



REPORT TO BEIS

**LONG-TERM ATMOSPHERIC MEASUREMENT AND INTERPRETATION
(OF RADIATIVELY ACTIVE TRACE GASES)**

BEIS contract number: GA0201

Annual Report (Sept 2016 - August 2017)

Date: 21st September 2017

University of Bristol: Simon O'Doherty, Kieran Stanley, Matt Rigby, Ann Stavert

Met Office: Alistair Manning, Alison Redington

INSCON: Peter Simmonds

Terra Modus Consultants Ltd: Dickon Young

University of East Anglia: Bill Sturges

University of Edinburgh: Paul Palmer

Contents

1	Executive Summary	4
1.1	Headline Summary	4
1.2	Project Summary	4
1.3	Summary of the main findings on inventory verification	5
1.4	Summary of Progress	5
1.5	Future Plans	6
1.6	Recent Publications	6
1.7	Meetings	8
1.8	Related information	8
2	Instrumentation	9
2.1	Sites	9
2.1.1	Mace Head (MHD)	9
2.1.2	Tacolneston (TAC)	9
2.1.3	Ridge Hill (RGL)	10
2.1.4	Bilsdale (BSD)	10
2.1.5	Heathfield (HFD) (Affiliated to UK DECC Network)	10
3	Annual Northern Hemispheric trends	12
3.1	Baseline Mole Fractions	12
4	Regional emission estimation	15
4.1	Introduction	15
4.2	Summary of InTEM inverse modelling	15
4.3	Summary of the greenhouse gases reported to the UNFCCC	17
4.4	Methane (CH ₄)	18
4.5	Nitrous oxide (N ₂ O)	21
4.6	Carbon dioxide (CO ₂)	24
4.7	HFC-125	25
4.8	HFC-134a	27
4.9	HFC-143a	29
4.10	HFC-152a	31
4.11	HFC-23	33
4.12	HFC-32	35
4.13	HFC-227ea	37
4.14	HFC-245fa	39
4.15	HFC-43-10mee	41
4.16	HFC-365mfc	43
4.17	PFC-14 (CF ₄)	45
4.18	PFC-116	47
4.19	PFC-218	49
4.20	PFC-318	51
4.21	SF ₆	53
4.22	NF ₃	55
5	Global emission estimates	56
5.1	Introduction	56
5.2	Recent trends in non-CO ₂ Kyoto gases	56
5.2.1	CH ₄	56
5.2.2	N ₂ O	56
5.2.3	HFCs	56
5.2.4	PFCs, SF ₆ and NF ₃	57
6	Use of satellite data in inversion modelling	65
6.1	Introduction	65
6.2	Preparation of existing satellite data	65
6.3	Future mission concepts	65
6.4	Ground-based networks	66
6.5	Emission estimates using satellite observations of CO ₂ and CH ₄	66
7	Estimating biogenic and anthropogenic emissions of CO ₂	68
8	Results and analysis of additional gases	69
8.1	Introduction	69
8.2	CFC-11	70

8.3	CFC-12	71
8.4	CFC-113	72
8.5	HCFC-124	73
8.6	HCFC-141b	74
8.7	HCFC-142b	75
8.8	HCFC-22	76
8.9	HFC-236fa	77
8.10	SO ₂ F ₂	78
8.11	CH ₃ Cl	79
8.12	CH ₂ Cl ₂	80
8.13	CHCl ₃ (chloroform)	81
8.14	CCl ₄ (carbon tetrachloride)	82
8.15	CH ₃ CCl ₃ (methyl chloroform)	83
8.16	CCl ₂ CCl ₂	84
8.17	Methyl bromide (CH ₃ Br)	85
8.18	Halon-1211	86
8.19	Halon-1301	87
8.20	Halon-2402	88
8.21	Carbon monoxide (CO)	89
8.22	Ozone (O ₃)	90
8.23	Hydrogen	91
9	UK HFC-143a Emissions	92
9.1	Introduction	92
9.2	Methodology	92
9.2.1	Initial RAC model analysis	92
9.2.2	Comparison of UNFCCC and InTEM emissions	93
9.2.3	Bottom-up estimation of UK HFC-143a emissions	93
9.3	Results and Discussion	93
9.3.1	Initial RAC model analysis	93
9.3.2	Comparison of UNFCCC and InTEM emissions	93
9.3.3	Bottom-up estimation of UK HFC-143a emissions	94
9.4	Conclusions	97
10	Use of optical methods for real-time atmospheric N ₂ O measurements	98
10.1	Introduction	98
10.2	Instrumentation	98
10.3	Description of data analysis methods	98
10.4	Results and discussion	99
10.5	Conclusions	99
11	Developments in methane isotopologue measurements	100
12	References	101

1 Executive Summary

1.1 *Headline Summary*

- The overriding aim of the project is to estimate UK emissions of the principle greenhouse gases using the UK Deriving Emissions related to Climate Change (DECC) network of observations and compare these to the compiled inventory. The Inversion Technique for Emission Modelling (InTEM) has been developed to deliver these estimates. These comparisons enable BEIS to be more informed in their inventory improvement programme.
- The northern hemisphere atmospheric concentrations of ALL of the 'Kyoto basket' of gases except HFC-152a are increasing.
- InTEM estimates for methane are lower than the reported inventory although in recent years the agreement is good. Nitrous oxide is in good agreement up until 2013. The principle HFCs are generally estimated to be lower by InTEM compared to the inventory, notably the most abundant, HFC-134a.

1.2 *Project Summary*

Monitoring the atmospheric concentrations of gases is important in assessing the impact of international policies related to the atmospheric environment. The effects of control measures on greenhouse gases in the so called 'Kyoto basket': carbon dioxide (CO₂), methane (CH₄), nitrous oxide (N₂O), hydrofluorocarbons (HFC), perfluorocarbons (PFC), nitrogen trifluoride (NF₃) and sulphur hexafluoride (SF₆), are now being observed. Likewise, measures introduced under the Montreal Protocol to protect the stratospheric ozone layer are also being observed in the atmosphere. Understanding the effectiveness and impacts of policies on the atmospheric abundance of these key gases is vitally important to policy makers.

This project has two principle aims:

- **Estimate the background atmospheric concentrations of the principle greenhouse and ozone-depleting gases from the DECC network of observations.**
- **Estimate the UK emissions of the principle greenhouse gases using the DECC network of observations and compare these to the compiled inventory.**

Since 1987, high frequency, real time measurements of the principal halocarbons and radiatively active trace gases have been made as part of the Global Atmospheric Gases Experiment (GAGE) and Advanced Global Atmospheric Gases Experiment (AGAGE) at Mace Head, County Galway, Ireland. For much of the time, the measurement station, which is situated on the Atlantic coast, monitors clean westerly air that has travelled across the North Atlantic Ocean. However, when the winds are easterly, Mace Head receives substantial regional scale pollution in air that has travelled from the populated and industrial regions of Europe. The site is therefore uniquely situated to record trace gas concentrations associated with both the northern hemisphere background levels and with the more polluted air arising from European emissions.

To this aim, the UK has developed a network of observation stations called the UK Deriving Emissions related to Climate Change (DECC) network. Along with Mace Head, it consists of three tall tower stations: Ridge Hill near Hereford; Tacolneston near Norwich; Bilsdale in North Yorkshire (originally Angus near Dundee). Ridge Hill became operational in February 2012, Tacolneston in July 2012 and Angus began operating for the network in April 2012, but was decommissioned and replaced with Bilsdale in September 2015. The expanded network makes it possible to resolve emissions on a higher resolution, both spatially and temporally, across the UK.

The UK DECC network measures, to very high precision, all of the principle greenhouse gases in the inventory 'Kyoto basket' of gases as well as many ozone-depleting gases. The Inversion Technique for Emission Modelling (InTEM) (please refer to Methodology report for more details) has been developed to use these observations to estimate both Northern Hemisphere concentration trends and UK emissions of each gas. The InTEM emission estimates, as well as those reported

through the inventory process, have uncertainties. The comparisons between the inventory and InTEM estimates enable BEIS to be more informed in their inventory improvement programme.

The atmospheric measurements and emission estimates of greenhouse gases provide an important independent cross-check for the national GreenHouse Gas Inventories (GHGI) of emissions submitted annually to the United Nations Framework Convention on Climate Change (UNFCCC). The GHGI are estimated through in-country submissions of Activity Data and Emission Factors that are, in some cases, very uncertain. Independent emissions verification is considered good practice by the Intergovernmental Panel on Climate Change (IPCC).

The UK is one of only two countries worldwide (Switzerland is the other) that currently routinely verify their reported inventory emissions as part of their annual UNFCCC submission of emissions.

1.3 Summary of the main findings on inventory verification

- The northern hemisphere atmospheric concentrations of ALL 'Kyoto basket' gases except HFC-152a are increasing.
- Methane (CH₄): The UK InTEM estimates are lower than the UK GHGI estimates (as reported to the UNFCCC in 2016) in the 1990s and 2000s. By 2002 the uncertainties of the two methods overlap and from 2013 onwards there is good agreement. The inclusion of the extended DECC network observations and the data from the NERC Greenhouse Gas UK and Global Emissions (GAUGE) project has allowed the InTEM time frame to be reduced from 3-years to 6-months, and even 1-month if a prior is used. Good agreement is seen between these different inversions. The 1-month inversions using the UK NAEI prior information reveals no significant seasonal cycle in the UK emissions of CH₄. Although the inventory is an annual value it is important to note that the UK emissions do vary across the year and understanding any particular seasonality could help improve the inventory. It should also be noted that higher frequency estimates allow more up-to-date UK emissions to be produced by InTEM ahead of the inventory.
- Nitrous oxide (N₂O): The UK GHGI and InTEM estimates are broadly in agreement up until 2012. The InTEM estimates show increased emissions in the latter period unlike the GHGI. The improvements to InTEM over the last year, notably boundary conditions, baselines and model uncertainty and, in the case of N₂O, calibration scale, have led to changes in the UK emission estimates from InTEM. The 5-site, 6-month, inversions now agree with the 3-year MHD-only inversion estimates from 2013 onwards, i.e. higher than the GHGI. 5-site, 1-month, InTEM results using the latest (2015) NAEI prior emissions to inform the inversions show a strong seasonal cycle in UK N₂O emissions with peaks in spring.
- HFC-134a: The UK GHGI is higher than that estimated by InTEM and the uncertainties of the two methods do not overlap. However, the agreement this year has improved compared to last year after further modifications to the emission factors and activity data used in the UK inventory and also improvements to the InTEM baseline and model uncertainties.
- HFC-125 and HFC-32: The UK GHGI estimates for these gases (used in refrigerant blends) are increasing. UK InTEM estimates are approximately one third lower than the GHGI but with a similar trend. In the later years the InTEM emission estimates may be starting to level off.
- For HFC-143a: UK InTEM estimates agree with the GHGI from 2011 onwards. The sharp step 2010-2011 in the GHGI, not seen in the InTEM results, is under investigation.
- Sulphur hexafluoride (SF₆): The UK InTEM estimates are consistently elevated compared to the GHGI; however, the InTEM uncertainty ranges do encompass the inventory estimates.

1.4 Summary of Progress

Significant progress has been made during the second 12 months of the contract period. There have been significant improvements to how uncertainty in the inversion process is represented and

how the baseline and boundary conditions are estimated. The section on satellite observations and how they are currently used in inversion modelling has been updated. Global emissions of the key greenhouse gases have also been updated in this report.

- **Mace Head** continues to be a baseline station at the forefront of global atmospheric research. This is evident through the high volume of peer-reviewed publications related to work using the Mace Head observational record. The recent publications related to this contract are detailed in the publication section of this report. In addition, the inclusion of Mace Head in many EU funded atmospheric research programmes, such as ICOS, InGOS, ACTRIS, and continued support from other global programmes such as AGAGE and NOAA-ESRL indicates its international significance.
- **Mid-latitude Northern Hemisphere baseline trends have been updated.** The trends have been extended up to and including June 2017 observations.
- **UK emission estimates.** Inversion emission estimates for the UK are reported up to and including 2016 and have been compared to the UK GHGI inventory submitted in 2017 (the 2017 GHGI submission covers UK emissions up to and including 2015).
- **UNFCCC verification appendix chapter** for the UK National Inventory Report (NIR) submission was delivered (March 2017).
- **6-month report** was completed (May 2017).
- **Sector-specific inversion capability** was developed within InTEM. However, the current coarseness of the mapped sector divisions, e.g. agriculture, waste, energy, are insignificant to really inform the inventory process.
- **New N₂O calibration scale** (SIO-16) was adopted across the UK DECC Network.

1.5 Future Plans

- High resolution modelling of the areas directly surrounding each station may improve the overall modelling of the observations. This will be investigated.
- Improve the uncertainty estimates of the InTEM emissions by including a factor related to the modelled vertical temperature profile at the observation station.

1.6 Recent Publications

Bader, W., Bovy, B., Conway, S., Strong, K., Smale, D., Turner, A. J., Blumenstock, T., Boone, C., Coen, M. C., Coulon, A., Garcia, O., Griffith, D. W. T., Hase, F., Hausmann, P., Jones, N., Krummel, P., Murata, I., Morino, I., Nakajima, H., **O'Doherty, S.**, Paton-Walsh, C., Robinson, J., Sandrin, R., Schneider, M., Servais, C., Sussmann, R. and Mahieu, E.: The recent increase of atmospheric methane from 10 years of ground-based NDACC FTIR observations since 2005, *Atmos. Chem. Phys.*, 17, 2255–2277, doi:10.5194/acp-17-2255-2017, 2017.

Brunner, D., Arnold, T., Henne, S., **Manning, A. J.**, Thompson, R. L., Maione, M., **O'Doherty, S.**, Reimann, S., Comparison of four inverse modelling systems applied to the estimation of HFC-125, HFC-134a and SF₆ emissions over Europe, *Atmos. Chem. Phys.*, 17, pp. 10651-10674, 2017.

Cain, M., Warwick, N., Fisher, R., Lowy, D., Lanoiselle, M., Nisbet, E., France, J., Pitt, J., O'Shea, S., Bower, K., Allen, G., Illingworth, S., **Manning, A. J.**, Bauguitte, S., Pissot, I., Pyle, J., A cautionary tale: Identifying the sources of a methane enhancement observed over the North Sea using a meteorological model and measurements of carbon isotopes, *J. Geophys. Res. Atmos.*, 122, pp. 7630-7645, 2017.

Chipperfield, M. P., Liang, Q., **Rigby, M.**, Hossaini, R., Montzka, S. A., Dhomse, S., Feng, W., Prinn, R. G., Weiss, R. F., Harth, C. M., Salameh, P. K., Mühle, J., **O'Doherty, S.**, **Young, D.**, **Simmonds, P. G.**, Krummel, P. B., Fraser, P. J., Steele, L. P., Happell, J. D., Rhew, R. C., Butler, J., Yvon-Lewis, S. A., Hall, B., Nance, D., Moore, F., Miller, B. R., Elkins, J. W., Harrison, J. J., Boone, C. D., Atlas, E. L., and Mahieu, E., Model sensitivity studies of the decrease in atmospheric carbon tetrachloride, *Atmos. Chem. Phys.*, 16(24), pp. 15741–15754, 2016.

Chirkov, M., Stiller, G. P., Laeng, A., Kellmann, S., von Clarmann, T., Boone, C. D., Elkins, J. W., Engel, A., Glatthor, N., Grabowski, U., Harth, C. M., Kiefer, M., Kolonjari, F., Krummel, P. B., Linden, A., Lunder, C. R., Miller, B. R., Montzka, S. A., Mühle, J., **O'Doherty, S.**, Orphal, J., Prinn, R. G., Toon, G., Vollmer, M. K., Walker, K. A., Weiss, R. F., Wiese, A. and **Young, D.**: Global HCFC-22 measurements with MIPAS: retrieval, validation, global

- distribution and its evolution over 2005–2012, *Atmos. Chem. Phys.*, 16(5), 3345–3368, doi:10.5194/acp-16-3345-2016, 2016.
- France, J., Cain, M., Fisher, R., Lowry, D., Allen, G., O’Shea, S., Illingworth, S., Pyle, J., Warwick, N., Jones, B., Gallagher, M., Bower, K., Le Breton, M., Percival, C., Muller, J., Wellpott, A., Bauguitte, S., George, C., Hayman, G., **Manning, A. J.**, Myhre, C., Lanoiselle, M., Nisbet, E., Using D13C in CH₄ and particle dispersion modelling to characterize sources of Arctic methane within an air mass, *JGR – Atmospheres*, 2017.
- Graziosi, F., Arduini, J., Bonasoni, P., Furlani, F., Giostra, U., **Manning, A. J.**, McCulloch, A., **O’Doherty, S.**, **Simmonds, P. G.**, Reimann, S., Vollmer, M. K., Maione, M., et al, Emissions of carbon tetrachloride (CCl₄) from Europe, *Atmos. Chem. Phys.*, 16, pp. 12849-12859, 2016.
- Graziosi, F., Arduini, J., Furlani, F., Giostra, U., Cristofanelli, P., Fang, X., Hermanssen, O., Lunder, C., Maenhout, G., **O’Doherty, S.**, Reimann, S., Schmidbauer, N., Vollmer, M. K., **Young, D.**, and Maione, M., European emissions of the powerful greenhouse gases hydrofluorocarbons inferred from atmospheric measurements and their comparison with annual national reports to UNFCCC, *Atmospheric Environment*, 158, pp. 85–97, 2017.
- Lunt, E. M., **Rigby, M.**, Ganesan, A., **Manning, A. J.**, Estimation of trace gas fluxes with objectively determined basis functions using reversible-jump Markov chain Monte Carlo, *Geosci. Model Dev.*, 9, pp. 3213-3229, 2016.
- Mahieu, E., Lejeune, B., Bovy, B., Servais, C., Toon, G. C., Bernath, P. F., Boone, C. D., Walker, K. A., Reimann, S., Vollmer, M. K. and **O’Doherty, S.**: Retrieval of HCFC-142b (CH₃CClF₂) from ground-based high-resolution infrared solar spectra: Atmospheric increase since 1989 and comparison with surface and satellite measurements, *J. Quant. Spectrosc. Radiat. Transf.*, 186, 96–105, doi:10.1016/j.jqsrt.2016.03.017, 2017.
- McNorton, J., Chipperfield, M. P., Gloor, M., Wilson, C., Feng, W., Hayman, G. D., **Rigby, M.**, Krummel, P. B., **O’Doherty, S.**, Prinn, R. G., Weiss, R. F., **Young, D.**, Dlugokencky, E. and Montzka, S. A.: Role of OH variability in the stalling of the global atmospheric CH₄ growth rate from 1999 to 2006, *Atmos. Chem. Phys. Discuss.*, 17(January), 1–24, doi:10.5194/acp-2015-1029, 2016.
- Meinshausen, M., Vogel, E., Nauels, A., Lorbacher, K., Meinshausen, N., Etheridge, D. M., Fraser, P. J., Montzka, S. A., Rayner, P. J., Trudinger, C. M., Krummel, P. B., Beyerle, U., Canadell, J. G., Daniel, J. S., Enting, I. G., Law, R. M., Lunder, C. R., **O’Doherty, S.**, Prinn, R. G., Reimann, S., Rubino, M., Velders, G. J. M., Vollmer, M. K., Wang, R. H. J. and Weiss, R.: Historical greenhouse gas concentrations for climate modelling (CMIP6), *Geosci. Model Dev.*, 10(5), 2057–2116, doi:10.5194/gmd-10-2057-2017, 2017.
- Obersteiner, F., Bönisch, H., Keber, T., **O’Doherty, S.** and Engel, A.: A versatile, refrigerant- and cryogen-free cryofocusing–thermodesorption unit for preconcentration of traces gases in air, *Atmos. Meas. Tech.*, 9(11), 5265–5279, doi:10.5194/amt-9-5265-2016, 2016.
- Rigby, M.**, Montzka, S., Prinn, R. G., White, J. W. C., **Young, D.**, **O’Doherty, S.**, Lunt, M. F., Ganesan, A., **Manning, A. J.**, **Simmonds, P.**, Salameh, P., Harth, C., Mühle, J., Weiss, R. F., Fraser, P., Steele, P., Krummel, P., McCulloch, A., Park, S., The role of atmospheric oxidation in recent methane growth, *PNAS*, 114 (21) pp. 5373-5377, 2017.
- Riddick, S., Connors, S., Robinson, A. D., **Manning, A. J.**, Jones, P. S. D., Lowry, D., Nisbet, E., Skelton, R. L., Allen, G., Pitt, J., Harris, N. R. P., Estimating the size of a methane emission point-source at different scales: from local to landscape, *Atmos. Chem. Phys.*, 17, pp. 7839-7851, 2017.
- Rózanski, K., Chmura, L., Gałkowski, M., NęCKI, J., Zimnoch, M., Bartyzel, J. and **O’Doherty, S.**: Monitoring of Greenhouse Gases in the Atmosphere-A Polish Perspective, *Pap. Glob. Chang. IGBP*, 23(1), 111–126, doi:10.1515/igbp-2016-0009, 2016.
- Saunois, M., Bousquet, P., Poulter, B., Peregon, A., Ciais, P., Canadell, J. G., Dlugokencky, E. J., Etiope, G., Bastviken, D., Houweling, S., Janssens-Maenhout, G., Tubiello, F. N., Castaldi, S., Jackson, R. B., Alexe, M., Arora, V. K., Beerling, D. J., Bergamaschi, P., Blake, D. R., Brailsford, G., Brovkin, V., Bruhwiler, L., Crevoisier, C., Crill, P., Curry, C., Frankenberg, C., Gedney, N., Höglund-Isaksson, L., Ishizawa, M., Ito, A., Joos, F., Kim, H.-S., Kleinen, T., Krummel, P., Lamarque, J.-F., Langenfelds, R., Locatelli, R., Machida, T., Maksyutov, S., McDonald, K. C., Marshall, J., Melton, J. R., Morino, I., **O’Doherty, S.**, Parmentier, F.-J. W., Patra, P. K., Peng, C., Peng, S., Peters, G. P., Pison, I., Prigent, C., Prinn, R., Ramonet, M., Riley, W. J., Saito, M., Schroder, R., Simpson, I. J., Spahni, R., Steele, P., Takizawa, A., Thornton, B. F., Tian, H., Tohjima, Y., Viovy, N., Voulgarakis, A., van Weele, M., van der Werf, G., Weiss, R., Wiedinmyer, C., Wilton, D. J., Wiltshire, A., Worthy, D., Wunch, D. B., Xu, X., Yoshida, Y., Zhang, B., Zhang, Z. and Zhu, Q.: The Global Methane Budget: 2000-2012, *Earth Syst. Sci. Data Discuss.*, (June), 1–79, doi:10.5194/essd-2016-25, 2016.
- Saunois, M., Bousquet, P., Poulter, B., Peregon, A., Ciais, P., Canadell, J. G., Dlugokencky, E. J., Etiope, G., Bastviken, D., Parmentier, F.-J. W., Patra, P. K., Peng, C., Peng, S., Peters, G. P., Pison, I., Prinn, R., Ramonet, M., Riley, **O’Doherty, S.**, W. J., Yoshida, Y., Zhang, B., Zhang, Z. and Zhu, Q.: Variability and quasi-decadal changes in the methane budget over the period 2000–2012, *Atmos. Chem. Phys.* *Atmos. Chem. Phys.*, 17(14), 11135–11161, doi:10.5194/acp-17-11135-2017, 2017.
- Say, D., **Manning, A. J.**, **O’Doherty, S.**, **Rigby, M.**, **Young, D.**, Grant, A., Re-evaluation of the UK’s HFC-134a emissions inventory based on atmospheric observations, *Environ. Sci. Technol.*, 50 (20), pp. 11129-11136, 2016.
- Simmonds, P. G.**, **Rigby, M.**, **Manning, A. J.**, Lunt, M. F., **O’Doherty, S.**, McCulloch, A., Fraser, P., Henne, S., Vollmer, M. K., Mühle, J., Weiss, R., Salameh, P., **Young, D.**, Reimann, S., Wenger, A., Arnold, A., Harth, C., et al,

Global and regional emissions estimates of HFC-152a from in situ and air archive observations, *Atmos. Chem. Phys.*, 16, pp. 365-382, 2016.

Simmonds, P. G., Rigby, M., McCulloch, A., Young, D., Mühle, J., Weiss, R., Salameh, P., Harth, C., Krummel, P., Fraser, P., Steele, P., Manning, A. J., Wang, R., Prinn, R., O'Doherty, S., Changing trends and emissions of hydrochlorofluorocarbons (HCFCs) and their hydrofluorocarbon (HFCs) replacements, *Atmos. Chem. Phys.*, 17, pp. 4641-4655, 2017.

Slemr, F., Brenninkmeijer, C. A., Rauthe-Schöch, A., Weigelt, A., Ebinghaus, R., Brunke, E.-G., Martin, L., Spain, T. G. and **O'Doherty, S.**: El Niño-Southern Oscillation influence on tropospheric mercury concentrations, *Geophys. Res. Lett.*, 43(4), 1766–1771, doi:10.1002/2016GL067949, 2016.

Trudinger, C. M., Fraser, P. J., Etheridge, D. M., Sturges, W. T., Vollmer, M. K., **Rigby, M.**, Martinerie, P., Mühle, J., Worton, D. R., Krummel, P. B., Paul Steele, L., Miller, B. R., Laube, J., Mani, F. S., Rayner, P. J., Harth, C. M., Witrant, E., Blunier, T., Schwander, J., **O'Doherty, S.** and Battle, M.: Atmospheric abundance and global emissions of perfluorocarbons CF₄, C₂F₆ and C₃F₈ since 1800 inferred from ice core, firn, air archive and in situ measurements, *Atmos. Chem. Phys.*, 16(18), doi:10.5194/acp-16-11733-2016, 2016.

Vollmer, M. K., Mühle, J., Trudinger, C. M., **Rigby, M.**, Montzka, S. A., Harth, C. M., Miller, B. R., Henne, S., Krummel, P. B., Hall, B. D., **Young, D.**, Kim, J., Arduini, J., Wenger, A., Yao, B., Reimann, S., **O'Doherty, S.**, Maione, M., Etheridge, D. M., Li, S., Verdonik, D. P., Park, S., Dutton, G., Steele, L. P., Lunder, C. R., Rhee, T. S., Hermansen, O., Schmidbauer, N., Wang, R. H. J., Hill, M., Salameh, P. K., Langenfelds, R. L., Zhou, L., Blunier, T., Schwander, J., Elkins, J. W., Butler, J. H., **Simmonds, P. G.**, Weiss, R. F., Prinn, R. G. and Fraser, P. J.: Atmospheric histories and global emissions of halons H-1211 (CBrClF₂), H-1301 (CBrF₃), and H-2402 (CBrF₂ CBrF₂), *J. Geophys. Res. Atmos.*, 121(7), 3663–3686, doi:10.1002/2015JD024488, 2016.

Zhang, G., Yao, B., Vollmer, M. K., Montzka, S. A., Mühle, J., Weiss, R. F., **O'Doherty, S.**, Li, Y., Fang, S. and Reimann, S.: Ambient mixing ratios of atmospheric halogenated compounds at five background stations in China, *Atmos. Environ.*, 160, 55–69, doi:10.1016/j.atmosenv.2017.04.017, 2017.

1.7 Meetings

- **AGAGE meeting (Tasmania, Australia, November 2016)**
- **DECC contract meeting (London, November 2016)**
- **NISC meeting (London, November 2016)**
- **AGAGE meeting (Mulranny, Ireland, June 2017)**
- **EU Modelling Inventory workshop (JRC, Italy 2017)**
- **DECC network meeting (Galway, July 2017)**

1.8 Related information

Project website: www.metoffice.gov.uk/atmospheric-trends

Methodology Report (Dec 2015)

Technical Document (May 2016)

2 Instrumentation

2.1 Sites

A brief summary of site operations over the last year is presented here. A more detailed account of the instruments and their operations is presented in the methodology report and also on the website (<http://www.metoffice.gov.uk/research/monitoring/atmospheric-trends/instrumentation>).

2.1.1 Mace Head (MHD)

- Medusa GC-MS: Overall, the Medusa GC-MS has experienced a number of sample pump related problems over the past 12-months.
- The air sample pump failed on 12th September 2016 due to a split diaphragm. A Viton coated diaphragm was installed but was replaced with a neoprene diaphragm on 20th September 2016 as there was concerns of outgassing of compounds measured on the Medusa GC-MS.
- At the end of September 2016, valve 1 was cleaned as there were concerns that parts of the broken pump diaphragm had entered the valve.
- A power issue resulted in the Cryotiger switching off and the baseplate warming, resulting in a day of data loss on 19th January 2017.
- The KNF pump failed again on 18th April 2017, and was replaced with a new pump on 25th May 2017. Problems continued with the sample module as a backpressure regulator developed a slight leak causing HFC-32 and HFC-125 samples to be contaminated by air from the lab A/C unit containing R410A (50:50 blend of HFC-32 and HFC-125). Data for these compounds between 29th June and 19th July 2017 were compromised and removed from the dataset as a result.
- GC-MD: The MD performed well for the reporting period. Most of the data loss resulted from the KNF pump failures described above.
- The complete N₂O data record was adjusted to the new SIO-16 calibration scale.

2.1.2 Tacolneston (TAC)

- There is extensive work being carried out on-site by Arqiva (preparing the site for 5G transmission). This work has and will continue to make access extremely difficult for the next year (or more).
- The lab AC started to leak slightly on 16th June, the unit was serviced, but continued to leak. Despite multiple site visits by an AC service company the AC finally failed on 4th Sept 2017, with lab temperature reaching 65°C before remote shutdown of all equipment was completed. All instruments are currently switched off awaiting a replacement AC unit.
- The UPS batteries were replaced on 1st February 2017 as they had exceeded their usage date.
- The TOC, which supplies dry gas to the Medusa GC-MS and GC-MD to dry the air, was replaced at site due to a leak in the system on 7th March 2017.
- Medusa GC-MS: Compressor failures on 7th November 2016, resulted in 5 days data loss. The system ran out of helium on 9th January 2017 after a large leak developed, which resulted in 4 days loss of data. The compressor failed on 26th January 2017, resulting in 42 days of data loss whilst waiting for a replacement. A new compressor and TOC was fitted on 7th March 2017. A helium leak in the GC EPC controller was found on 8th March 2017 and fixed. The Medusa vacuum shell leak-rate was also tested and subsequently had the majority of the O-rings re-greased to reduce the shell vacuum leak-rate. On the 9th March 2017, the sampling inlet for the Medusa was changed to 185 m, from the 100 m inlet. The PCC refrigerant was topped up on 22nd May to try to improve the baseplate cooling. Another leak on the EPC control module was found on 23rd May and subsequently fixed.
- GC-MD: The GC-MD has been running well. On the 9th March 2017, the sampling inlet for the GC-MD was changed to 185 m, from the 100 m inlet. A new mercuric oxide filter was installed on 6th July 2017 and a new mercury lamp on 20th July 2017.
- CRDS: The CRDS has been running well.
- OA-ICOS: The Off Axis-Integrated Cavity Output Spectrometer (OA-ICOS) was installed at site on 31st August 2016 and has been running well since. Originally the instrument was

setup to sample each inlet sequentially for 20 minutes. However, on 9th March 2017, the hourly repeating sampling sequence was changed to analyse the 185 m inlet for 40 minutes and the other two inlets for 10 minutes each.

- The ICOS comparison drift experiment in collaboration with LSCE (France) has been running for almost a year and is set to continue for a couple more months.

2.1.3 Ridge Hill (RGL)

- GC-MD: The GC-MD has been running well over the past 12 months. Problems with the UPS system resulted in 22 days of data loss (7 days from 29th October 2016 and 15 days from 9th May 2017). Four cylinders spanning below and above ambient N₂O mole fractions were installed in May 2017 and were analysed on the instrument until 12th August 2017 to characterise instrument nonlinearity.
- CRDS: The CRDS has been working well over the last 12 months. Problems with the UPS has resulted in 22 days data loss (7 in November 2016 and 15 in May 2017). The mid-high calibration cylinder was reinstalled at site after recalibration at EMPA in April 2017.
- The UPS at site failed twice and drained the batteries on 29th October 2016 and on 9th May 2017. The UPS unit and batteries were replaced both times.

2.1.4 Bilsdale (BSD)

- Bilsdale became part of the UK DECC network in September 2016 (previously it was part of the GAUGE project with measurements starting in January 2014).
- GC-MD: The MD at Bilsdale has been running well during the past 12 months. The sampling height was switched from 108 m to 248 m on 17th March 2017. The compressor was switched off accidentally by workmen in laboratory on the 7th April, resulting in the instrument being run with humid air until the site was visited on 20th April 2017. Four cylinders spanning below and above ambient N₂O mole fractions were installed on 22nd August 2017 and were analysed on the instrument overnight to investigate instrument nonlinearity.
- CRDS: The CRDS has been working well over the last 12 months. The original sampling regime of analysing the 42, 108 and 248 m inlets sequentially for 20 minutes was changed to analyse the 248 m inlet for 40 minutes and then the other two inlets for 10 minutes each. H₂O tests were re-run on the instrument on 22nd to 24th August 2017.

2.1.5 Heathfield (HFD) (Affiliated to UK DECC Network)

- Future of the station after completion of NERC's GAUGE project
 1. As of 5th September 2017, the National Physical Laboratory (NPL) took over the running of the GHG measurements and the site sharing license with Arqiva at the Heathfield site.
 2. NPL aim to make the site a centre for atmospheric measurement and metrology for the UK community, while maintaining and building on the current suite of GHG measurements at the site.
 3. NPL plan to continue to link in to the DECC network via use of the current traceable chain of standards and maintaining the QA/QC procedure for data analysis.
 4. Plans for 2017/2018 include installation of meteorological sensors for wind speed, temperature, pressure and relative humidity, and air quality sensors. The University of Edinburgh have a grant as part of a larger NERC investment in 'atmospheric hazards' and plan to install a Picarro CRDS for N₂O and CO measurements (G5310) and a Rd detector from ANSTO for helping trace the air history to the site.
- Site technical issues
 1. The Picarro CRDS has been running without any issues.
 2. The pump for the 50 m sampling line failed at the end of 2016 and was replaced in February. During the 2 months air was sampled from only the 100 m inlet by the Picarro. The MD was unaffected as it only samples the 100 m inlet.
 3. A second multiposition valve and controller were installed along with 5 cylinders of calibration gases gravimetrically prepared by NPL. These are sampled monthly by both the Picarro and MD to characterise long-term drift in instrument linearity.
 4. The GC carrier gas ran out in November 2016 and the instrument automatically shut down. After replacing the gas the amount of noise – characterised by the plot of RL for

the standard gas – had increased significantly. This noise persisted until July, when a small air leak in the GC column connection was found and repaired.

5. The GC peak integration parameters have been changed by UoB to match those used at the other sites.
- Greenhouse gas summer school.
 1. Heathfield was used as a field-trip site for the 2017 International Summer School on Global Greenhouse Gases. This was part of a two-week summer school on greenhouse gases organised by the National Oceanography Centre in Southampton and the University of Edinburgh.
 2. Tim Arnold, Tom Gardiner, Chris Rennick, Neil Howes and Jessica Connolly from the Emissions and Atmospheric Metrology Group (EAMG) gave lectures and demonstrations on metrology, spectroscopy, atmospheric chemistry, and greenhouse gas measurements and modelling. The students visited the tall tower monitoring site in groups to understand how measurements of CO₂, CH₄, N₂O and SF₆ are made for the purpose of validating the UK's greenhouse gas inventory.

3 Annual Northern Hemispheric trends

3.1 Baseline Mole Fractions

For each gas observed at Mace Head a baseline analysis has been performed. ECMWF meteorology is used from 1989 – 2002 inclusive and Met Office meteorology from 2003 – 2017 inclusive. For each gas, monthly and annual northern hemisphere (NH) baselines, annual growth rates and the average seasonal cycle seen within the observations are calculated. Table 1 – Table 4 summarises the annual baseline mole fractions for each of the gases observed.

Gas	CH ₄	N ₂ O	CO ₂	HFC-125	HFC-134a	HFC-143a	HFC-152a	HFC-23	HFC-32
	ppb	ppb	ppm	ppt	ppt	ppt	ppt	ppt	ppt
1990	1787	309							
1991	1802	310							
1992	1798	310							
1993	1813	310	357						
1994	1810	311	358						
1995	1815	312	360		2.3		1.2		
1996	1818	313	361		4.3		1.2		
1997	1818	314	364		6.1		1.4		
1998	1828	314	366		9.7		1.7		
1999	1832	315	368	1.4	13.1		2.1		
2000	1832	316	368	1.7	16.9		2.4		
2001	1834	317	371	2.3	20.7		2.8		
2002	1836	318	373	2.6	24.8		3.3		
2003	1842	319	374	3.2	29.4		4.1		
2004	1842	319	377	3.8	34.4	5.4	4.7		1
2005	1841	320	379	4.6	39	6.3	5.5		1.5
2006	1835	320	381	5.3	43.4	7.4	6.6		2
2007	1845	321	383	6.2	47.5	8.3	7.7		2.7
2008	1858	322	385	7.4	52.9	9.5	8.7	22.4	3.3
2009	1862	323	387	8.5	57.5	10.6	8.8	22.9	4
2010	1868	324	389	9.9	62.9	11.8	9.4	23.6	5.1
2011	1870	325	391	11.6	68	13	9.8	24.6	6.4
2012	1877	326	394	13.4	73	14.4	9.9	25.4	7.6
2013	1881	327	396	15.4	78.4	15.8	9.8	26.6	9.2
2014	1894	328	398	17.8	83.7	17.3	9.9	27.7	10.9
2015	1905	328	400	20.2	89.2	18.7	9.7	28.7	12.9
2016	1916	329	403	22.5	95.6	20.4	9.8	29.5	14.9
AvGrow	5.04	0.79	2.01	1.25	4.48	1.25	0.42	0.9	1.17
AvGr12	10.47	0.75	2.91	2.4	6.18	1.58	0.03	0.8	2.13

Table 1: Annual northern hemisphere baseline mass mixing ratios for Kyoto gases measured at Mace Head (ppt unless stated) and growth rates (ppt yr⁻¹ unless stated). AvGrow = Average growth since records began and AvGr12 = Average growth over most recent year.

Gas	HFC-227ea	HFC-4310mee	HFC-365mfc	PFC-14	PFC-116	PFC-218	PFC-318	SF ₆	NF ₃
	ppt	ppt	ppt	ppt	ppt	ppt	ppt	ppt	ppt
2004				74.8	3.6	0.4		5.5	
2005			0.3	75.4	3.7	0.4		5.8	
2006			0.4	76.1	3.8	0.5		6	
2007	0.5		0.5	76.8	3.9	0.5		6.3	
2008	0.5		0.6	77.6	4	0.5		6.6	
2009	0.6		0.6	78.1	4	0.5		6.9	
2010	0.7		0.7	78.7	4.1	0.5		7.1	
2011	0.8	0.2	0.8	79.4	4.2	0.6	1.3	7.5	
2012	0.9	0.2	0.8	80.2	4.3	0.6	1.4	7.8	
2013	1	0.2	0.9	80.9	4.4	0.6	1.4	8.1	
2014	1.1	0.3	1	81.7	4.4	0.6	1.5	8.4	1.2
2015	1.2	0.3	1.1	82.5	4.5	0.6	1.5	8.8	1.4
2016	1.3	0.3	1.2	83.4	4.6	0.6	1.6	9.1	1.5
AvGrow	0.09	0.01	0.08	0.72	0.08	0.02	0.05	0.3	0.15
AvGr12	0.12	0.01	0.08	0.87	0.07	0.01	0.05	0.31	0.16

Table 2: Annual northern hemisphere baseline mass mixing ratios for Kyoto gases measured at Mace Head (ppt) and growth rates (ppt yr⁻¹). AvGrow = Average growth since records began and AvGr12 = Average growth over most recent year.

Gas	CFC-11	CFC-12	CFC-113	HCFC-124	HCFC-141b	HCFC-142b	HCFC-22	HFC-236fa	HFC-245fa	SO ₂ F ₂	CH ₃ Cl	CH ₂ Cl ₂
	ppt	ppt	ppt	ppt	ppt	ppt	ppt	ppt	ppt	ppt	ppt	ppt
1990	263	495	74.8									
1991	267	505	81.7									
1992	267	515	83.9									
1993	269	520	84.9									
1994	268	528	83.9									
1995	267	532	84.1		5.2	7.9						
1996	266	537	84		7.4	9.2						36.3
1997	264	540	83.5		9.6	10.5						36.2
1998	263	542	82.8		11.5							31
1999	261	543	82.3	1.2	13.1	12.3	144				524	30.8
2000	260	545	82	1.4	15	13.5	150				514	29.5
2001	258	546	81.2	1.5	16.2	14.5	158				508	28.6
2002	256	546	80.4	1.6	17.5	15	163				505	28.7
2003	254	546	79.7	1.6	18.4	15.5	168				514	30.2
2004	252	545	78.9	1.6	19.1	16.2	173				519	30
2005	250	544	78.4	1.6	19	16.9	179			1.4	522	30.1
2006	248	542	77.6	1.6	19.5	18	186			1.5	513	
2007	246	540	76.8	1.6	20.2	19.2	194	0.1	1.1	1.5	533	
2008	244	538	76.3	1.6	20.8	20.5	203	0.1	1.2	1.6	529	35.7
2009	242	535	75.7	1.5	21.2	21.3	211	0.1	1.4	1.7	534	36.1
2010	240	533	74.9	1.5	21.9	21.8	218	0.1	1.5	1.7	523	39.6
2011	238	530	74.3	1.4	23	22.6	225	0.1	1.8	1.8	514	38.6
2012	236	527	73.8	1.4	24.1	23	230	0.1	2	1.9	522	
2013	234	525	73.2	1.3	24.8	23.2	236	0.1	2.2	2	528	
2014	233	523	72.6	1.3	25.3	23.3	241	0.1	2.4	2.1	529	
2015	232	520	72.1	1.2	25.6	23.3	245	0.1	2.5	2.2	532	
2016	230	516	71.3	1.1	25.9	23.4	249	0.2	2.8	2.4	537	49.6
AvGrw	-1.16	1.06	-0.04	-0.01	0.94	0.73	6.19	0.01	0.19	0.09	0.64	0.34
AvGr12	-1.49	-3.73	-0.73	-0.06	0.25	0.03	3.58	0.01	0.21	0.14	3.04	1.97

Table 3: Annual northern hemisphere baseline mass mixing ratios for other gases measured at Mace Head and growth rates (ppt yr⁻¹). AvGrow = Average growth since records began and AvGr12 = Average growth over most recent year.

Gas	CHCl ₃	CCl ₄	CH ₃ - CCl ₃	CCl ₂ = CCl ₂	CH ₃ Br	Halon- 1211	Halon- 1301	Halon- 2402	CO	H ₂	O ₃
	ppt	ppt	ppt	ppt	ppt	ppt	ppt	ppt	ppb	ppb	ppb
1990		107	150								33.4
1991			151								33.4
1992		104	148								32.6
1993		103	138								33.3
1994	10.7	103	124							499	34.6
1995	11.3	102	110							500	33.2
1996	11.5	101	95							502	34.7
1997	11.2	100	79						116	501	34.5
1998	11.2	99	66						143	514	37.4
1999	10.6	97	55		10.7	4.1	2.7		121	516	40.4
2000	10.4	97	46		10.4	4.3	2.9		117	505	38.5
2001	10.5	96	38	5	9.8	4.4	3		113	501	38.6
2002	10.3	95	32	4.6	9	4.4	3		118	500	39.3
2003	10.5	94	27	4.6	8.6	4.4	3		135	503	39.7
2004	10.7	93	22	4.3	9.1	4.5	3	0.5	120	502	38.8
2005	10.6	92	18	3.7	10.1	4.5	3.1	0.5	122	506	37.8
2006	10.6	91	15	3.7	9.3	4.4	3.2	0.5	121	508	38.8
2007	10.8	90	13	3.5	9.1	4.4	3.2	0.5	121	506	39.3
2008	10.8	89	11	3.3	9.1	4.4	3.2	0.5	119	508	39.4
2009	10.6	88	9	2.9	8.6	4.3	3.2	0.5	114	505	39.4
2010	11.2	87	8	3.1	8.2	4.2	3.3	0.5	122	501	39.2
2011	10.9	86	6	2.7	8.3	4.1	3.3	0.4	115	510	38.7
2012	11.1	85	5	2.5	8.2	4.1	3.3	0.4	123	510	38.2
2013	12.2	84	4	2.4	7.9	3.9	3.3	0.4	118	513	39.3
2014	13.2	83		2.4	7.6	3.9	3.4	0.4	122	512	39.6
2015	13.7	81	3	2.4	7.4	3.7	3.4	0.4	118	509	38.5
2016	14.5	80	2	2.3	7.3	3.6	3.4	0.4	115	511	38.3
AvGrow	0.16	-1.06	-5.58	-0.18	-0.2	-0.03	0.04	-0.01	-0.12	0.49	0.22
AvGr12	0.82	-1.41	-0.64	-0.11	-0.11	-0.12	-0.01	-0.01	-4.77	0.62	-0.15

Table 4: Annual northern hemisphere baseline mass mixing ratios for other gases measured at Mace Head and growth rates (ppt yr⁻¹ unless stated). AvGrow = Average growth since records began and AvGr12 = Average growth over most recent year.

4 Regional emission estimation

4.1 Introduction

This chapter presents the InTEM inversion results, showing the atmospheric trends and regional emissions of the gases that are measured in the UK DECC network and that are reported to the UNFCCC (United Nations Framework Convention on Climate Change). For each gas, the Northern Hemisphere baselines are presented, followed by the UK estimated emissions, where a comparison is made to the reported inventory values (2017 submission).

InTEM is briefly presented but for more information the reader is referred to the Methodology report. The uses, atmospheric lifetimes, and global warming potentials for the different gases reported under the UNFCCC are presented in Table 5.

4.2 Summary of InTEM inverse modelling

By removing the time-varying baseline concentrations from the raw measurement data, a time-series of excursions from the baseline, averaged over each 2-hour period, for each observed gas has been generated. The perturbations above baseline, observed across the UK DECC network, are driven by emissions on regional scales that have yet to be fully mixed on the hemisphere scale and are the principle tool used to estimate surface emissions across north-west Europe. A method for estimating emissions from observations, referred to as 'Inversion Technique for Emission Modelling' (InTEM), has been developed over many years and is used here to estimate UK emissions using the observations from the UK DECC network, and other networks where available.

InTEM links the observation time-series with the NAME air history estimates of how surface emissions dilute as they travel to the observation stations. An estimated emission distribution, when combined with the NAME output, can be transformed into a modelled time-series at each of the measurement stations. The modelled, and the observed time-series can be compared using a single or a range of statistics (referred to as cost functions) to produce a skill score for that particular emission distribution. InTEM uses a Bayesian statistical technique with a non-negative least squares solver to find the emission distributions that produces the modelled times-series at each observation station that has the best statistical match to the observations. The Bayesian method requires the use of a prior emission distribution with magnitudes as the starting point for the inversion. The prior information can influence and inform the inversion (posterior) solution. In these inversions the prior emission information has been obtained from the EDGAR v4.2 FT2010 database, using the 1990, 1995, 2000, 2005 and 2010 estimates, as appropriate. However, to preserve the independence of the inversion results presented here from the prior estimates, the priors chosen for the UK and Ireland were unconstrained by geographical distribution within each country (i.e. a uniform or flat prior over each country) and given very large uncertainties ($\pm 10,000\%$); this ensured the inversion was negligibly constrained by the prior over these regions, and thus dominated by the impact of the observations. For the rest of the domain, each defined geographical region (France, Spain/Portugal, Germany, Benelux, Denmark, Norway, SE Europe, NE Europe) also had no geographical distribution within each region but used a reduced uncertainty of $\pm 50\%$. The outer domain regions, as discussed in the May 2017 6-month report, were likewise specified with $\pm 50\%$ uncertainty.

In order for InTEM to provide robust solutions for every area within the modelled domain, each region needs to significantly contribute to the air concentrations at the UK DECC network sites on a reasonable number of time periods. If the signal from an area is only rarely or poorly seen by the network, then its impact on the cost function is minimal and the inversion method will have little skill at determining its true emission. The contributions that different grid boxes make to the observed air concentration varies from grid to grid. Grid boxes that are distant from the observation site contribute little to the observation, whereas those that are close have a large impact. In order to balance the contribution from different grid boxes, those that are more distant are grouped together into increasingly larger regions. The grouping cannot extend beyond country, region or Devolved Administration (DA) boundaries. The country boundaries extend into the surrounding seas to reflect both emissions from shipping, off-shore installations and river runoff but also because the inversion has geographical uncertainty.

For each greenhouse gas two types of inversion are performed. The first, using only Mace Head data, were performed with an inversion timeframe of 3 years. For CH₄ and N₂O the inversions were started in February 1989 to coincide with the availability of ECMWF ERA-Interim meteorology, the other gases, from when the observations were first available. So, for each gas a 3-year inversion was performed and then the 3-year timeframe was advanced by one month and another inversion performed, this was repeated up until the end of the available data with an associated baseline, April 2017 (e.g. inversion periods Feb 1989 – Jan 1992, Mar 1989 – Feb 1992, ..., May 2014 – Apr 2017). Annual (and monthly) emission estimates were made by averaging those inversion results where the entire time period of interest was covered by the inversion timeframe. The second type of inversion involved using the observations from the UK tall tower network combined with those from Mace Head, but were performed with smaller inversion timeframes. For CH₄, N₂O and SF₆, where observations are available from 5 or 6 sites, the inversion timeframe was set to 6-months, for the remaining compounds, where only TAC and MHD data are available, the inversion timeframe was 2-years.

There are significant uncertainties in the emissions that are estimated. Uncertainty arises from many factors: errors in the baseline estimate; emissions that vary over time-scales shorter than the inversion time-period e.g. diurnal, seasonal or intermittent; heterogeneous emissions i.e. emissions that vary within the regions solved for; errors in the transport model (NAME) or the underpinning 3-dimensional meteorology; errors in the observations themselves. The potential magnitudes of these uncertainties have been estimated and are incorporated within InTEM to inform the uncertainty of the modelled results.

4.3 Summary of the greenhouse gases reported to the UNFCCC

Table 5 describes the principle uses of each of the gases, their radiative efficiency, atmospheric lifetime and global warming potential in a 100-year framework (GWP₁₀₀).

Gas	Chemical Formula	Main Use	Radiative Efficiency (W m ⁻² ppb ⁻¹)	Atmos. lifetime (years)	GWP ₁₀₀
CH ₄	CH ₄	Landfill, farming, energy, wetlands	0.00036	12.4	28
N ₂ O	N ₂ O	Nylon manufacture, farming	0.003	121	265
CO ₂	CO ₂	Combustion	0.0000138	indefinite	1
HFC-125	CHF ₂ CF ₃	Refrigeration blend, fire suppression	0.23	28.2	3,170
HFC-134a	CH ₂ FCF ₃	Mobile air conditioner	0.16	13.4	1,300
HFC-143a	CH ₃ CF ₃	Refrigeration blend	0.16	47.1	4,800
HFC-152a	CH ₃ CHF ₂	Aerosol propellant, foam-blowing agent	0.10	1.5	138
HFC-23	CHF ₃	Bi-product of manufacture of HCFC-22	0.18	222	12,400
HFC-32	CH ₂ F ₂	Refrigeration blend	0.11	5.2	677
HFC-227ea	CF ₃ CHFCF ₃	Fire suppression, inhalers, foam blowing	0.26	38.9	3,350
HFC-245fa	C ₃ H ₃ F ₅	Blowing and insulation agent	0.28	7.6	1030
HFC-43-10mee	C ₅ H ₂ F ₁₀	Electronics industry	0.42	16.1	1,650
HFC-365mfc	C ₄ H ₅ F ₅	Foam blowing	0.22	8.7	804
PFC-14	CF ₄	Bi-product alum. production, electronics	0.09	50,000	6,630
PFC-116	C ₂ F ₆	Electronics, bi-product alum. production	0.25	>10,000	11,100
PFC-218	C ₃ F ₈	Electronics, bi-product alum. production	0.28	2,600	8,900
PFC-318	C ₄ F ₈	Semiconductor and electronics industries	0.32	3,200	9,540
SF ₆	SF ₆	Circuit breaker in high voltage switchgear	0.57	3,200	23,500
NF ₃	NF ₃	Electronics	0.2	500	16,100

Table 5: The principle use, radiative efficiency, atmospheric lifetime and 100-year global warming potential of the gases measured by the UK DECC network and that are reported to the UNFCCC. Data taken from the 5th IPCC Assessment Report Chapter 8 Appendix 8.A

4.4 Methane (CH₄)

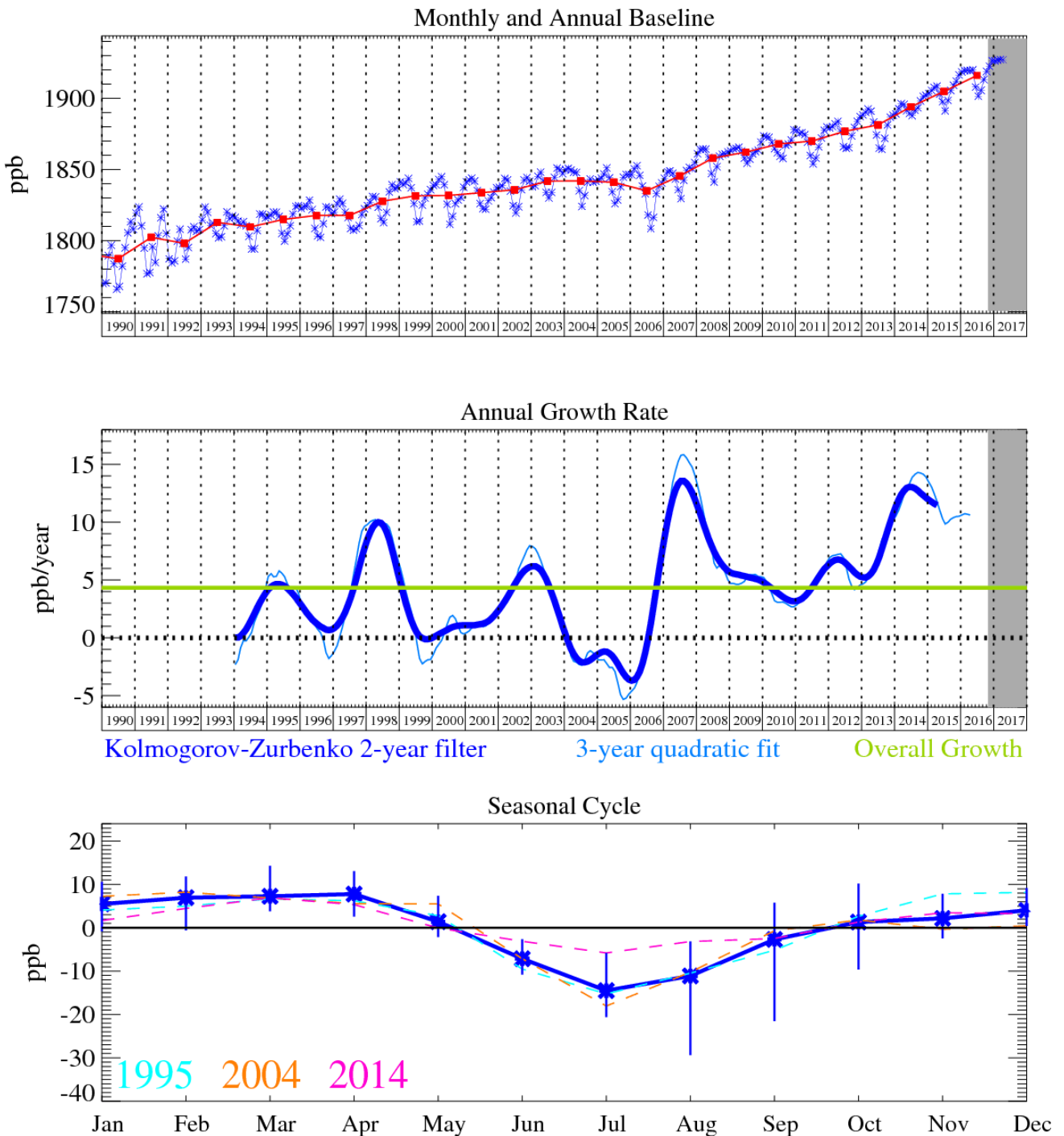


Figure 1: Methane (CH₄): Monthly (blue) and annual (red) Northern Hemisphere baseline mole fractions (top plot). Annual (blue) and overall average growth rate (green) (middle plot). Seasonal cycle (de-trended) with year-to-year variability (lower plot). Grey area covers un-ratified and therefore provisional data.

The amount of CH₄ in the atmosphere is continuing to grow at a strong rate, currently it is growing at more than 10 ppb yr⁻¹, a rate it has sustained for over two years. It has a strong seasonal cycle, with the dip in the summer caused by its chemical removal by the OH radical.

UK Methane

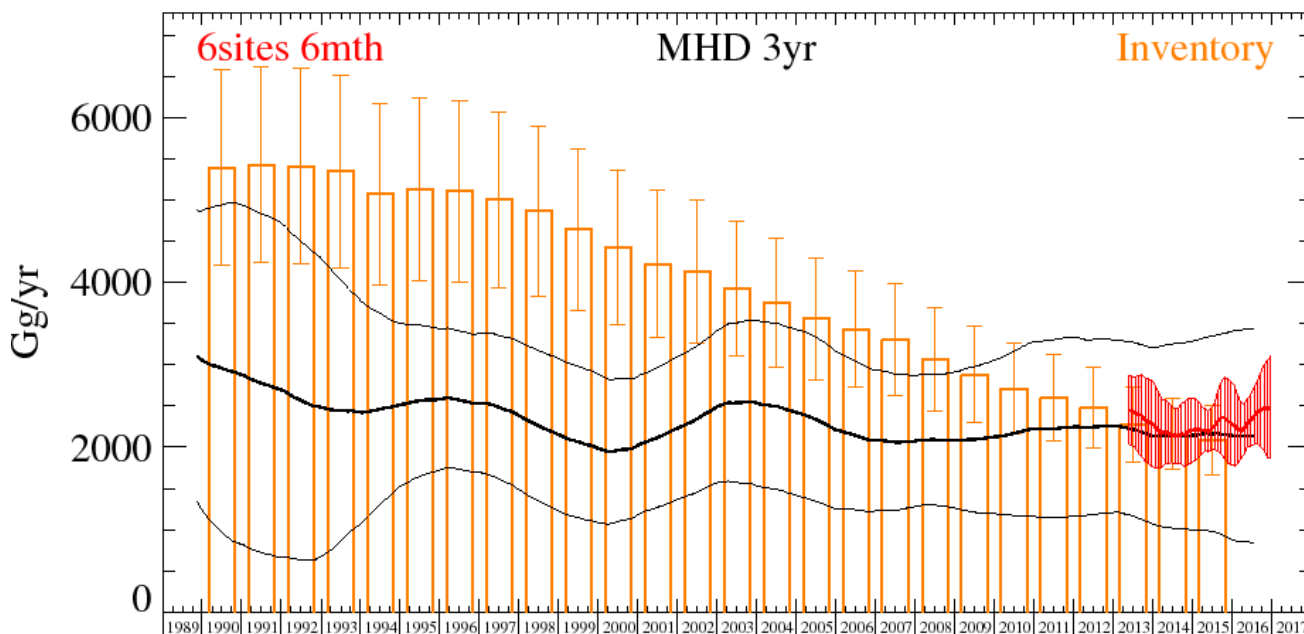


Figure 2: CH₄ UK Emission estimates (Gg yr⁻¹) from the UNFCCC Inventory (orange) and InTEM; 3-year MHD-only (black) and 6-month DECC + GAUGE network (red). The uncertainty bars represent the 5th and 95th percentiles.

UK Methane

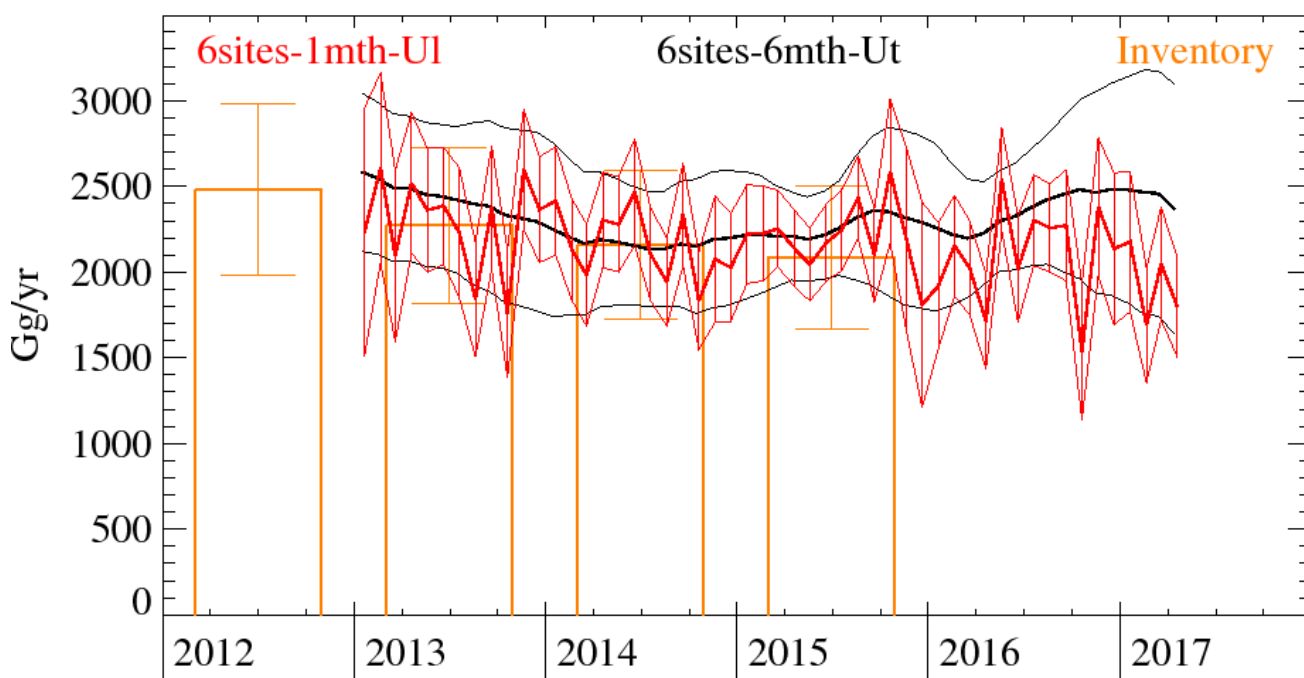


Figure 3: CH₄ emission estimates (Gg yr⁻¹) from the UNFCCC Inventory (orange) and InTEM using the DECC + GAUGE networks for the UK. 6-month, 5-site UK-prior (flat, very uncertain) InTEM inversions (black) and 1-month 80% uncertain NAEI 2015 UK-prior InTEM inversions (red) are shown. The non-UK prior information are the same, namely EDGAR FT2010 with each region having 50% uncertainty. The uncertainty bars represent the 5th and 95th percentiles.

The InTEM estimated emissions for the UK for CH₄ show only a very modest decline over the 27 years, from ~3000 Gg yr⁻¹ to ~2100 Gg yr⁻¹. The inventory has declined from 5400 Gg yr⁻¹ to 2100 Gg yr⁻¹ over the same period. Both methods have significant uncertainty, especially InTEM in the early 1990s when the observations were less precise. The uncertainties overlap from 2003 onwards. The use of the extended UK network from mid-2012, including the towers at Bilsdale (formerly GAUGE now in the UK DECC network) and Heathfield (formerly GAUGE now operated by NPL), has yielded results that are similar to the MHD-only inversions. The use of the extended network has allowed the inversions to be performed at the higher temporal resolution of 6-months with a very uncertain UK prior.

The UK inventory team has produced a high resolution (1 km) emission map for CH₄ covering the UK, the NAEI (National Atmospheric Emissions Inventory). The latest release is the 2015 map from the 2017 submission. A global inventory is produced by the EU Joint Research Centre (JRC) called the Emissions Database for Global Atmospheric Research (EDGAR) on a 0.5 degree resolution (~50 km), the latest release is for 2010. For each of the non-UK geographical regions the emissions have been uniformly distributed across the region (referred to as a flat prior) and each region is defined to have a combined uncertainty of 50%. These two maps have been combined to produce a prior emission map covering the same domain as solved for in the InTEM inversions, the higher resolution NAEI (with a combined UK uncertainty of 40%) is used wherever available in preference to EDGAR. This prior has been used as extra information to allow 1-month inversions 2013-2017. The results are compared to the inversions without the use of the UK NAEI prior information, Figure 3. The results are very comparable. All of the inversion solutions are very close to the inventory from 2013 onwards. The 1-month inversions do not reveal any strong seasonal cycle in UK CH₄ emissions.

Years	Inventory	MHD 3yr	6sites 6mth
1990	5390. (4210.-6580.)	3040. (1210.-4880.)	
1991	5420. (4240.-6610.)	2870. (810.-4930.)	
1992	5410. (4230.-6590.)	2520. (410.-4630.)	
1993	5340. (4180.-6500.)	2380. (810.-3940.)	
1994	5070. (3970.-6170.)	2460. (1410.-3520.)	
1995	5130. (4030.-6240.)	2570. (1670.-3460.)	
1996	5100. (4010.-6200.)	2600. (1780.-3430.)	
1997	5000. (3930.-6070.)	2500. (1660.-3340.)	
1998	4860. (3830.-5900.)	2270. (1320.-3210.)	
1999	4640. (3660.-5620.)	2040. (1100.-2980.)	
2000	4420. (3490.-5360.)	1900. (1060.-2740.)	
2001	4220. (3330.-5110.)	2080. (1250.-2910.)	
2002	4130. (3260.-4990.)	2390. (1500.-3270.)	
2003	3920. (3100.-4740.)	2610. (1640.-3580.)	
2004	3750. (2970.-4530.)	2520. (1490.-3550.)	
2005	3560. (2820.-4290.)	2300. (1280.-3310.)	
2006	3430. (2720.-4140.)	2120. (1230.-3010.)	
2007	3300. (2620.-3980.)	2030. (1220.-2830.)	
2008	3070. (2440.-3700.)	2100. (1320.-2880.)	
2009	2880. (2290.-3460.)	2130. (1280.-2980.)	
2010	2710. (2160.-3260.)	2100. (1100.-3110.)	
2011	2600. (2070.-3120.)	2290. (1160.-3410.)	
2012	2480. (1980.-2980.)	2310. (1220.-3390.)	
2013	2270. (1820.-2730.)	2160. (1170.-3140.)	2390. (1920.-2870.)
2014	2160. (1730.-2590.)	2130. (1020.-3240.)	2170. (1770.-2570.)
2015	2090. (1670.-2510.)	2140. (890.-3400.)	2280. (1900.-2660.)
2016		2200. (880.-3520.)	2340. (1920.-2770.)
2017			2460. (1740.-3170.)

Table 6: CH₄ emission (Gg yr⁻¹) estimates for the UK with uncertainty (5th - 95th percentile).

4.5 Nitrous oxide (N₂O)

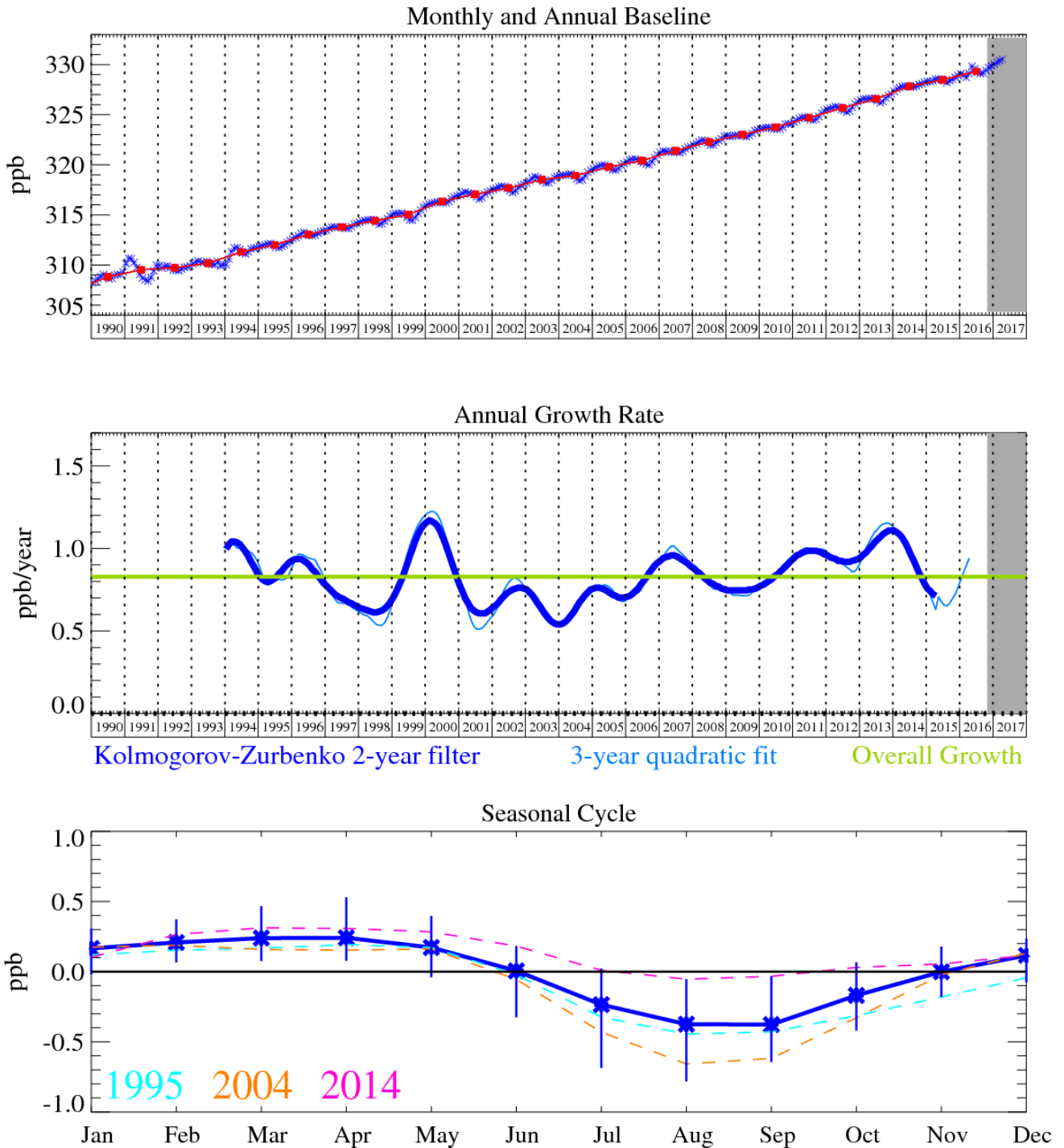


Figure 4: Nitrous oxide (N₂O): Monthly (blue) and annual (red) Northern Hemisphere baseline mole fractions (top). Annual (blue) and overall growth rate (green) (middle). Seasonal cycle (de-trended) with year-to-year variability (lower plot). Grey area covers un-ratified and therefore provisional data.

The atmospheric concentration of N₂O continues to grow strongly in the atmosphere. The seasonal cycle in the baseline is driven by the seasonal cycle in the interaction of the stratosphere (relatively low concentration) with the troposphere (relatively high concentration). The stratosphere is the main atmospheric sink of N₂O.

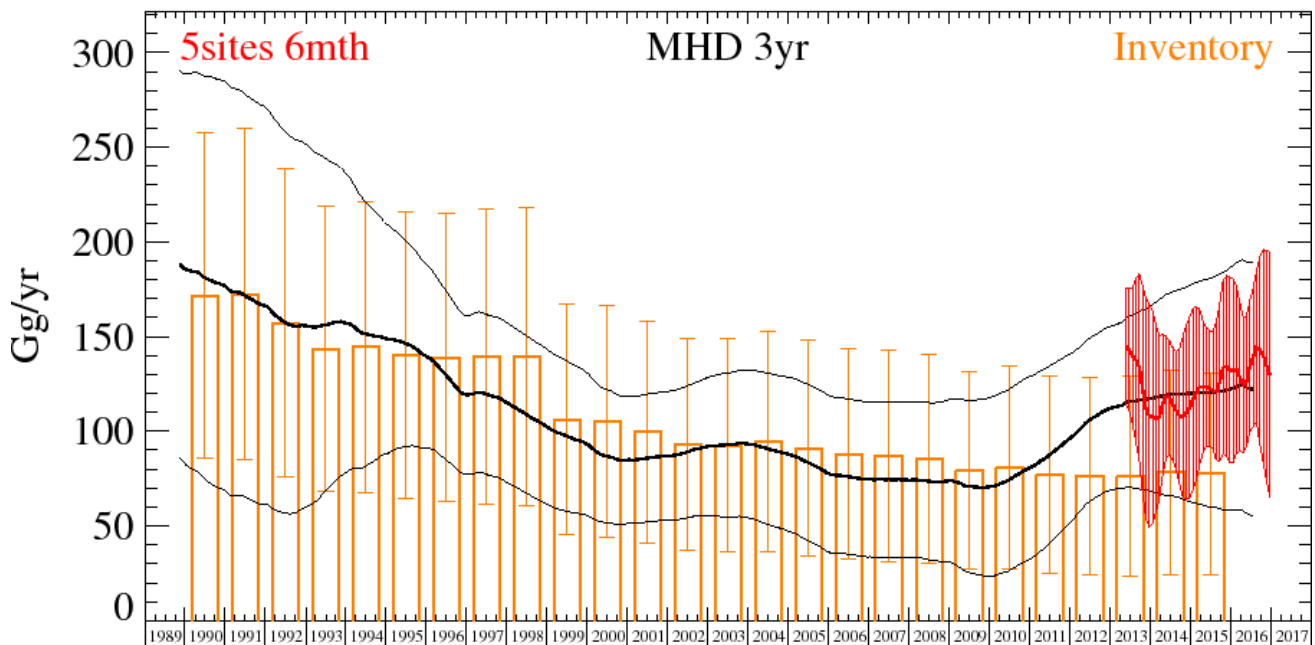


Figure 5: N₂O UK Emission estimates (Gg yr⁻¹) from the UNFCCC Inventory (orange) and InTEM; 3-year MHD-only (black) and 6-month DECC + GAUGE network (red). The uncertainty bars represent the 5th and 95th percentiles.

The UK inventory and InTEM estimates are in good agreement until 2010. By 2013 there is a significant difference although the uncertainties do overlap. This is quite different from the results presented in the 2016 annual report where the agreement between the 5-site inversion was close to the inventory estimates, although it is important to note that the uncertainties then and now do overlap significantly. There are several improvements that have been made over the last year, namely:

- The N₂O calibration scale has been significantly revised. This has enhanced the modelled pollution events in the later years as a previous non-linearity has been corrected.
- The baseline algorithm has been improved. This has had the effect of lowering the baseline by a small degree, again this would enhance the magnitude of the modelled pollution events.
- The outer regions (South Atlantic, America, W. and E. Arctic, East Europe, Africa) have been included, giving the inversion more flexibility in discerning the mole fraction of the air entering the inversion domain.
- The model uncertainty algorithm has been improved by incorporating the boundary layer height to complement the previous 'localness' criteria.
- The prior emissions used in these inversions have prevented the regions distant from the UK and Ireland having unrealistic emissions. It is important to note that UK and Ireland emissions are not restricted by the prior.
- The inventory estimates have been changed significantly over different UNFCCC submissions, for example UK 2011 estimates were 110 in the 2013 submission, 117 in 2014, 93 in 2015, 72 in 2016 and 77 in the 2017 submission.

These improvements will be re-investigated to determine the impact of each in turn.

The uncertainties in the modelling when only MHD data are used with a 3-year inversion timeframe are comparable to those in the inventory. When 5 sites are used with a 6-month inversion timeframe the model uncertainties are smaller than the inventory uncertainties.

The use of high-resolution emission priors are investigated in Figure 6. The 6-month 5-site InTEM inversions with unrestrained UK-prior emissions (black) are compared to those performed with the 1-month 5-site inversions with a more detailed NAEI 2015 (2017 submission) UK-prior (red). In both cases the non-UK prior estimates are identical. The strong seasonal cycle in the emissions are very clearly seen with peaks in spring. In 2015 and 2016 the peak in spring is smaller than in 2013 and 2014 but is sustained throughout the summer. It is also interesting to note that the 1-month inversions are lower than the 6-month inversions; this is not surprising because of the impact of the UK prior – which is lower than most of the estimated UK emissions.

Years	Inventory	MHD 3yr	5sites 6mth
1990	172. (86.-258.)	185. (82.-289.)	
1991	172. (85.-260.)	176. (68.-284.)	
1992	157. (76.-239.)	157. (52.-263.)	
1993	144. (68.-219.)	150. (63.-238.)	
1994	144. (67.-222.)	162. (93.-231.)	
1995	140. (64.-216.)	147. (93.-200.)	
1996	139. (63.-215.)	124. (82.-166.)	
1997	139. (62.-217.)	118. (77.-159.)	
1998	139. (61.-218.)	110. (67.-153.)	
1999	106. (45.-167.)	98. (58.-139.)	
2000	105. (44.-166.)	85. (51.-119.)	
2001	100. (41.-158.)	84. (51.-117.)	
2002	93. (37.-149.)	89. (54.-124.)	
2003	92. (36.-149.)	96. (58.-134.)	
2004	95. (36.-153.)	93. (53.-133.)	
2005	91. (34.-148.)	83. (41.-124.)	
2006	88. (32.-144.)	72. (31.-114.)	
2007	87. (31.-143.)	73. (33.-114.)	
2008	85. (30.-140.)	77. (36.-118.)	
2009	79. (27.-132.)	72. (27.-116.)	
2010	81. (27.-134.)	68. (19.-118.)	
2011	77. (25.-129.)	88. (39.-137.)	
2012	77. (24.-129.)	109. (68.-151.)	
2013	76. (24.-129.)	114. (72.-156.)	131. (86.-175.)
2014	78. (24.-132.)	120. (64.-175.)	108. (67.-150.)
2015	77. (24.-131.)	122. (58.-186.)	128. (85.-170.)
2016		122. (54.-189.)	134. (88.-181.)
2017			114. (47.-180.)

Table 7: N₂O emission (Gg yr⁻¹) estimates for the UK with uncertainty (5th - 95th percentile).

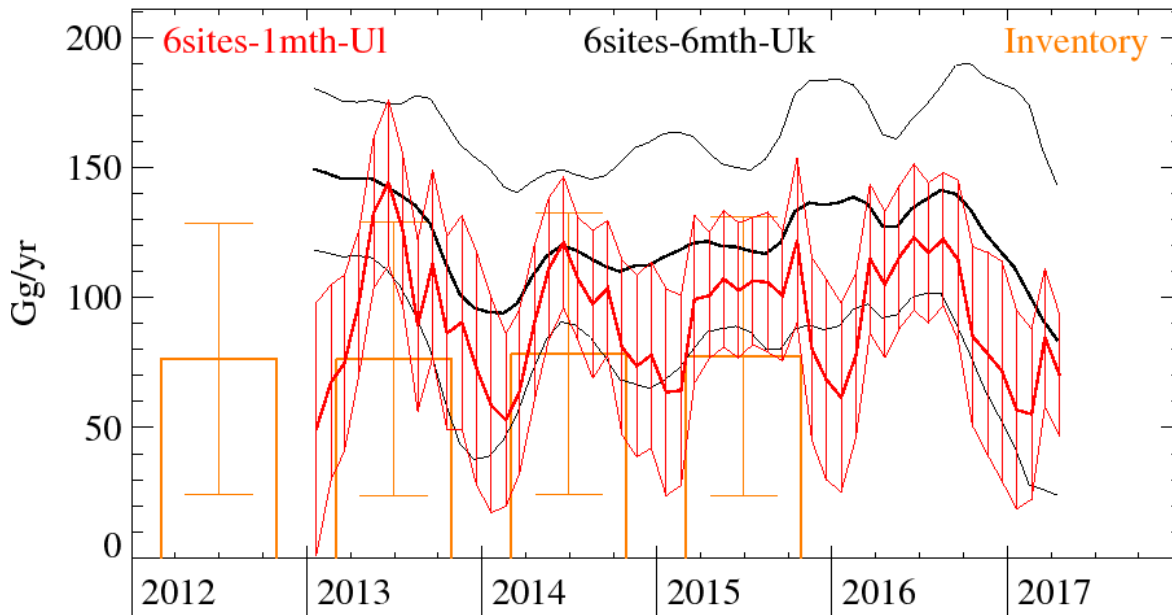


Figure 6: N₂O emission estimates (Gg yr⁻¹) from the UNFCCC Inventory and InTEM using the DECC + GAUGE network for the UK. 6-month 5-site UK-prior (flat, very uncertain) InTEM inversions (black) and 1-month 80% uncertain NAEI 2015 UK-prior InTEM inversions (red). The non-UK prior information are the same, namely EDGAR FT2010 with each region having 50% uncertainty. The uncertainty bars represent the 5th and 95th percentiles.

4.6 Carbon dioxide (CO₂)

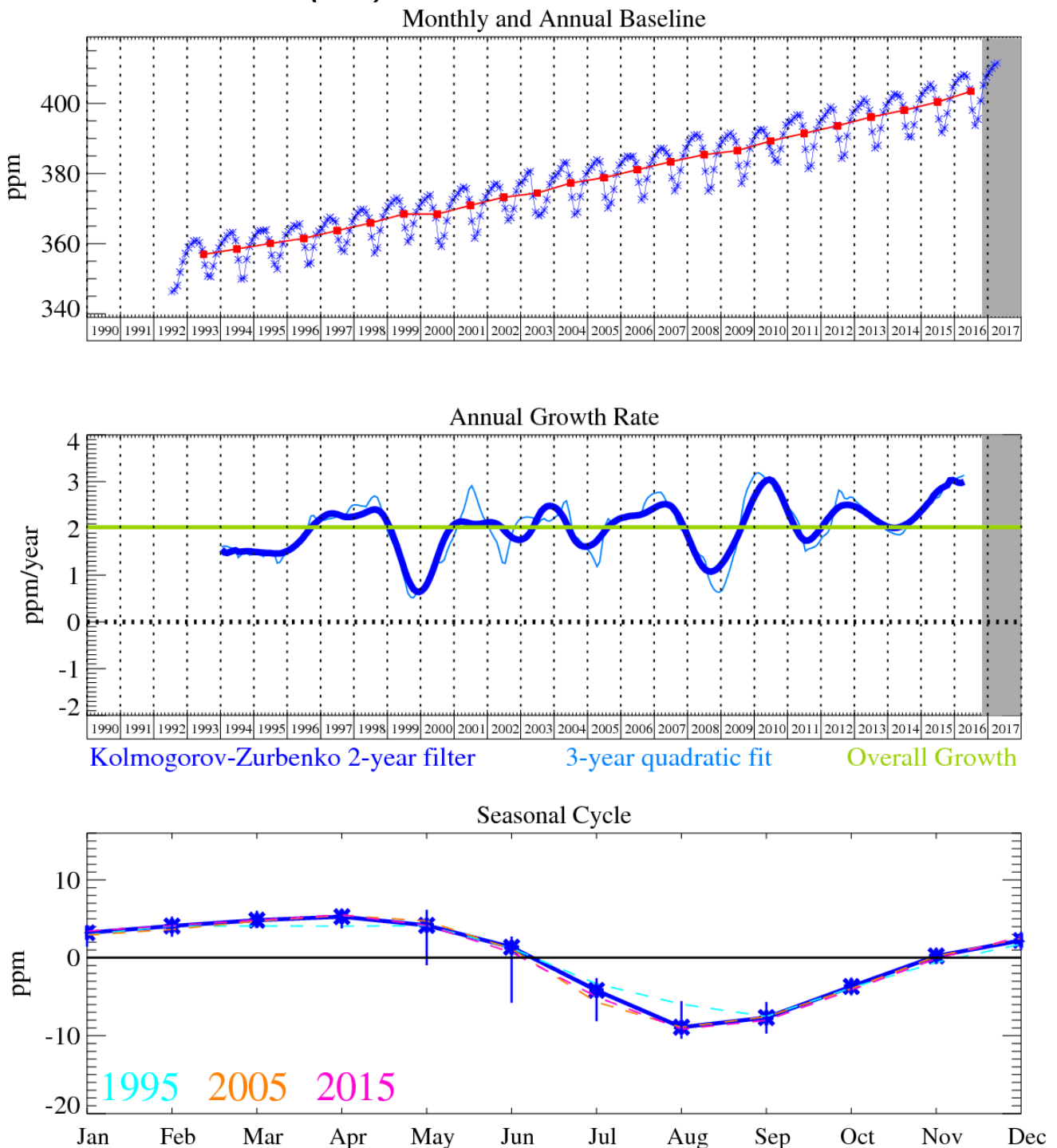


Figure 7: Carbon dioxide (CO₂): Monthly (blue) and annual (red) Northern Hemisphere baseline mole fractions (top plot). Annual (blue) and overall average growth rate (green) (middle plot). Seasonal cycle (de-trended) with year-to-year variability (lower plot). Grey area covers un-ratified and therefore provisional data.

CO₂ is the most important greenhouse gas, and has steadily grown at an annual average rate of 2 ppm yr⁻¹, calculated from the baseline-selected monthly means. Since 2010 the growth rate has averaged more than 2 ppm yr⁻¹. It has now reached a monthly mole fraction of 411.5 ppm (Apr 2017), the highest yet recorded at Mace Head, Ireland, and has shown significant growth rate anomalies in 1998/99 and 2002/03, which we suggest are a result of the global biomass burning events in those years. The average annual baseline mole fraction in the mid-latitude northern hemisphere surpassed 400 ppm in 2015.

4.7 HFC-125

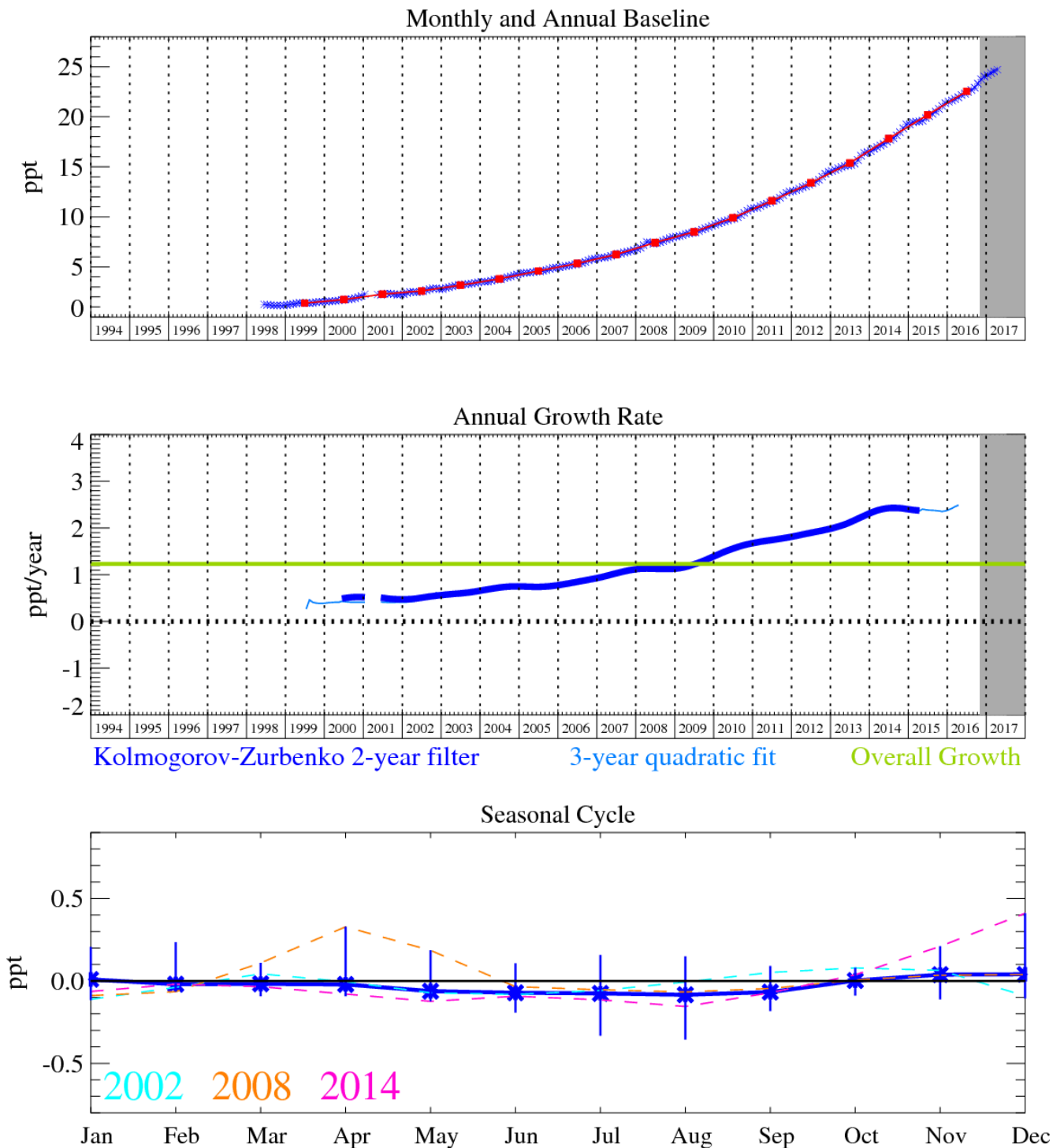


Figure 8: HFC-125 (CHF_2CF_3): Monthly (blue) and annual (red) Northern Hemisphere baseline mole fractions (top plot). Annual (blue) and overall average growth rate (green) (middle plot). Seasonal cycle (de-trended) with year-to-year variability (lower plot). Grey area covers un-ratified provisional data.

Unfortunately, the observations of HFC-125 (and HFC-32) at Mace Head were compromised by contamination from the air conditioning system (May 2014 – June 2015) and these data had to be removed. The current solution is to flush the air sample module with clean ambient air to minimise contamination from laboratory air. A long-term solution will require modification of the air conditioner to use a chilled water heat exchanger with the refrigerant gases contained in a unit external to the laboratory. The northern hemisphere baseline during this period has been estimated using another AGAGE northern hemisphere station, Zeppelin (Ny-Ålesund).

Relative to the magnitude of the baseline the pollution events are very significant. Therefore, InTEM has plenty of clear information on which to base the emission estimates. The agreement in trend between the inventory and InTEM for the UK is good. It is interesting to note that with InTEM the UK

MHD+TAC estimates in the recent years have started to fall in contrast to the inventory that continues to grow strongly.

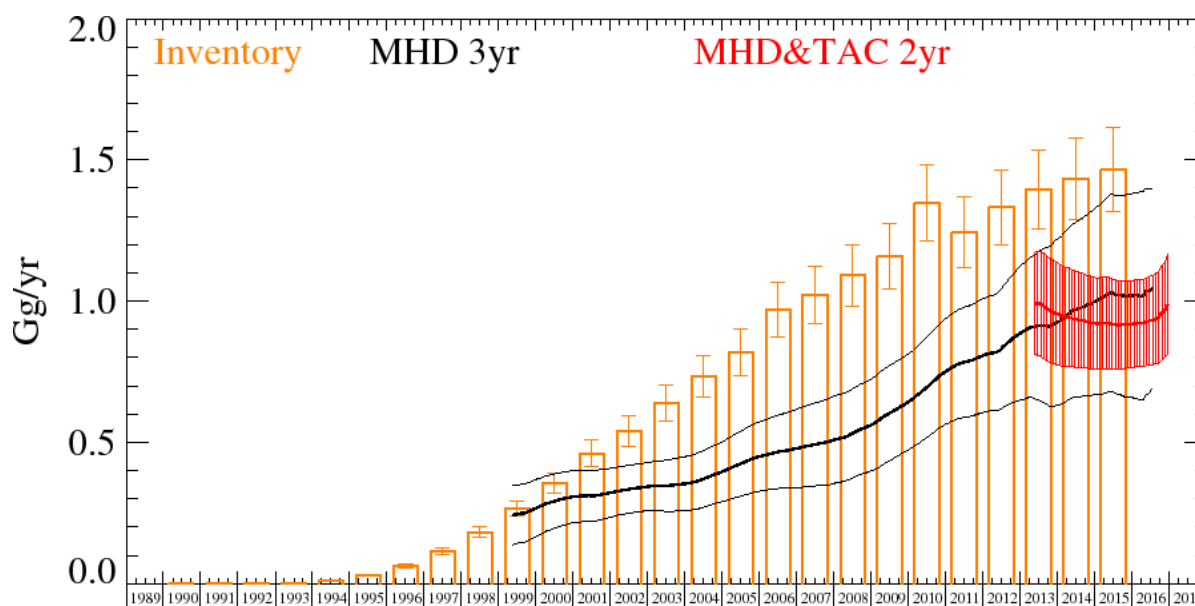


Figure 9: HFC-125 UK emission estimates (Gg yr⁻¹) from the UNFCCC Inventory (orange) and InTEM; MHD-only (black) and DECC network (red). The uncertainty bars represent the 5th and 95th percentiles.

Years	Inventory	MHD 3yr	MHD&TAC 2yr
1990	0.000 (0.000-0.000)		
1991	0.000 (0.000-0.001)		
1992	0.001 (0.001-0.002)		
1993	0.003 (0.003-0.004)		
1994	0.012 (0.011-0.013)		
1995	0.030 (0.027-0.033)		
1996	0.063 (0.057-0.070)		
1997	0.114 (0.103-0.126)		
1998	0.183 (0.165-0.201)		
1999	0.265 (0.239-0.292)	0.235 (0.127-0.343)	
2000	0.356 (0.321-0.392)	0.270 (0.169-0.370)	
2001	0.462 (0.416-0.508)	0.324 (0.235-0.413)	
2002	0.541 (0.487-0.595)	0.341 (0.261-0.422)	
2003	0.638 (0.574-0.702)	0.334 (0.246-0.422)	
2004	0.735 (0.661-0.808)	0.372 (0.270-0.475)	
2005	0.819 (0.737-0.901)	0.421 (0.310-0.533)	
2006	0.968 (0.871-1.065)	0.475 (0.347-0.604)	
2007	1.023 (0.921-1.126)	0.496 (0.344-0.649)	
2008	1.091 (0.982-1.200)	0.511 (0.353-0.669)	
2009	1.158 (1.042-1.274)	0.599 (0.434-0.764)	
2010	1.349 (1.214-1.484)	0.698 (0.523-0.873)	
2011	1.243 (1.118-1.367)	0.792 (0.598-0.987)	
2012	1.332 (1.199-1.465)	0.84 (0.63-1.06)	
2013	1.397 (1.257-1.536)	0.90 (0.65-1.15)	0.954 (0.780-1.128)
2014	1.435 (1.291-1.578)	0.97 (0.64-1.30)	0.952 (0.773-1.131)
2015	1.466 (1.320-1.613)	1.02 (0.66-1.38)	0.889 (0.746-1.031)
2016		1.13 (0.83-1.43)	0.988 (0.811-1.165)

Table 8: HFC-125 emission (Gg yr⁻¹) estimates for the UK with uncertainty (5th – 95th percentile).

4.8 HFC-134a

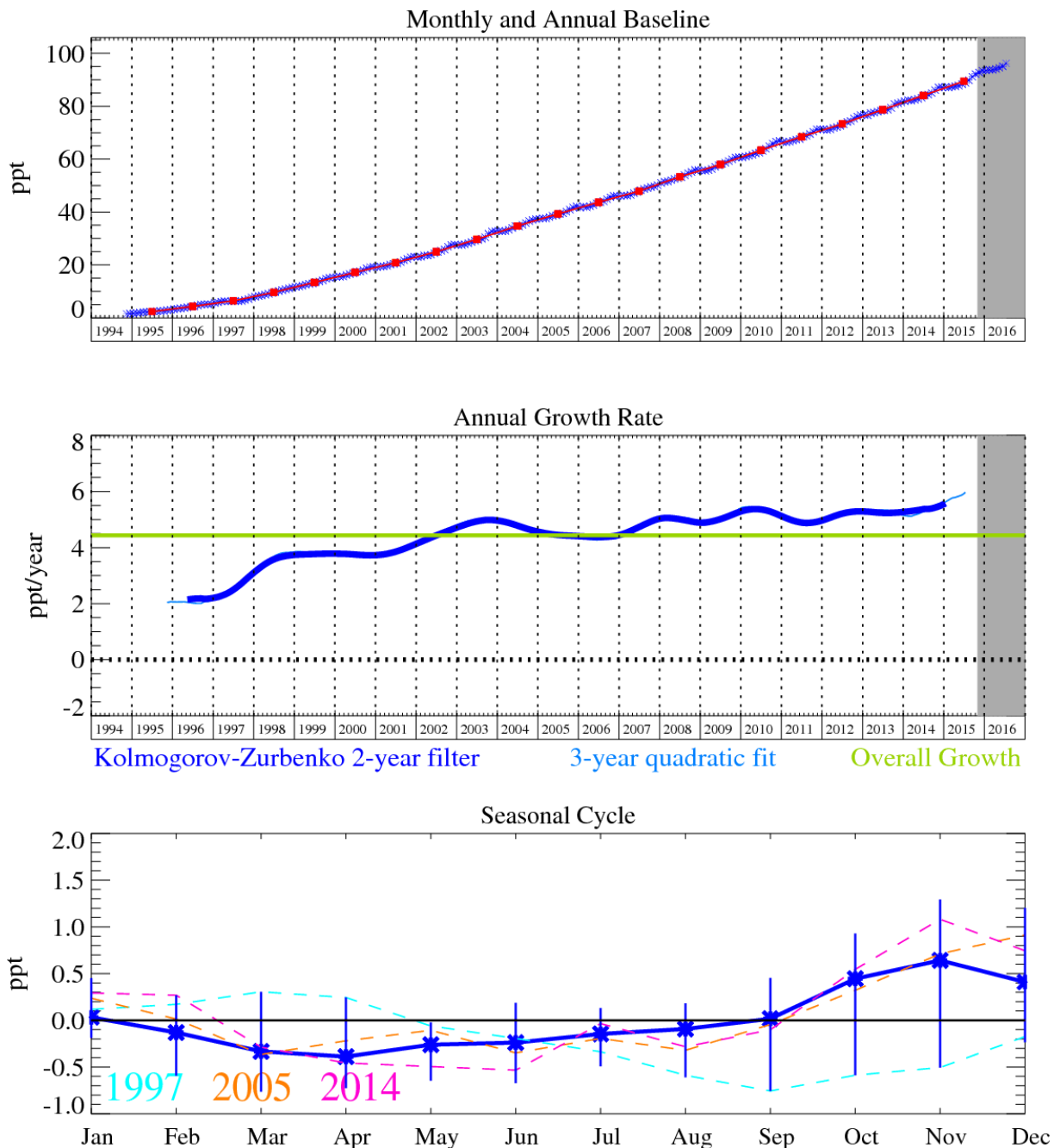


Figure 10: HFC-134a (CH_2FCF_3): Monthly (blue) and annual (red) Northern Hemisphere baseline mole fractions (top plot). Annual (blue) and overall average growth rate (green) (middle plot). Seasonal cycle (de-trended) with year-to-year variability (lower plot). Grey area covers un-ratified and therefore provisional data.

Globally HFC-134a (CH_2FCF_3) is the most abundant HFC present in the atmosphere and is used predominantly in refrigeration and mobile air conditioning (MAC). Due to its long lifetime, 13.5 years, and relatively high GWP_{100} of 1370 (Forster *et al.*, 2007), the use of HFC-134a (and any other HFCs with a $\text{GWP}_{100} > 150$) is being phased out in Europe between 2011 and 2017. It is proposed that a very gradual phase-out of the use of HFC-134a in cars will also take place outside Europe because of the global nature of the car industry. However, in developing countries the potential for growth of HFC-134a is still large (Velders *et al.*, 2009).

The UK inventory and InTEM estimates increased from the mid-1990s until 2009. Since then the InTEM estimates have continued to increase unlike the inventory which has remained largely constant. The InTEM estimates for the UK are consistently around two thirds of the inventory estimates. A significant proportion of the HFC-134a emitted is estimated to come from in-use vehicles (it is used in mobile air conditioning units). Inspection of the inventory shows that different EU countries use surprisingly different values for the leakage rates from in-use vehicles. The UK inventory was modified downwards (5%) for the 2017 submission for data from 2009 onwards after

further work on the activity data and emission factors used was undertaken. However, a key factor, the annual re-fill frequency, was kept at the conservative, albeit unrealistic, rate of 100% because of a limitation present in the inventory model.

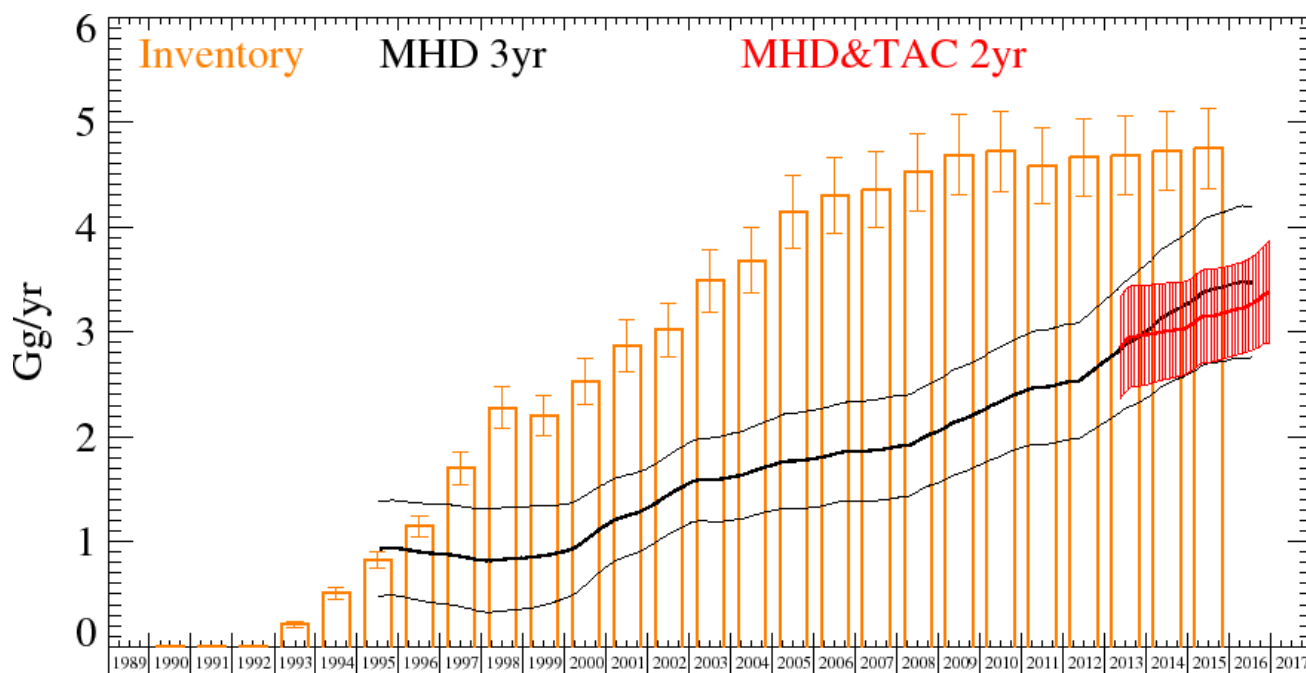


Figure 11: HFC-134a UK emission estimates (Gg yr⁻¹) from the UNFCCC Inventory (orange) and InTEM; MHD-only (black) and DECC network (red). The uncertainty bars represent the 5th and 95th percentiles.

Years	Inventory	MHD 3yr	MHD&TAC 2yr
1990	0.001 (0.000-0.001)		
1991	0.003 (0.003-0.003)		
1992	0.007 (0.006-0.008)		
1993	0.214 (0.188-0.240)		
1994	0.508 (0.454-0.562)		
1995	0.828 (0.753-0.902)	0.92 (0.47-1.37)	
1996	1.146 (1.043-1.248)	0.93 (0.48-1.39)	
1997	1.700 (1.549-1.851)	0.88 (0.40-1.35)	
1998	2.27 (2.07-2.48)	0.77 (0.26-1.28)	
1999	2.202 (2.010-2.395)	0.86 (0.38-1.35)	
2000	2.53 (2.31-2.75)	1.00 (0.59-1.41)	
2001	2.87 (2.62-3.12)	1.24 (0.86-1.61)	
2002	3.02 (2.76-3.28)	1.48 (1.11-1.86)	
2003	3.49 (3.19-3.78)	1.60 (1.21-2.00)	
2004	3.68 (3.37-3.99)	1.67 (1.25-2.10)	
2005	4.15 (3.80-4.49)	1.75 (1.30-2.20)	
2006	4.30 (3.94-4.66)	1.86 (1.39-2.33)	
2007	4.36 (4.00-4.72)	1.87 (1.38-2.35)	
2008	4.52 (4.15-4.89)	1.92 (1.44-2.40)	
2009	4.69 (4.31-5.07)	2.15 (1.66-2.65)	
2010	4.72 (4.34-5.10)	2.36 (1.85-2.88)	
2011	4.58 (4.22-4.95)	2.48 (1.93-3.02)	
2012	4.66 (4.29-5.04)	2.56 (2.00-3.12)	
2013	4.68 (4.31-5.06)	2.81 (2.21-3.41)	2.79 (2.30-3.28)
2014	4.72 (4.34-5.10)	3.21 (2.54-3.88)	2.97 (2.50-3.45)
2015	4.75 (4.37-5.13)	3.44 (2.73-4.15)	3.12 (2.71-3.53)
2016		3.54 (2.85-4.24)	3.38 (2.90-3.87)

Table 9: HFC-134a emission (Gg yr⁻¹) estimates for the UK with uncertainty (5th - 95th percentile).

4.9 HFC-143a

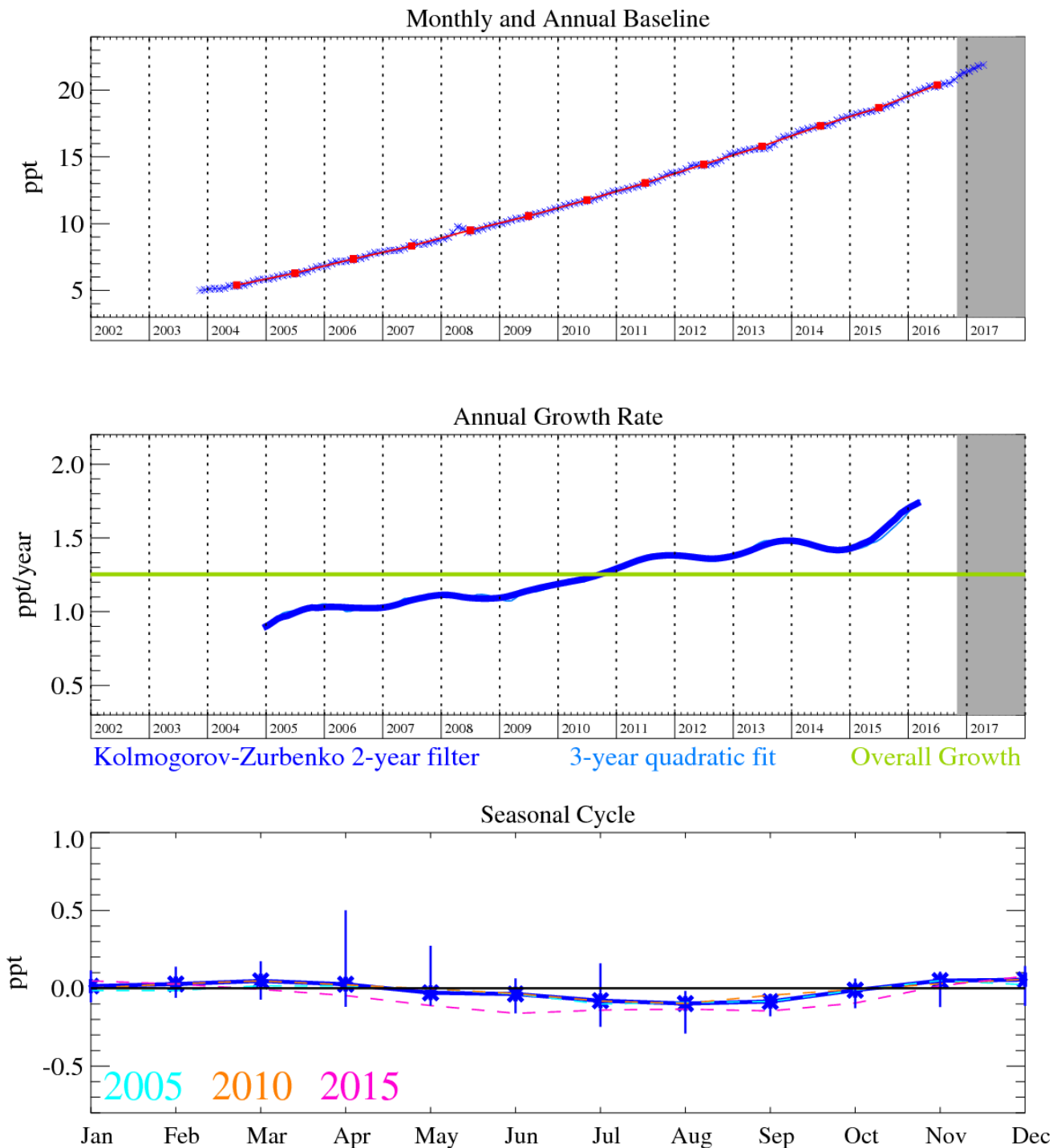


Figure 12: HFC-143a (CH₃CF₃): Monthly (blue) and annual (red) Northern Hemisphere baseline mole fractions (top plot). Annual (blue) and overall average growth rate (green) (middle plot). Seasonal cycle (de-trended) with year-to-year variability (lower plot). Grey area covers un-ratified and therefore provisional data.

HFC-143a (CH₃CF₃) is used mainly as a working fluid in refrigerant blends (R-404A and R-507A) for low and medium temperature commercial refrigeration systems. In 2016 the NH baseline mole exceeded 20 ppt for the first time. These levels have increased dramatically from the low levels observed in 2003 with an increasing growth rate. It has a relatively long atmospheric lifetime of 51.4 years and a significant radiative forcing value (third largest of all the HFCs) with a GWP₁₀₀ of 4400.

The indications are that the InTEM emission estimates for the UK have started to decline. The higher frequency (2-year) DECC network InTEM estimates show a declining UK total throughout from 2013, the (3-year) MHD-only InTEM estimates for the UK may have peaked in 2015. The inventory estimates an increase across the years until 2011 when there is dramatic step down in emissions.

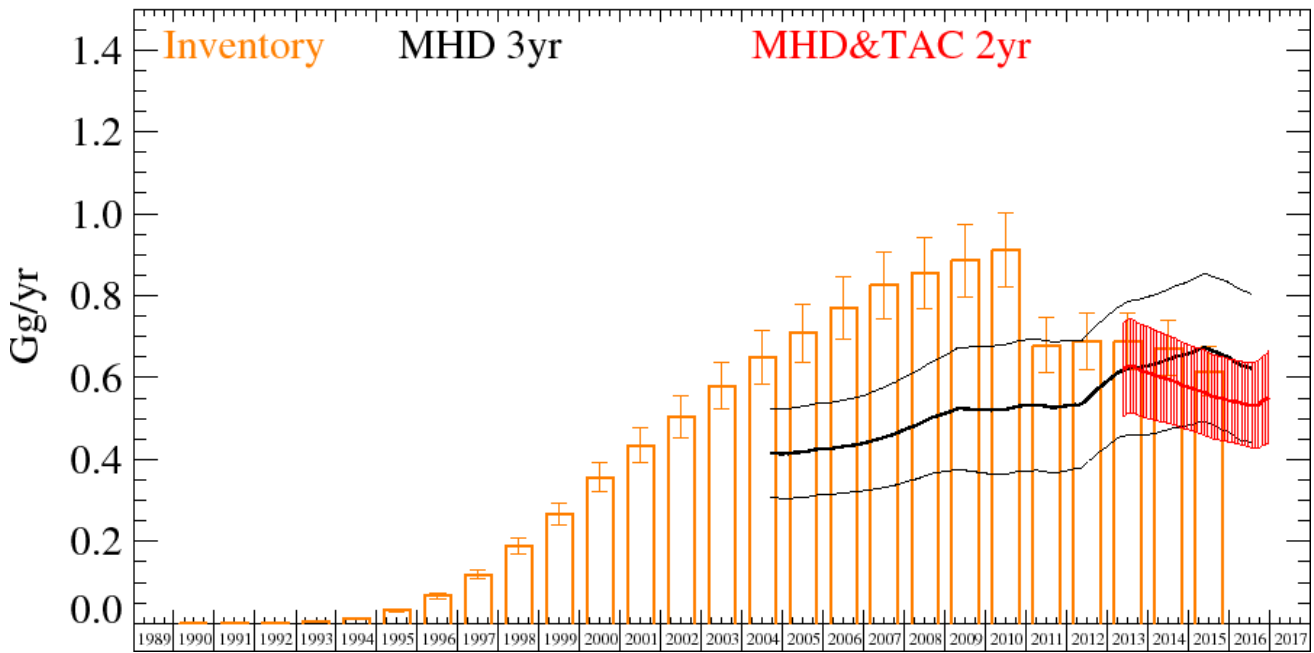


Figure 13: HFC-143a UK emission estimates (Gg yr^{-1}) from the UNFCCC Inventory (orange) and InTEM; MHD-only (black) and DECC network (red). The uncertainty bars represent the 5th and 95th percentiles.

Years	Inventory	MHD 3yr	MHD&TAC 2yr
1990	0.000 (0.000-0.000)		
1991	0.001 (0.001-0.001)		
1992	0.002 (0.001-0.002)		
1993	0.004 (0.003-0.004)		
1994	0.013 (0.012-0.014)		
1995	0.032 (0.029-0.035)		
1996	0.067 (0.060-0.074)		
1997	0.119 (0.108-0.131)		
1998	0.190 (0.171-0.209)		
1999	0.268 (0.241-0.295)		
2000	0.356 (0.320-0.391)		
2001	0.435 (0.391-0.478)		
2002	0.505 (0.454-0.555)		
2003	0.580 (0.522-0.638)		
2004	0.651 (0.586-0.716)	0.418 (0.315-0.521)	
2005	0.709 (0.638-0.780)	0.414 (0.305-0.524)	
2006	0.769 (0.692-0.846)	0.427 (0.315-0.539)	
2007	0.825 (0.743-0.908)	0.453 (0.334-0.572)	
2008	0.855 (0.769-0.940)	0.490 (0.355-0.624)	
2009	0.886 (0.797-0.974)	0.535 (0.385-0.685)	
2010	0.911 (0.820-1.002)	0.526 (0.366-0.685)	
2011	0.679 (0.611-0.746)	0.520 (0.358-0.682)	
2012	0.688 (0.619-0.757)	0.549 (0.394-0.705)	
2013	0.689 (0.620-0.758)	0.616 (0.457-0.775)	0.603 (0.486-0.720)
2014	0.671 (0.604-0.738)	0.663 (0.487-0.839)	0.609 (0.498-0.720)
2015	0.615 (0.554-0.677)	0.651 (0.468-0.834)	0.540 (0.444-0.636)
2016		0.626 (0.457-0.794)	0.551 (0.438-0.664)

Table 10: HFC-143a emission (Gg yr^{-1}) estimates for the UK with uncertainty (5th - 95th percentile).

4.10 HFC-152a

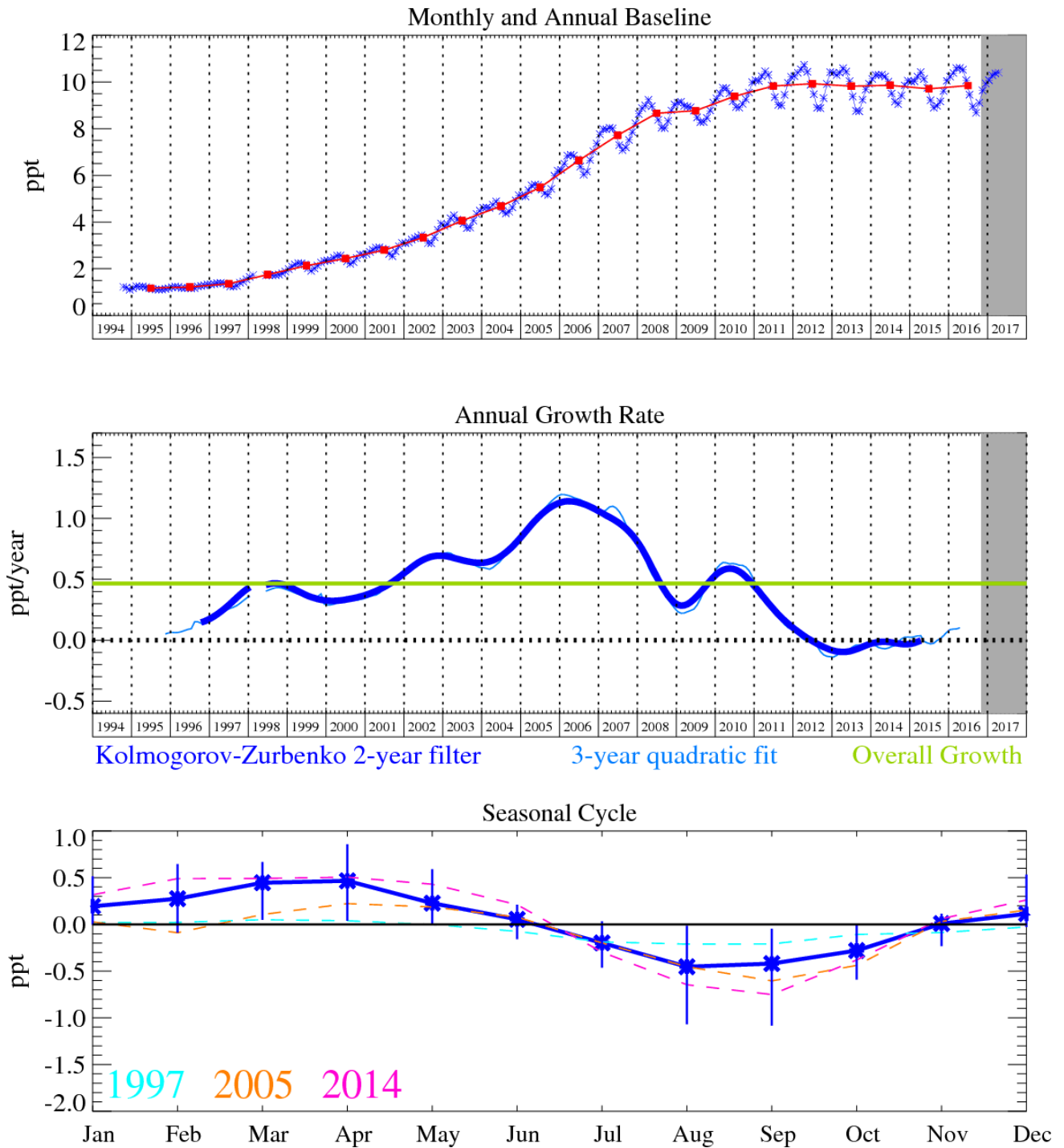


Figure 14: HFC-152a (CH₃CHF₂): Monthly (blue) and annual (red) Northern Hemisphere baseline mole fractions (top plot). Annual (blue) and overall average growth rate (green) (middle plot). Seasonal cycle (de-trended) with year-to-year variability (lower plot). Grey area covers un-ratified and therefore provisional data.

HFC-152a (CH₃CHF₂) has a relatively short lifetime of 1.6 years due to its efficient removal by OH oxidation in the troposphere, consequently it has the smallest GWP₁₀₀ at 133 of all of the major HFCs. It is used as a foam-blowing agent and aerosol propellant, and given its short lifetime has exhibited substantial growth in the atmosphere since measurements began in 1994, implying a substantial increase in emissions in these years. However, in the last few years the rate of growth slowed considerably and is now zero to negative. The maximum NH monthly mole fraction reached was 10.7 ppt (Apr 2012).

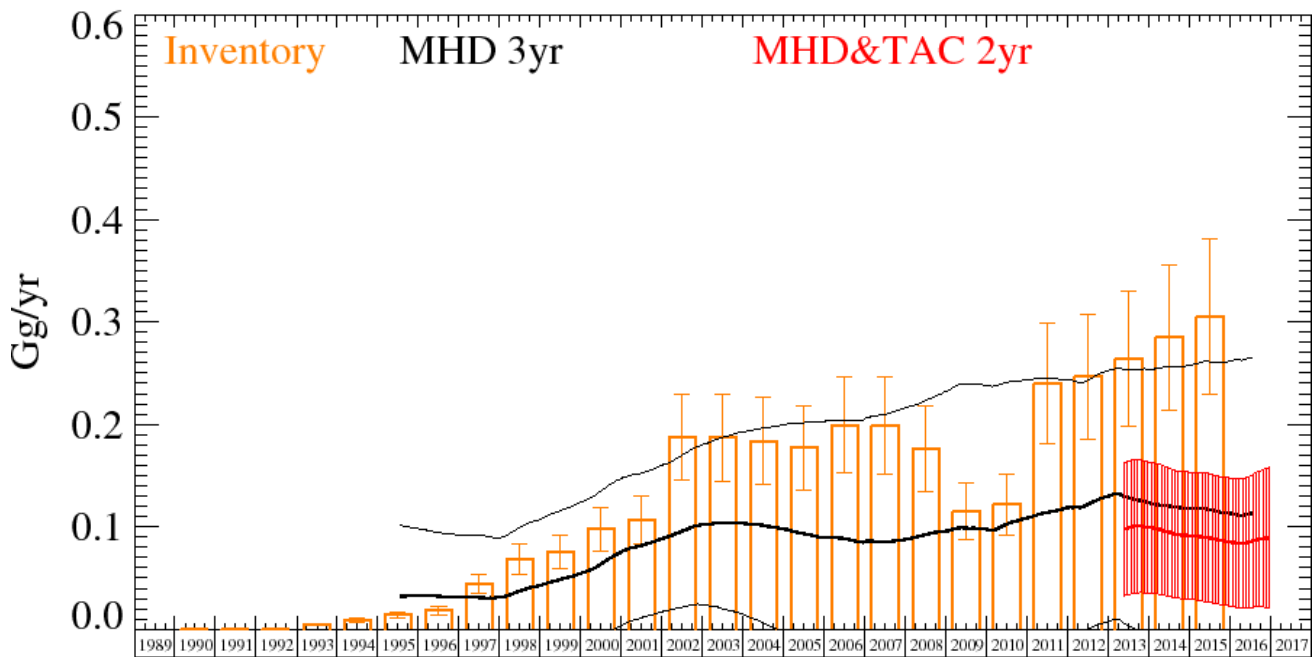


Figure 15: HFC-152a UK emission estimates (Gg yr^{-1}) from the UNFCCC Inventory (orange) and InTEM; MHD-only (black) and DECC network (red). The uncertainty bars represent the 5th and 95th percentiles.

The comparison for the UK shows that the InTEM estimates are substantially lower than the inventory although the uncertainties do overlap in the early and later years.

Years	Inventory	MHD 3yr	MHD&TAC 2yr
1990	0.000 (0.000-0.000)		
1991	0.000 (0.000-0.000)		
1992	0.000 (0.000-0.000)		
1993	0.005 (0.004-0.006)		
1994	0.009 (0.007-0.011)		
1995	0.014 (0.011-0.017)	0.028 (0.000-0.120)	
1996	0.018 (0.014-0.022)	0.033 (0.000-0.098)	
1997	0.044 (0.035-0.054)	0.032 (0.000-0.088)	
1998	0.068 (0.053-0.083)	0.030 (0.000-0.089)	
1999	0.076 (0.059-0.092)	0.050 (0.000-0.119)	
2000	0.098 (0.076-0.119)	0.067 (0.000-0.139)	
2001	0.107 (0.083-0.131)	0.079 (0.010-0.149)	
2002	0.187 (0.145-0.230)	0.100 (0.027-0.173)	
2003	0.187 (0.145-0.230)	0.106 (0.024-0.188)	
2004	0.184 (0.141-0.226)	0.101 (0.005-0.197)	
2005	0.177 (0.136-0.218)	0.094 (0.000-0.202)	
2006	0.199 (0.152-0.246)	0.085 (0.000-0.203)	
2007	0.199 (0.152-0.246)	0.084 (0.000-0.207)	
2008	0.176 (0.134-0.218)	0.092 (0.000-0.222)	
2009	0.115 (0.088-0.143)	0.101 (0.000-0.244)	
2010	0.122 (0.092-0.151)	0.098 (0.000-0.238)	
2011	0.240 (0.181-0.299)	0.111 (0.000-0.240)	
2012	0.246 (0.185-0.308)	0.132 (0.011-0.252)	
2013	0.264 (0.198-0.330)	0.130 (0.007-0.252)	0.094 (0.028-0.160)
2014	0.285 (0.214-0.356)	0.117 (0.000-0.254)	0.099 (0.035-0.163)
2015	0.305 (0.229-0.382)	0.113 (0.000-0.262)	0.084 (0.024-0.144)
2016		0.118 (0.000-0.273)	0.090 (0.021-0.158)

Table 11: HFC-152a emission (Gg yr^{-1}) estimates for the UK with uncertainty (5th - 95th percentile).

4.11 HFC-23

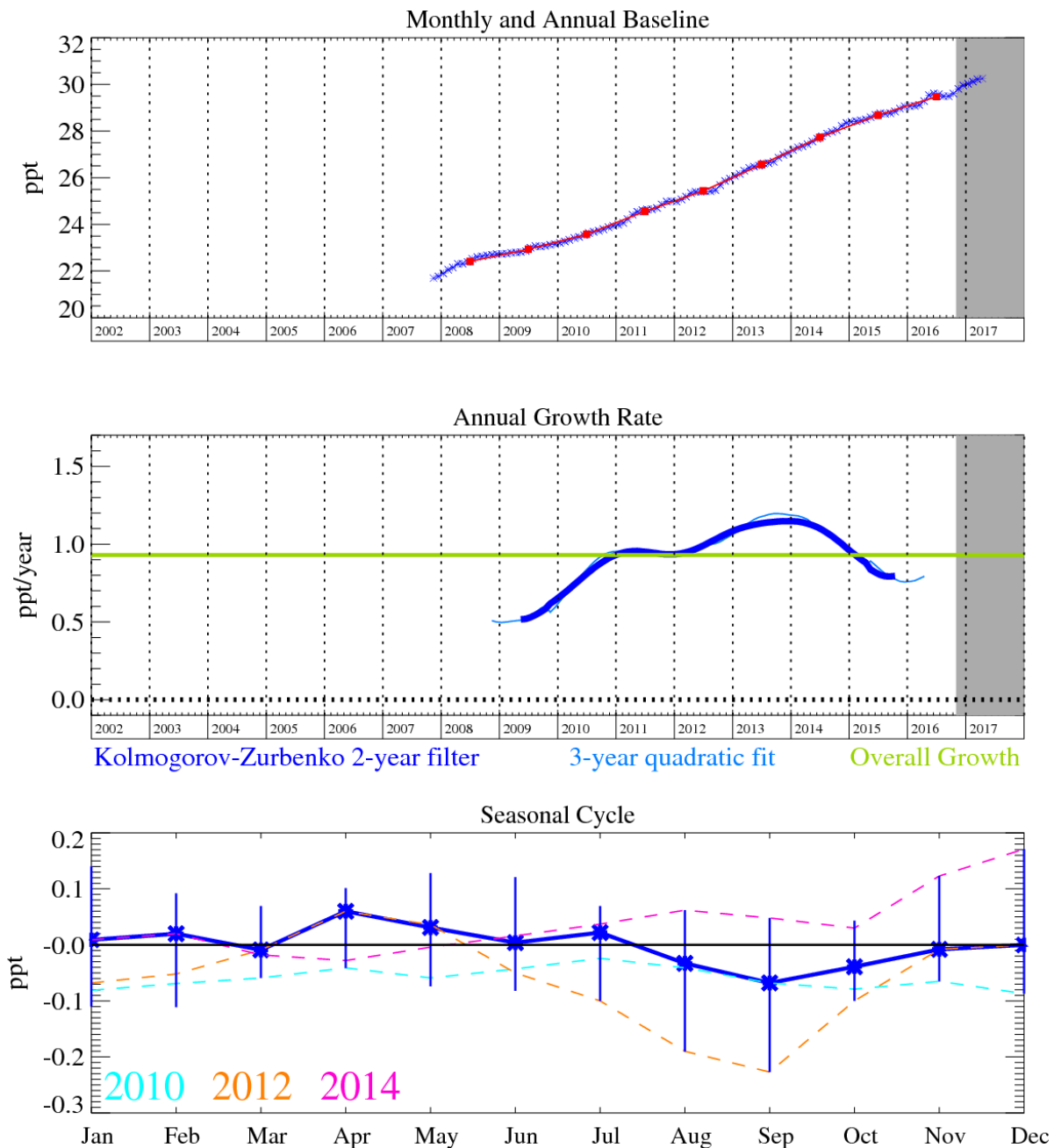


Figure 16: HFC-23 (CHF₃): Monthly (blue) and annual (red) Northern Hemisphere baseline mole fractions. Annual (blue) and overall average growth rate (green) (lower plot). Grey area covers un-ratified provisional data.

HFC-23 (CHF₃) is primarily a by-product formed by the over fluorination of chloroform during the production of HCFC-22. Other minor emissions arise from the electronic industry and fire extinguishers. It is the second most abundant HFC in the atmosphere after HFC-134a; this, combined with a long atmospheric lifetime of 228 years, makes this compound a potent GHG. Emissions of HFC-23 in developed countries have declined due to the Montreal Protocol phase-out schedule for HCFC-22; however, emissions from developing countries continues to drive global atmospheric concentrations up.

Although the InTEM estimates on average are higher than the inventory estimates, the uncertainty ranges entirely overlap for the UK. The baseline uncertainty is of a similar magnitude to the pollution events and so the emission estimates are very uncertain. The use of the Mace Head baseline at Tacolneston is a particular concern for this gas because of this issue; hence, the even larger uncertainty when the DECC network observations are included.

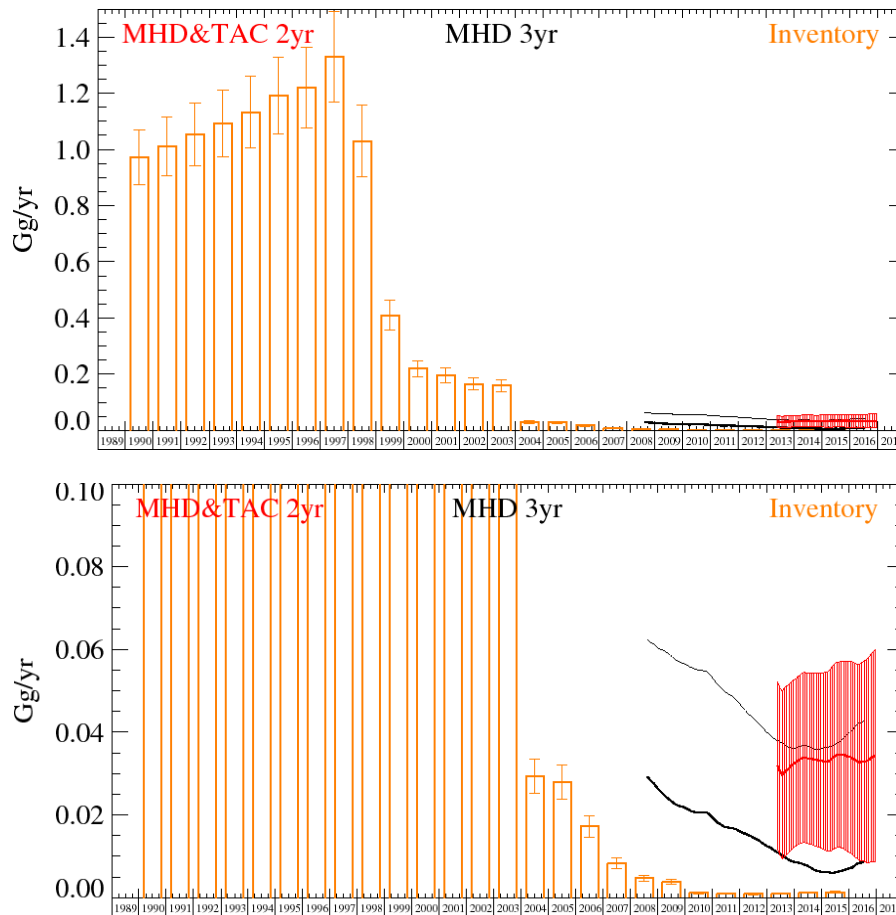


Figure 17: HFC-23 UK emission estimates (Gg yr^{-1}) from the UNFCCC Inventory (orange) and InTEM; MHD-only (black) and DECC network (red). The uncertainty bars represent the 5th and 95th percentiles. Lower plot is zoom of the upper plot.

Years	Inventory	MHD 3yr	MHD&TAC 2yr
1990	0.972 (0.875-1.070)		
1991	1.012 (0.908-1.117)		
1992	1.052 (0.941-1.164)		
1993	1.092 (0.973-1.212)		
1994	1.133 (1.005-1.260)		
1995	1.193 (1.055-1.330)		
1996	1.221 (1.076-1.365)		
1997	1.331 (1.169-1.492)		
1998	1.030 (0.902-1.158)		
1999	0.410 (0.358-0.462)		
2000	0.219 (0.191-0.248)		
2001	0.197 (0.171-0.223)		
2002	0.165 (0.143-0.188)		
2003	0.159 (0.137-0.181)		
2004	0.029 (0.025-0.034)		
2005	0.028 (0.024-0.032)		
2006	0.017 (0.015-0.020)		
2007	0.008 (0.007-0.010)		
2008	0.005 (0.004-0.005)	0.035 (0.002-0.068)	
2009	0.004 (0.003-0.004)	0.026 (0.000-0.060)	
2010	0.001 (0.001-0.001)	0.021 (0.000-0.055)	
2011	0.001 (0.001-0.001)	0.017 (0.000-0.050)	
2012	0.001 (0.001-0.001)	0.016 (0.000-0.044)	
2013	0.001 (0.001-0.001)	0.010 (0.000-0.035)	0.035 (0.015-0.054)
2014	0.001 (0.001-0.001)	0.006 (0.000-0.033)	0.033 (0.012-0.053)
2015	0.001 (0.001-0.002)	0.007 (0.000-0.040)	0.034 (0.012-0.056)
2016		0.009 (0.000-0.045)	0.034 (0.009-0.060)

Table 12: HFC-23 emission (Gg yr^{-1}) estimates for the UK with uncertainty (5th - 95th percentile).

4.12 HFC-32

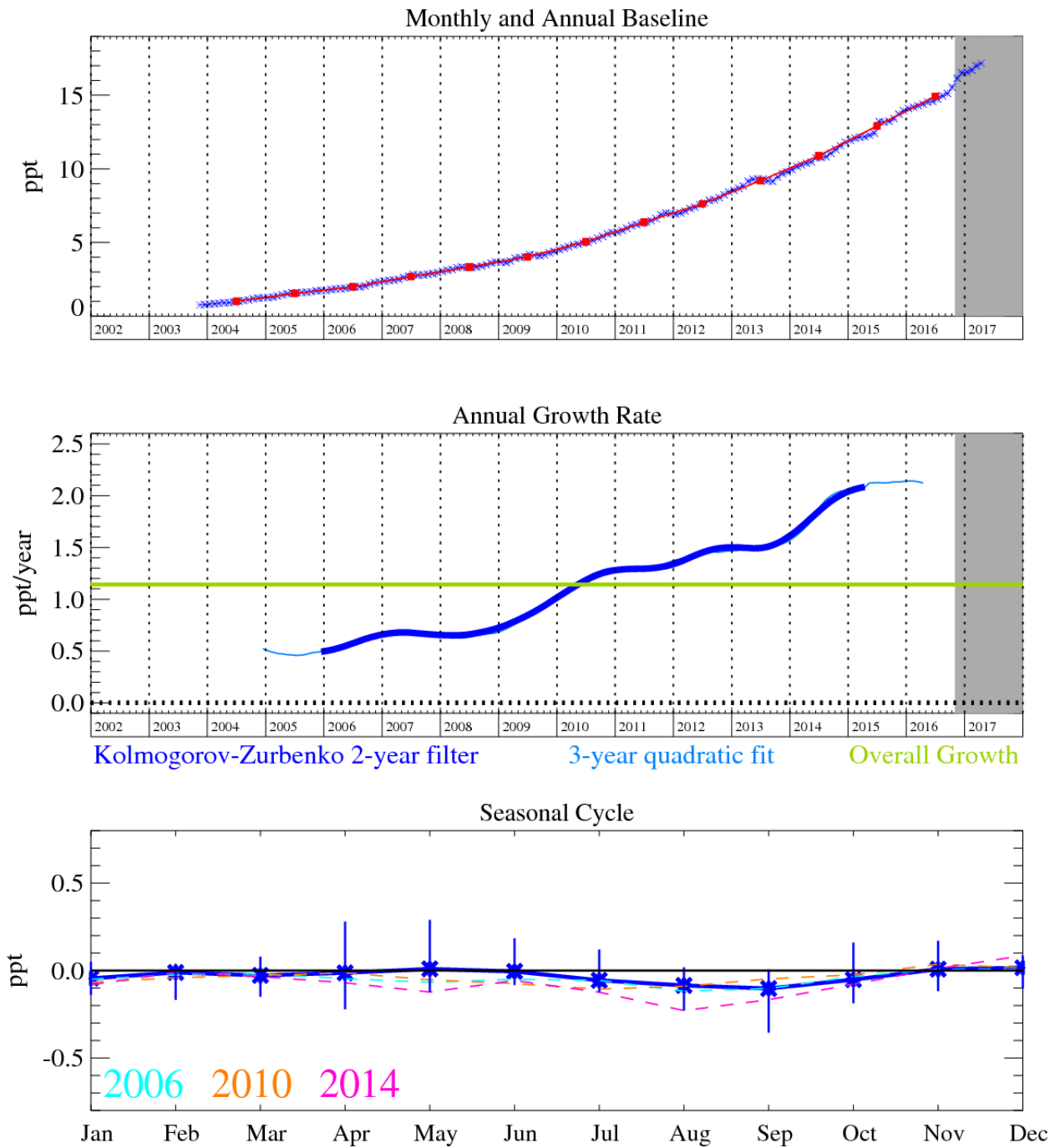


Figure 18: HFC-32 (CH_2F_2): Monthly (blue) and annual (red) Northern Hemisphere baseline mole fractions (top plot). Annual (blue) and overall average growth rate (green) (middle plot). Seasonal cycle (de-trended) with year-to-year variability (lower plot). Grey area covers un-ratified and therefore provisional data.

HFC-32 (CH_2F_2) has an atmospheric lifetime of 5.4 years and a GWP_{100} of 716. It is used in air conditioning and refrigeration applications; R-410A (50% HFC-32, 50% HFC-125 by weight) and R-407C (23% HFC-32, 52% HFC-134a, 25% HFC-125 by weight) are used as replacements to HCFC-22. As the phase-out of HCFC-22 gains momentum it might be expected that demand for these refrigerant blends will increase. The pollution events measured at Mace Head are highly correlated with that of HFC-125.

Unfortunately, the observations of HFC-32 at Mace Head (and HFC-125) were compromised by contamination from the air conditioning system (May 2014 – June 2015) and these data had to be removed. The current solution is to flush the air sample module with clean ambient air to minimise contamination from laboratory air. A long-term solution will require modification of the air conditioner to use a chilled water heat exchanger with the refrigerant gases contained in a unit external to the

laboratory. The NH baseline during this period has been estimated using another AGAGE NH station, Zeppelin (Ny-Ålesund).

The UK inventory estimates are growing strongly throughout the time-series. The InTEM estimates using only MHD data are increasing throughout. The InTEM estimates for the UK using the additional TAC observations remain flat. The InTEM results using either data set are lower than the inventory estimates and are outside the uncertainties.

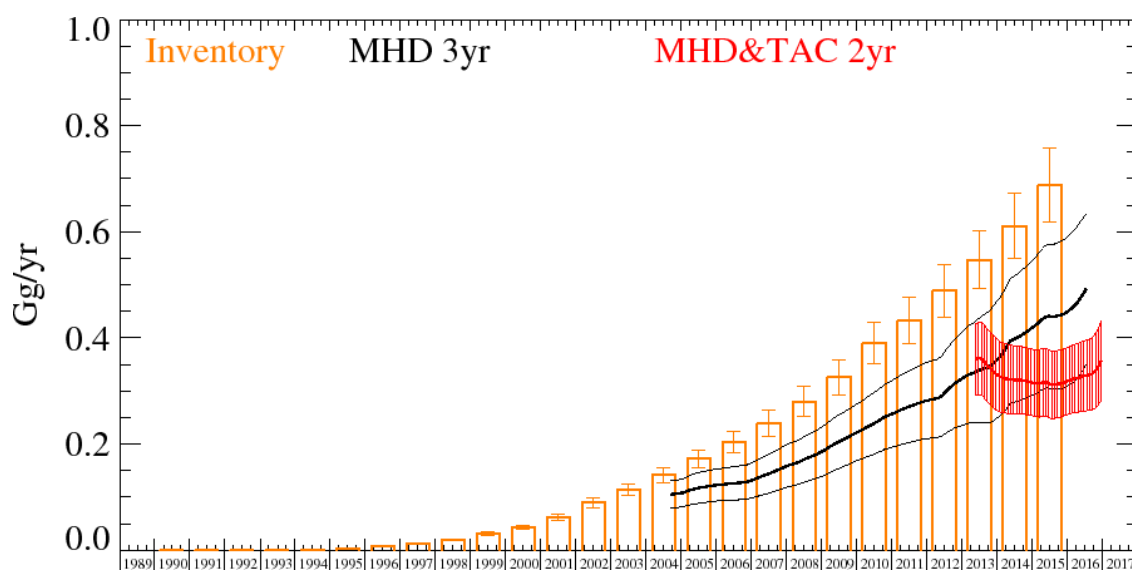


Figure 19: HFC-32 UK emission estimates (Gg yr^{-1}) from the UNFCCC Inventory (orange) and InTEM; MHD-only (black) and DECC network (red). The uncertainty bars represent the 5th and 95th percentiles.

Years	Inventory	MHD 3yr	MHD&TAC 2yr
1990	0.000 (0.000-0.000)		
1991	0.000 (0.000-0.000)		
1992	0.000 (0.000-0.000)		
1993	0.000 (0.000-0.000)		
1994	0.000 (0.000-0.000)		
1995	0.003 (0.003-0.004)		
1996	0.007 (0.006-0.008)		
1997	0.013 (0.011-0.014)		
1998	0.020 (0.018-0.021)		
1999	0.031 (0.028-0.034)		
2000	0.043 (0.039-0.047)		
2001	0.063 (0.056-0.069)		
2002	0.090 (0.081-0.099)		
2003	0.114 (0.103-0.126)		
2004	0.142 (0.128-0.156)	0.081 (0.061-0.101)	
2005	0.172 (0.155-0.190)	0.108 (0.082-0.135)	
2006	0.203 (0.183-0.223)	0.125 (0.094-0.155)	
2007	0.240 (0.216-0.264)	0.142 (0.106-0.178)	
2008	0.280 (0.252-0.308)	0.168 (0.125-0.211)	
2009	0.326 (0.293-0.358)	0.206 (0.156-0.257)	
2010	0.390 (0.351-0.429)	0.236 (0.181-0.292)	
2011	0.433 (0.390-0.477)	0.274 (0.207-0.342)	
2012	0.489 (0.440-0.538)	0.296 (0.218-0.374)	
2013	0.547 (0.492-0.602)	0.337 (0.242-0.431)	0.353 (0.286-0.419)
2014	0.611 (0.550-0.672)	0.390 (0.266-0.515)	0.328 (0.262-0.395)
2015	0.688 (0.620-0.757)	0.447 (0.307-0.588)	0.301 (0.243-0.359)
2016		0.563 (0.428-0.698)	0.357 (0.282-0.432)

Table 13: HFC-32 emission (Gg yr^{-1}) estimates for the UK with uncertainty (5th - 95th percentile).

4.13 HFC-227ea

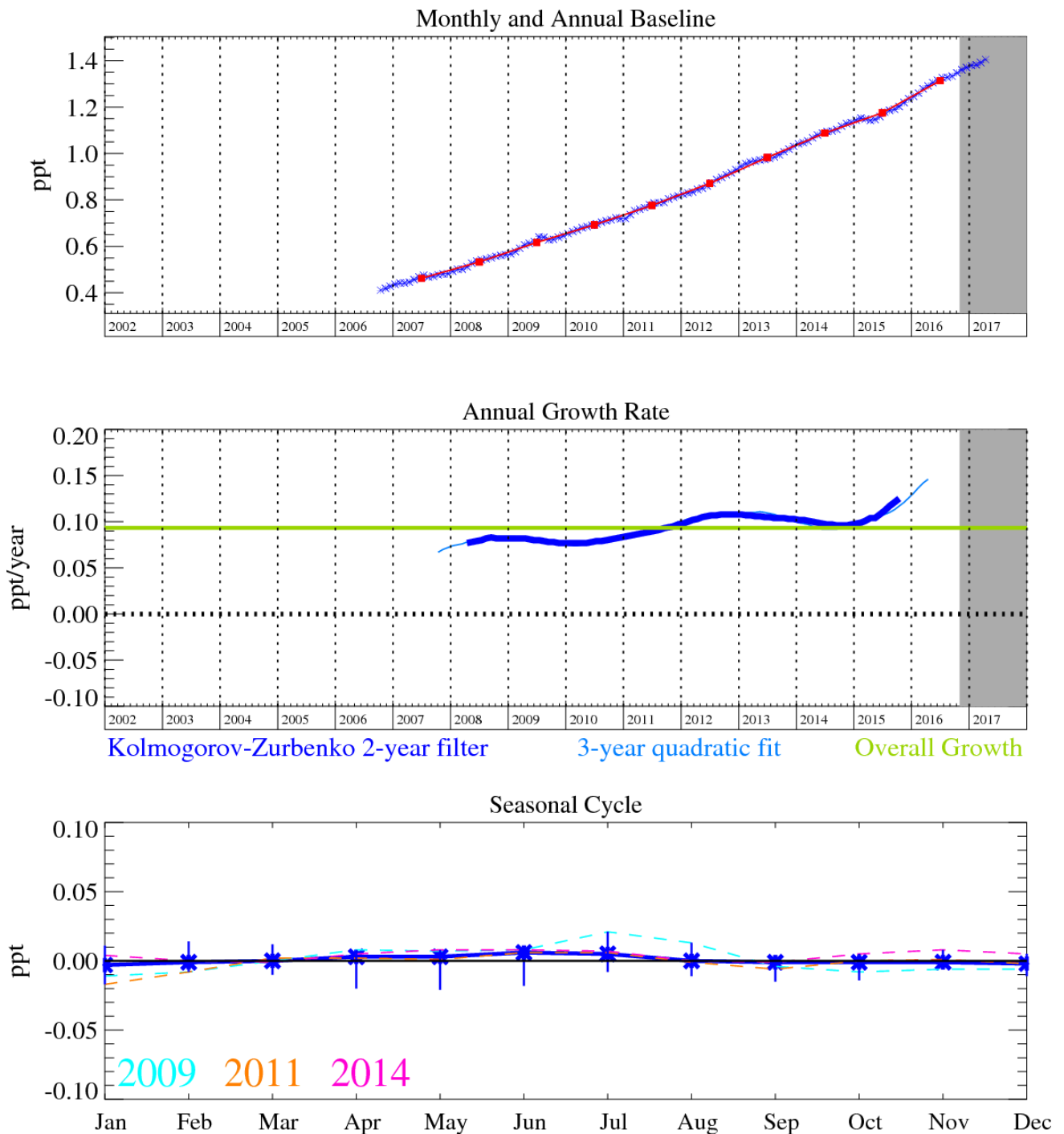


Figure 20: HFC-227ea (C₃HF₇): Monthly (blue) and annual (red) Northern Hemisphere baseline mole fractions (top plot). Annual (blue) and overall average growth rate (green) (middle plot). Seasonal cycle (de-trended) with year-to-year variability (lower plot). Grey area covers un-ratified and therefore provisional data.

HFC-227ea (C₃HF₇) was added to the Medusa analysis in October 2006. HFC-227ea is used as a propellant for medical aerosols and a fire-fighting agent and to a lesser extent in metered-dose inhalers, and foam blowing (atmospheric lifetime 35.8 years and GWP₁₀₀ of 3580).

The InTEM results are significantly lower (~50%) than the inventory estimates. The reason for this difference is unknown. The results, when the new observations from Tacolneston are incorporated, are similar to, but lower than, the Mace Head only InTEM results.

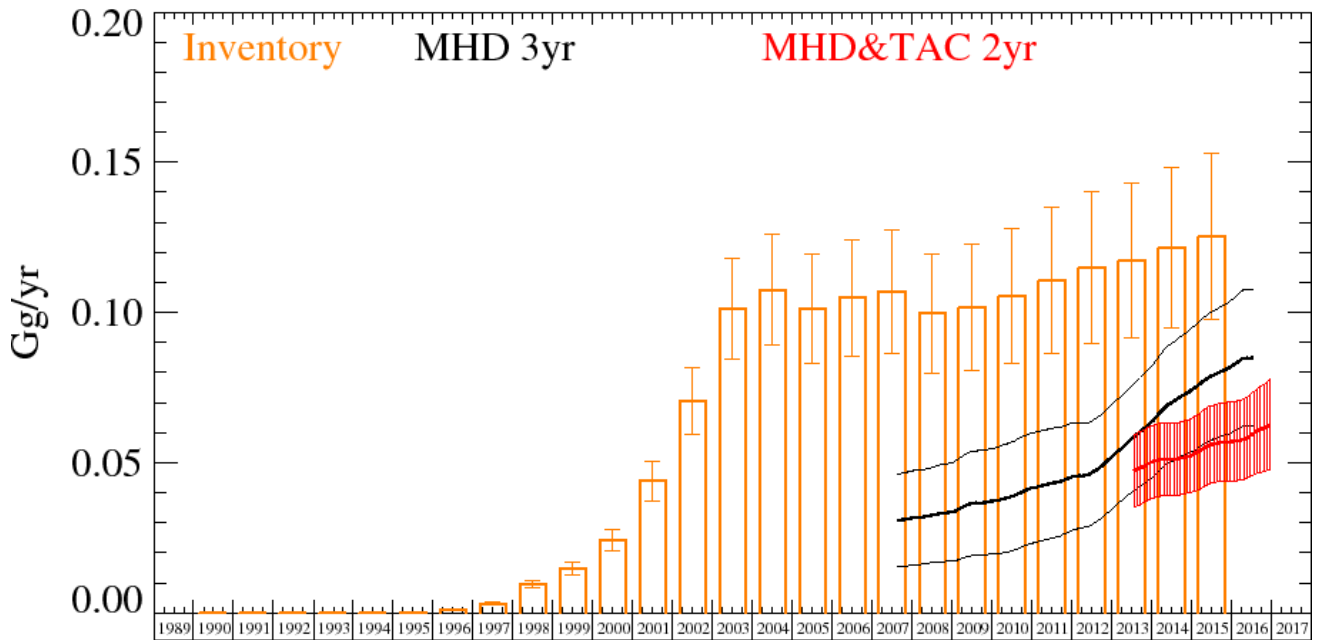


Figure 21: HFC-227ea UK emission estimates (Gg yr^{-1}) from the UNFCCC Inventory (orange) and InTEM; MHD-only (black) and DECC network (red). The uncertainty bars represent the 5th and 95th percentiles.

Years	Inventory	MHD 3yr	MHD&TAC 2yr
1990	0.0 (0.0-0.0)		
1991	0.0 (0.0-0.0)		
1992	0.0 (0.0-0.0)		
1993	0.0 (0.0-0.0)		
1994	0.0 (0.0-0.0)		
1995	0.0 (0.0-0.0)		
1996	0.001 (0.001-0.002)		
1997	0.003 (0.038-0.004)		
1998	0.010 (0.008-0.011)		
1999	0.015 (0.013-0.017)		
2000	0.024 (0.021-0.028)		
2001	0.044 (0.037-0.051)		
2002	0.071 (0.054-0.082)		
2003	0.101 (0.085-0.118)		
2004	0.108 (0.089-0.126)		
2005	0.101 (0.083-0.120)		
2006	0.105 (0.085-0.124)		
2007	0.107 (0.086-0.128)	0.028 (0.013-0.043)	
2008	0.100 (0.080-0.120)	0.032 (0.010-0.047)	
2009	0.102 (0.081-0.123)	0.034 (0.086-0.051)	
2010	0.105 (0.083-0.128)	0.040 (0.021-0.058)	
2011	0.111 (0.086-0.135)	0.044 (0.025-0.063)	
2012	0.115 (0.090-0.140)	0.046 (0.023-0.063)	
2013	0.117 (0.091-0.143)	0.055 (0.038-0.072)	0.046 (0.037-0.056)
2014	0.122 (0.095-0.148)	0.072 (0.052-0.092)	0.051 (0.038-0.063)
2015	0.125 (0.098-0.153)	0.082 (0.060-0.104)	0.055 (0.043-0.067)
2016		0.087 (0.064-0.109)	0.063 (0.048-0.078)

Table 14: HFC-227ea emission (Gg yr^{-1}) estimates for the UK with uncertainty (5th - 95th percentile).

4.14 HFC-245fa

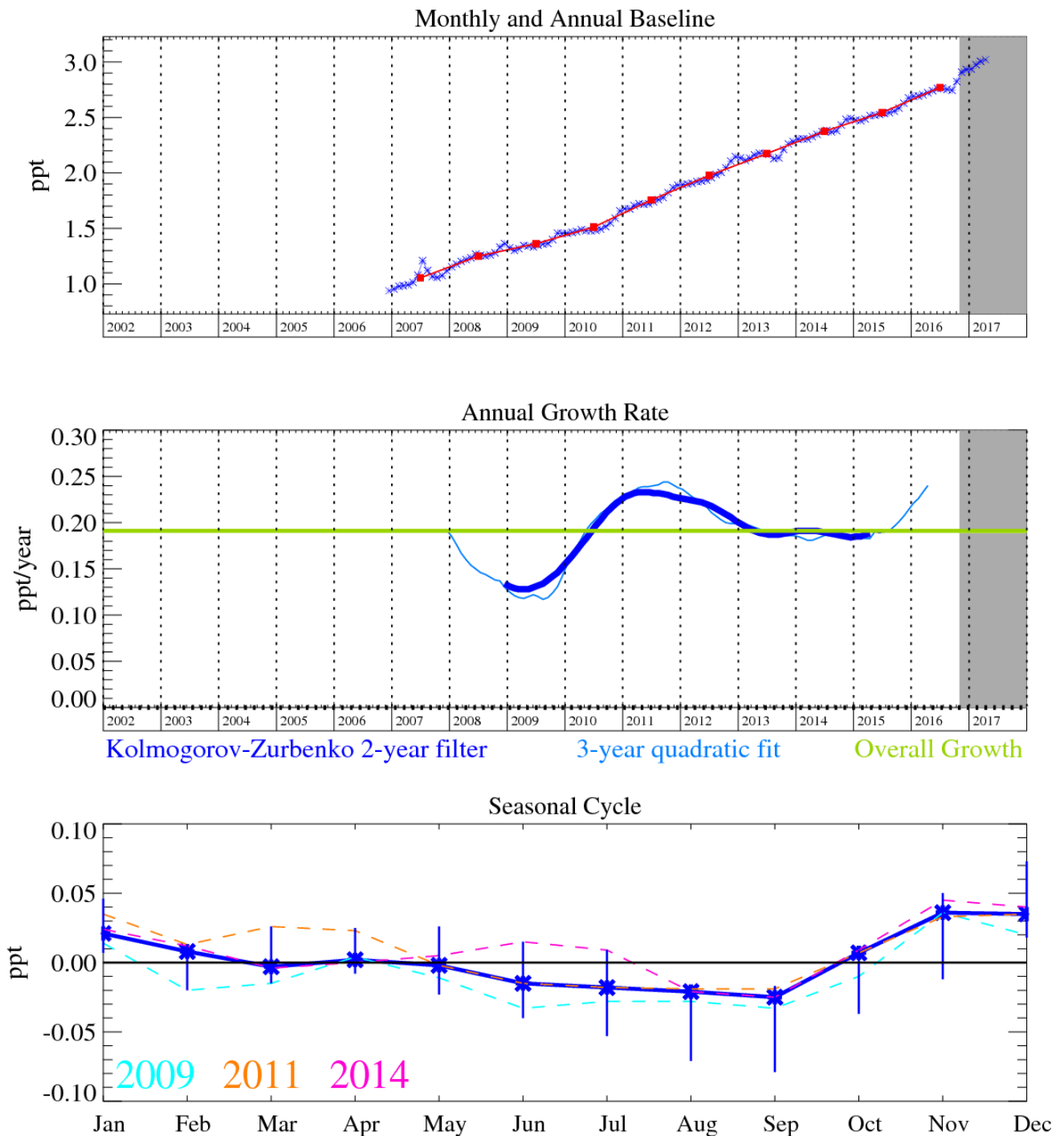


Figure 22: HFC-245fa ($C_3H_3F_5$): Monthly (blue) and annual (red) baseline (top plot). Annual (blue) and overall average growth rate (green) (middle plot). Seasonal cycle (de-trended) with year-to-year variability (lower plot). Grey area covers un-ratified and therefore provisional data.

The inversion results for this gas are on the whole lower than those estimated in the inventory. The uncertainty bars for the MHD-only results overlap with inventory estimates but are large. The inclusion of TAC observations lowers the InTEM estimates below the inventory estimates but the uncertainties overlap strongly with the MHD-only estimates.

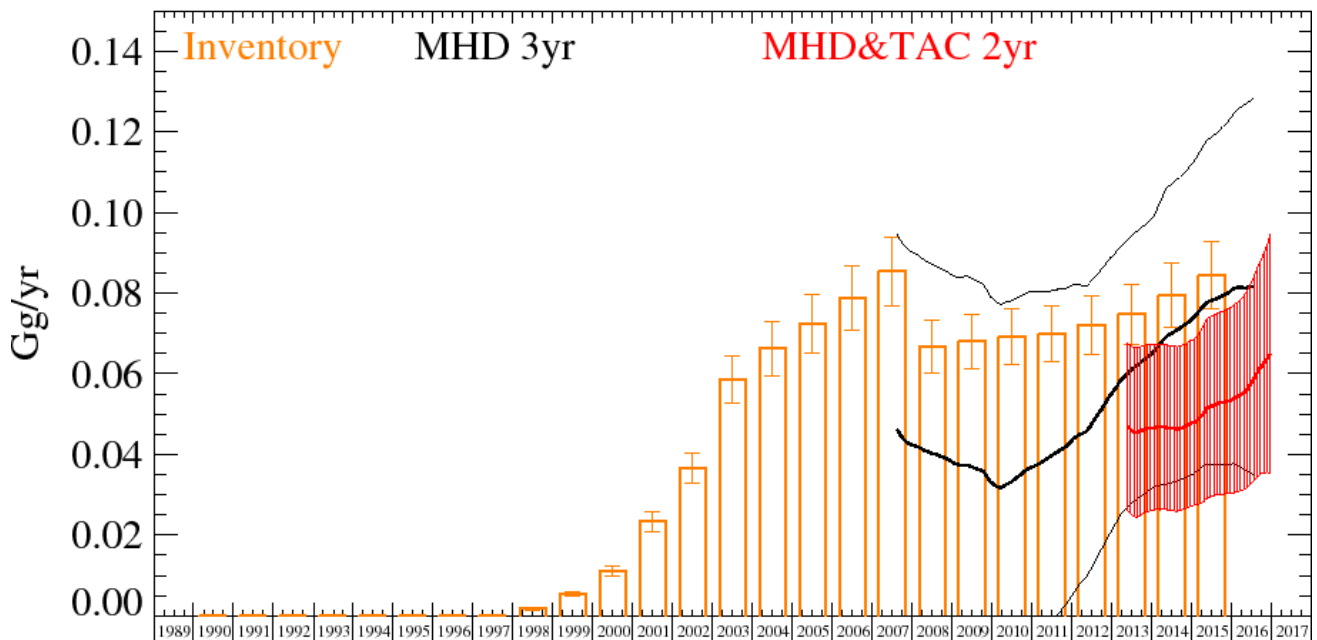


Figure 23: HFC-245fa UK emission estimates (Gg yr⁻¹) from the UNFCCC Inventory (orange) and InTEM; MHD-only (black) and DECC network (red).. The uncertainty bars represent the 5th and 95th percentiles.

Years	Inventory	MHD 3yr	MHD&TAC 2yr
1990	0.0 (0.0-0.0)		
1991	0.0 (0.0-0.0)		
1992	0.0 (0.0-0.0)		
1993	0.0 (0.0-0.0)		
1994	0.0 (0.0-0.0)		
1995	0.0 (0.0-0.0)		
1996	0.0 (0.0-0.0)		
1997	0.0 (0.0-0.0)		
1998	0.002 (0.001-0.002)		
1999	0.005 (0.005-0.006)		
2000	0.011 (0.010-0.012)		
2001	0.023 (0.021-0.026)		
2002	0.037 (0.033-0.040)		
2003	0.059 (0.053-0.064)		
2004	0.066 (0.060-0.073)		
2005	0.073 (0.065-0.080)		
2006	0.079 (0.071-0.087)		
2007	0.085 (0.077-0.094)	0.065 (0.014-0.116)	
2008	0.067 (0.060-0.073)	0.042 (0.000-0.090)	
2009	0.068 (0.061-0.075)	0.035 (0.000-0.081)	
2010	0.069 (0.062-0.076)	0.031 (0.000-0.076)	
2011	0.070 (0.063-0.077)	0.039 (0.000-0.081)	
2012	0.072 (0.065-0.079)	0.051 (0.016-0.086)	
2013	0.075 (0.067-0.082)	0.058 (0.027-0.089)	0.050 (0.029-0.071)
2014	0.079 (0.071-0.087)	0.071 (0.036-0.106)	0.047 (0.026-0.067)
2015	0.084 (0.076-0.093)	0.080 (0.038-0.123)	0.049 (0.029-0.070)
2016		0.085 (0.031-0.139)	0.065 (0.035-0.094)

Table 15: HFC-245fa emission (Gg yr⁻¹) estimates for the UK with uncertainty (5th - 95th percentile).

4.15 HFC-43-10mee

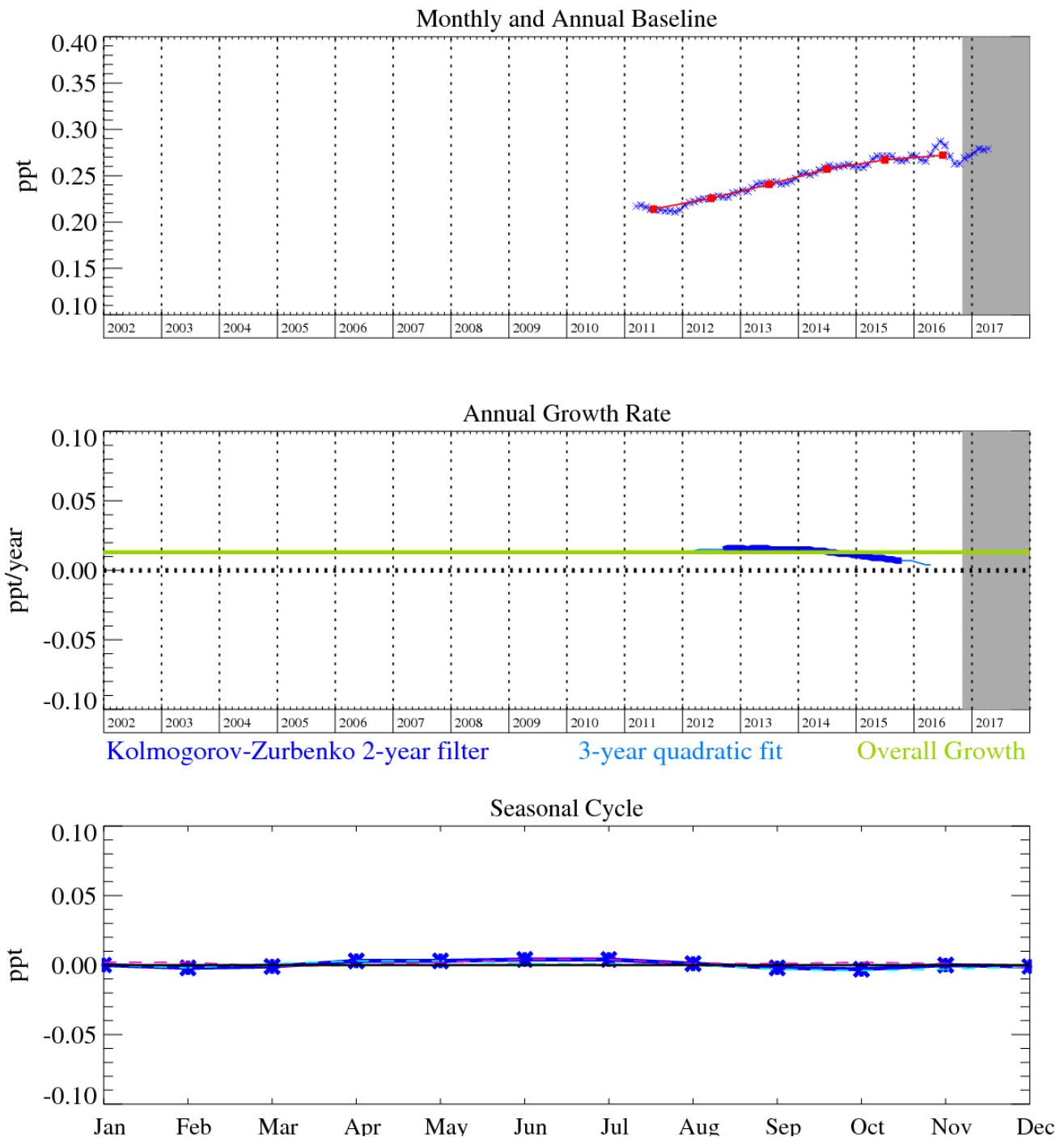


Figure 24: HFC-43-10mee (C₅H₂F₁₀): Monthly (blue) and annual (red) Northern Hemisphere baseline mole fractions (top plot). Annual (blue) and overall average growth rate (green) (middle plot). Seasonal cycle (de-trended) with year-to-year variability (lower plot). Grey area covers un-ratified and therefore provisional data.

HFC-43-10mee (C₅H₂F₁₀) was introduced in the mid 1990s as a replacement for CFC-113. It meets many requirements in the electronics industries and replaces PFCs in some uses such as a carrier fluid for lubricants applied to computer hard disks. It has an atmospheric lifetime of 16.1 years, a GWP₁₀₀ of 1,650 and a radiative efficiency of 0.42 W m⁻² ppb⁻¹.

The inversion results for HFC-43-10mee show that there is disagreement between the inventory and the InTEM results, although the emissions are relatively small in both estimates. The InTEM estimates are less than half of the inventory estimates and the uncertainties do not overlap.

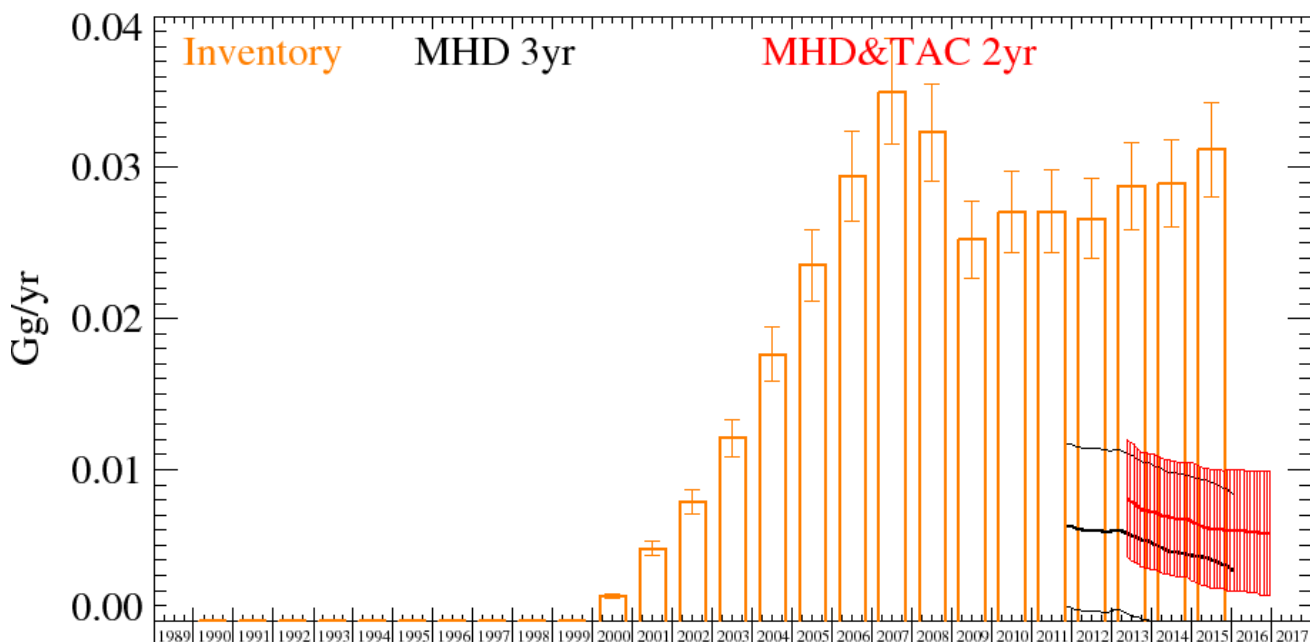


Figure 25: HFC-43-10mee emission estimates (Gg yr^{-1}) from the UNFCCC Inventory and InTEM (4y MH-only and 2y DECC network) for the UK. The uncertainty bars represent the 5th and 95th percentiles.

Years	Inventory	MHD 3yr	MHD&TAC 2yr
1990	0.0 (0.0-0.0)		
1991	0.0 (0.0-0.0)		
1992	0.0 (0.0-0.0)		
1993	0.0 (0.0-0.0)		
1994	0.0 (0.0-0.0)		
1995	0.0 (0.0-0.0)		
1996	0.0 (0.0-0.0)		
1997	0.0 (0.0-0.0)		
1998	0.0 (0.0-0.0)		
1999	0.0 (0.0-0.0)		
2000	0.002 (0.001-0.002)		
2001	0.005 (0.004-0.005)		
2002	0.008 (0.007-0.009)		
2003	0.012 (0.011-0.013)		
2004	0.018 (0.016-0.019)		
2005	0.024 (0.021-0.026)		
2006	0.029 (0.027-0.032)		
2007	0.035 (0.032-0.039)		
2008	0.032 (0.029-0.036)		
2009	0.025 (0.023-0.028)		
2010	0.027 (0.024-0.030)		
2011	0.027 (0.024-0.030)		
2012	0.027 (0.024-0.029)	0.006 (0.001-0.012)	
2013	0.029 (0.026-0.032)	0.006 (0.001-0.011)	0.009 (0.005-0.013)
2014	0.029 (0.026-0.032)	0.005 (0.000-0.010)	0.007 (0.003-0.011)
2015	0.031 (0.028-0.034)	0.004 (0.000-0.009)	0.006 (0.002-0.010)
2016		0.003 (0.000-0.008)	0.006 (0.002-0.010)

Table 16: HFC-43-10mee emission (Gg yr^{-1}) estimates for the UK with uncertainty (5th - 95th percentile).

4.16 HFC-365mfc

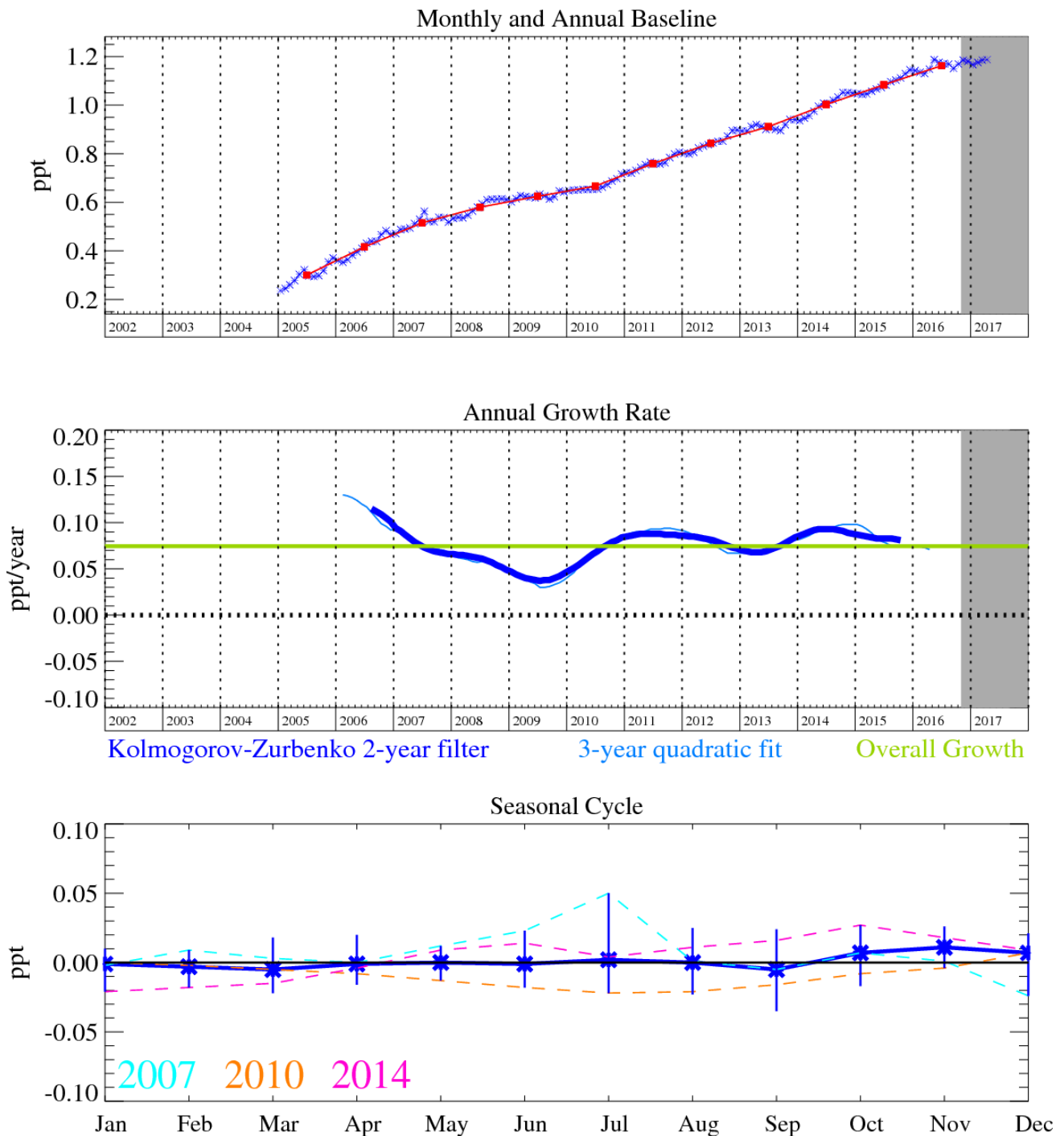


Figure 26: HFC-365mfc (C₄H₅F₅): Monthly (blue) and annual (red) baseline (top plot). Annual (blue) and overall average growth rate (green) (middle plot). Seasonal cycle (de-trended) with year-to-year variability (lower plot). Grey area covers un-ratified and therefore provisional data.

HFC-365mfc (C₄H₅F₅) is used mainly for polyurethane structural foam blowing as a replacement for HCFC-141b, and to a minor extent as a blend component for solvents. It has an atmospheric lifetime of 8.6 years and a GWP estimated at 790-997 (100-year time horizon).

The InTEM emissions for the UK show a significant decrease between 2006-2009, then a flat period until 2013 before starting to rise. The inventory shows a similar decline, flat period and rise over the same time period. The agreement between the inventory and the MHD+TAC inversion results is excellent in both magnitude and trend.

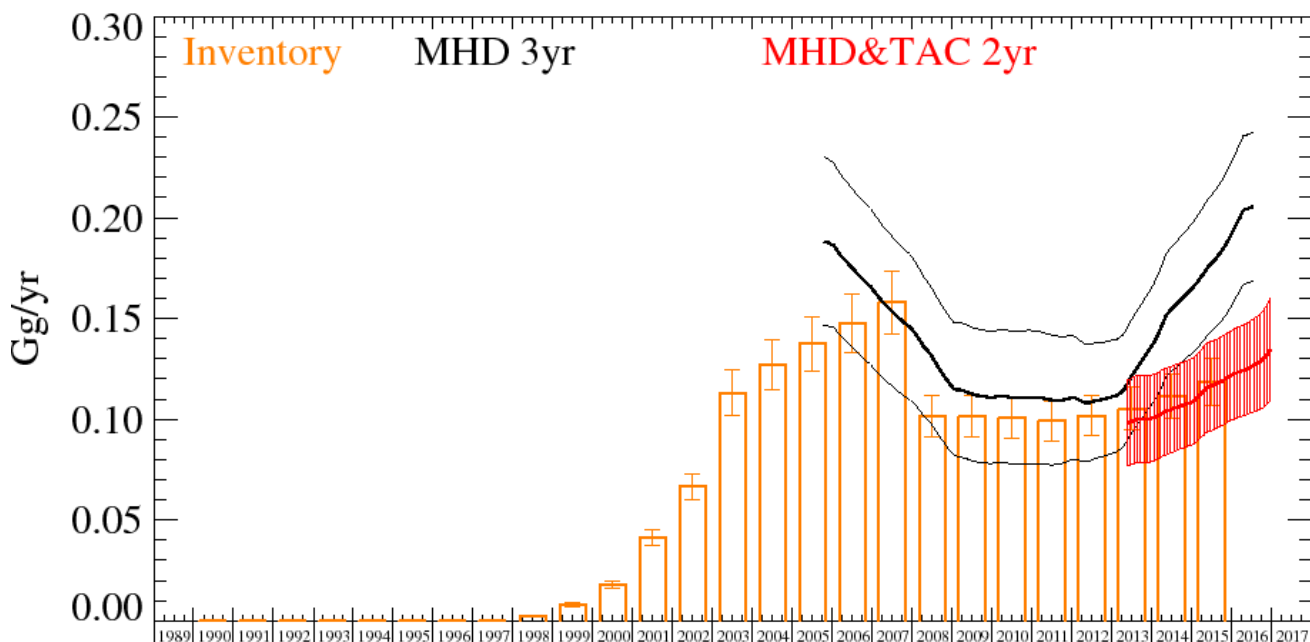


Figure 27: HFC-365mfc emission estimates (Gg yr^{-1}) from InTEM (MHD-only and DECC network) for the UK. The uncertainty bars represent the 5th and 95th percentiles.

Years	Inventory	MHD 3yr	MHD&TAC 2yr
1990	0.0 (0.0-0.0)		
1991	0.0 (0.0-0.0)		
1992	0.0 (0.0-0.0)		
1993	0.0 (0.0-0.0)		
1994	0.0 (0.0-0.0)		
1995	0.0 (0.0-0.0)		
1996	0.0 (0.0-0.0)		
1997	0.0 (0.0-0.0)		
1998	0.002 (0.002-0.003)		
1999	0.008 (0.007-0.009)		
2000	0.018 (0.016-0.020)		
2001	0.041 (0.037-0.045)		
2002	0.067 (0.060-0.073)		
2003	0.113 (0.102-0.125)		
2004	0.127 (0.114-0.140)		
2005	0.137 (0.124-0.151)	0.184 (0.139-0.228)	
2006	0.148 (0.133-0.162)	0.186 (0.145-0.227)	
2007	0.158 (0.142-0.174)	0.164 (0.125-0.202)	
2008	0.101 (0.091-0.112)	0.124 (0.091-0.158)	
2009	0.101 (0.091-0.112)	0.103 (0.072-0.135)	
2010	0.101 (0.091-0.111)	0.114 (0.080-0.147)	
2011	0.099 (0.089-0.109)	0.115 (0.082-0.149)	
2012	0.102 (0.092-0.112)	0.104 (0.075-0.132)	
2013	0.105 (0.095-0.116)	0.114 (0.088-0.140)	0.097 (0.076-0.118)
2014	0.112 (0.100-0.123)	0.154 (0.123-0.185)	0.101 (0.080-0.122)
2015	0.118 (0.107-0.130)	0.190 (0.155-0.226)	0.117 (0.096-0.138)
2016		0.219 (0.181-0.257)	0.134 (0.109-0.160)

Table 17: HFC-365mfc emission (Gg yr^{-1}) estimates for the UK with uncertainty (5th - 95th percentile).

4.17 PFC-14 (CF₄)

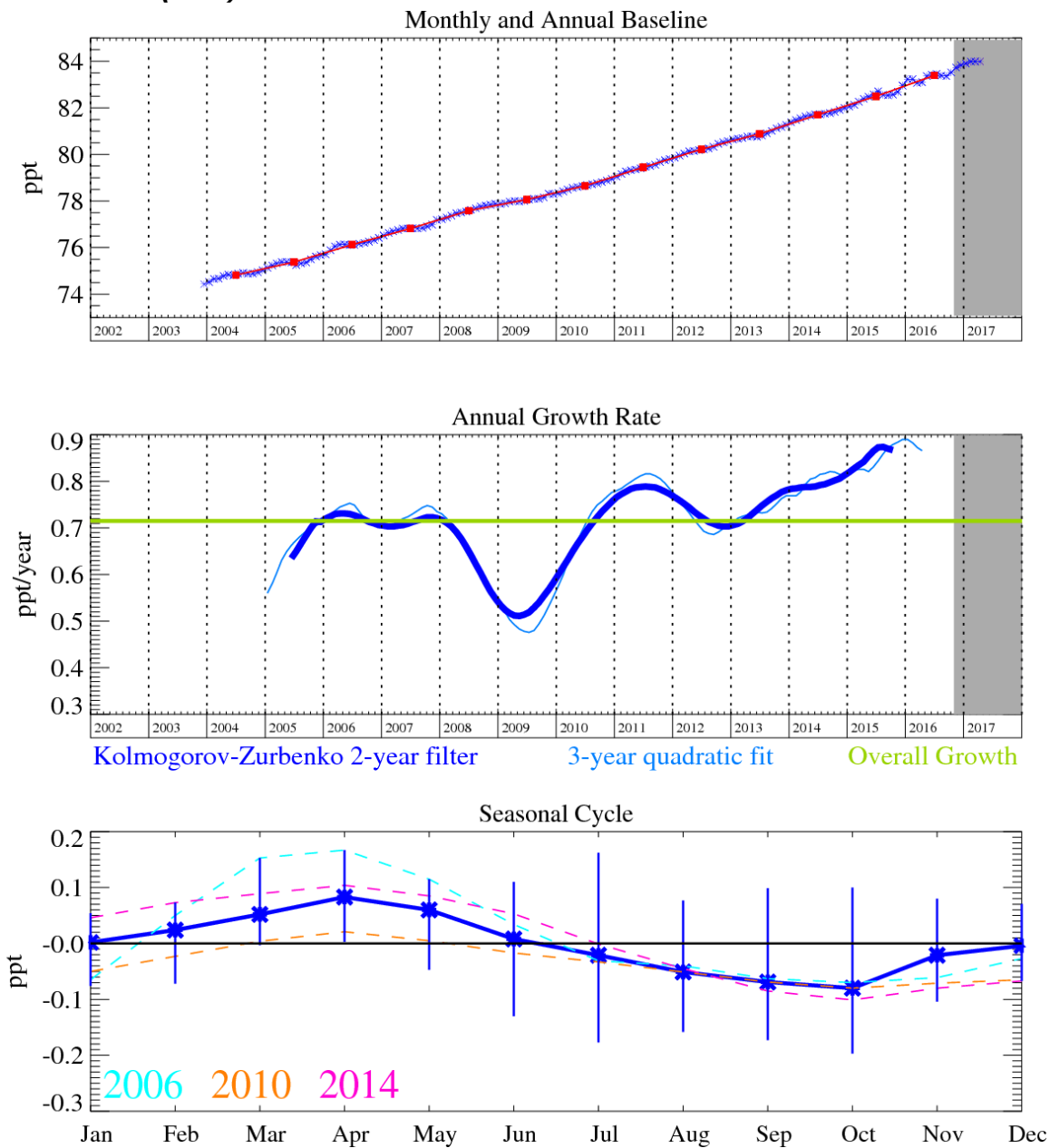


Figure 28: PFC-14 (CF₄): Monthly (blue) and annual (red) Northern Hemisphere baseline mole fractions (top plot). Annual (blue) and overall average growth rate (green) (middle plot). Seasonal cycle (de-trended) with year-to-year variability (lower plot). Grey area covers un-ratified and therefore provisional data.

PFC-14 (CF₄) possesses the longest known lifetime of anthropogenic molecules (>50,000 years), which, when coupled with its high absolute radiative forcing (0.08 W m⁻² ppb⁻¹) gives rise to a high GWP₁₀₀ of 5,820 and can equate to upwards of 1% of total radiative forcing. Its primary emission source is as an unwanted by-product of aluminium smelting during a fault condition known as an anode effect. Thus, the frequency of occurrence and duration of an anode effect event will determine the regional and global CF₄ emissions. CF₄ has some additional minor applications in the semiconductor industry (as a source of F radicals), but industry has shied away from using CF₄ knowing that its GWP is so high. The aluminium industry has recognised the CF₄ (and C₂F₆) emission problem and has been undergoing processes of replacement of older, less efficient aluminium production cells with more efficient designs, and automated and quicker intervention policies to prevent the occurrence of these anode effects. It is also thought that CF₄ has a natural source from crustal degassing. The current growth rate of atmospheric CF₄ in the NH is close to 0.9 ppt yr⁻¹. This compound will accumulate in the atmosphere due to its very long atmospheric lifetime.

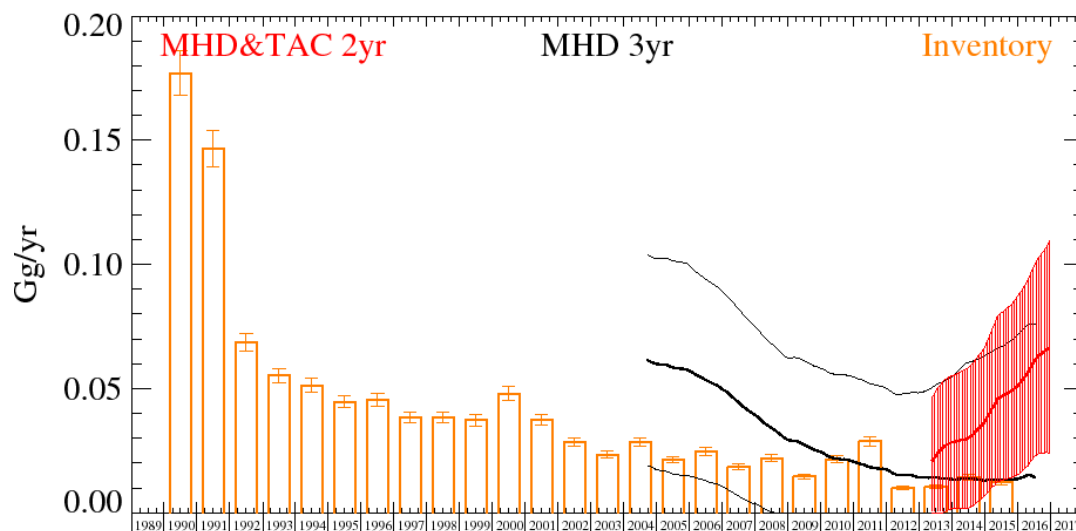


Figure 29: PFC-14 emission estimates (Gg yr^{-1}) from the UNFCCC Inventory and InTEM (MHD-only and DECC network) for the UK. The uncertainty bars represent the 5th and 95th percentiles.

The large uncertainties in the InTEM results entirely overlap with the inventory estimates although the median results are generally higher. In the InTEM inversions, the statistical match in time-series between the model time-series and the observations is weak. This is because the emissions are principally from point sources (aluminium smelters). If the locations of the smelters are included and solved for as single grid cells (25 km) then the agreement between model and observation is much improved. The largest smelter in the UK, at Lynemouth on the north east coast of England ceased operations in March 2012. This is very clearly seen in the modelled emissions when the smelter locations are included as prior information – please refer to the 2014 annual report for details. The MHD+TAC InTEM results at the higher time resolution of 2 years show a strong upward trend unlike the inventory, although the uncertainties are large.

Years	Inventory	MHD 3yr	MHD&TAC 2yr
1990	0.177 (0.168-0.186)		
1991	0.147 (0.139-0.154)		
1992	0.069 (0.065-0.072)		
1993	0.055 (0.052-0.058)		
1994	0.051 (0.049-0.054)		
1995	0.045 (0.042-0.047)		
1996	0.046 (0.043-0.048)		
1997	0.039 (0.036-0.041)		
1998	0.039 (0.036-0.041)		
1999	0.037 (0.035-0.039)		
2000	0.048 (0.045-0.051)		
2001	0.038 (0.035-0.040)		
2002	0.029 (0.027-0.030)		
2003	0.023 (0.022-0.025)		
2004	0.029 (0.027-0.030)	0.064 (0.021-0.107)	
2005	0.021 (0.020-0.023)	0.060 (0.017-0.102)	
2006	0.025 (0.023-0.026)	0.056 (0.014-0.099)	
2007	0.018 (0.017-0.020)	0.045 (0.007-0.083)	
2008	0.022 (0.021-0.023)	0.032 (0.000-0.065)	
2009	0.015 (0.014-0.016)	0.026 (0.000-0.059)	
2010	0.022 (0.020-0.023)	0.023 (0.000-0.057)	
2011	0.029 (0.027-0.031)	0.019 (0.000-0.053)	
2012	0.010 (0.0094-0.0108)	0.015 (0.000-0.047)	
2013	0.010 (0.0097-0.0111)	0.013 (0.000-0.048)	0.016 (0.000-0.039)
2014	0.014 (0.013-0.015)	0.013 (0.000-0.060)	0.029 (0.002-0.055)
2015	0.012 (0.011-0.013)	0.014 (0.000-0.071)	0.046 (0.013-0.079)
2016		0.014 (0.000-0.080)	0.067 (0.024-0.109)

Table 18: Emission (Gg yr^{-1}) estimates for the UK with uncertainty (5th - 95th percentile).

4.18 PFC-116

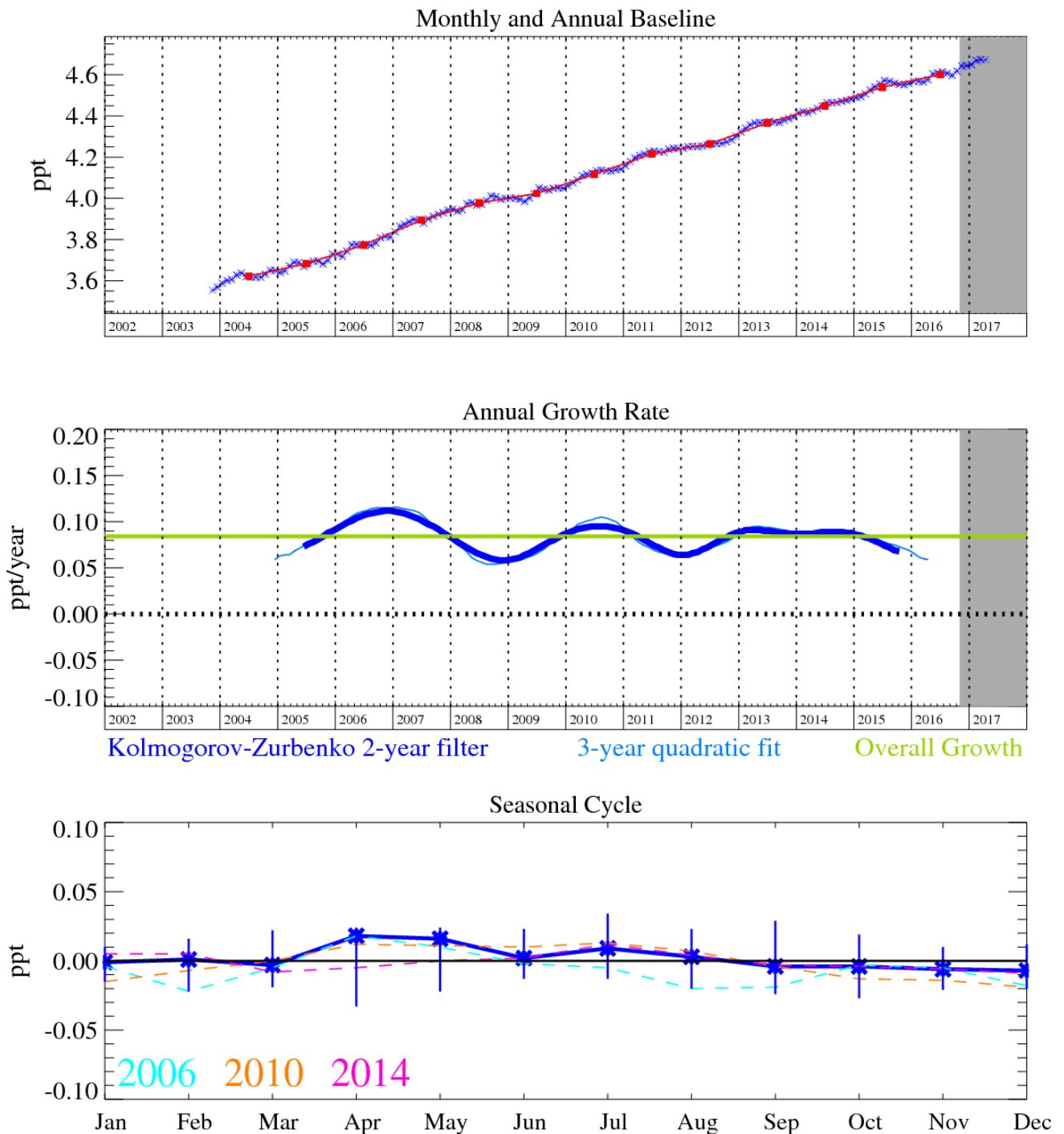


Figure 30: PFC-116 (C_2F_6): Monthly (blue) and annual (red) Northern Hemisphere baseline mole fractions (top plot). Annual (blue) and overall average growth rate (green) (middle plot). Seasonal cycle (de-trended) with year-to-year variability (lower plot). Grey area covers un-ratified and therefore provisional data.

PFC-116 (C_2F_6) is also a potent greenhouse gas with an atmospheric lifetime of >10,000 years. It has many common sources to CF_4 , and serves to help explain why most of the CF_4 above-baseline (pollution) events are correlated with those of C_2F_6 . However, we note that there are more frequent, and greater magnitude of, C_2F_6 emissions relative to CF_4 . This is due to the dominant source of C_2F_6 being from plasma etching in the semiconductor industry.

The InTEM uncertainty ranges for the regional emissions are large but consistently overlap the inventory estimates.

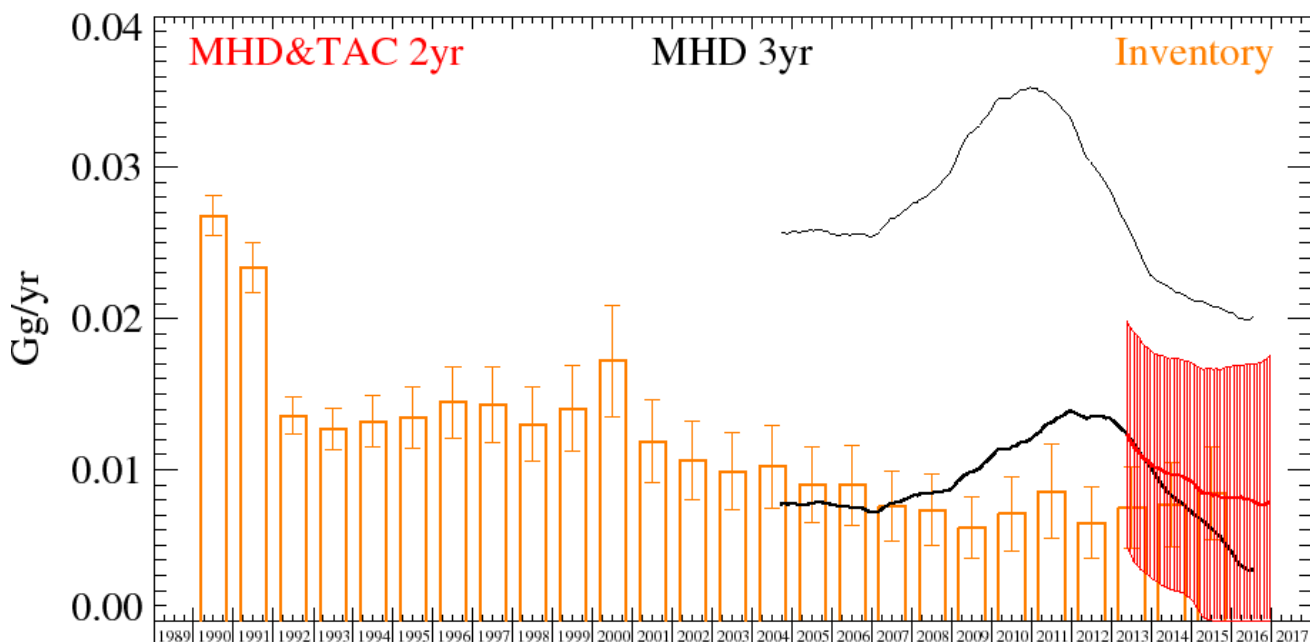


Figure 31: PFC-116 emission estimates (Gg yr^{-1}) from the UNFCCC Inventory and InTEM (MHD-only and DECC network) for the UK. The uncertainty bars represent the 5th and 95th percentiles.

Years	Inventory	MHD 3yr	MHD&TAC 2yr
1990	0.027 (0.025-0.028)		
1991	0.023 (0.022-0.025)		
1992	0.014 (0.012-0.015)		
1993	0.013 (0.011-0.014)		
1994	0.013 (0.011-0.015)		
1995	0.014 (0.011-0.016)		
1996	0.014 (0.012-0.017)		
1997	0.014 (0.012-0.017)		
1998	0.013 (0.011-0.016)		
1999	0.014 (0.011-0.017)		
2000	0.017 (0.014-0.021)		
2001	0.012 (0.009-0.015)		
2002	0.011 (0.008-0.013)		
2003	0.010 (0.007-0.012)		
2004	0.010 (0.008-0.013)	0.008 (0.000-0.026)	
2005	0.009 (0.007-0.012)	0.008 (0.000-0.026)	
2006	0.009 (0.006-0.012)	0.008 (0.000-0.026)	
2007	0.008 (0.005-0.010)	0.007 (0.000-0.025)	
2008	0.007 (0.005-0.010)	0.009 (0.000-0.029)	
2009	0.006 (0.004-0.008)	0.010 (0.000-0.032)	
2010	0.007 (0.005-0.010)	0.011 (0.000-0.035)	
2011	0.009 (0.006-0.012)	0.014 (0.000-0.037)	
2012	0.007 (0.004-0.009)	0.015 (0.000-0.031)	
2013	0.008 (0.005-0.010)	0.013 (0.001-0.024)	0.014 (0.006-0.021)
2014	0.008 (0.005-0.010)	0.008 (0.000-0.021)	0.010 (0.003-0.018)
2015	0.009 (0.005-0.012)	0.005 (0.000-0.020)	0.008 (0.000-0.016)
2016		0.004 (0.000-0.022)	0.008 (0.000-0.018)

Table 19: PFC-116 emission (Gg yr^{-1}) estimates for the UK with uncertainty (5th - 95th percentile).

4.19 PFC-218

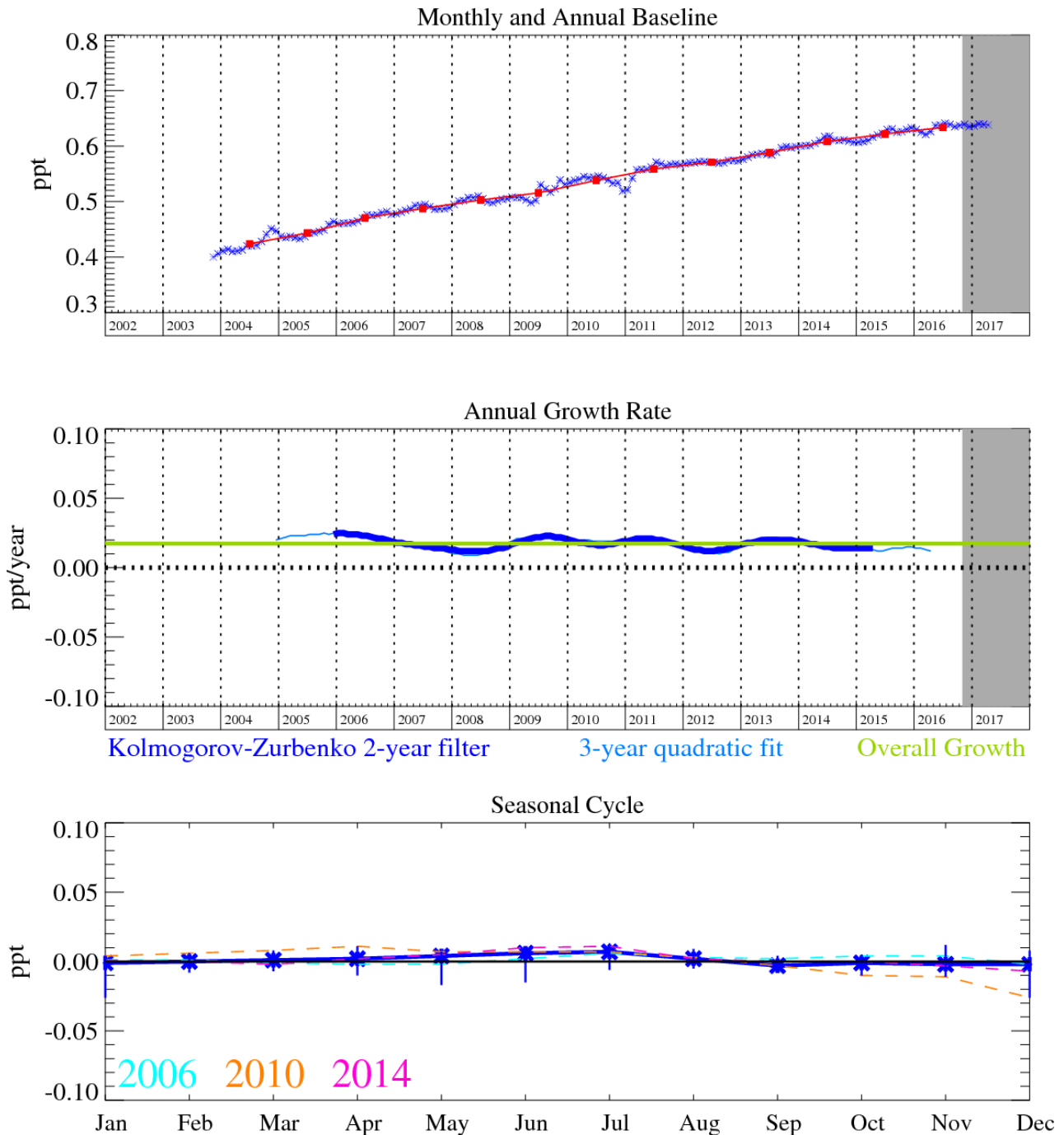


Figure 32: PFC-218 (C_3F_8): Monthly (blue) and annual (red) Northern Hemisphere baseline mole fractions (top plot). Annual (blue) and overall average growth rate (green) (middle plot). Seasonal cycle (de-trended) with year-to-year variability (lower plot). Grey area covers un-ratified and therefore provisional data.

PFC-218 (C_3F_8) has an atmospheric lifetime of 2600 years and a GWP_{100} of 8690. It is also used in semiconductor manufacturing, but to a lesser extent than C_2F_6 . It also has a very small contribution from aluminium smelting and has an increasing contribution from refrigeration use. Observations of above-baseline C_3F_8 emissions are less frequent than those of C_2F_6 but are of a higher relative magnitude.

There is a large uncertainty in the InTEM emission estimates because the pollution events are relatively difficult to model due to their intermittent and sparse occurrences. It is likely that the significant sources of this gas are specific, potentially intermittent, point sources that cannot be readily resolved by the large inversion grids used. Prior knowledge would be required to pin-point the significant point sources within the UK. The InTEM and inventory results are remarkably

consistent in trend, both showing a dip in emissions in 2008 – 2010. The InTEM estimates are higher than those estimated in the inventory.

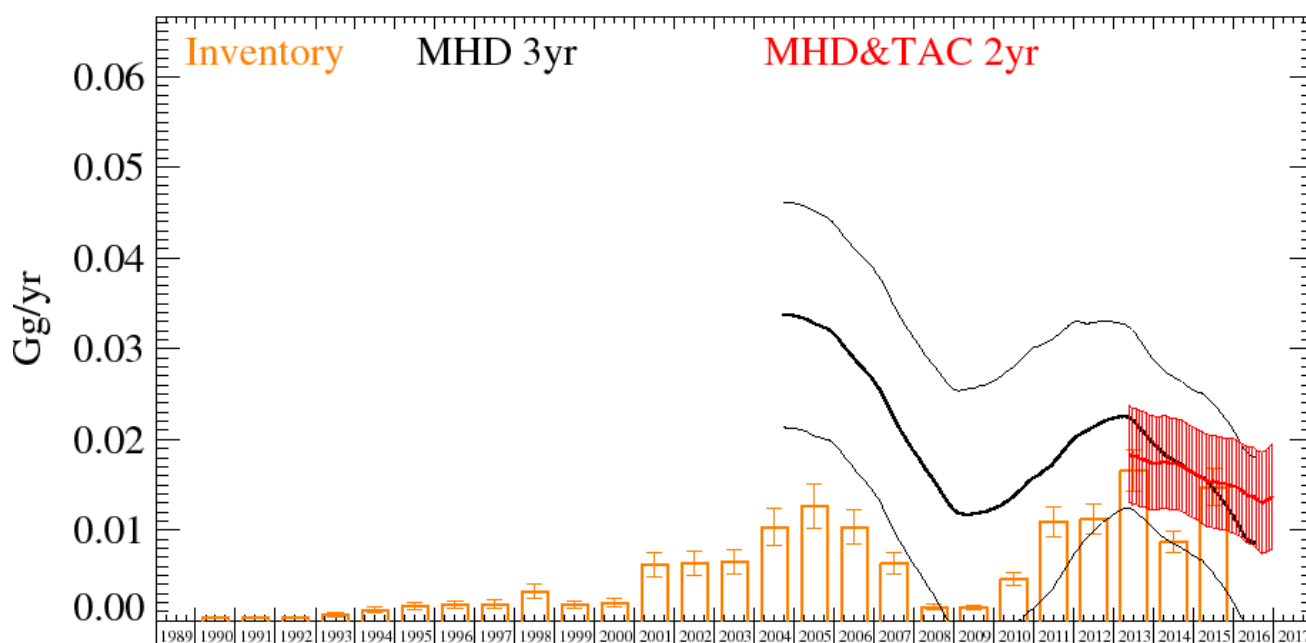


Figure 33: PFC-218 emission estimates (Gg yr^{-1}) from the UNFCCC Inventory and InTEM (MHD-only and DECC network) for the UK. The uncertainty bars represent the 5th and 95th percentiles.

Years	Inventory	MHD 3yr	MHD&TAC 2yr
1990	0.000 (0.000-0.000)		
1991	0.000 (0.000-0.000)		
1992	0.000 (0.000-0.000)		
1993	0.001 (0.000-0.001)		
1994	0.001 (0.001-0.002)		
1995	0.002 (0.001-0.002)		
1996	0.002 (0.001-0.002)		
1997	0.002 (0.001-0.002)		
1998	0.003 (0.002-0.004)		
1999	0.002 (0.001-0.002)		
2000	0.002 (0.001-0.002)		
2001	0.006 (0.005-0.008)		
2002	0.006 (0.005-0.008)		
2003	0.006 (0.005-0.008)		
2004	0.010 (0.008-0.012)	0.030 (0.018-0.043)	
2005	0.013 (0.010-0.015)	0.034 (0.021-0.046)	
2006	0.010 (0.008-0.012)	0.031 (0.019-0.044)	
2007	0.006 (0.005-0.007)	0.022 (0.010-0.035)	
2008	0.001 (0.001-0.002)	0.013 (0.001-0.026)	
2009	0.001 (0.001-0.002)	0.010 (0.000-0.024)	
2010	0.005 (0.004-0.005)	0.013 (0.000-0.028)	
2011	0.011 (0.009-0.013)	0.018 (0.004-0.033)	
2012	0.011 (0.009-0.013)	0.022 (0.010-0.034)	
2013	0.017 (0.014-0.019)	0.023 (0.014-0.032)	0.019 (0.013-0.024)
2014	0.009 (0.007-0.010)	0.018 (0.009-0.027)	0.017 (0.012-0.022)
2015	0.015 (0.013-0.017)	0.012 (0.002-0.021)	0.015 (0.010-0.020)
2016		0.009 (0.000-0.018)	0.014 (0.008-0.019)

Table 20: PFC-218 emission (Gg yr^{-1}) estimates for the UK with uncertainty (5th - 95th percentile).

4.20 PFC-318

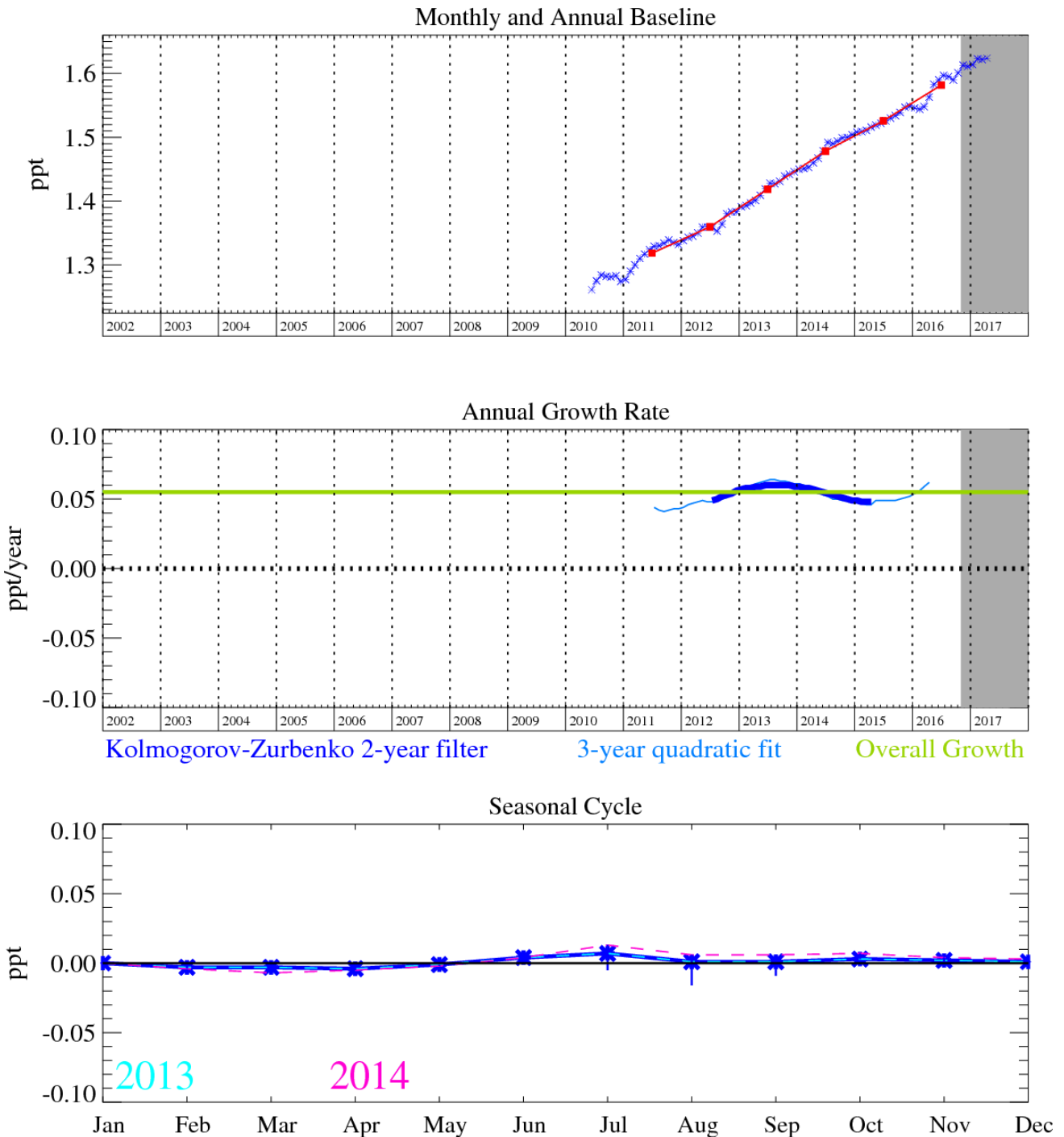


Figure 34: PFC-318 (c-C₄F₈): Monthly (blue) and annual (red) Northern Hemisphere baseline mole fractions (top plot). Annual (blue) and overall average growth rate (green) (middle plot). Seasonal cycle (de-trended) with year-to-year variability (lower plot). Grey area covers un-ratified and therefore provisional data.

PFC-319 (c-C₄F₈) is increasingly used in the semiconductor and electronics industries for cleaning, plasma etching and deposition gas, also it has more minor use in aerolyzed foods, retinal detachment surgery, size estimation of natural gas and oil reservoirs, specialist military applications, tracer experiments and may also replace SF₆ as an electrically insulating gas. It has an atmospheric lifetime of 3,200 years, a GWP₁₀₀ of 10,300 and a radiative efficiency of 0.32 W m⁻² ppb⁻¹.

The reported UK inventory emissions of PFC-318 are very small (less than 0.00002 Gg yr⁻¹) compared to the median InTEM emission estimates; however, the InTEM estimates have very significant uncertainty extending down to zero. The pollution episodes observed are very small and largely lost within the baseline noise. Also, it is likely that this gas is released intermittently thereby challenging one of the InTEM assumptions of uniform emissions within the inversion time-window.

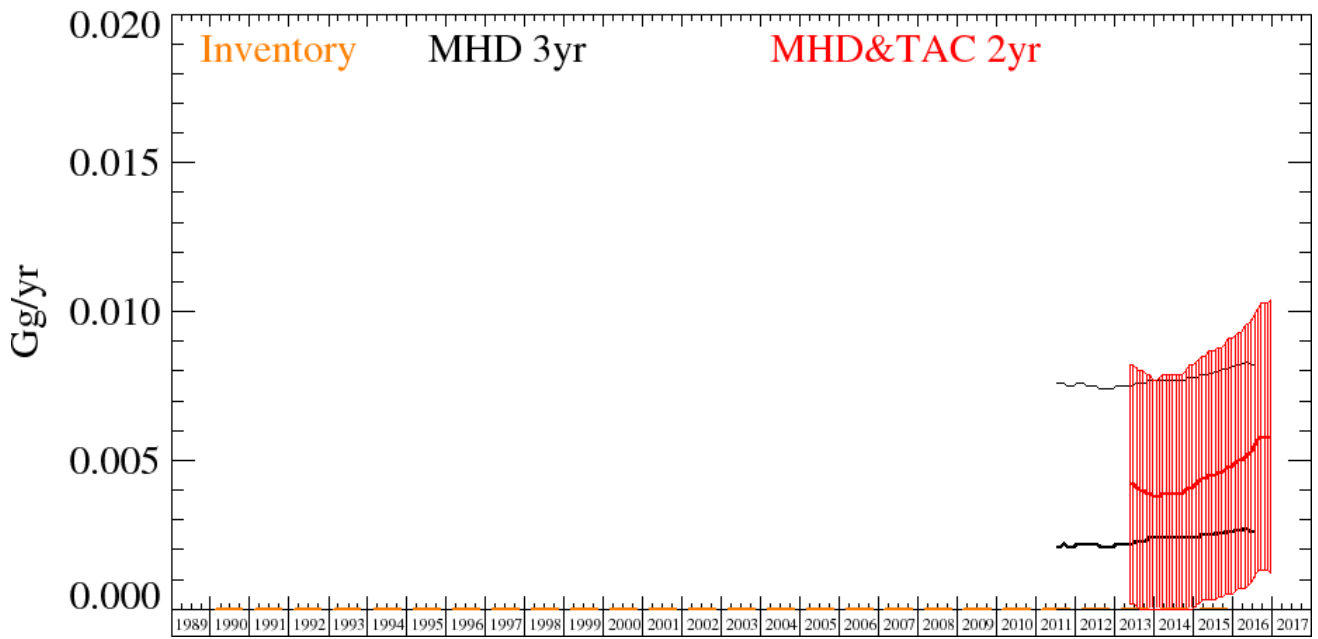


Figure 35: PFC-318 emission estimates (Gg yr^{-1}) from the UNFCCC Inventory and InTEM (MHD-only and DECC network) for the UK. The uncertainty bars represent the 5th and 95th percentiles

4.21 SF₆

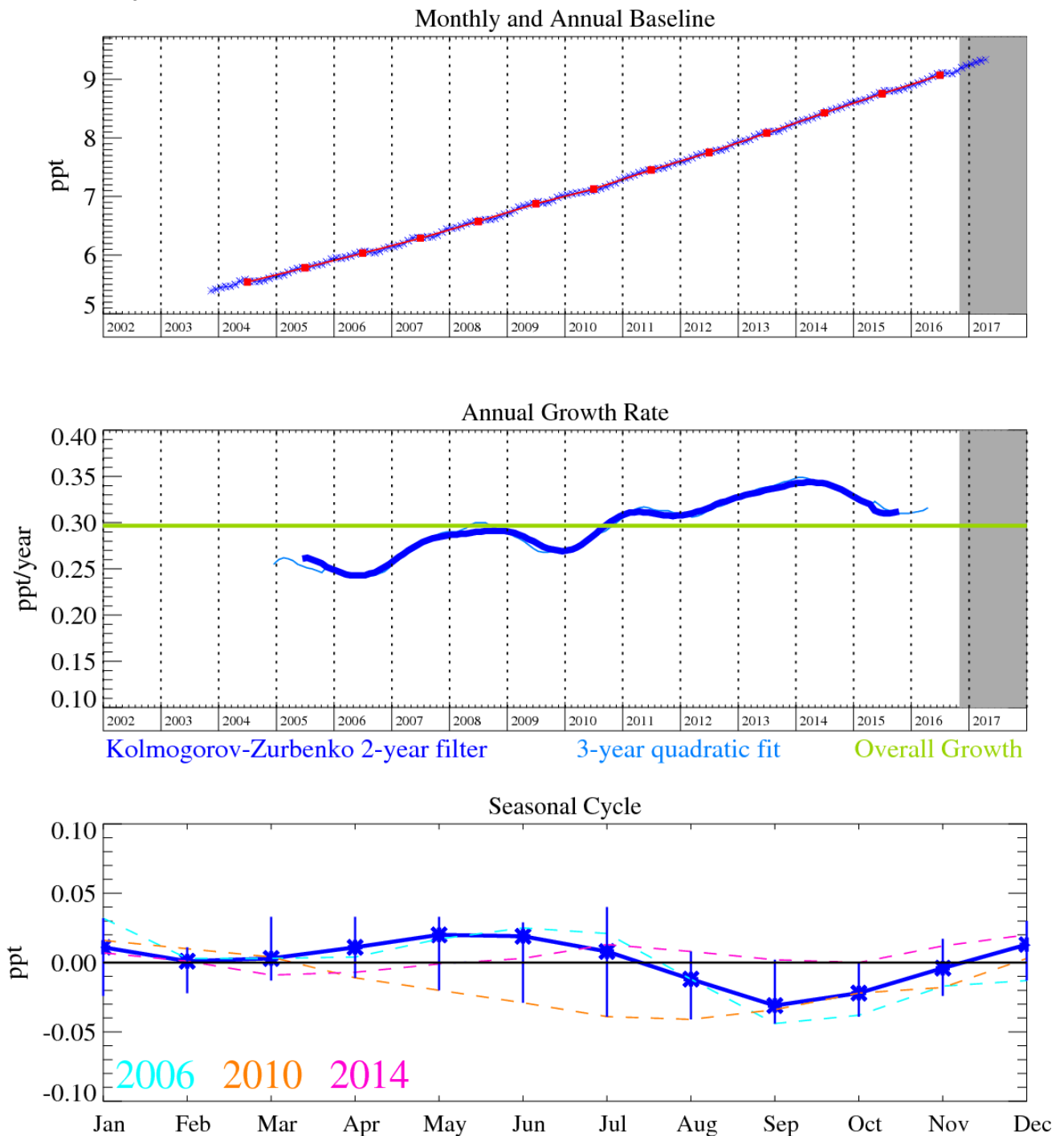


Figure 36: SF₆: Monthly (blue) and annual (red) Northern Hemisphere baseline mole fractions (top plot). Annual (blue) and overall average growth rate (green) (middle plot). Seasonal cycle (de-trended) with year-to-year variability (lower plot). Grey area covers un-ratified and therefore provisional data.

SF₆ is an important greenhouse gas since it has a long atmospheric lifetime of 3,200 years and a high radiative efficiency; giving rise to a GWP₁₀₀ of 22,800. Although having minor usage in the semiconductor industry, it is predominantly used in electrical circuit breakers, heavy-duty gas-insulated switchgear (GIS) for systems with voltages from 5,000-38,000 volts, and other switchgear used in the electrical transmission systems to manage high voltages (>38 kV). The electrical power industry uses roughly 80% of all SF₆ produced worldwide. Although the units themselves are hermetically sealed and pressurised, aging equipment, breakdown and disposal, alongside leakage from wear-and-tear will cause this sector to emit SF₆. A minor use of this gas is also reported in its use as a blanketing (i.e. oxygen inhibiting inert gas) agent during magnesium production. Hence SF₆ will have many, and more diffuse, sources relative to the other perfluorinated species. Its atmospheric trend was predicted to rise at a rate faster than linear, as older electrical switchgear is

switched to higher efficiency units; this is corroborated by the constantly increasing atmospheric growth rate over the last several years

Post 2009, the UK InTEM estimates are consistently elevated compared to the inventory; however, the InTEM uncertainty ranges are large and do encompass the inventory estimates. 5-site 6-month InTEM modelling indicates that SF₆ UK emissions may have a seasonal cycle, this is still under investigation.

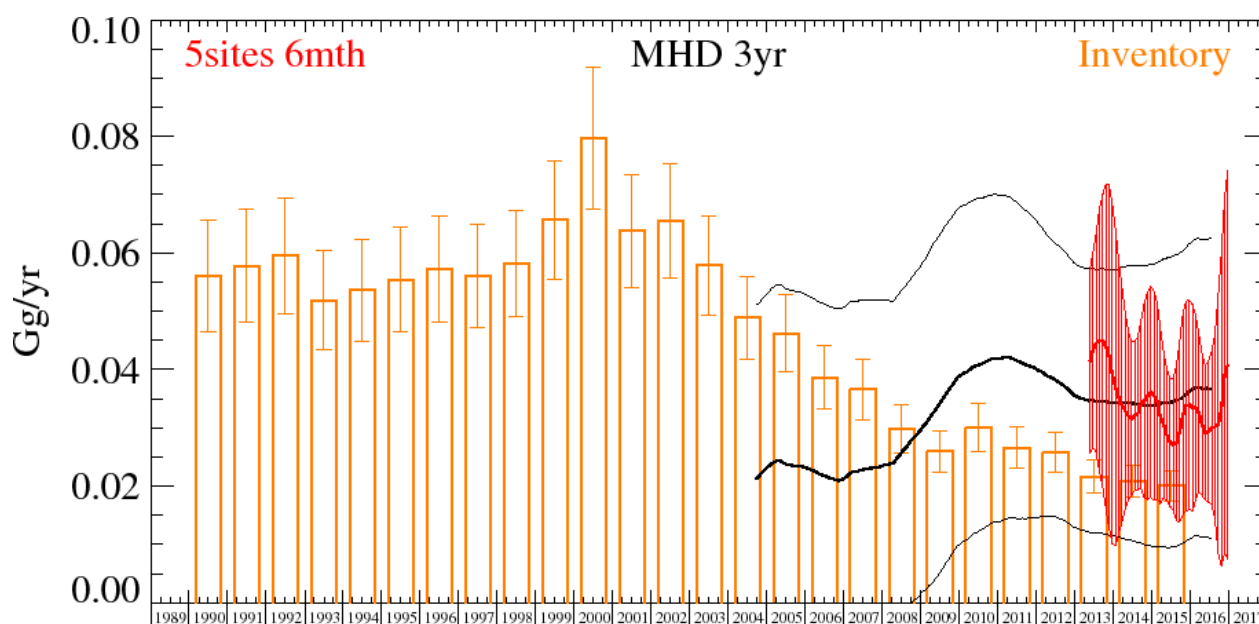


Figure 37: SF₆ emission estimates (Gg yr⁻¹) from the UNFCCC Inventory and InTEM (MHD-only and DECC + GAUGE network) for the UK. The uncertainty bars represent the 5th and 95th percentiles.

Years	Inventory	MHD 3yr	5sites 6mth
1990	0.056 (0.047-0.066)		
1991	0.058 (0.048-0.068)		
1992	0.060 (0.049-0.069)		
1993	0.052 (0.043-0.060)		
1994	0.053 (0.049-0.064)		
1995	0.055 (0.046-0.064)		
1996	0.057 (0.048-0.064)		
1997	0.056 (0.047-0.060)		
1998	0.058 (0.049-0.064)		
1999	0.066 (0.055-0.076)		
2000	0.080 (0.067-0.092)		
2001	0.064 (0.054-0.073)		
2002	0.066 (0.056-0.075)		
2003	0.058 (0.049-0.066)		
2004	0.049 (0.042-0.056)	0.014 (0.000-0.043)	
2005	0.046 (0.039-0.053)	0.023 (0.000-0.053)	
2006	0.039 (0.033-0.044)	0.023 (0.000-0.053)	
2007	0.037 (0.031-0.042)	0.020 (0.000-0.049)	
2008	0.030 (0.026-0.034)	0.024 (0.000-0.052)	
2009	0.026 (0.022-0.029)	0.036 (0.009-0.064)	
2010	0.030 (0.026-0.034)	0.043 (0.013-0.073)	
2011	0.027 (0.023-0.030)	0.042 (0.014-0.070)	
2012	0.026 (0.022-0.029)	0.038 (0.015-0.061)	
2013	0.022 (0.019-0.024)	0.033 (0.012-0.055)	0.043 (0.020-0.065)
2014	0.021 (0.018-0.023)	0.033 (0.010-0.057)	0.034 (0.016-0.052)
2015	0.020 (0.017-0.023)	0.036 (0.011-0.062)	0.031 (0.016-0.047)
2016		0.037 (0.011-0.063)	0.032 (0.013-0.052)
2017			0.054 (0.017-0.090)

Table 21: SF₆ emission (Gg yr⁻¹) estimates for the UK with uncertainty (5th - 95th percentile).

4.22 NF_3

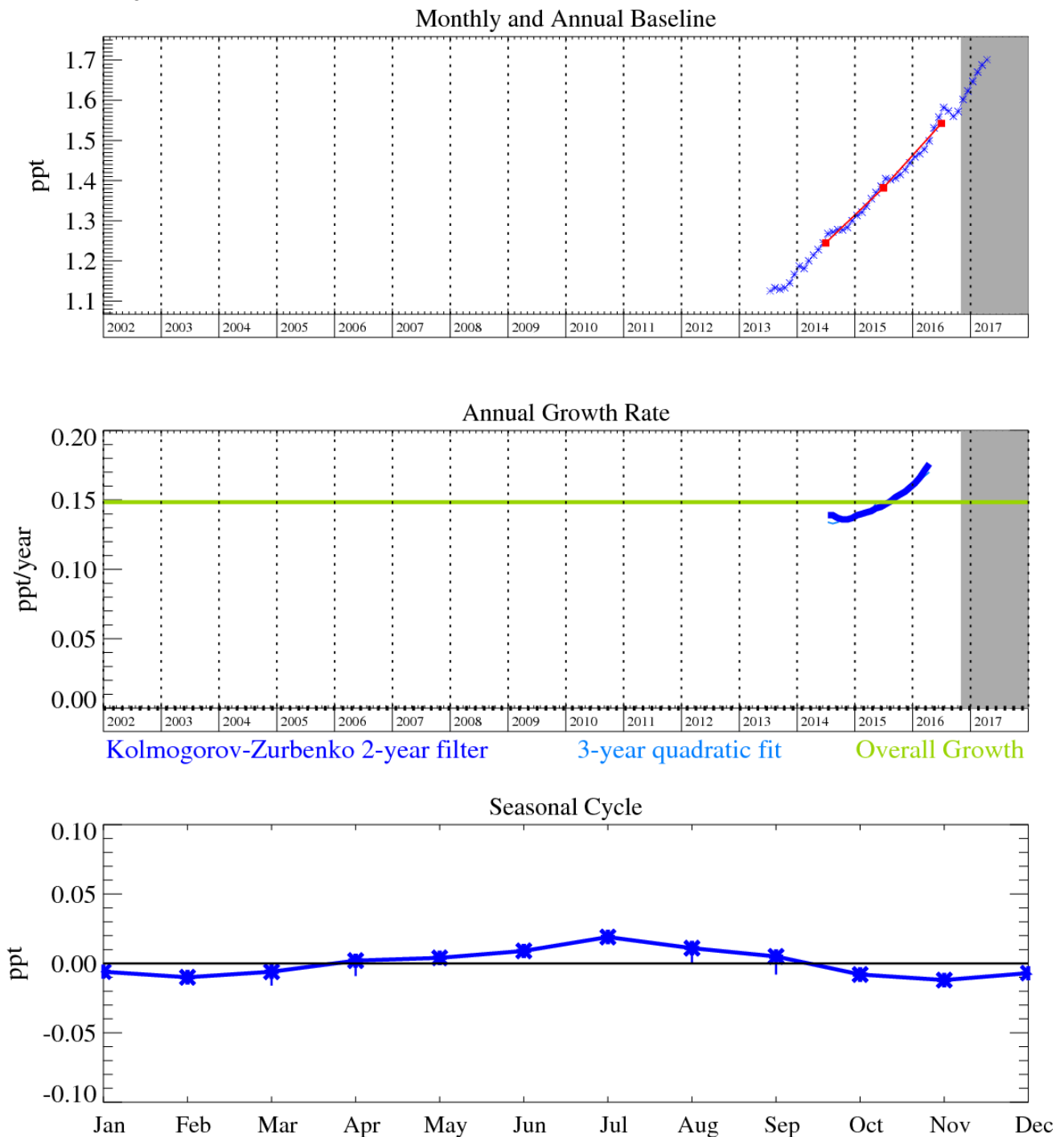


Figure 38: NF_3 : Monthly (blue) baseline mole fractions. Grey area covers un-ratified and therefore provisional data.

Production of nitrogen trifluoride (NF_3) has been increasing rapidly to meet demand in end use applications (the manufacture of semiconductor devices, flat panel displays and photovoltaic cells). The new ambient air measurements from the Advanced Global Atmospheric Gases Experiment have shown the rapidly rising global atmospheric abundance of this gas due to this market expansion. Although the current contribution of NF_3 to radiative forcing is small, its potential to impact the climate is significant (its GWP_{100} is 16,100).

The UK emissions of this gas, both estimated in the inventory and using InTEM, are very small. The pollution events seen at Mace Head are almost all lost within the baseline noise. The only exception to this was an episode when the air travelled quickly and directly from the NE USA (please refer to the 2015 report for more details).

5 Global emission estimates

5.1 Introduction

Global emissions and mole fraction estimates were made using baseline AGAGE observations from five “background” AGAGE stations (Mace Head, Ireland; Trinidad Head, California; Ragged Point, Barbados; Cape Matatula, American Samoa; and Cape Grim, Tasmania) using the method outlined in Rigby et al. (2014). A two-dimensional model of global atmospheric chemistry and transport was used to simulate baseline mole fractions in four latitudinal bands, separated at the equator and ± 30 degrees (Rigby et al., 2013). The modelled mole fractions were brought into consistency with the AGAGE observations using a Bayesian method in which an initial estimate of the emissions growth rate was adjusted in the inversion. Uncertainties in the derived global emissions estimates are determined by the observational uncertainty, model uncertainty and uncertainties in the atmospheric lifetimes of each gas. Global mole fractions and emissions of each of the measured gases reported to the UNFCCC are shown in Table 22 - Table 25 and Table 26 - Table 29 respectively.

5.2 Recent trends in non-CO₂ Kyoto gases

5.2.1 CH₄

Methane concentrations grew at 8 ppt yr⁻¹ between 2015 and 2016. This positive growth trend has continued since 2007, before which, growth was relatively constant between 2000 and 2006. In the previous report, studies were described that attributed the rise in methane to growth in livestock emissions or the growth in oil and gas extraction (Schaefer et al., 2016; Helmig et al., 2016). Some more recent studies have suggested an increase in tropical methane emissions as being the primary driver of the rise (Nisbet et al., 2016), although others also implicate fossil fuel extraction (Hausmann et al., 2016). In contrast, two studies have examined whether changes in the methane atmospheric sink could be responsible for recent growth trends (Rigby et al., 2017; Turner et al., 2017). Both studies find evidence for a rise and fall in the concentration of the hydroxyl radical (OH), which destroys methane in the atmosphere and is coincident with the methane pause and renewed growth. Although the derived OH changes explain much of the variability in methane growth, Rigby et al. (2017) still find a gradual rise in global emissions throughout this period. In contrast, Turner et al. (2017) find a maximum likelihood solution in which global methane emissions have declined in recent years. In both cases, uncertainties were very large, and a trajectory in which OH had not changed substantially could not be ruled out.

5.2.2 N₂O

Nitrous oxide is the third most important greenhouse gas after CO₂ and CH₄. It has grown steadily in the atmosphere, at a rate of around 0.8 ppb yr⁻¹ for the last decade. This steady growth is reflected in the derived global emissions rates, which have remained close to 28 Tg yr⁻¹. Sources of N₂O remain very uncertain. Recent studies have attempted to re-evaluate the global N₂O emissions distribution using multiple atmospheric models (Thompson et al. 2014). They find that the majority of N₂O emissions are likely to originate from land in the tropics, although the northern hemisphere extra-tropics were found to be more important sources than previously assumed. Recent work has suggested that the currently accepted lifetime for N₂O of 123 years (Ko et al. 2013) may be over-estimated, and a downward revision to 116 years may be required (Prather et al., 2015). This decrease in lifetime would lead to an increase in emissions inferred from atmospheric observations.

5.2.3 HFCs

Emissions of most of the major HFCs continued to grow between 2015 and 2016. This global growth is expected, as the phase-out of hydrochlorofluorocarbons (HCFCs) continues under the Montreal Protocol, with HFCs being the replacements for these compounds in refrigeration, air conditioning and foam blowing. Recently, Simmonds et al. (2017) showed that the growth since 2010 in combined emissions of HFC-134a, -142a, -32, and -125 have been somewhat slower than was predicted (Velders et al., 2009). However, the growth of HFC-32 and -125 has intensified, possibly reflecting the increased adoption of blends of these compounds in refrigeration (Lunt et al., 2015). Emissions of HFC-23 continued to decline between 2015 and 2016, perhaps reflecting the global freeze in HCFC-22 production, although the reasons for this change is currently under investigation. Emissions of HFC-152a have remained relatively constant since around 2010 (as noted in Simmonds et al., 2016).

5.2.4 PFCs, SF₆ and NF₃

Emissions of PFC-14 (CF₄) increased slightly between 2015 and 2016, although the emissions of this compound have been relatively low in the last decade. Trudinger et al. (2016) examined atmospheric CF₄ trends and inferred that the intensity of emissions from Aluminium production has dropped over time, causing a reduction in emissions despite continued growth in production. CF₄ and PFC-116 (C₂F₆) are also emitted from semiconductor manufacture, although the contribution of this source to the global total is poorly quantified (Kim et al., 2014). Following a decline since the 1990s (when emissions from the developed world were reported to have been reduced), emissions of SF₆ have continued to grow strongly since 2000, and are now at levels of 8.58 (8.23 - 8.99) Gg yr⁻¹. Emissions of NF₃ are rising rapidly, increasing by around 10% between 2015 and 2016. This rise is thought to reflect its increasing use in the electronics industry, where it is a replacement for C₂F₆ (Arnold et al., 2013).

Date	CH ₄ (ppb)	N ₂ O (ppb)	HFC-23 (ppt)	HFC-32 (ppt)	HFC-125 (ppt)
1978	(-)	300 (298 - 301)	(-)	(-)	(-)
1979	(-)	301 (299 - 302)	(-)	(-)	(-)
1980	(-)	301 (299 - 303)	(-)	(-)	(-)
1981	(-)	302 (300 - 303)	(-)	(-)	(-)
1982	(-)	303 (301 - 305)	(-)	(-)	(-)
1983	(-)	304 (302 - 305)	(-)	(-)	(-)
1984	(-)	304 (302 - 306)	(-)	(-)	(-)
1985	1680 (1670 - 1690)	304 (303 - 306)	(-)	(-)	(-)
1986	1670 (1660 - 1680)	305 (304 - 307)	(-)	(-)	(-)
1987	1680 (1670 - 1690)	306 (304 - 307)	(-)	(-)	(-)
1988	1690 (1680 - 1700)	307 (305 - 308)	(-)	(-)	(-)
1989	1710 (1700 - 1720)	308 (306 - 309)	(-)	(-)	(-)
1990	1710 (1710 - 1720)	309 (307 - 310)	(-)	(-)	(-)
1991	1730 (1720 - 1740)	310 (308 - 311)	(-)	(-)	(-)
1992	1740 (1730 - 1750)	310 (308 - 312)	(-)	(-)	(-)
1993	1740 (1730 - 1750)	310 (309 - 312)	(-)	(-)	(-)
1994	1740 (1740 - 1750)	311 (309 - 313)	(-)	(-)	(-)
1995	1750 (1740 - 1760)	312 (310 - 313)	(-)	(-)	(-)
1996	1750 (1740 - 1760)	313 (311 - 314)	(-)	(-)	(-)
1997	1750 (1740 - 1760)	314 (312 - 315)	(-)	(-)	(-)
1998	1760 (1750 - 1770)	314 (313 - 316)	(-)	0.126 (0.072 - 0.180)	0.99 (0.94 - 1.05)
1999	1770 (1760 - 1780)	315 (313 - 317)	(-)	0.173 (0.120 - 0.226)	1.22 (1.16 - 1.29)
2000	1770 (1760 - 1780)	316 (314 - 318)	(-)	0.229 (0.184 - 0.274)	1.53 (1.45 - 1.61)
2001	1770 (1760 - 1780)	317 (315 - 319)	(-)	0.304 (0.251 - 0.354)	1.93 (1.83 - 2.03)
2002	1770 (1760 - 1780)	318 (316 - 319)	(-)	0.414 (0.366 - 0.465)	2.34 (2.23 - 2.46)
2003	1780 (1770 - 1790)	318 (317 - 320)	(-)	0.565 (0.521 - 0.607)	2.87 (2.73 - 3.02)
2004	1780 (1770 - 1780)	319 (317 - 321)	(-)	0.832 (0.804 - 0.864)	3.43 (3.27 - 3.61)
2005	1770 (1770 - 1780)	320 (318 - 321)	(-)	1.20 (1.17 - 1.24)	4.06 (3.87 - 4.27)
2006	1770 (1770 - 1780)	320 (319 - 322)	(-)	1.61 (1.56 - 1.66)	4.78 (4.55 - 5.03)
2007	1780 (1770 - 1790)	321 (319 - 323)	21.1 (20.6 - 21.5)	2.13 (2.07 - 2.20)	5.62 (5.35 - 5.91)
2008	1790 (1780 - 1800)	322 (320 - 324)	21.9 (21.4 - 22.3)	2.69 (2.61 - 2.77)	6.60 (6.28 - 6.94)
2009	1790 (1780 - 1800)	323 (321 - 325)	22.6 (22.1 - 23.0)	3.27 (3.18 - 3.37)	7.67 (7.30 - 8.07)
2010	1800 (1790 - 1810)	324 (322 - 325)	23.3 (22.8 - 23.7)	4.08 (3.96 - 4.20)	8.94 (8.50 - 9.40)
2011	1800 (1790 - 1810)	325 (323 - 326)	24.1 (23.6 - 24.5)	5.14 (4.99 - 5.29)	10.5 (9.94 - 11.0)
2012	1810 (1800 - 1820)	326 (324 - 327)	25.0 (24.5 - 25.4)	6.23 (6.04 - 6.41)	12.1 (11.5 - 12.7)
2013	1810 (1810 - 1820)	327 (325 - 328)	26.0 (25.5 - 26.5)	7.51 (7.28 - 7.73)	14.0 (13.3 - 14.7)
2014	1820 (1810 - 1830)	328 (326 - 329)	27.0 (26.5 - 27.5)	8.96 (8.70 - 9.23)	16.1 (15.3 - 16.9)
2015	1830 (1820 - 1840)	329 (327 - 330)	28.0 (27.5 - 28.6)	10.7 (10.4 - 11.0)	18.5 (17.6 - 19.4)
2016	1840 (1830 - 1850)	329 (328 - 331)	28.9 (28.3 - 29.5)	12.4 (12.0 - 12.8)	20.7 (19.7 - 21.8)

Table 22: Modelled global mole fractions with uncertainties

Date	HFC-134a (ppt)	HFC-143a (ppt)	HFC-152a (ppt)	HFC-227ea (ppt)	HFC-236fa (ppt)
1978	(-)	(-)	(-)	(-)	(-)
1979	(-)	(-)	(-)	(-)	(-)
1980	(-)	0.098 (0.041 - 0.155)	(-)	(-)	(-)
1981	(-)	0.214 (0.061 - 0.351)	(-)	(-)	(-)
1982	(-)	0.196 (0.092 - 0.294)	(-)	(-)	(-)
1983	(-)	0.195 (0.140 - 0.244)	(-)	(-)	(-)
1984	(-)	0.210 (0.111 - 0.307)	(-)	(-)	(-)
1985	(-)	0.243 (0.180 - 0.303)	(-)	(-)	(-)
1986	(-)	0.290 (0.245 - 0.334)	(-)	(-)	(-)
1987	(-)	0.310 (0.221 - 0.392)	(-)	(-)	(-)
1988	(-)	0.368 (0.315 - 0.420)	(-)	(-)	(-)
1989	(-)	0.426 (0.378 - 0.473)	(-)	(-)	(-)
1990	(-)	0.483 (0.420 - 0.542)	(-)	(-)	(-)
1991	(-)	0.538 (0.490 - 0.583)	(-)	(-)	(-)
1992	(-)	0.574 (0.523 - 0.622)	(-)	(-)	(-)
1993	(-)	0.619 (0.563 - 0.677)	(-)	(-)	(-)
1994	1.03 (0.94 - 1.13)	0.691 (0.644 - 0.739)	0.82 (0.78 - 0.86)	(-)	(-)
1995	1.99 (1.91 - 2.09)	0.810 (0.762 - 0.857)	1.05 (1.01 - 1.09)	(-)	(-)
1996	3.43 (3.35 - 3.54)	0.995 (0.944 - 1.04)	1.15 (1.12 - 1.20)	(-)	(-)
1997	5.35 (5.23 - 5.47)	1.24 (1.17 - 1.31)	1.27 (1.23 - 1.32)	(-)	(-)
1998	8.02 (7.87 - 8.16)	1.61 (1.55 - 1.68)	1.54 (1.49 - 1.59)	(-)	(-)
1999	11.1 (10.9 - 11.3)	2.00 (1.93 - 2.08)	1.69 (1.63 - 1.75)	(-)	(-)
2000	14.5 (14.3 - 14.7)	2.45 (2.36 - 2.54)	1.87 (1.81 - 1.93)	(-)	(-)
2001	17.9 (17.7 - 18.2)	2.97 (2.86 - 3.09)	2.10 (2.03 - 2.17)	(-)	(-)
2002	21.7 (21.4 - 22.1)	3.59 (3.47 - 3.71)	2.40 (2.33 - 2.48)	(-)	(-)
2003	25.9 (25.5 - 26.3)	4.20 (4.07 - 4.34)	2.82 (2.73 - 2.91)	(-)	(-)
2004	30.3 (29.9 - 30.8)	4.92 (4.78 - 5.07)	3.25 (3.15 - 3.36)	(-)	(-)
2005	34.7 (34.2 - 35.2)	5.71 (5.54 - 5.88)	3.75 (3.64 - 3.88)	(-)	(-)
2006	39.0 (38.4 - 39.6)	6.62 (6.43 - 6.82)	4.48 (4.35 - 4.63)	0.364 (0.333 - 0.394)	0.058 (0.046 - 0.070)
2007	43.4 (42.8 - 44.0)	7.59 (7.35 - 7.81)	5.27 (5.12 - 5.45)	0.429 (0.393 - 0.463)	0.065 (0.051 - 0.079)
2008	48.0 (47.4 - 48.7)	8.63 (8.37 - 8.88)	5.81 (5.64 - 6.01)	0.497 (0.454 - 0.535)	0.073 (0.057 - 0.088)
2009	52.7 (52.0 - 53.5)	9.73 (9.42 - 10.0)	5.97 (5.80 - 6.18)	0.573 (0.525 - 0.617)	0.081 (0.063 - 0.098)
2010	57.8 (57.0 - 58.6)	10.9 (10.5 - 11.2)	6.26 (6.08 - 6.48)	0.654 (0.598 - 0.704)	0.089 (0.070 - 0.108)
2011	62.8 (61.9 - 63.7)	12.1 (11.7 - 12.4)	6.61 (6.41 - 6.83)	0.736 (0.675 - 0.794)	0.099 (0.078 - 0.120)
2012	67.7 (66.7 - 68.7)	13.4 (13.0 - 13.8)	6.77 (6.58 - 7.01)	0.822 (0.754 - 0.884)	0.109 (0.086 - 0.132)
2013	72.7 (71.7 - 73.8)	14.7 (14.3 - 15.2)	6.73 (6.54 - 6.96)	0.922 (0.845 - 0.992)	0.120 (0.094 - 0.145)
2014	77.9 (76.9 - 79.1)	16.2 (15.7 - 16.7)	6.64 (6.45 - 6.86)	1.02 (0.936 - 1.10)	0.130 (0.102 - 0.158)
2015	83.4 (82.2 - 84.6)	17.7 (17.2 - 18.2)	6.61 (6.41 - 6.83)	1.12 (1.03 - 1.21)	0.140 (0.110 - 0.170)
2016	89.2 (88.0 - 90.5)	19.3 (18.7 - 19.9)	6.71 (6.51 - 6.94)	1.24 (1.13 - 1.33)	0.150 (0.118 - 0.182)

Table 23: Modelled global mole fractions with uncertainties

Date	HFC-245fa (ppt)	HFC-365mfc (ppt)	PFC-14 (ppt)	PFC-116 (ppt)
1978	(-)	(-)	50.8 (49.4 - 52.3)	1.04 (1.01 - 1.07)
1979	(-)	(-)	52.2 (50.7 - 53.7)	1.13 (1.09 - 1.16)
1980	(-)	(-)	53.5 (52.0 - 55.0)	1.21 (1.18 - 1.26)
1981	(-)	(-)	54.6 (53.1 - 56.2)	1.30 (1.26 - 1.34)
1982	(-)	(-)	55.6 (54.0 - 57.3)	1.37 (1.32 - 1.41)
1983	(-)	(-)	56.6 (55.0 - 58.3)	1.44 (1.40 - 1.48)
1984	(-)	(-)	57.7 (56.1 - 59.5)	1.53 (1.48 - 1.58)
1985	(-)	(-)	58.7 (57.1 - 60.5)	1.62 (1.57 - 1.66)
1986	(-)	(-)	59.7 (58.0 - 61.5)	1.71 (1.66 - 1.76)
1987	(-)	(-)	60.7 (59.0 - 62.5)	1.80 (1.75 - 1.85)
1988	(-)	(-)	61.7 (60.0 - 63.5)	1.89 (1.84 - 1.95)
1989	(-)	(-)	62.8 (61.0 - 64.7)	1.98 (1.93 - 2.04)
1990	(-)	(-)	63.8 (62.0 - 65.7)	2.07 (2.02 - 2.14)
1991	(-)	(-)	64.8 (63.0 - 66.8)	2.16 (2.10 - 2.23)
1992	(-)	(-)	65.7 (63.8 - 67.7)	2.25 (2.19 - 2.32)
1993	(-)	(-)	66.5 (64.6 - 68.5)	2.34 (2.27 - 2.41)
1994	(-)	(-)	67.2 (65.3 - 69.2)	2.42 (2.36 - 2.49)
1995	(-)	(-)	67.9 (66.0 - 69.9)	2.51 (2.44 - 2.59)
1996	(-)	(-)	68.7 (66.7 - 70.7)	2.62 (2.55 - 2.70)
1997	(-)	(-)	69.4 (67.5 - 71.5)	2.73 (2.66 - 2.82)
1998	(-)	(-)	70.1 (68.2 - 72.2)	2.86 (2.78 - 2.94)
1999	(-)	(-)	70.8 (68.8 - 72.9)	2.99 (2.91 - 3.08)
2000	(-)	(-)	71.5 (69.4 - 73.6)	3.11 (3.03 - 3.21)
2001	(-)	(-)	72.1 (70.1 - 74.3)	3.23 (3.15 - 3.33)
2002	(-)	(-)	72.8 (70.7 - 75.0)	3.35 (3.26 - 3.45)
2003	(-)	0.059 (0.049 - 0.069)	73.5 (71.5 - 75.7)	3.46 (3.37 - 3.57)
2004	(-)	0.126 (0.108 - 0.145)	74.3 (72.2 - 76.5)	3.57 (3.47 - 3.67)
2005	(-)	0.217 (0.185 - 0.247)	75.0 (72.9 - 77.2)	3.66 (3.56 - 3.77)
2006	0.60 (0.55 - 0.65)	0.316 (0.271 - 0.359)	75.7 (73.6 - 77.9)	3.75 (3.65 - 3.87)
2007	0.83 (0.77 - 0.90)	0.406 (0.349 - 0.462)	76.4 (74.3 - 78.7)	3.85 (3.74 - 3.96)
2008	1.03 (0.95 - 1.11)	0.480 (0.413 - 0.548)	77.1 (74.9 - 79.4)	3.93 (3.83 - 4.05)
2009	1.18 (1.09 - 1.28)	0.537 (0.459 - 0.613)	77.7 (75.5 - 80.0)	4.01 (3.90 - 4.13)
2010	1.34 (1.24 - 1.44)	0.589 (0.504 - 0.673)	78.3 (76.1 - 80.6)	4.09 (3.98 - 4.21)
2011	1.51 (1.40 - 1.63)	0.648 (0.555 - 0.736)	79.0 (76.8 - 81.4)	4.17 (4.06 - 4.29)
2012	1.70 (1.57 - 1.83)	0.711 (0.611 - 0.807)	79.7 (77.5 - 82.1)	4.25 (4.13 - 4.38)
2013	1.88 (1.74 - 2.03)	0.776 (0.666 - 0.883)	80.5 (78.2 - 82.8)	4.33 (4.21 - 4.45)
2014	2.05 (1.90 - 2.21)	0.845 (0.726 - 0.962)	81.2 (78.9 - 83.6)	4.41 (4.28 - 4.54)
2015	2.23 (2.06 - 2.41)	0.919 (0.788 - 1.05)	81.9 (79.6 - 84.3)	4.49 (4.36 - 4.62)
2016	2.42 (2.23 - 2.61)	0.994 (0.851 - 1.14)	82.7 (80.4 - 85.2)	4.57 (4.44 - 4.70)

Table 24: Modelled global mole fractions with uncertainties

Date	PFC-318 (ppt)	SF ₆ (ppt)	NF ₃ (ppt)
1978	(-)	0.66 (0.64 - 0.68)	(-)
1979	(-)	0.76 (0.74 - 0.79)	(-)
1980	(-)	0.87 (0.85 - 0.89)	(-)
1981	(-)	0.98 (0.96 - 1.01)	(-)
1982	(-)	1.11 (1.08 - 1.13)	(-)
1983	0.072 (0.066 - 0.077)	1.21 (1.19 - 1.24)	(-)
1984	0.076 (0.072 - 0.080)	1.33 (1.30 - 1.36)	(-)
1985	0.082 (0.078 - 0.086)	1.48 (1.45 - 1.51)	(-)
1986	0.089 (0.085 - 0.093)	1.66 (1.62 - 1.69)	(-)
1987	0.096 (0.092 - 0.101)	1.84 (1.80 - 1.88)	(-)
1988	0.104 (0.099 - 0.108)	2.00 (1.96 - 2.05)	(-)
1989	0.111 (0.106 - 0.116)	2.17 (2.13 - 2.21)	(-)
1990	0.118 (0.113 - 0.123)	2.36 (2.31 - 2.40)	(-)
1991	0.126 (0.120 - 0.132)	2.57 (2.52 - 2.61)	(-)
1992	0.135 (0.128 - 0.140)	2.76 (2.71 - 2.82)	(-)
1993	0.145 (0.138 - 0.151)	2.97 (2.91 - 3.02)	(-)
1994	0.157 (0.149 - 0.163)	3.19 (3.13 - 3.25)	(-)
1995	0.171 (0.163 - 0.179)	3.44 (3.38 - 3.51)	(-)
1996	0.189 (0.180 - 0.196)	3.70 (3.62 - 3.77)	(-)
1997	0.209 (0.200 - 0.218)	3.93 (3.85 - 4.01)	(-)
1998	0.232 (0.222 - 0.241)	4.15 (4.07 - 4.23)	(-)
1999	0.257 (0.245 - 0.268)	4.34 (4.26 - 4.43)	(-)
2000	0.284 (0.271 - 0.296)	4.53 (4.44 - 4.62)	(-)
2001	0.312 (0.298 - 0.325)	4.73 (4.63 - 4.82)	(-)
2002	0.341 (0.326 - 0.355)	4.94 (4.84 - 5.04)	(-)
2003	0.371 (0.354 - 0.385)	5.17 (5.06 - 5.27)	(-)
2004	0.400 (0.382 - 0.415)	5.40 (5.29 - 5.50)	(-)
2005	0.427 (0.408 - 0.444)	5.62 (5.51 - 5.73)	(-)
2006	0.453 (0.433 - 0.471)	5.87 (5.76 - 5.98)	(-)
2007	0.477 (0.456 - 0.495)	6.14 (6.02 - 6.25)	(-)
2008	0.498 (0.476 - 0.518)	6.42 (6.30 - 6.54)	(-)
2009	0.518 (0.495 - 0.538)	6.70 (6.57 - 6.83)	(-)
2010	0.537 (0.513 - 0.558)	6.99 (6.85 - 7.12)	(-)
2011	0.554 (0.529 - 0.576)	7.28 (7.14 - 7.42)	(-)
2012	0.571 (0.546 - 0.594)	7.58 (7.44 - 7.73)	(-)
2013	0.587 (0.561 - 0.610)	7.90 (7.75 - 8.05)	1.05 (1.01 - 1.08)
2014	0.603 (0.576 - 0.626)	8.23 (8.07 - 8.38)	1.17 (1.13 - 1.20)
2015	0.619 (0.591 - 0.643)	8.55 (8.39 - 8.72)	1.30 (1.27 - 1.34)
2016	0.635 (0.606 - 0.660)	8.88 (8.71 - 9.06)	1.45 (1.41 - 1.49)

Table 25: Modelled global mole fractions with uncertainties

Date	CH ₄ (Tg yr ⁻¹)	N ₂ O (Tg yr ⁻¹)	HFC-23 (Gg yr ⁻¹)	HFC-32 (Gg yr ⁻¹)	HFC-125 (Gg yr ⁻¹)
1978	(-)	24.4 (22.1 - 26.6)	(-)	(-)	(-)
1979	(-)	22.9 (20.6 - 24.9)	(-)	(-)	(-)
1980	(-)	23.0 (20.9 - 24.9)	(-)	(-)	(-)
1981	(-)	25.3 (23.2 - 27.3)	(-)	(-)	(-)
1982	(-)	26.7 (24.5 - 28.8)	(-)	(-)	(-)
1983	(-)	22.4 (20.2 - 24.5)	(-)	(-)	(-)
1984	(-)	22.5 (20.3 - 24.7)	(-)	(-)	(-)
1985	357 (285 - 433)	23.3 (21.2 - 25.3)	(-)	(-)	(-)
1986	479 (408 - 553)	24.7 (22.5 - 26.8)	(-)	(-)	(-)
1987	502 (433 - 573)	24.8 (22.4 - 26.9)	(-)	(-)	(-)
1988	536 (466 - 610)	25.4 (23.3 - 27.5)	(-)	(-)	(-)
1989	493 (424 - 565)	26.4 (24.2 - 28.6)	(-)	(-)	(-)
1990	549 (480 - 625)	27.3 (25.2 - 29.4)	(-)	(-)	(-)
1991	543 (471 - 618)	24.3 (22.0 - 26.4)	(-)	(-)	(-)
1992	491 (419 - 566)	22.4 (20.3 - 24.5)	(-)	(-)	(-)
1993	527 (457 - 603)	22.4 (20.2 - 24.5)	(-)	(-)	(-)
1994	518 (446 - 593)	25.1 (23.0 - 27.2)	(-)	(-)	(-)
1995	515 (445 - 591)	25.4 (23.3 - 27.4)	(-)	(-)	(-)
1996	517 (446 - 592)	26.7 (24.5 - 28.8)	(-)	(-)	(-)
1997	516 (447 - 590)	25.7 (23.5 - 27.7)	(-)	(-)	(-)
1998	552 (482 - 628)	25.9 (23.8 - 27.9)	(-)	0.838 (-0.270 - 1.91)	7.38 (6.83 - 8.00)
1999	522 (452 - 599)	26.4 (24.3 - 28.4)	(-)	0.662 (-0.281 - 1.62)	6.26 (5.78 - 6.74)
2000	514 (444 - 590)	27.2 (25.1 - 29.3)	(-)	0.675 (-0.212 - 1.54)	8.51 (7.89 - 9.14)
2001	517 (447 - 592)	24.8 (22.7 - 26.8)	(-)	1.35 (0.540 - 2.20)	8.98 (8.37 - 9.72)
2002	520 (448 - 595)	24.5 (22.3 - 26.6)	(-)	1.69 (0.645 - 2.71)	11.2 (10.4 - 12.0)
2003	526 (455 - 602)	25.8 (23.6 - 27.8)	(-)	3.06 (2.22 - 3.95)	13.7 (12.6 - 14.7)
2004	510 (439 - 586)	24.9 (22.7 - 27.0)	(-)	4.14 (3.77 - 4.54)	14.3 (13.3 - 15.4)
2005	522 (451 - 599)	25.7 (23.5 - 27.7)	(-)	5.40 (4.93 - 5.92)	16.6 (15.4 - 17.8)
2006	513 (441 - 588)	25.3 (23.1 - 27.4)	(-)	6.83 (6.23 - 7.46)	19.2 (17.9 - 20.6)
2007	543 (471 - 619)	26.7 (24.4 - 28.8)	11.5 (10.8 - 12.2)	8.31 (7.53 - 9.10)	21.7 (20.2 - 23.3)
2008	533 (461 - 609)	26.8 (24.7 - 28.8)	11.2 (10.6 - 11.7)	9.74 (8.78 - 10.7)	26.1 (24.5 - 28.0)
2009	524 (452 - 598)	26.1 (23.9 - 28.2)	9.56 (9.00 - 10.2)	11.1 (9.99 - 12.3)	27.9 (26.1 - 29.9)
2010	550 (476 - 627)	26.7 (24.5 - 28.8)	10.4 (9.85 - 10.9)	15.4 (14.0 - 17.0)	35.2 (32.9 - 37.6)
2011	539 (468 - 616)	27.5 (25.2 - 29.6)	11.6 (11.0 - 12.2)	18.0 (16.2 - 19.8)	39.4 (36.7 - 42.1)
2012	540 (467 - 616)	27.1 (24.8 - 29.3)	12.9 (12.3 - 13.5)	20.8 (18.8 - 23.0)	44.4 (41.5 - 47.7)
2013	545 (472 - 623)	27.8 (25.6 - 29.9)	14.0 (13.3 - 14.6)	24.5 (22.0 - 27.1)	49.3 (46.0 - 52.9)
2014	557 (482 - 634)	28.3 (26.1 - 30.4)	14.5 (13.8 - 15.1)	29.9 (26.9 - 33.0)	58.8 (55.0 - 63.0)
2015	559 (485 - 638)	26.8 (24.6 - 29.0)	13.0 (12.4 - 13.7)	33.4 (29.8 - 37.1)	59.5 (55.5 - 63.8)
2016	559 (484 - 638)	26.8 (24.6 - 28.9)	12.3 (11.6 - 13.0)	36.5 (32.7 - 40.8)	63.7 (59.1 - 68.7)

Table 26: Modelled global emissions with uncertainties

Date	HFC-134a (Gg yr ⁻¹)	HFC-143a (Gg yr ⁻¹)	HFC-152a (Gg yr ⁻¹)	HFC-227ea (Gg yr ⁻¹)	HFC-236fa (Gg yr ⁻¹)
1978	(-)	(-)	(-)	(-)	(-)
1979	(-)	(-)	(-)	(-)	(-)
1980	(-)	2.37 (0.112 - 4.39)	(-)	(-)	(-)
1981	(-)	0.950 (-1.397 - 3.29)	(-)	(-)	(-)
1982	(-)	-0.501 (-2.573 - 1.66)	(-)	(-)	(-)
1983	(-)	0.173 (-1.589 - 1.76)	(-)	(-)	(-)
1984	(-)	0.0463 (-1.487 - 1.55)	(-)	(-)	(-)
1985	(-)	0.601 (-0.938 - 2.49)	(-)	(-)	(-)
1986	(-)	0.830 (-0.511 - 2.10)	(-)	(-)	(-)
1987	(-)	0.405 (-0.739 - 1.50)	(-)	(-)	(-)
1988	(-)	1.38 (0.157 - 2.75)	(-)	(-)	(-)
1989	(-)	0.786 (-0.227 - 1.83)	(-)	(-)	(-)
1990	(-)	0.921 (-0.171 - 2.07)	(-)	(-)	(-)
1991	(-)	1.10 (-0.206 - 2.35)	(-)	(-)	(-)
1992	(-)	0.584 (-0.736 - 2.00)	(-)	(-)	(-)
1993	(-)	1.34 (-0.077 - 2.87)	(-)	(-)	(-)
1994	15.0 (12.5 - 17.6)	1.12 (-0.063 - 2.37)	10.8 (9.44 - 12.0)	(-)	(-)
1995	21.3 (20.3 - 22.4)	2.46 (1.32 - 3.51)	10.8 (9.38 - 12.0)	(-)	(-)
1996	33.1 (31.8 - 34.6)	3.44 (2.41 - 4.46)	11.6 (10.1 - 13.0)	(-)	(-)
1997	43.0 (40.9 - 45.0)	4.54 (3.34 - 5.70)	13.3 (11.6 - 14.9)	(-)	(-)
1998	60.6 (57.5 - 63.4)	5.63 (4.34 - 7.05)	14.7 (12.6 - 16.5)	(-)	(-)
1999	71.5 (68.0 - 75.1)	6.29 (4.80 - 7.78)	16.1 (13.9 - 18.1)	(-)	(-)
2000	79.8 (75.6 - 83.9)	7.36 (5.82 - 8.82)	18.0 (15.7 - 20.2)	(-)	(-)
2001	86.6 (81.4 - 91.8)	9.05 (7.38 - 10.7)	19.6 (16.7 - 22.1)	(-)	(-)
2002	100. (93.7 - 106)	9.71 (8.08 - 11.5)	23.3 (20.2 - 26.2)	(-)	(-)
2003	109 (102 - 117)	11.4 (9.81 - 12.9)	27.0 (23.2 - 30.2)	(-)	(-)
2004	117 (109 - 125)	11.8 (11.1 - 12.6)	29.9 (25.7 - 33.8)	(-)	(-)
2005	124 (115 - 134)	13.8 (12.9 - 14.7)	35.9 (31.0 - 40.3)	(-)	(-)
2006	129 (119 - 139)	15.6 (14.7 - 16.5)	42.9 (36.9 - 48.0)	2.21 (1.74 - 2.69)	0.194 (0.149 - 0.239)
2007	138 (126 - 149)	16.0 (15.0 - 16.9)	47.8 (40.9 - 54.1)	2.21 (1.89 - 2.53)	0.203 (0.154 - 0.251)
2008	149 (137 - 162)	18.5 (17.4 - 19.6)	48.7 (40.7 - 55.2)	2.53 (2.21 - 2.86)	0.214 (0.164 - 0.265)
2009	156 (142 - 170)	18.6 (17.4 - 19.7)	47.5 (39.8 - 54.6)	2.76 (2.43 - 3.09)	0.224 (0.175 - 0.275)
2010	170 (154 - 185)	20.4 (19.1 - 21.7)	52.4 (44.2 - 59.4)	2.97 (2.58 - 3.35)	0.245 (0.192 - 0.301)
2011	172 (156 - 188)	21.6 (20.1 - 22.8)	53.7 (45.1 - 61.4)	3.05 (2.63 - 3.48)	0.273 (0.213 - 0.331)
2012	178 (161 - 196)	23.1 (21.8 - 24.6)	52.2 (43.6 - 60.1)	3.36 (2.92 - 3.81)	0.287 (0.226 - 0.349)
2013	188 (169 - 206)	24.3 (22.7 - 25.7)	50.8 (42.1 - 58.5)	3.73 (3.22 - 4.24)	0.290 (0.226 - 0.353)
2014	202 (182 - 222)	25.9 (24.2 - 27.5)	50.3 (41.5 - 57.7)	3.81 (3.31 - 4.31)	0.289 (0.226 - 0.355)
2015	211 (190 - 233)	27.5 (25.9 - 29.2)	50.7 (42.0 - 58.1)	3.97 (3.45 - 4.50)	0.286 (0.222 - 0.351)
2016	224 (201 - 247)	29.2 (27.2 - 30.9)	52.1 (43.2 - 59.9)	4.54 (3.88 - 5.13)	0.289 (0.221 - 0.357)

Table 27: Modelled global emissions with uncertainties

Date	HFC-245fa (Gg yr ⁻¹)	HFC-365mfc (Gg yr ⁻¹)	PFC-14 (Gg yr ⁻¹)	PFC-116 (Gg yr ⁻¹)
1978	(-)	(-)	21.2 (20.0 - 22.7)	2.21 (1.88 - 2.49)
1979	(-)	(-)	20.5 (19.4 - 21.6)	2.23 (1.99 - 2.47)
1980	(-)	(-)	19.4 (18.4 - 20.8)	2.15 (1.95 - 2.36)
1981	(-)	(-)	17.1 (16.0 - 18.2)	1.89 (1.70 - 2.08)
1982	(-)	(-)	15.7 (14.6 - 16.9)	1.74 (1.53 - 1.95)
1983	(-)	(-)	16.4 (15.2 - 17.6)	1.91 (1.70 - 2.13)
1984	(-)	(-)	16.5 (15.4 - 17.7)	2.17 (1.96 - 2.37)
1985	(-)	(-)	15.7 (14.7 - 16.8)	2.17 (1.97 - 2.38)
1986	(-)	(-)	15.6 (14.5 - 16.8)	2.16 (1.95 - 2.36)
1987	(-)	(-)	15.7 (14.6 - 17.0)	2.18 (1.99 - 2.37)
1988	(-)	(-)	16.1 (15.1 - 17.2)	2.25 (2.06 - 2.45)
1989	(-)	(-)	16.1 (15.0 - 17.2)	2.26 (2.05 - 2.49)
1990	(-)	(-)	16.0 (15.0 - 17.1)	2.23 (2.03 - 2.45)
1991	(-)	(-)	14.8 (13.8 - 15.9)	2.16 (1.96 - 2.36)
1992	(-)	(-)	13.0 (12.1 - 14.1)	2.09 (1.90 - 2.29)
1993	(-)	(-)	12.3 (11.3 - 13.3)	2.12 (1.92 - 2.31)
1994	(-)	(-)	11.7 (10.8 - 12.8)	2.16 (1.95 - 2.35)
1995	(-)	(-)	11.9 (11.1 - 13.0)	2.35 (2.16 - 2.56)
1996	(-)	(-)	11.5 (10.6 - 12.5)	2.60 (2.42 - 2.81)
1997	(-)	(-)	11.3 (10.4 - 12.2)	2.86 (2.67 - 3.06)
1998	(-)	(-)	11.1 (10.2 - 12.1)	3.02 (2.81 - 3.23)
1999	(-)	(-)	10.8 (9.76 - 11.7)	3.11 (2.90 - 3.31)
2000	(-)	(-)	10.5 (9.54 - 11.5)	3.03 (2.81 - 3.25)
2001	(-)	(-)	10.2 (9.32 - 11.2)	2.90 (2.69 - 3.12)
2002	(-)	(-)	10.7 (9.78 - 11.6)	2.86 (2.64 - 3.05)
2003	(-)	1.22 (0.985 - 1.47)	11.6 (10.8 - 12.5)	2.71 (2.50 - 2.91)
2004	(-)	2.33 (1.96 - 2.70)	11.4 (10.7 - 12.3)	2.45 (2.28 - 2.62)
2005	(-)	2.97 (2.50 - 3.47)	10.7 (10.1 - 11.3)	2.31 (2.14 - 2.47)
2006	7.36 (6.52 - 8.29)	3.36 (2.83 - 3.92)	11.3 (10.7 - 12.0)	2.29 (2.14 - 2.45)
2007	7.39 (6.47 - 8.34)	3.28 (2.75 - 3.83)	10.8 (10.2 - 11.4)	2.26 (2.11 - 2.42)
2008	7.37 (6.38 - 8.43)	3.13 (2.55 - 3.70)	10.6 (10.1 - 11.3)	2.08 (1.92 - 2.22)
2009	7.16 (6.09 - 8.27)	2.95 (2.38 - 3.50)	9.06 (8.52 - 9.67)	1.89 (1.74 - 2.04)
2010	7.88 (6.71 - 9.14)	3.12 (2.53 - 3.72)	10.1 (9.58 - 10.8)	1.93 (1.78 - 2.08)
2011	8.77 (7.47 - 10.2)	3.41 (2.75 - 4.06)	11.3 (10.8 - 12.0)	1.93 (1.78 - 2.08)
2012	9.46 (8.03 - 10.9)	3.65 (2.95 - 4.37)	11.3 (10.7 - 12.0)	1.91 (1.77 - 2.06)
2013	9.74 (8.19 - 11.4)	3.88 (3.15 - 4.61)	11.0 (10.4 - 11.7)	1.94 (1.80 - 2.08)
2014	10.2 (8.57 - 11.9)	4.20 (3.41 - 4.99)	11.1 (10.6 - 11.8)	1.95 (1.81 - 2.10)
2015	10.9 (9.08 - 12.8)	4.49 (3.60 - 5.35)	11.8 (11.2 - 12.5)	1.95 (1.80 - 2.10)
2016	11.7 (9.76 - 13.8)	4.71 (3.81 - 5.66)	12.4 (11.8 - 13.2)	1.97 (1.80 - 2.15)

Table 28: Modelled global emissions with uncertainties

Date	PFC-318 (Gg yr ⁻¹)	SF ₆ (Gg yr ⁻¹)	NF ₃ (Gg yr ⁻¹)
1978	(-)	2.67 (2.12 - 3.20)	(-)
1979	(-)	2.65 (2.29 - 3.02)	(-)
1980	(-)	2.76 (2.32 - 3.20)	(-)
1981	(-)	3.07 (2.65 - 3.48)	(-)
1982	(-)	3.04 (2.68 - 3.42)	(-)
1983	0.263 (0.202 - 0.321)	2.86 (2.48 - 3.28)	(-)
1984	0.257 (0.202 - 0.307)	3.38 (2.99 - 3.77)	(-)
1985	0.250 (0.199 - 0.295)	4.08 (3.71 - 4.48)	(-)
1986	0.254 (0.209 - 0.298)	4.75 (4.34 - 5.14)	(-)
1987	0.249 (0.209 - 0.289)	4.37 (3.99 - 4.78)	(-)
1988	0.244 (0.205 - 0.279)	4.26 (3.89 - 4.66)	(-)
1989	0.242 (0.206 - 0.281)	4.35 (3.99 - 4.74)	(-)
1990	0.248 (0.212 - 0.281)	4.94 (4.57 - 5.32)	(-)
1991	0.265 (0.229 - 0.302)	5.21 (4.84 - 5.64)	(-)
1992	0.297 (0.261 - 0.332)	5.07 (4.69 - 5.49)	(-)
1993	0.348 (0.312 - 0.385)	5.47 (5.05 - 5.85)	(-)
1994	0.418 (0.377 - 0.457)	6.05 (5.67 - 6.47)	(-)
1995	0.504 (0.460 - 0.547)	6.43 (6.06 - 6.90)	(-)
1996	0.598 (0.549 - 0.644)	6.31 (5.91 - 6.75)	(-)
1997	0.689 (0.641 - 0.740)	5.85 (5.46 - 6.27)	(-)
1998	0.771 (0.719 - 0.825)	5.50 (5.09 - 5.90)	(-)
1999	0.841 (0.787 - 0.893)	5.03 (4.64 - 5.42)	(-)
2000	0.898 (0.840 - 0.952)	4.97 (4.56 - 5.39)	(-)
2001	0.939 (0.881 - 0.990)	5.26 (4.85 - 5.68)	(-)
2002	0.963 (0.904 - 1.02)	5.68 (5.31 - 6.10)	(-)
2003	0.968 (0.910 - 1.02)	5.87 (5.51 - 6.27)	(-)
2004	0.950 (0.891 - 1.01)	5.78 (5.48 - 6.15)	(-)
2005	0.905 (0.848 - 0.959)	6.09 (5.80 - 6.41)	(-)
2006	0.840 (0.788 - 0.888)	6.42 (6.14 - 6.75)	(-)
2007	0.770 (0.719 - 0.818)	7.02 (6.72 - 7.36)	(-)
2008	0.706 (0.659 - 0.753)	7.36 (7.05 - 7.70)	(-)
2009	0.655 (0.608 - 0.699)	7.09 (6.78 - 7.41)	(-)
2010	0.615 (0.570 - 0.658)	7.35 (7.04 - 7.66)	(-)
2011	0.581 (0.540 - 0.623)	7.67 (7.37 - 8.02)	(-)
2012	0.554 (0.514 - 0.595)	7.98 (7.66 - 8.32)	(-)
2013	0.539 (0.499 - 0.582)	8.22 (7.91 - 8.58)	1.40 (1.30 - 1.48)
2014	0.531 (0.486 - 0.571)	8.43 (8.13 - 8.82)	1.55 (1.46 - 1.64)
2015	0.528 (0.480 - 0.572)	8.32 (7.99 - 8.70)	1.73 (1.64 - 1.82)
2016	0.526 (0.472 - 0.580)	8.58 (8.23 - 8.99)	1.90 (1.80 - 2.00)

Table 29: Modelled global emissions with uncertainties

6 Use of satellite data in inversion modelling

6.1 Introduction

Each section in this chapter builds on the work presented in the previous annual report. It is widely agreed that space-borne observations have a role to play in verifying nationwide GHG emission. They represent global, and high geographical coverage of the atmosphere subject to the constraints imposed by clouds and sub-optimal viewing geometries (e.g. high solar zenith angle associated with sampling polar regions during winter months). The number of satellite instruments in space with a sensitivity to measure changes in CO₂ and CH₄ associated with fossil emissions has increased by one since the 2015/16 report, although access to data from this new instrument has not been possible yet. Various political and programmatic changes have had positive and negative impacts on future missions, which we detail below.

6.2 Preparation of existing satellite data

The primary vehicle for the development of satellite-derived GHG data products was until recently the ESA Climate Change Initiative (CCI) (Chevallier et al, 2017). Key retrieval groups have produced self-consistent CO₂ and CH₄ data using data from SCIAMACHY, GOSAT, and OCO-2 (CO₂ only), and to a lesser extent using data from thermal IR measurements from the Infrared Atmospheric Sounding Interferometer (IASI) aboard the ESA MetOp satellites. The current GHG CCI study has now concluded with a Climate Assessment report published online in March 2017. There is consensus among this group to continue working together to take advantage of data produced.

Analysis of collected spectra from GOSAT and OCO-2 continues with individual science teams spending effort to minimize systematic biases that continue to affect retrievals; even a sub-one ppm regional bias for CO₂ translates into a large bias in CO₂ fluxes. OCO-2 is now processing version 8 of an official data product, with the associated bias correction stable and well-behaved. The OCO-2 science team activities also include an ongoing large-scale modelling effort to inter-compare regional CO₂ fluxes inferred from OCO-2 CO₂ column data. A number of studies are due to be published in the peer-review literature over the next few months.

Validation activities (vicarious or otherwise) continue with aircraft campaigns and ground-based column remote sensing instruments (TCCON, Total Carbon Column Observing Network). Preparatory science activities in support of the NASA ASCENDS space-borne mission (Active Sensing of CO₂ Emissions over Nights, Days, and Seasons) include flights to test a multi-frequency laser that is being designed to fly in space. OCO-2 and GOSAT are taking advantage of aircraft campaigns over North America (ACT-America, NASA funded) and on a global-scale (ATom, Atmospheric Tomography Mission, NSF funded)

The Chinese TanSat was launched in December 2016 and closely based on the design of OCO-2. At the time of writing, extensive validation activities are underway to ensure retrievals of CO₂ are similar to those measured from the ground.

6.3 Future mission concepts

The most impending launch is TROPOMI (TROPOspheric Monitoring Instrument), which is due for launch in 2017. TROPOMI is an instrument aboard the Copernicus Sentinel-5 Precursor satellite. It measures a wide range of wavelengths that include CH₄ and range of reactive trace gases that help identify its sources, e.g. formaldehyde, nitrogen dioxide, and CO.

The current US administration has changed the scientific landscape associated with GHG satellite missions. The 2018 Federal Budget has proposed terminating five Earth science missions (<https://www.whitehouse.gov/sites/whitehouse.gov/files/omb/budget/fy2018/msar.pdf>) including OCO-3, which was due for launch on the International Space Station (ISS), in 2019. The ISS uses an inclined, precessing orbit so that OCO-3 would have provided more information about tropical CO₂ fluxes (i.e. more time is spent over the tropics resulting in more cloud-free scenes) at different times of day. At the time of writing this budget has not been passed by US congress.

In December 2016, NASA allocated funding for the GeoCARB (Geostationary Carbon Cycle Observatory) as an Earth Venture Mission. GeoCARB will, over the Americas, spatially resolve (at 5-10 kms) a number of carbon cycle gases (CO₂, CH₄, and CO) and also measure solar induced fluorescence, which has been related to changes in vegetation. It is due for launch in 2021.

The follow-on to GOSAT, GOSAT-2, has a launch date in 2018 or soon afterwards and has a nominal lifetime of 5 years. It will use similar but updated hardware to GOSAT, which will help to eventually link the two time series. GOSAT-2 will observe CO₂ and CH₄ with an accuracy of 0.5 ppm and 5 ppb respectively over a 500 km mesh grid. As an approach to separating fossil fuel combustion from other sources, GOSAT-2 will also measure CO. The GOSAT-2 science team are planning to use their aerosol optical measurements to help study PM_{2.5} (particulate matter with diameters less than 2.5 microns). This will be the first GHG satellite that includes measurements to help improve identification of fossil fuel CO₂.

The French MicroCarb space-borne mission is now a bilateral mission with the UK, with science team involvement from the Universities of Leicester and Edinburgh. MicroCarb will measure CO₂ at a horizontal resolution of 9 km with a precision comparable to OCO-2. It has a proposed launch of 2020 and a nominal lifetime of 3 years.

In a bilateral between France and Germany, CNES and DLR are developing the MERLIN satellite (Methane Remote Sensing Lidar Mission) that has a proposed launch of 2021. It will measure atmospheric CH₄ using an active approach with an integrated Path Differential Absorption Lidar. The active approach has the advantage that it can observe atmospheric CH₄ day or night throughout the year so will be particularly suited for polar regions during winter months.

6.4 Ground-based networks

The Total Carbon Column Observing Network (TCCON) still represents the only ground-based network to validate satellite observations. Maintaining such a network, funded with multinational sources, is difficult and while there are no immediate signs of a gap in funding, recent political changes in science funding in the US have emphasised the fragility of such a network.

Complementary networks of simpler and cheaper instruments are being proposed. For example, miniaturised laser heterodyne radiometers (mini-LHRs) have been developed by NASA, which can take advantage of an existing global measurement infrastructure that supports aerosol optical measurements (<https://aeronet.gsfc.nasa.gov/>). Based on calculations soon to be submitted for peer-review, a network of mini-LHRs could potentially outperform TCCON in terms of contributing to knowledge about CO₂ fluxes; but ideally they would help fill in geographical gaps left by the sparse but highly-accurate TCCON network.

6.5 Emission estimates using satellite observations of CO₂ and CH₄

Horizon 2020, the EU Research and Innovation programme, has just funded two large (each approximately 10 million euro) projects focussed on quantifying European anthropogenic CO₂ emissions. These are:

- CO₂ Human Emissions (CHE) in response to call EO-3-2017 “Preparation for a European capacity to monitor CO₂ anthropogenic emissions”.
- An observation-based system for monitoring and verification of greenhouse gases (VERIFY) in response to call SC5-04-2017 “Towards a robust and comprehensive greenhouse gas verification system”.

CHE is coordinated by ECMWF and VERIFY is coordinated by LSCE. The CHE and VERIFY projects will eventually support broader efforts to quantify fossil fuel CO₂ (ffCO₂) emissions over Europe that will be required as part of the global stocktake required by the Paris Agreement. CHE and VERIFY will design and integrate monitoring subsystems (e.g. emission modelling, measurements, models) to estimate ffCO₂. To achieve these goals both projects bring together (mainly) existing ground-based and space-borne remote sensing and in situ measurements, with enhanced modelling capabilities for ffCO₂ emissions in the context of natural and other

anthropogenic emissions. In terms of satellite observations, CHE and VERIFY will mainly work on using data that already exists with some forward-planning experiments to understand how planned missions will improve the monitoring system. There is a major effort to engage with key European and international stakeholders, allowing them to take advantage of the infrastructure built as part of these projects.

As part of the wider European effort ESA/European Commission (EC) have commissioned two CO₂ task forces to specify the (ESA Task Force A) space component and the (EC Task Force B) end-to-end operational emission monitoring system, including the space component, inverse modelling, in situ observation networks, and emission inventories. These task forces build on the 2015 EC report “Towards a European Operational Observing System to Monitor Fossil CO₂ emissions” (http://edgar.jrc.ec.europa.eu/news_docs/CO2_report_22-10-2015.pdf). The first reports from Task Forces A and B will appear later in 2017.

7 Estimating biogenic and anthropogenic emissions of CO₂

Atmospheric variations of carbon dioxide (CO₂) mole fraction reflects changes in atmospheric transport and regional patterns of surface emission and uptake. Measurements of CO₂ mole fraction therefore represent a superposition of fast and slow variations due to different physical and biological processes. Without further information, attributing atmospheric CO₂ variations to these processes is an ill-posed problem. This chapter builds on the work from the previous annual report.

There remains no single, robust methodology to isolate ffCO₂ from atmospheric measurements of CO₂. The two complementary approaches are geographical disaggregation, taking advantage of geographically isolated sources and the use of an additional tracer (e.g. co-emitted gas or an isotope).

Several new approaches will be pursued by the two Horizon2020 (EU-funded) projects (mentioned previously). The integrative modelling infrastructure will include the development and implementation of high temporally (hourly) and spatially (<10 km) resolved emission inventories. The emissions model will ingest near-real time activity data (e.g. energy demand, traffic intensity, and socio-economic drivers) that will improve our understanding of observed atmospheric variations of CO₂ on larger city-scales. The modelling components will bring together traditionally separate approaches to understanding the carbon cycle, Fossil Fuel Data Assimilation and Carbon Cycle Data Assimilation systems (FFDAS and CCDAS), to provide emission estimates from fossil fuel and natural fluxes simultaneously. This will be achieved by using, for example, correlative land surface data such as leaf area index. The project will also consider for the first time the use of reactive trace gases (e.g. nitrogen dioxide and formaldehyde) that provide chemical source signatures. These reactive gases, measured on a number of existing space-borne platforms, have the potential to improve the source attribution of ffCO₂.

Recent work has shown how Atmospheric Potential Oxygen (APO) can be used effectively to quantify ffCO₂ (Pickers, 2017). It has the advantage that it does not suffer from contamination from other source (e.g. nuclear power plant emissions of ¹⁴CO₂) or from large variations in combustion ratios (e.g. CO:CO₂). APO is given by $O_2 : -1.1CO_2$, where the -1.1 factor represents the mean global O₂:CO₂ ratio between fluxes of CO₂ and O₂ between the atmosphere and terrestrial biosphere. Determination of ffCO₂ from APO is analogous to the approach used for estimating ffCO₂ from CO, e.g. $APO - APO_{baseline} / R_{APO:CO_2}$, where R denotes the combustion ratio for fossil fuel. Pickers argues that $R_{CO:CO_2}$ varies much more than the corresponding value for APO, suggesting the ffCO₂ values derived from APO are potentially more robust. Pickers compared ffCO₂(APO) against ffCO₂(CO) and ffCO₂(¹⁴CO₂) at three sites over East Anglia. After taking into account uncertainties associated with the baseline, measurements, and emission ratios, values of ffCO₂(APO) are approximately half as uncertain as ffCO₂(CO). This is a promising approach but needs to be tested more widely, for example in urban environments where ffCO₂ will be higher than on the east coast of England. This approach demands continuous, high-precision O₂ measurements over cities.

Radiocarbon remains the mainstay of ffCO₂ estimation. It is a difficult measurement to make with strict associated precision requirements and consequently only a few groups routinely analyse samples. Optical technology capable of measuring radiocarbon is in its infancy but saturated-absorption cavity ring-down technology is beginning to show promise (e.g. Giusfredi et al, 2015). The device measures radiocarbon by measuring how the light interacts with the CO₂ produced when a given sample is burned; the frequency of the laser at 2209.11 cm⁻¹ resonates with the ν_3 antisymmetric stretching of ¹⁴C¹⁶O₂. Continued development of this kind of technology towards the precision requirements of ffCO₂ analysis will potentially allow the construction of a global ffCO₂ network.

8 Results and analysis of additional gases

8.1 Introduction

This section discusses the atmospheric trends and regional emissions of the other gases that are measured at Mace Head. The table below describes, if applicable, the principle uses of each of the gases, their radiative efficiency, atmospheric lifetime, global warming potential in a 100-year framework (GWP_{100}) and ozone depleting potential (ODP). In the following sections each of these gases are presented.

Gas	Primary use	Radiative Efficiency ($W\ m^{-2}\ ppb^{-1}$)	Atmospheric Lifetime (years)	GWP_{100}	ODP
CFC-11	Widespread	0.26	45	4,660	1
CFC-12	Refrigerant	0.32	100	10,200	0.82
CFC-113	Coolant, electronics	0.30	85	5,820	0.85
CFC-115	Refrigerant	0.20	1,020	7,670	0.57
HCFC-124	Refrigerant, fire suppression	0.20	5.9	527	0.02
HCFC-141b	Foam blowing	0.16	9.2	782	0.12
HCFC-142b	Chem. synthesis/foam blowing	0.19	17.2	1,980	0.06
HCFC-22	Propellant, air conditioning	0.21	11.9	1,760	0.04
HFC-236fa	Fire extinguisher	0.24	242	8060	
HFC-245fa	Foam blowing	0.24	7.7	858	
SO ₂ F ₂	Fumigant	0.2	36	4090	
CH ₃ Cl	Natural, refrigerant	0.01	1	12	0.02
CH ₂ Cl ₂	Foam plastic, solvent, natural		144 days		
CHCl ₃	Bi-product, natural		149 days		
CCl₄	Fire suppression, precursor	0.17	26	1,730	0.82
CH₃CCl₃	Solvent	0.07	5.0	160	0.16
CHClCCl ₂	Degreasing solvent		5 days	5	
CCl ₂ CCl ₂	Solvent, dry cleaning		90 days	15	
CH ₃ Br	Natural (seaweed), fumigant		0.8		
CH ₂ Br ₂	Natural (seaweed)		123 days		
CHBr₃	Fumigant, natural (seaweed)		24 days		0.66
CBrClF₂	Fire suppression (military)	0.29	16	1,750	7.9
CBrF₃	Fire suppression	0.30	65	6,290	15.9
C₂Br₂F₄	Fire suppression	0.31	20	1,470	13.0
CH ₃ I	Natural (seaweed)		7 days		
C ₂ H ₆	Combustion, gas leakage				
CO	Combustion		30-90 days		
O ₃	Reactions in atmosphere				
H ₂	Combustion, photolysis				

Table 30: The principle uses of the gases observed at Mace Head, their radiative efficiency, atmospheric lifetime, global warming potential in a 100-year framework (GWP_{100}) and ozone depleting potential (ODP). The gases listed in red are specifically covered by the Montreal Protocol. All of the gases with a GWP are GHGs but not all GHGs are covered by the Kyoto Protocol.

8.2 CFC-11

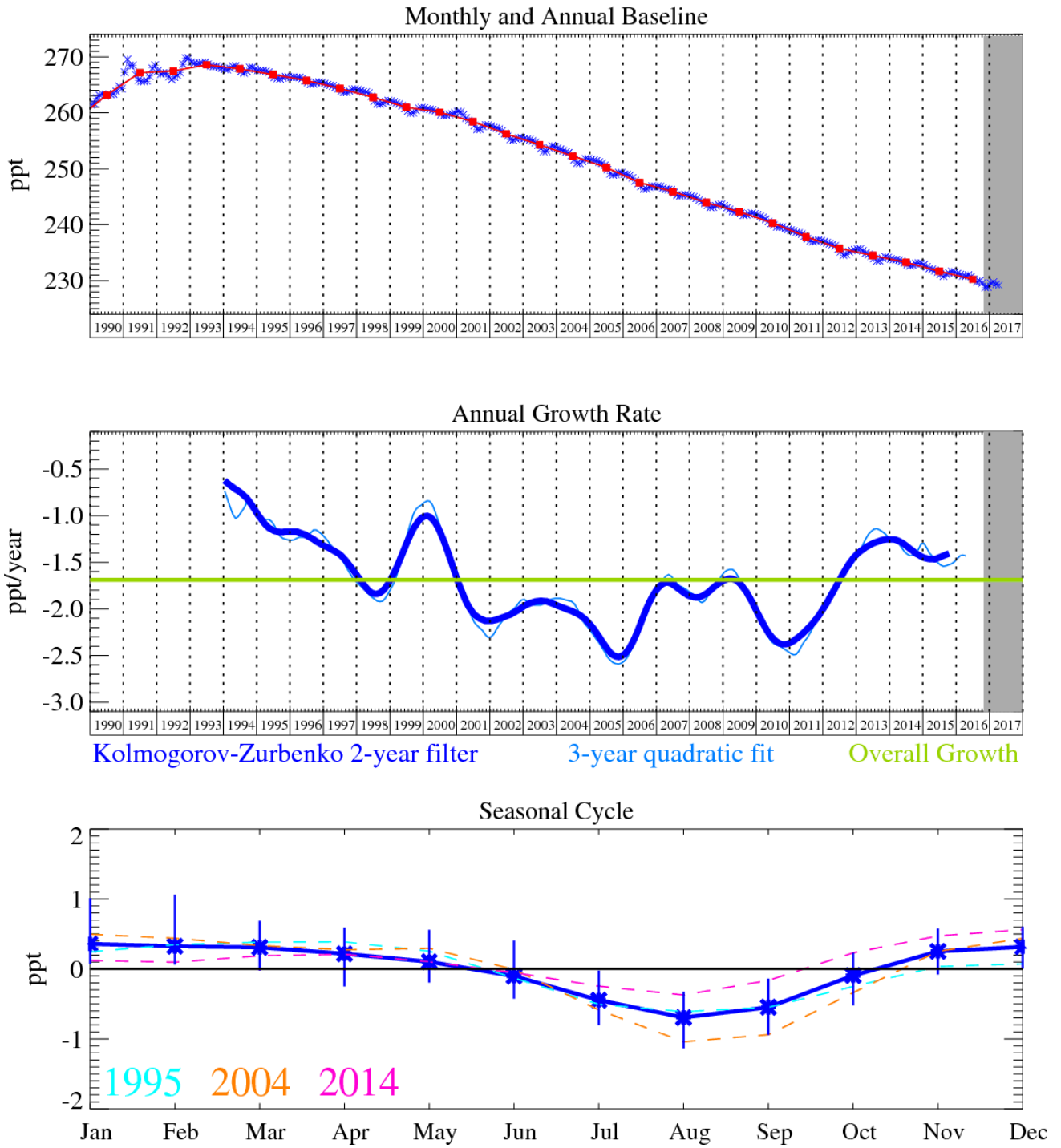


Figure 39: CFC-11 (CCl₃F): Monthly (blue) and annual (red) baseline (top plot). Annual (blue) and overall average growth rate (green) (middle plot). Seasonal cycle (de-trended) with year-to-year variability (lower plot). The grey area covers un-ratified and therefore provisional data.

8.3 CFC-12

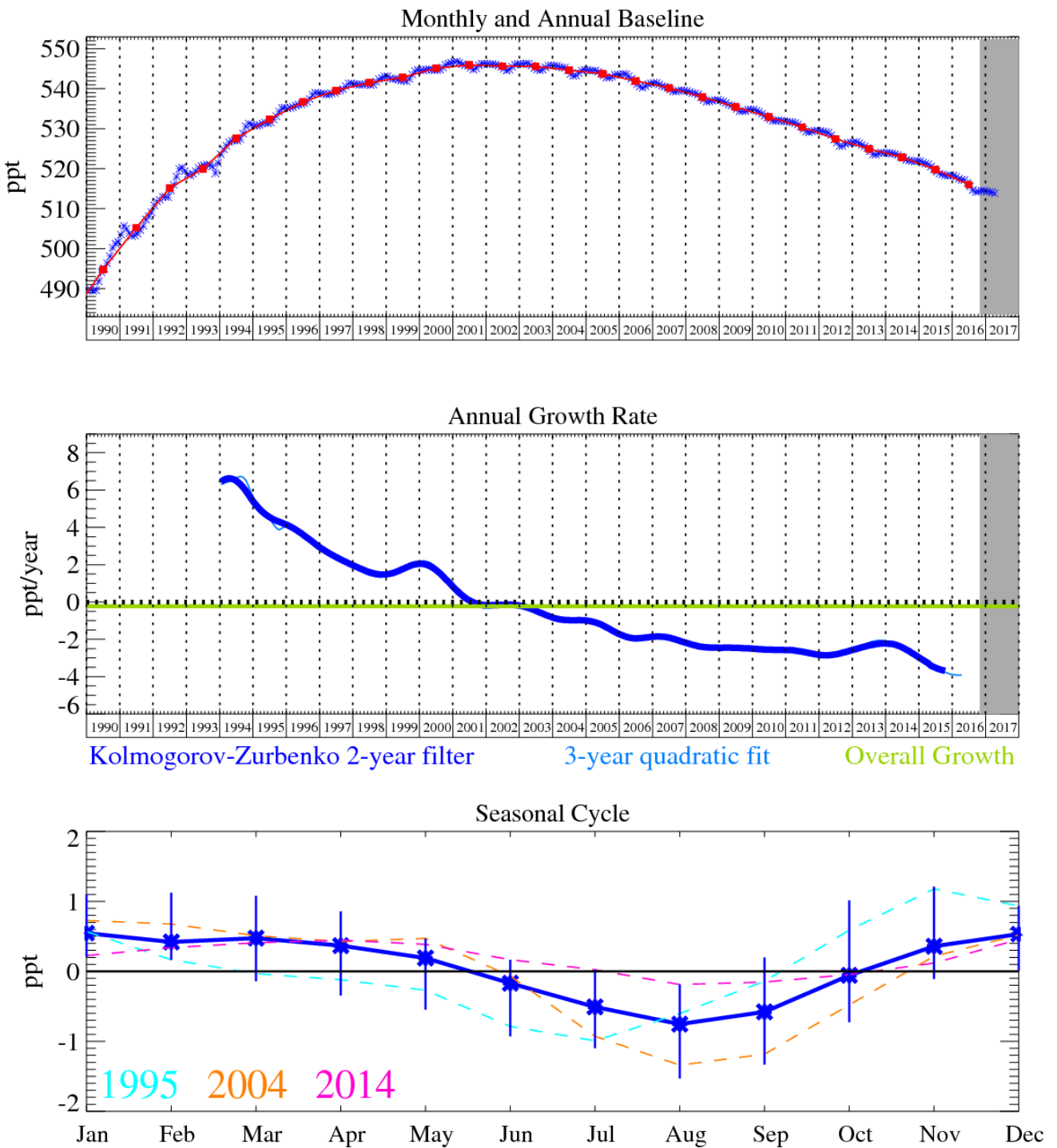


Figure 40: CFC-12 (CCl_2F_2): Monthly (blue) and annual (red) baseline (top plot). Annual (blue) and overall average growth rate (green) (middle plot). Seasonal cycle (de-trended) with year-to-year variability (lower plot). The grey area covers un-ratified and therefore provisional data.

8.4 CFC-113

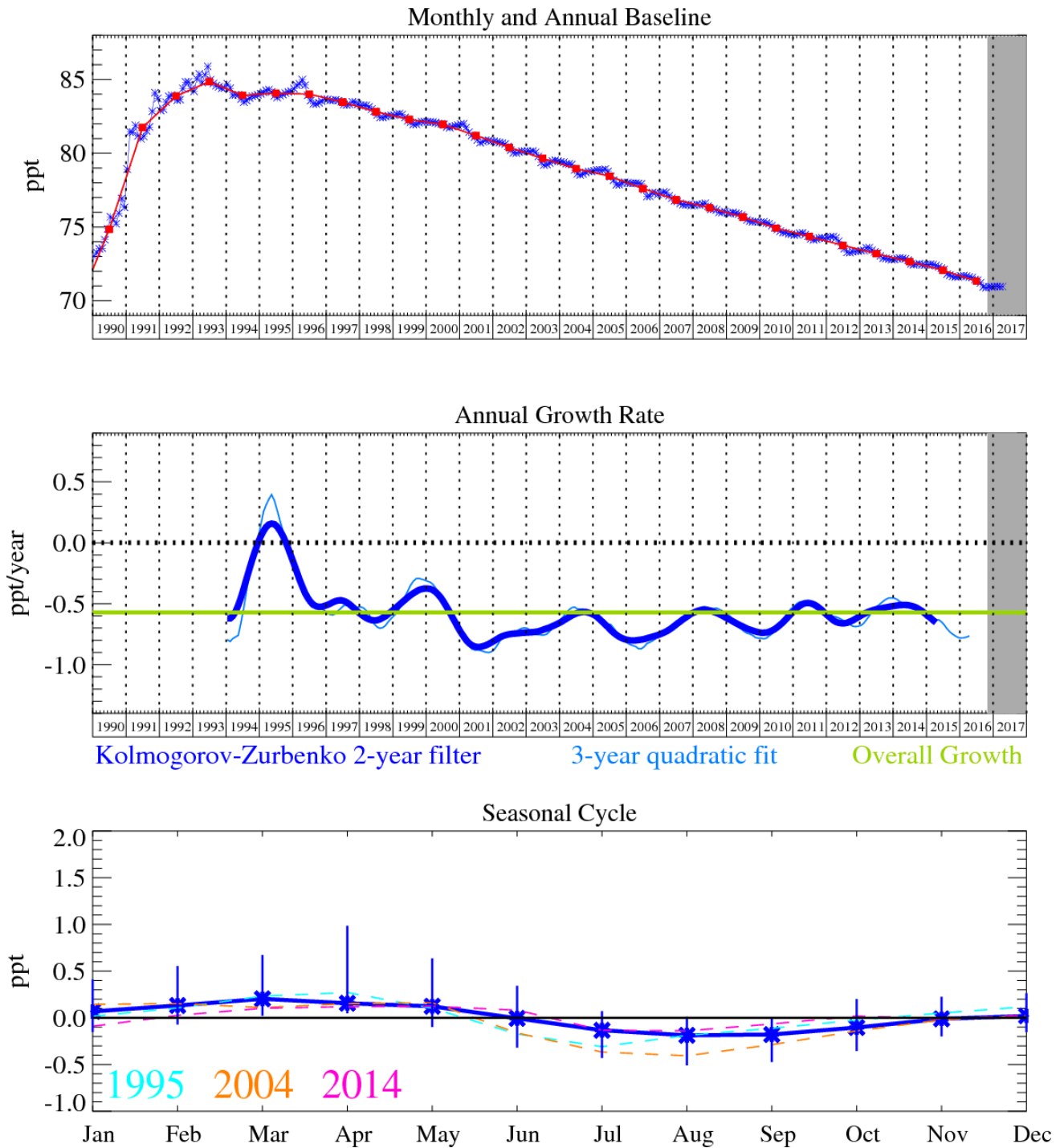


Figure 41: CFC-113 ($C_2Cl_3F_3$): Monthly (blue) and annual (red) baseline (top plot). Annual (blue) and overall average growth rate (green) (middle plot). Seasonal cycle (de-trended) with year-to-year variability (lower plot). The grey area covers un-ratified and therefore provisional data.

8.5 HCFC-124

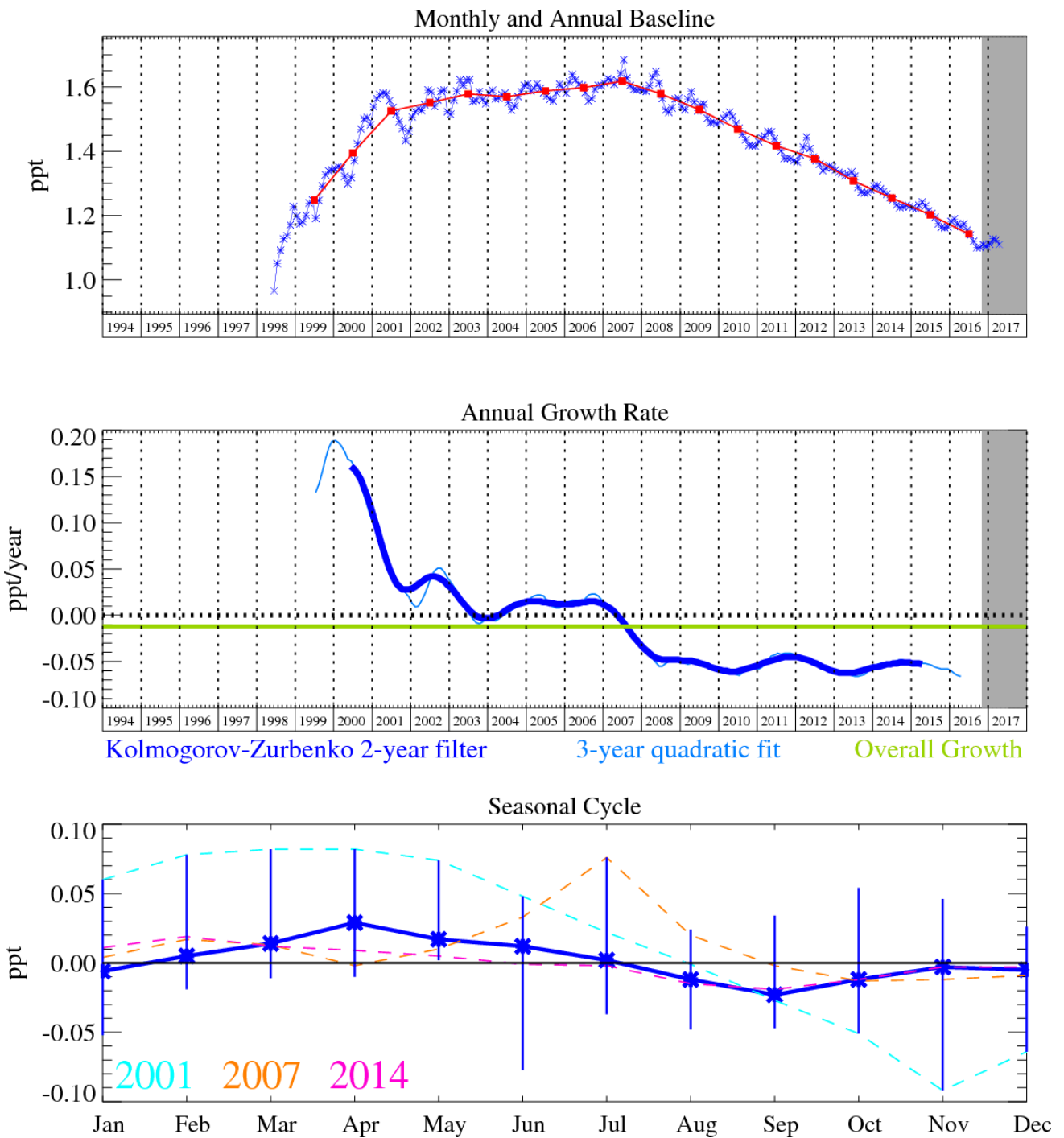


Figure 42: HCFC-124 (C_2HClF_4): Monthly (blue) and annual (red) baseline (top plot). Annual (blue) and overall average growth rate (green) (middle plot). Seasonal cycle (de-trended) with year-to-year variability (lower plot). The grey area covers un-ratified and therefore provisional data.

8.6 HCFC-141b

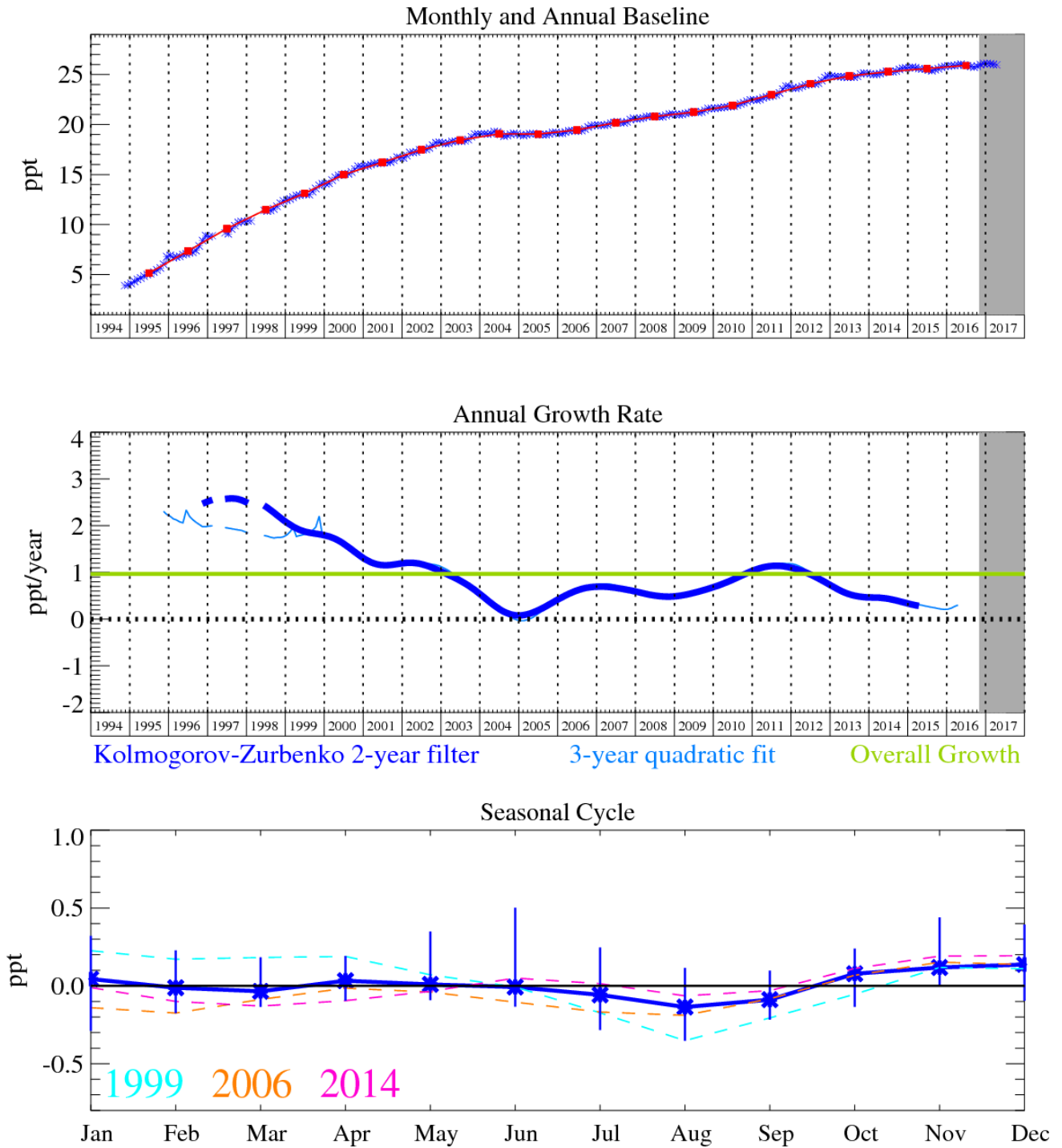


Figure 43: HCFC-141b ($C_2H_3Cl_2F$): Monthly (blue) and annual (red) baseline (top). Annual (blue) and overall average growth rate (green) (middle plot). Seasonal cycle (de-trended) with year-to-year variability (lower plot). The grey area covers un-ratified and therefore provisional data.

8.7 HCFC-142b

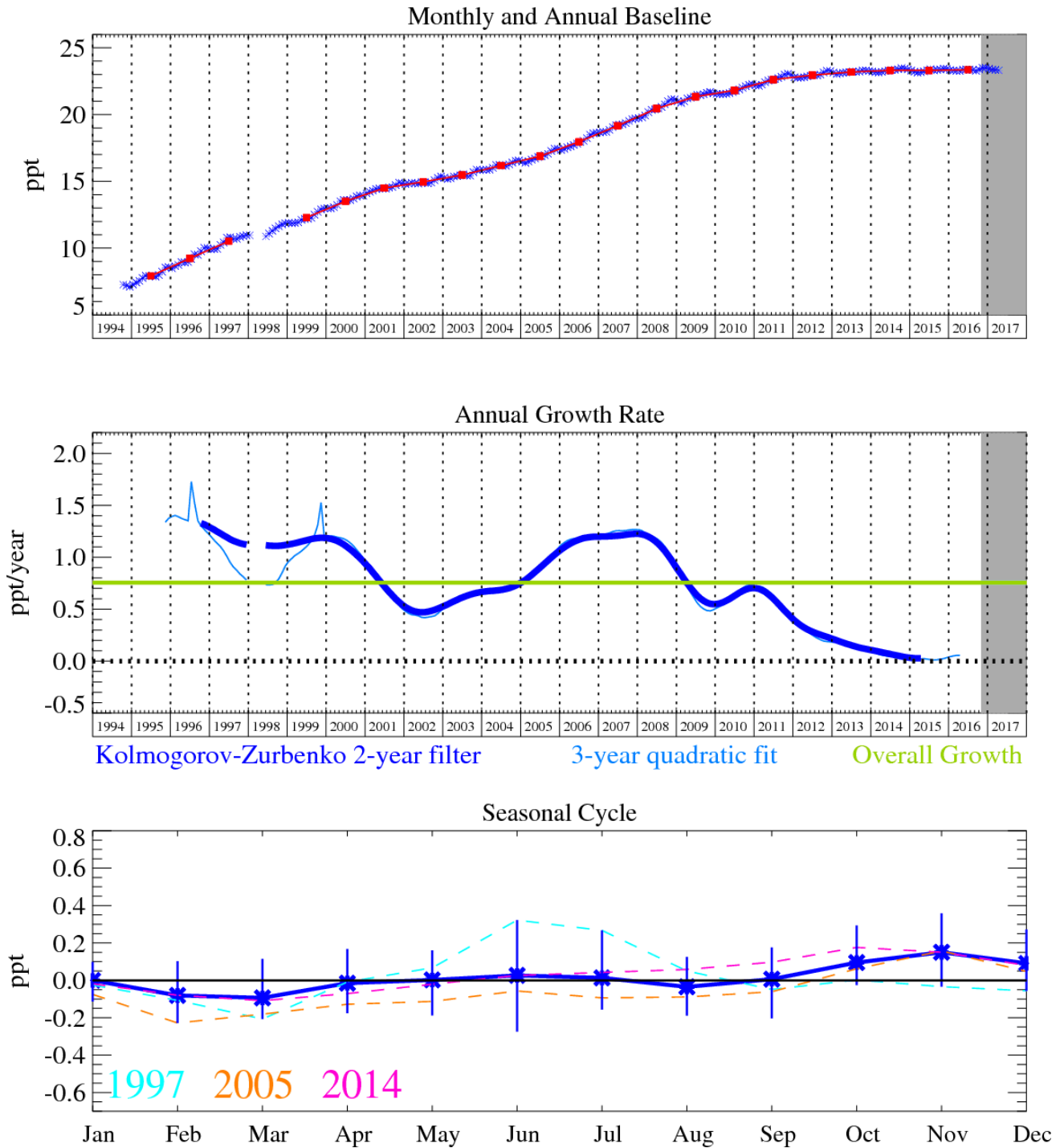


Figure 44: HCFC-142b ($C_2H_3ClF_2$): Monthly (blue) and annual (red) baseline (top). Annual (blue) and overall average growth rate (green) (middle plot). Seasonal cycle (de-trended) with year-to-year variability (lower plot). The grey area covers un-ratified and therefore provisional data.

8.8 HCFC-22

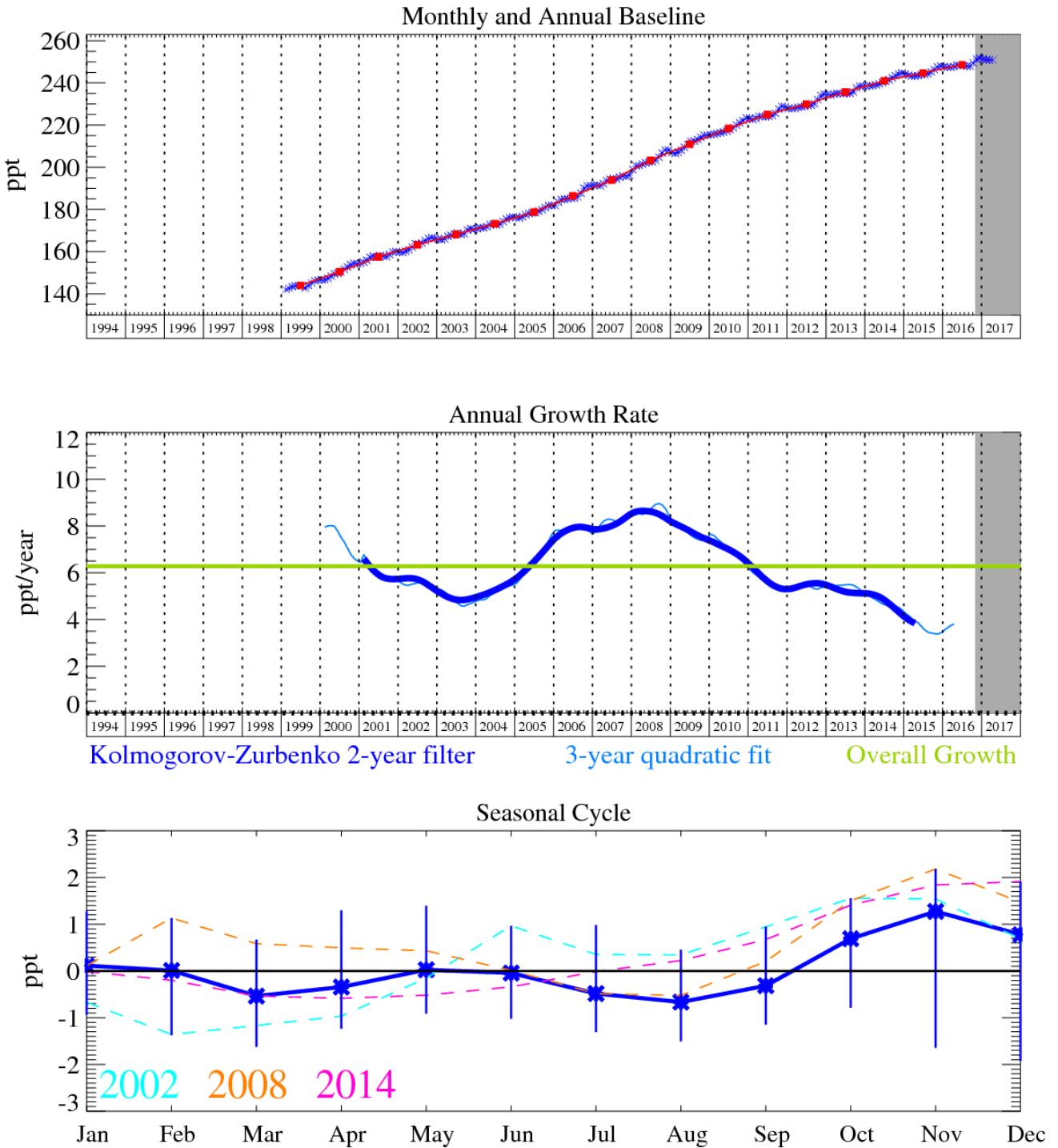


Figure 45: HCFC-22 (CHClF₂): Monthly (blue) and annual (red) baseline (top plot). Annual (blue) and overall average growth rate (green) (middle plot). Seasonal cycle (de-trended) with year-to-year variability (lower plot). Grey area covers un-ratified and therefore provisional data.

8.9 HFC-236fa

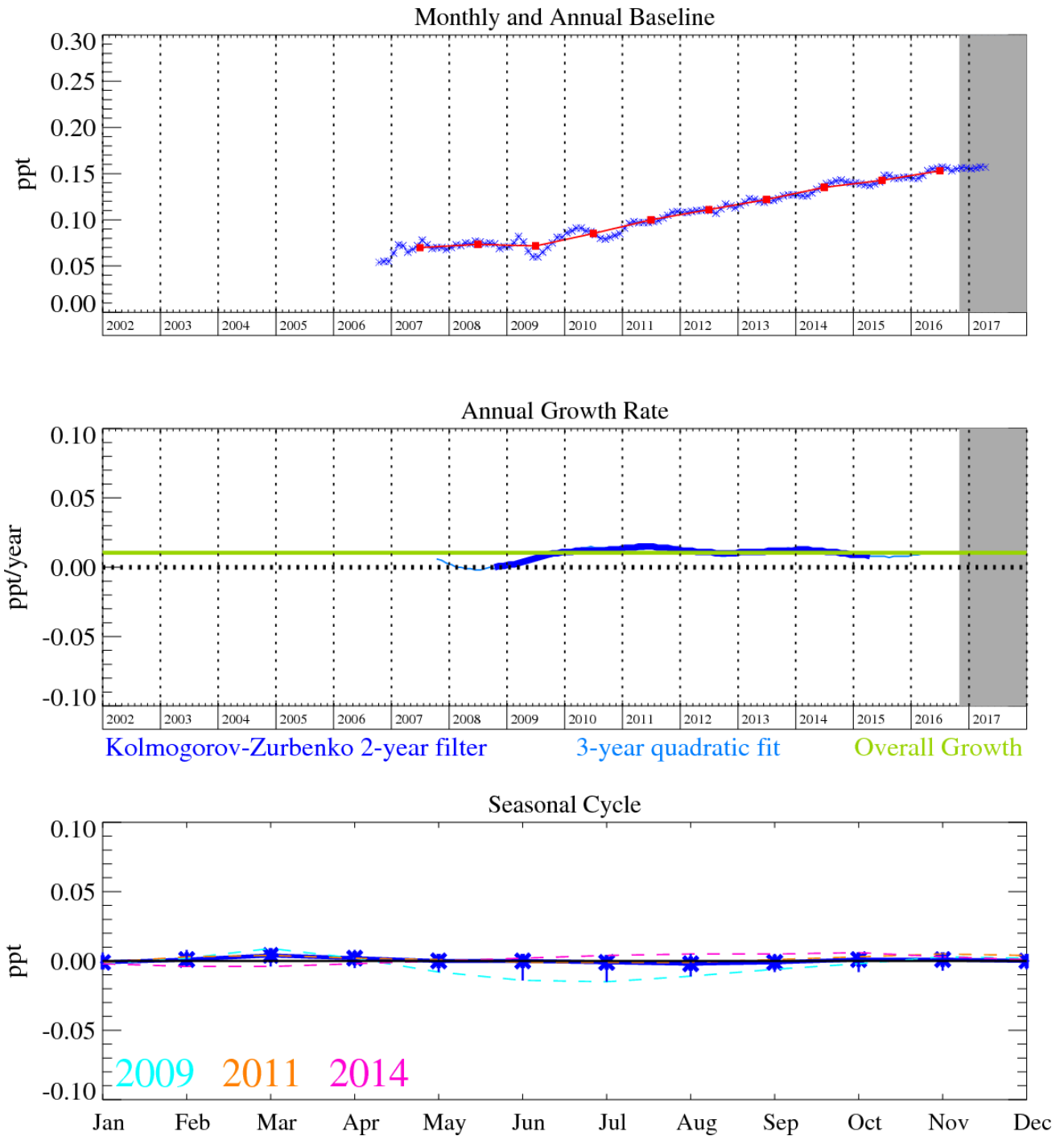


Figure 46: HFC-236fa ($C_3H_2F_6$): Monthly (blue) and annual (red) baseline (top plot). Annual (blue) and overall average growth rate (green) (middle plot). Seasonal cycle (de-trended) with year-to-year variability (lower plot). Grey area covers un-ratified and therefore provisional data.

8.10 SO₂F₂

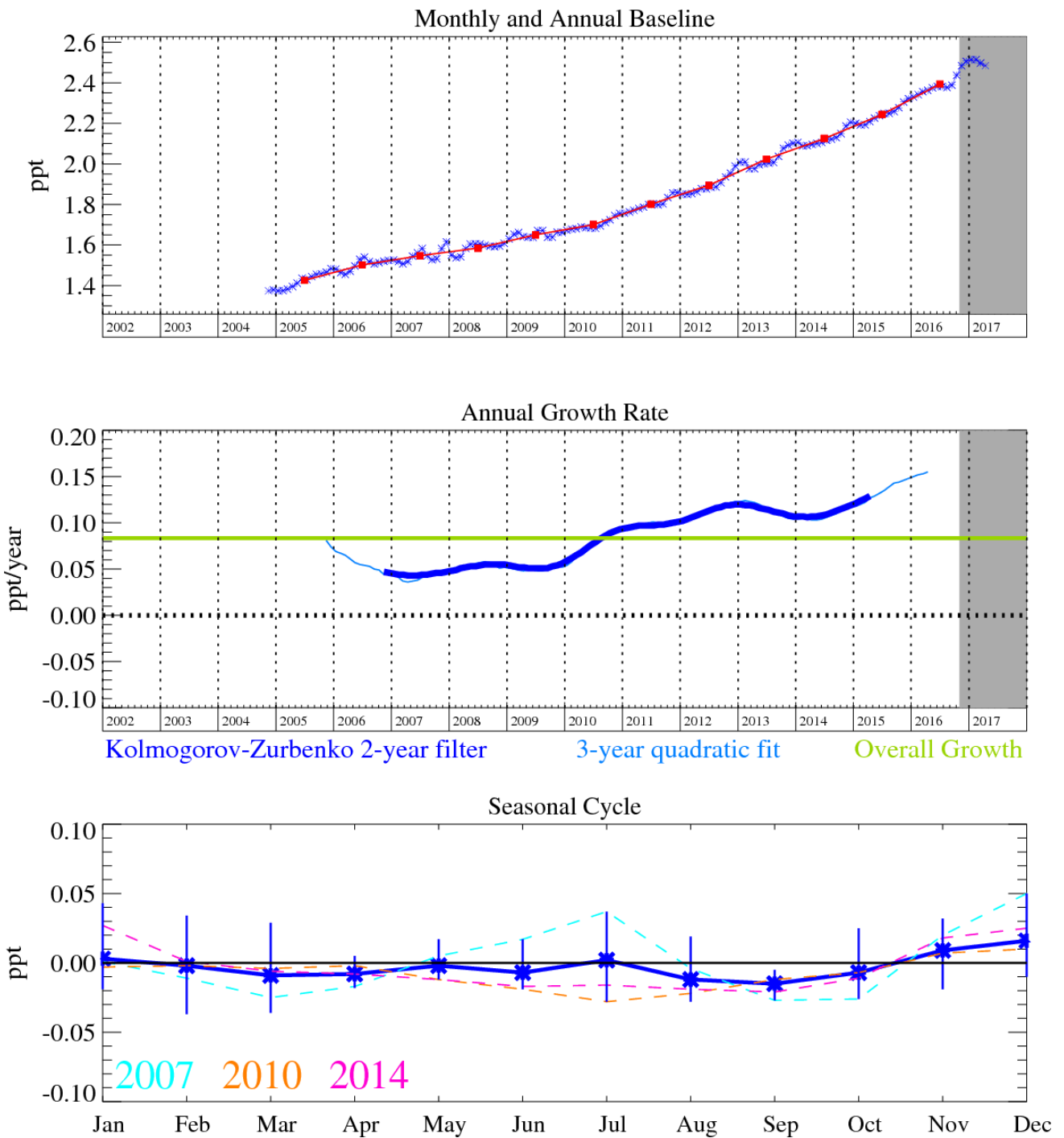


Figure 47: SO₂F₂: Monthly (blue) and annual (red) Northern Hemisphere baseline mole fractions (top plot). Annual (blue) and overall average growth rate (green) (middle plot). Seasonal cycle (de-trended) with year-to-year variability (lower plot). Grey area covers un-ratified and therefore provisional data.

8.11 CH₃Cl

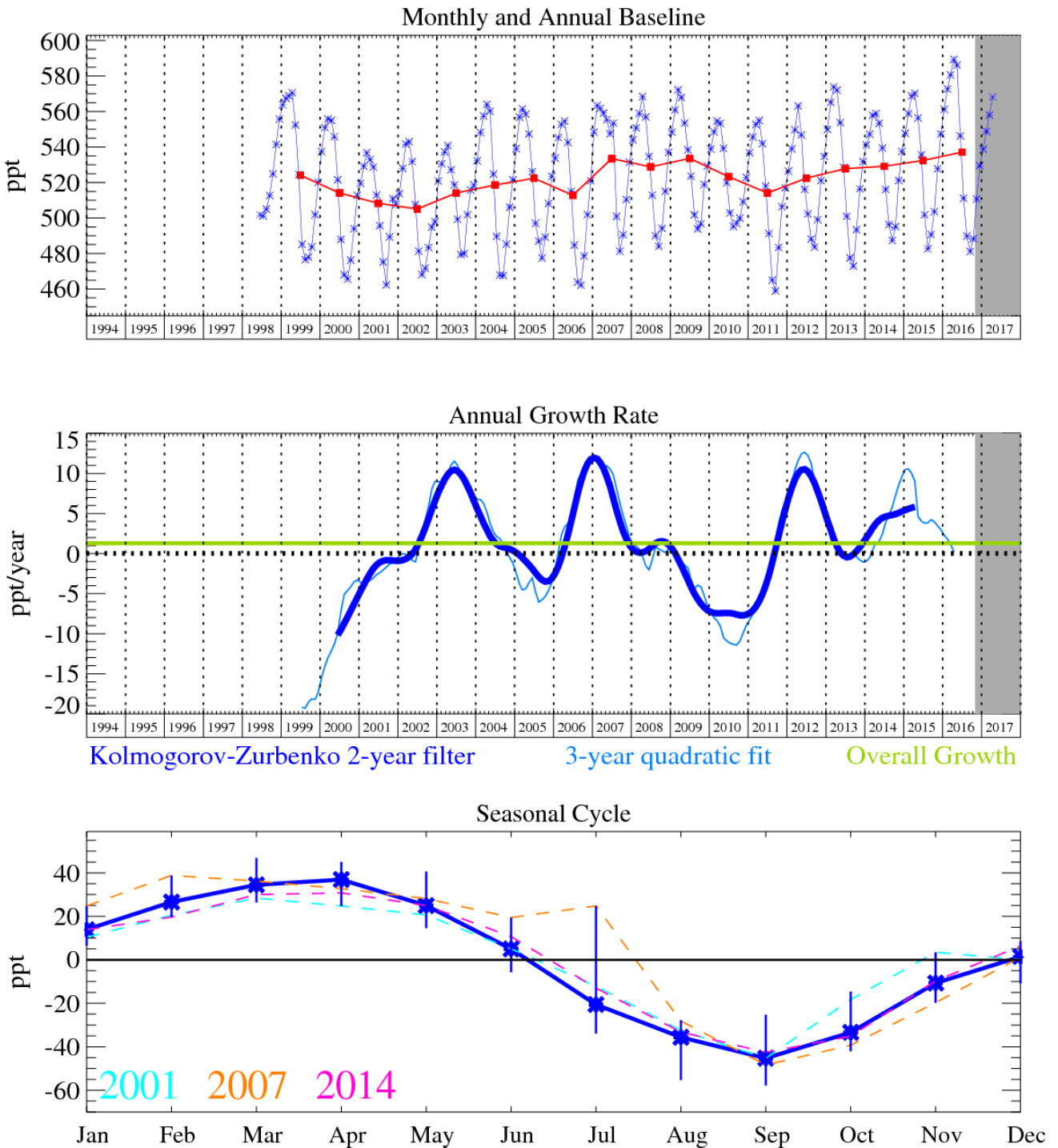


Figure 48: CH₃Cl: Monthly (blue) and annual (red) Northern Hemisphere baseline mole fractions (top plot). Annual (blue) and overall growth rate (green) (middle). Seasonal cycle (de-trended) with year-to-year variability (lower plot). Grey area covers un-ratified and therefore provisional data.

8.12 CH₂Cl₂

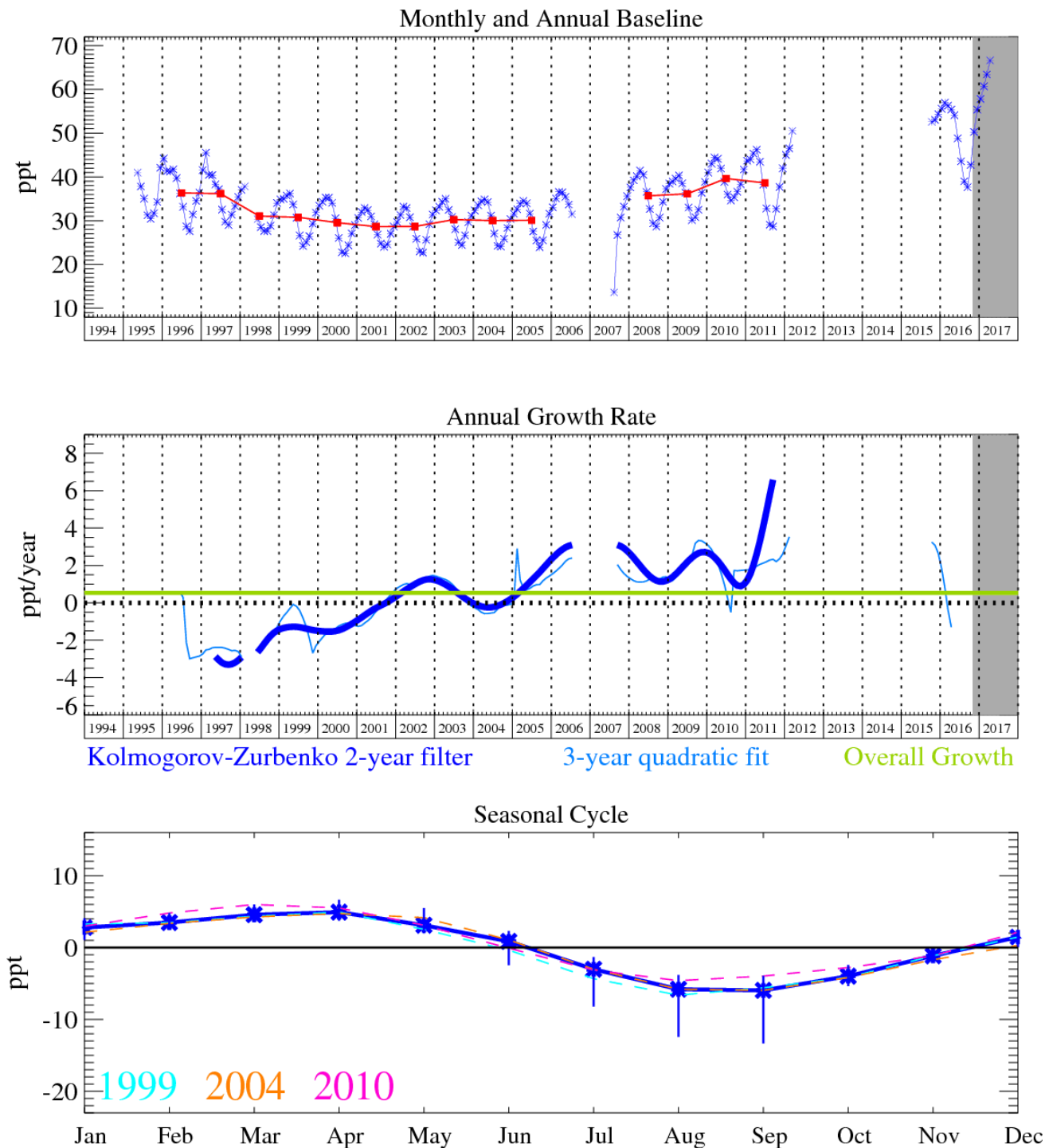


Figure 49: CH₂Cl₂: Monthly (blue) and annual (red) Northern Hemisphere baseline mole fractions (top plot). Annual (blue) and overall average growth rate (green) (middle plot). Seasonal cycle (de-trended) with year-to-year variability (lower plot). Grey area covers un-ratified and therefore provisional data.

There are significant gaps in the Mace Head observation record, 2006-2007 and 2012-2015. This gas can co-elute with CFC-11 due to GC column aging and was analysed using identical mass-to-charge ratios for fragmentation ions. This made isolation of the peaks in the chromatography very difficult; where co-elution happens the data have had to be removed. Other, less abundant, ions are now routinely analysed to ensure interference by CFC-11 co-elution will not happen in the future.

8.13 CHCl₃ (chloroform)

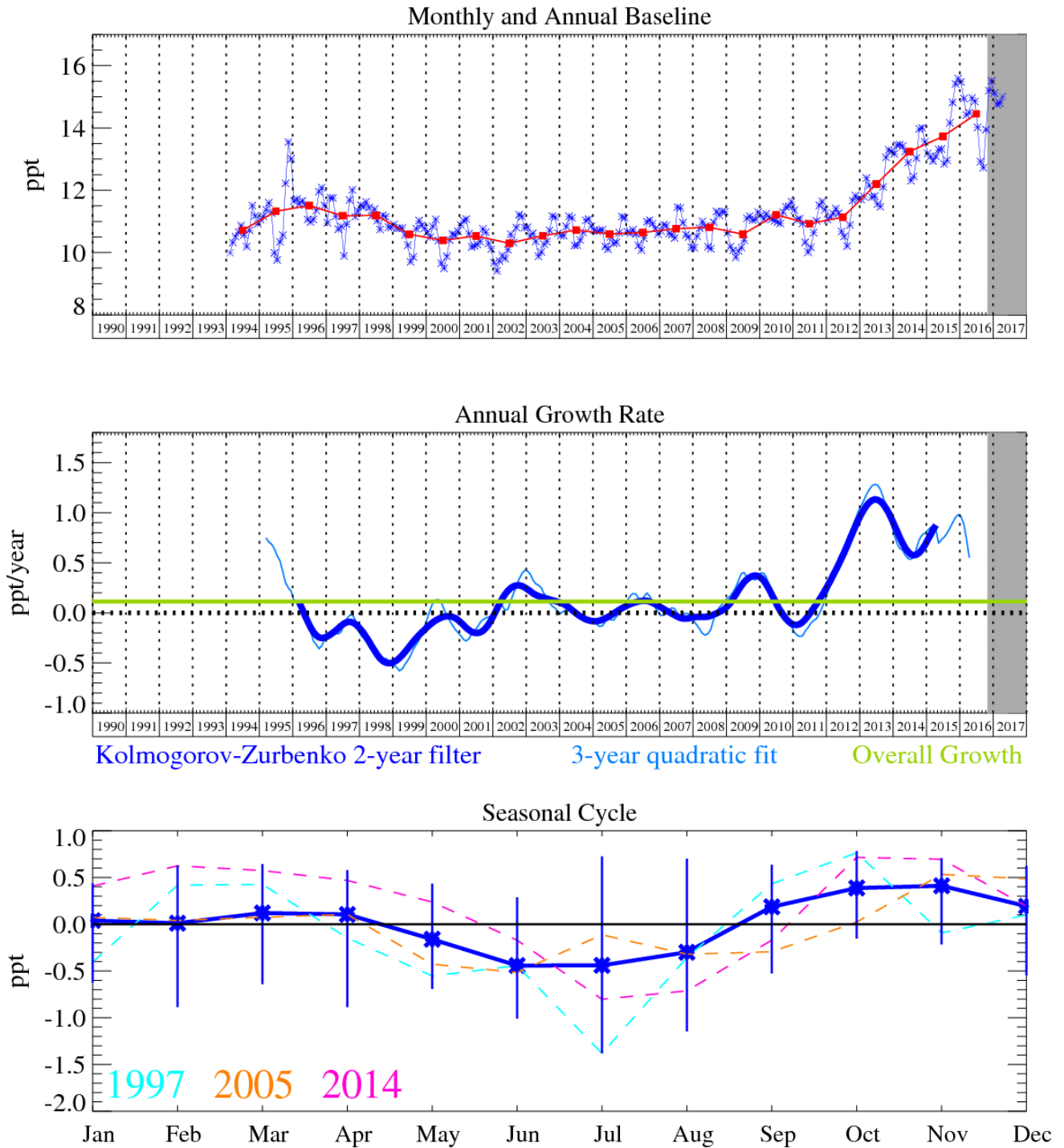


Figure 50: CHCl₃: Monthly (blue) and annual (red) Northern Hemisphere baseline mole fractions (top plot). Annual (blue) and overall average growth rate (green) (middle plot). Seasonal cycle (de-trended) with year-to-year variability (lower plot). Grey area covers un-ratified and therefore provisional data.

8.14 CCl₄ (carbon tetrachloride)

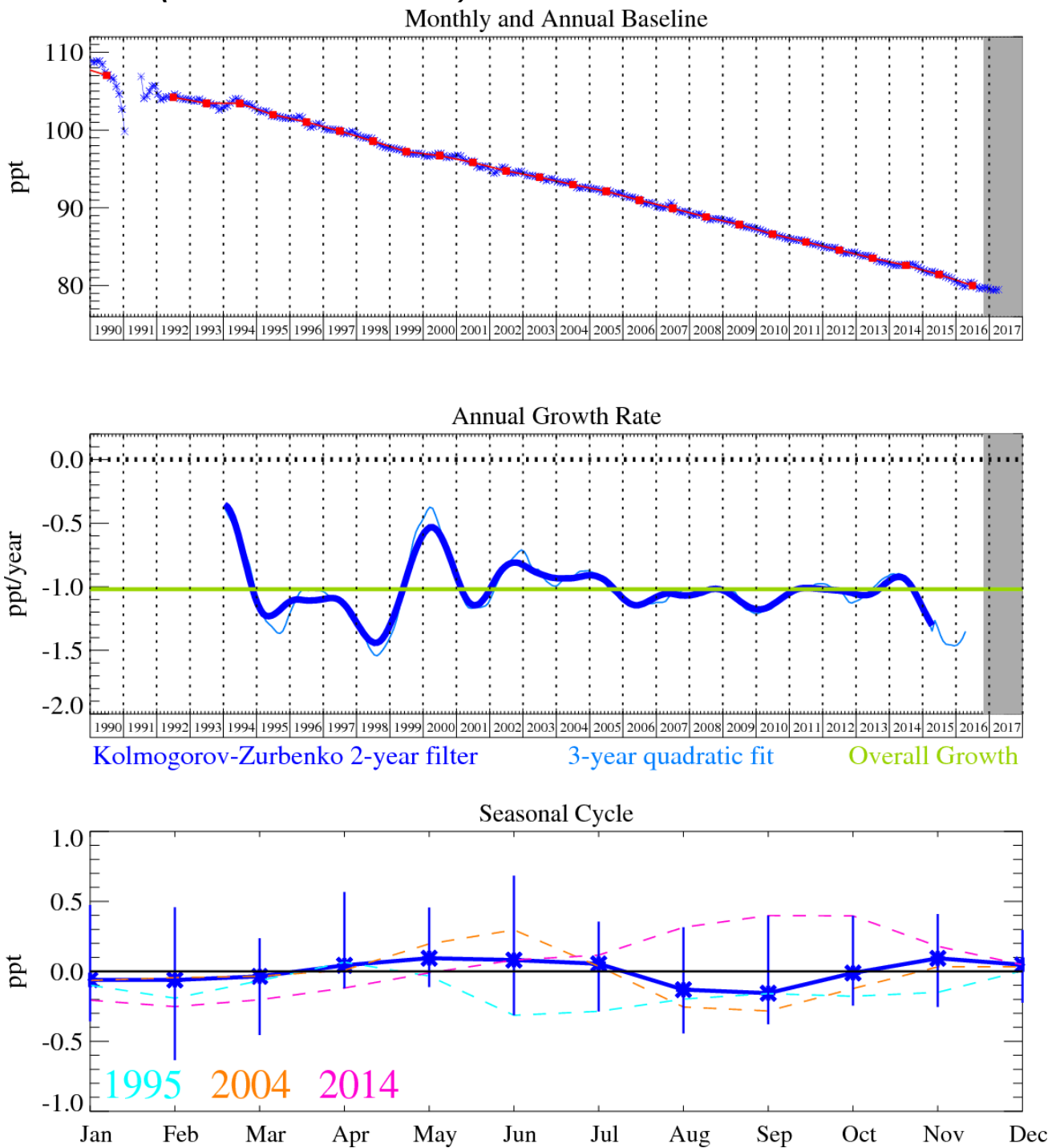


Figure 51: CCl₄: Monthly (blue) and annual (red) Northern Hemisphere baseline mole fractions (top plot). Annual (blue) and overall average growth rate (green) (middle plot). Seasonal cycle (de-trended) with year-to-year variability (lower plot). Grey area covers un-ratified and therefore provisional data.

8.15 CH₃CCl₃ (methyl chloroform)

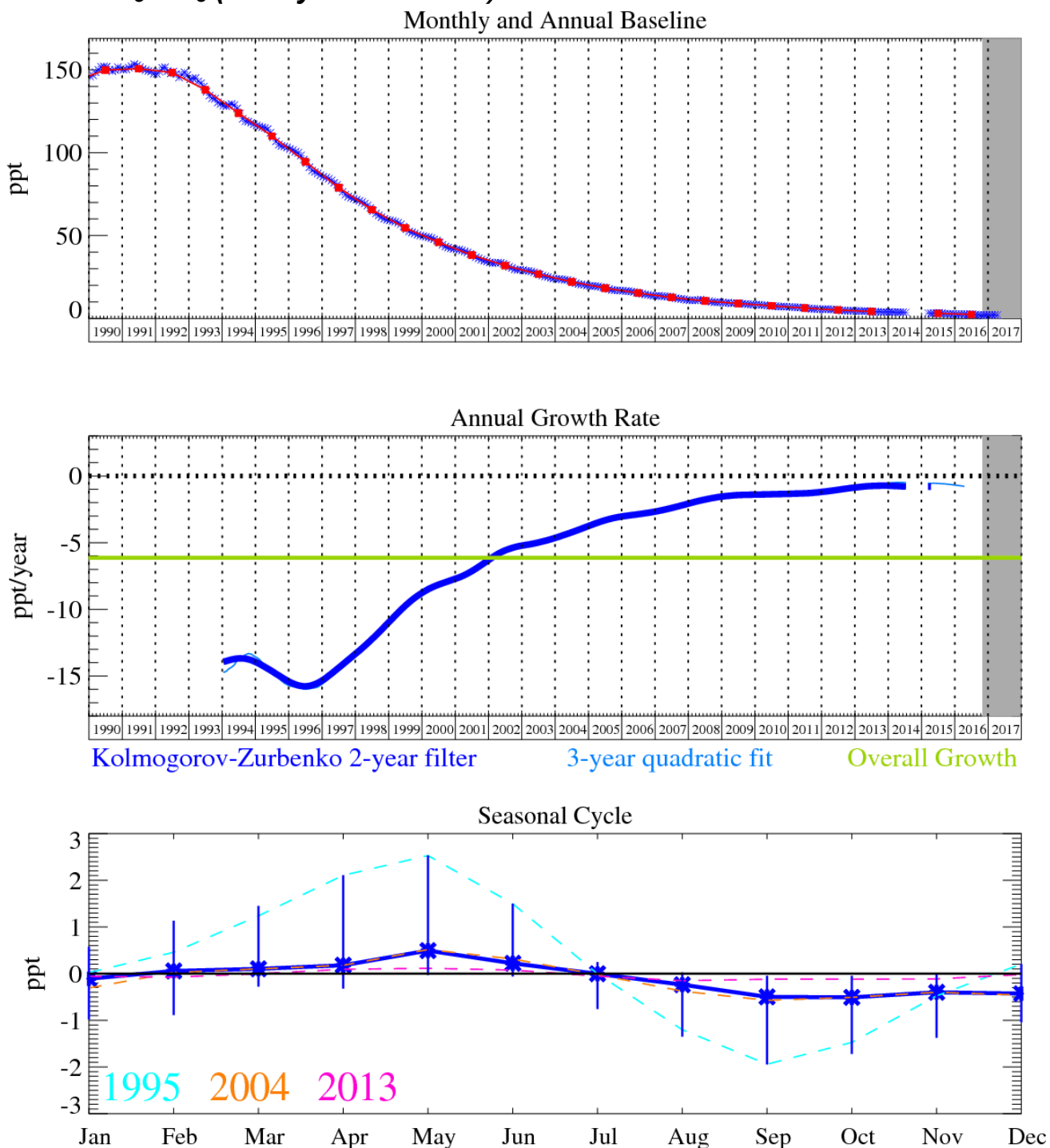


Figure 52: CH₃CCl₃: Monthly (blue) and annual (red) Northern Hemisphere baseline mole fractions (top plot). Annual (blue) and overall average growth rate (green) (middle plot). Seasonal cycle (de-trended) with year-to-year variability (lower plot). Grey area covers un-ratified and therefore provisional data.

8.16 CCl₂CCl₂

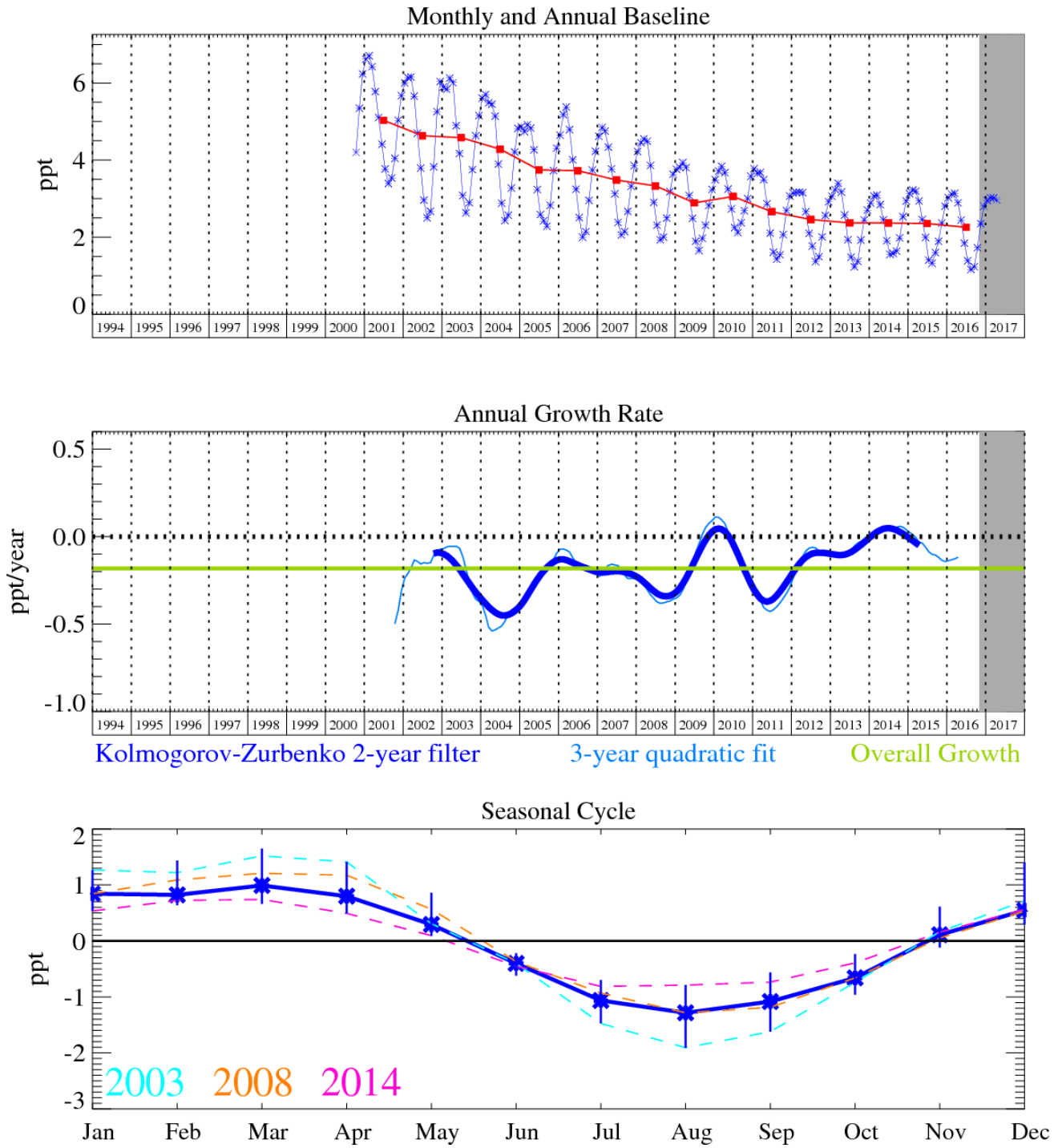


Figure 53: CCl₂CCl₂: Monthly (blue) and annual (red) Northern Hemisphere baseline mole fractions (top plot). Annual (blue) and overall average growth rate (green) (middle plot). Seasonal cycle (de-trended) with year-to-year variability (lower plot). Grey area covers un-ratified and therefore provisional data.

8.17 Methyl bromide (CH₃Br)

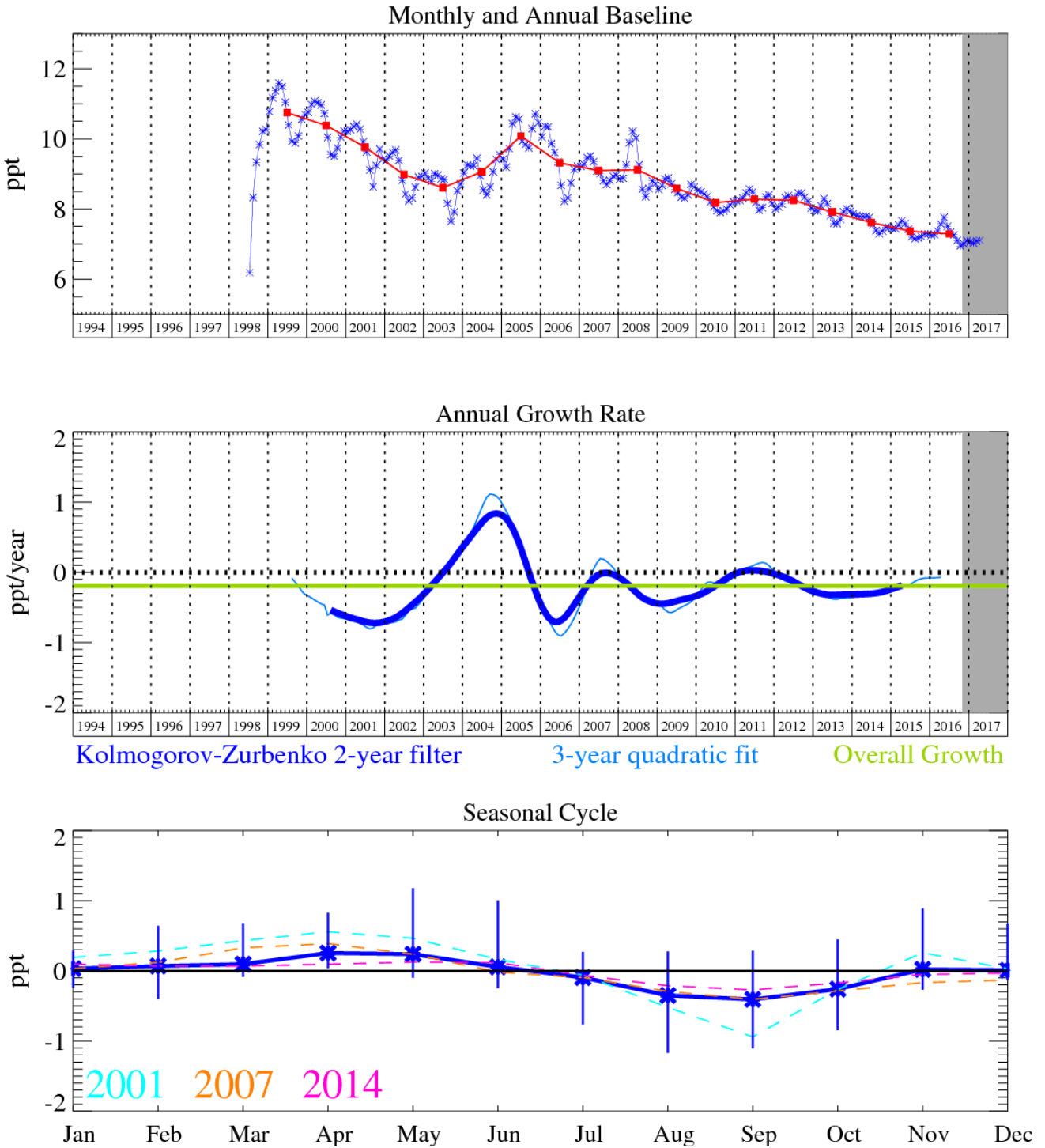


Figure 54: Methyl bromide: Monthly (blue) and annual (red) baseline (top plot). Annual (blue) and overall average growth rate (green) (middle plot). Seasonal cycle (de-trended) with year-to-year variability (lower plot). Grey area covers un-ratified and therefore provisional data.

The instrument change in 2005 to the Medusa system produced a discontinuity in the methyl bromide record, this jump should be discounted as it is an artefact of the measurement system.

8.18 Halon-1211

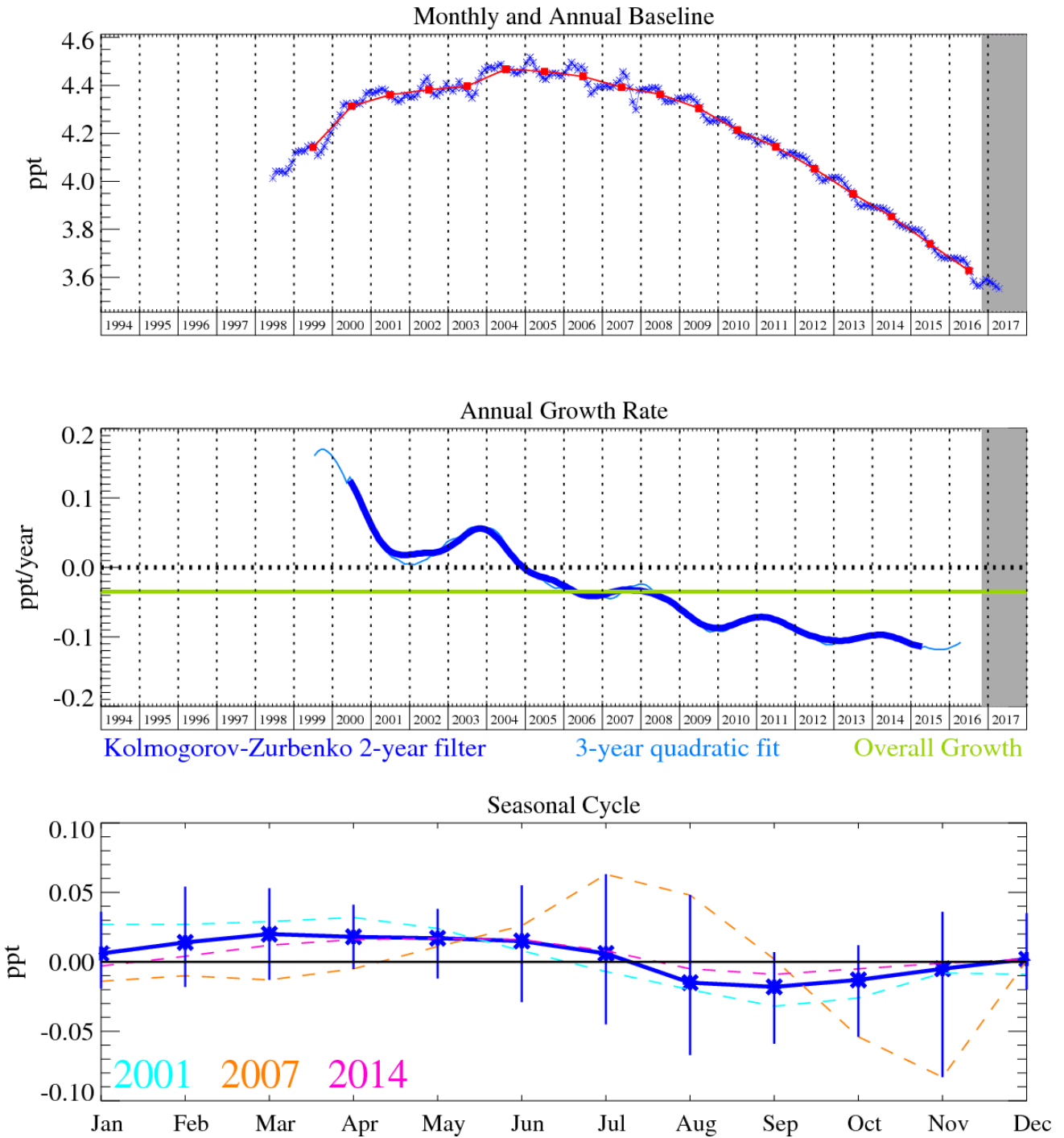


Figure 55: Halon-1211 (CBrClF₂): Monthly (blue) and annual (red) baseline (top plot). Annual (blue) and overall average growth rate (green) (middle plot). Seasonal cycle (de-trended) with year-to-year variability (lower plot). Grey area covers un-ratified and therefore provisional data.

8.19 Halon-1301

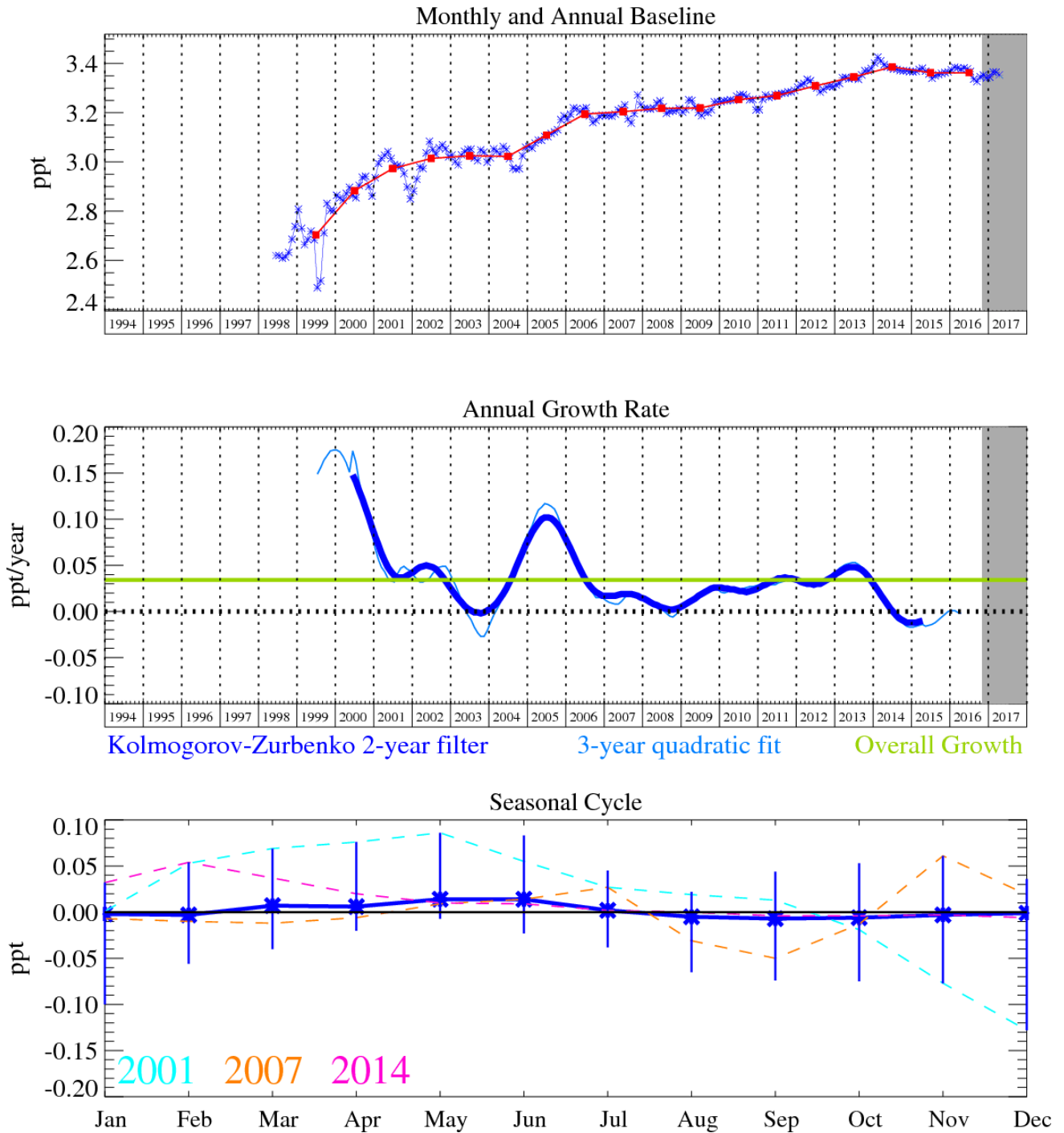


Figure 56: Halon-1301 (CBrF₃): Monthly (blue) and annual (red) baseline (top plot). Annual (blue) and overall average growth rate (green) (middle plot). Seasonal cycle (de-trended) with year-to-year variability (lower plot). Grey area covers un-ratified and therefore provisional data.

8.20 Halon-2402

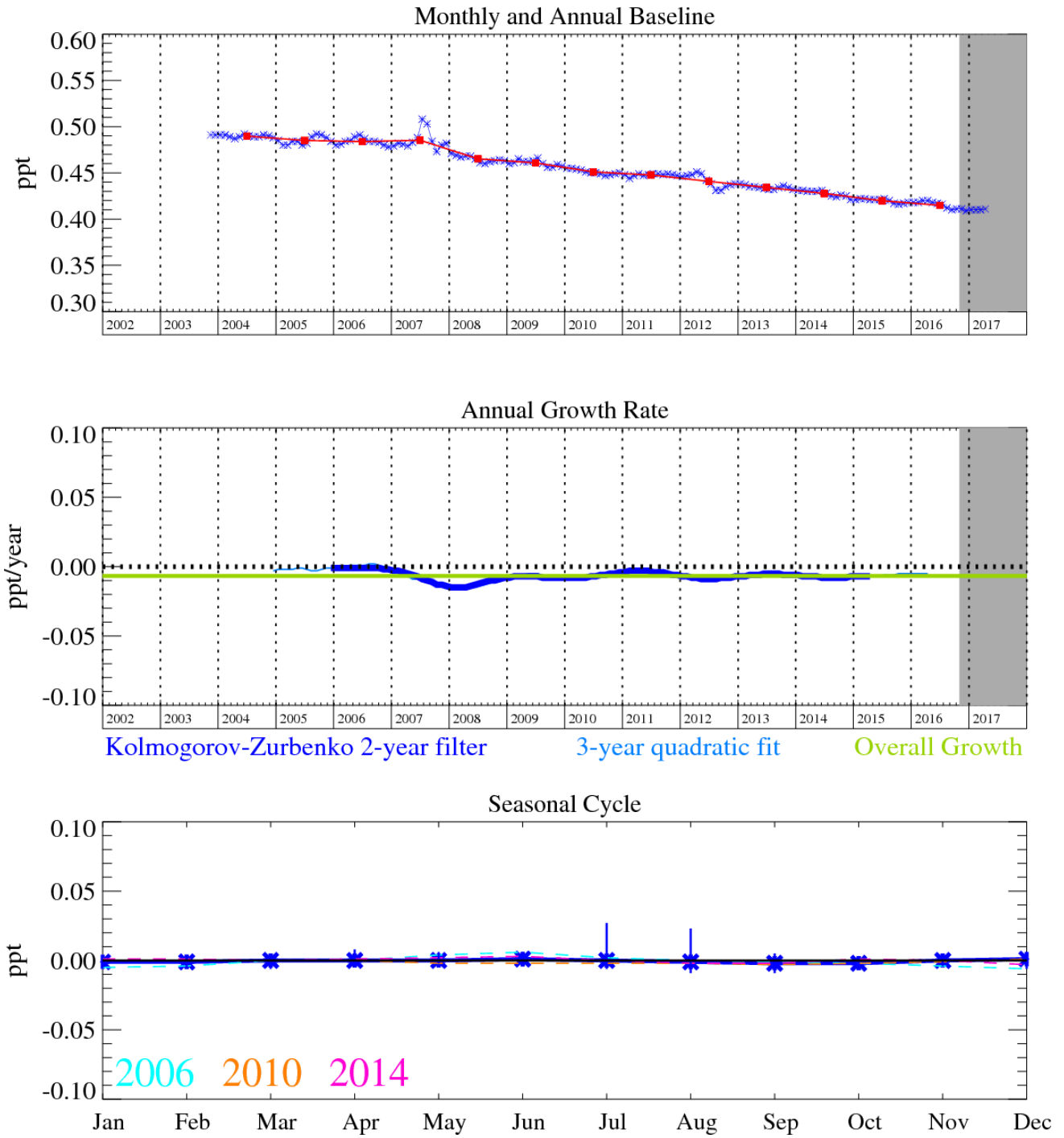


Figure 57: Halon-2402 ($C_2Br_2F_4$): Monthly (blue) and annual (red) baseline (top plot). Annual (blue) and overall average growth rate (green) (middle plot). Seasonal cycle (de-trended) with year-to-year variability (lower plot). Grey area covers un-ratified and therefore provisional data.

8.21 Carbon monoxide (CO)

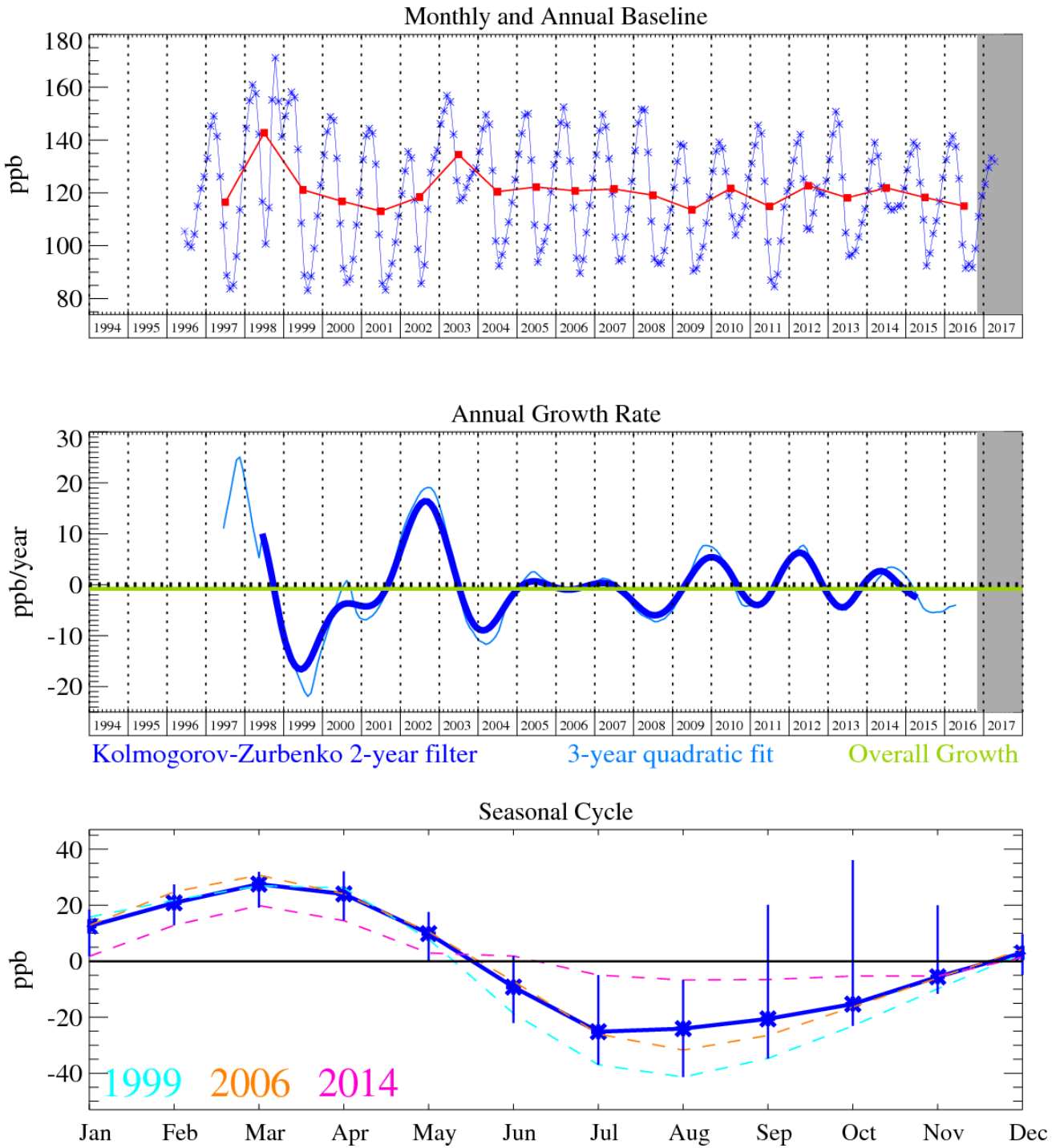


Figure 58: CO: Monthly (blue) and annual (red) Northern Hemisphere baseline mole fractions (top plot). Annual (blue) and overall average growth rate (green) (middle plot). Seasonal cycle (de-trended) with year-to-year variability (lower plot). Grey area covers un-ratified and therefore provisional data.

8.22 Ozone (O₃)

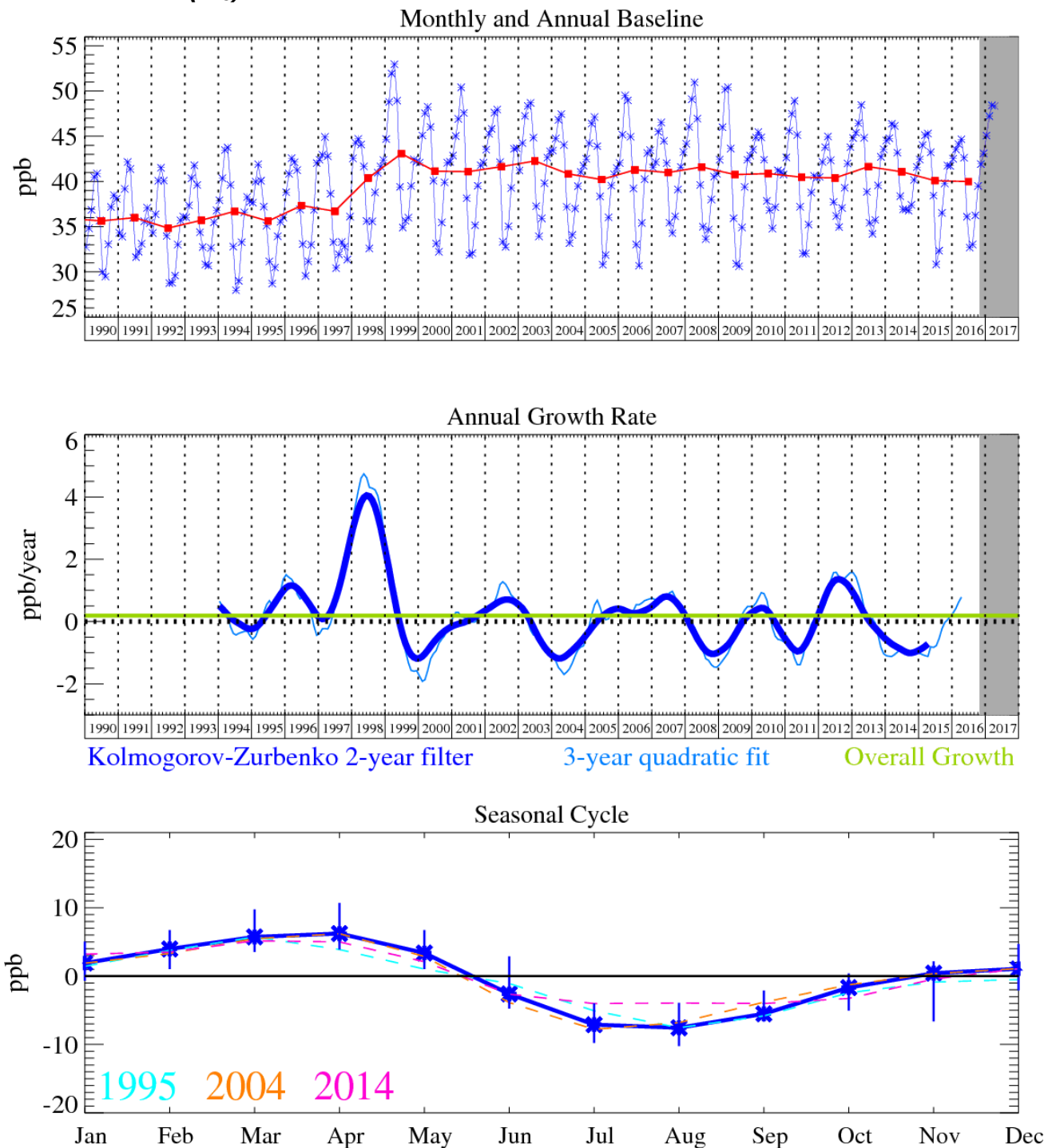


Figure 59: Ozone (O₃): Monthly (blue) and annual (red) Northern Hemisphere baseline mole fractions (top plot). Annual (blue) and overall average growth rate (green) (middle plot). Seasonal cycle (de-trended) with year-to-year variability (lower plot). Grey area covers un-ratified and therefore provisional data.

8.23 Hydrogen

Hydrogen is an oxidation product of CH₄ and isoprene, whose main sink is ground surface uptake, mainly in the northern hemisphere. Annual mean baseline levels have remained roughly constant (within measurement uncertainty) for much of the Mace Head record. There is evidence of anomalous growth in 2010-2011 through the influence of the forest fires in the Russian Federation.

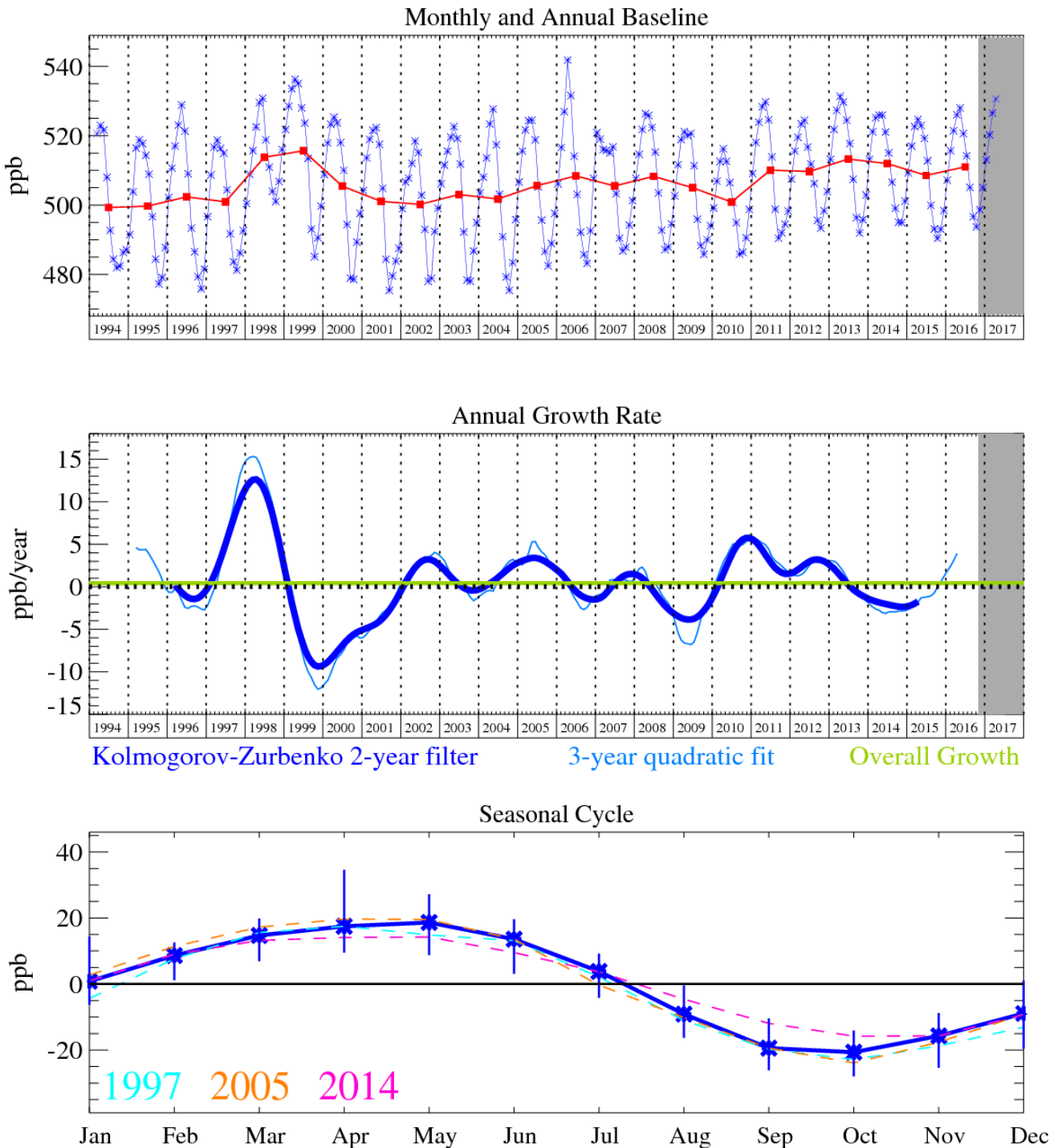


Figure 60: Hydrogen (H₂): Monthly (blue) and annual (red) baseline (top plot). Annual (blue) and overall average growth rate (green) (middle plot). Seasonal cycle (de-trended) with year-to-year variability (lower plot). Grey area covers un-ratified and therefore provisional data.

9 UK HFC-143a Emissions

9.1 Introduction

Hydrofluorocarbon HFC-143a (CH_3CF_3) is a commonly used refrigerant and propellant, either by itself or in blends. The gas is a potent greenhouse gas due to its high chemical stability and infrared absorbency (lifetime of 51 years and GWP of 4470). Of a few existing refrigerant blends containing HFC-143a, R-404A contains the most composition of HFC-143a (52%) with HFC-125 (44%) and HFC-134a (4%). HFC-143a will be the main gas studied in this report.

UK emission inventories are constructed using a bottom-up approach. In the RAC industry, RAC model, developed by ICF International, (Development of the GHG Refrigeration and Air Conditioning Model final report by ICF International, December 2011) (GHG Refrigeration and Air Conditioning Model Version 12 by ICF International, May 2015) is used to calculate emissions of gases specifically from the RAC sectors. There are 6 categories of RAC under the model which split into 13 'end use' sectors summarized in Table 31.

RAC Sector	Source	RAC Category
RAC-1	Domestic Refrigeration	Domestic Refrigeration
RAC-2	Small Hermetic Stand-alone Refrigeration	Commercial Refrigeration
RAC-3	Condensing Units	
RAC-4	Centralised Supermarket Refrigeration Systems	
RAC-5	Industrial Refrigeration	Industrial Refrigeration
RAC-6	Small Stationary Air- Conditioning	Stationary Air-Conditioning
RAC-7	Medium Stationary Air- Conditioning	
RAC-8	Large Stationary Air- Conditioning (Chillers)	
RAC-9	Heat Pumps	
RAC-10	Land Transport Refrigeration	Transport Air-Conditioning
RAC-11	Marine Transport Refrigeration	
RAC-12	Light-duty Mobile Air Conditioning	Mobile Air-Conditioning
RAC-13	Other Mobile Air-Conditioning	

Table 31: Summary of RAC sectors

Calculations to quantify emissions are derived from input assumptions based on findings from several research organisations and industry stakeholders. These parameters include lifetime, refill status, average charge size and emission rates for manufacture, operation and disposal, exist as default values but can be changed to showcase different scenarios.

Independent research to estimate gas emissions are carried out using top-down approach which mainly involves atmospheric observations. Measurements of trace-gases in the atmosphere are recorded at observatories such as Mace Head observatory located on the west coast Ireland. Numerical Atmospheric-dispersion Modelling Environment (NAME) is a Lagrangian particle model used to simulate atmospheric dispersion events. It is used to derive the probable history of air at specific locations, in order to show the likely contribution of different regions. Inversion Technique for Emission Modelling (InTEM) is an inversion modelling system developed by the Met Office which makes use of Bayesian statistics. Using an iterative best-fit technique, InTEM searches for emissions map which minimizes the difference between model and atmospheric observations. Therefore, combination of NAME and atmospheric observations within InTEM is used to quantify emissions of GHGs.

9.2 Methodology

9.2.1 Initial RAC model analysis

RAC model was used to determine from which RAC category and sectors R-404A (and consequently HFC-143a) emissions originate. This was done by collating output data for R-404A in

each category. To determine results specific to HFC-143a, the data were then scaled according to its specific compositions in the blend which were also used in data comparison later.

9.2.2 Comparison of UNFCCC and InTEM emissions

UK's inventory emissions submitted to the UNFCCC were compared with the InTEM emission estimates, with their uncertainties, derived from atmospheric measurements. Both data were obtained from Met Office's annual report to DECC (September 2016). Latest InTEM estimates of HFC-143a (June 2017) by Manning from the Met Office were incorporated for the year 2013-2014.

9.2.3 Bottom-up estimation of UK HFC-143a emissions

Calculation of HFC-143a emissions in the RAC model depends on input assumptions with their respective default values. Varying these parameters (within the allowed ranges) could possibly justify the emission gaps as will be discussed below. For higher calculation speed, the parameters were varied using calculation carried out by Python programming language. Key input data for calculations were collected into comma-separated value (CSV) files for each sector which were then imported into Python.

Within the script, which was derived from previous author(s), calculations used in the model were reproduced to yield individual calculations for manufacturing, operating and disposal emissions. The script was first tested and modified before any data manipulation. This was done by running the individual calculations to reproduce the results calculated in the RAC model. When combined, resultant total emissions should also reproduce the model total emissions. (Linear relationships should be expected).

Input parameters were then varied in turn within the allowed range by modifying relevant parts of the script. The change in the total inventory was recorded for upper and lower bounds. The resultant plots were reproduced which also include plots of original total inventory and InTEM emissions data for comparison as will be discussed below.

9.3 Results and Discussion

9.3.1 Initial RAC model analysis

Analysis of RAC model showed that out of 6 RAC categories, only 3 contributed towards the emissions of HFC-143a: Commercial Refrigeration, Industrial Refrigeration and Transport Air-Conditioning. All sectors under the 3 categories contribute towards HFC-143a emissions and is summarized in Figure 61 below. In this report, the focus will only be in 3 sectors: RAC-3, RAC-4 and RAC-5, which have major contribution towards HFC-143a emissions.

9.3.2 Comparison of UNFCCC and InTEM emissions

In each subplot below, plot of dashed lines (- - -) represent the original total inventory emissions of HFC-143a with default values of parameters. Green plots with error bars resemble the InTEM emissions and their uncertainties while the coloured shaded plots represent the total inventory emissions when each parameter were varied between upper and lower bounds.

Generally, the original total inventory emissions of HFC-143a is at a higher value than that of InTEM emissions up until 2012, with similar trend of increasing to a maximum and then decreases (Figure 62). Higher InTEM estimates from 2013 were derived from the latest, revised set of emissions data by Met Office. From 2011, the inventory emissions decrease sharply from the highest in 2010 (from 911 to 679 tonnes) such that emissions are within the uncertainties of InTEM emissions. This is thought to be due to the improvements in the RAC model over the years with the reductions in leak/loss rates post-2010. Efforts in improving the accuracy of RAC and InTEM models deemed necessary proven from the observed smaller emission gaps in 2013 and 2014 (33.1 and 13.9 tonnes respectively).

The trend of increasing emissions in both sets of data in the earlier reporting years is mainly due to the development in technology and the rise of RAC sectors resulting in the increase number of emissive products and their usage. The estimated decreasing trend from 2010 is presumably due to

the efforts in reducing the HFC-143a usage, with other lower-GWP gases considered as alternatives.

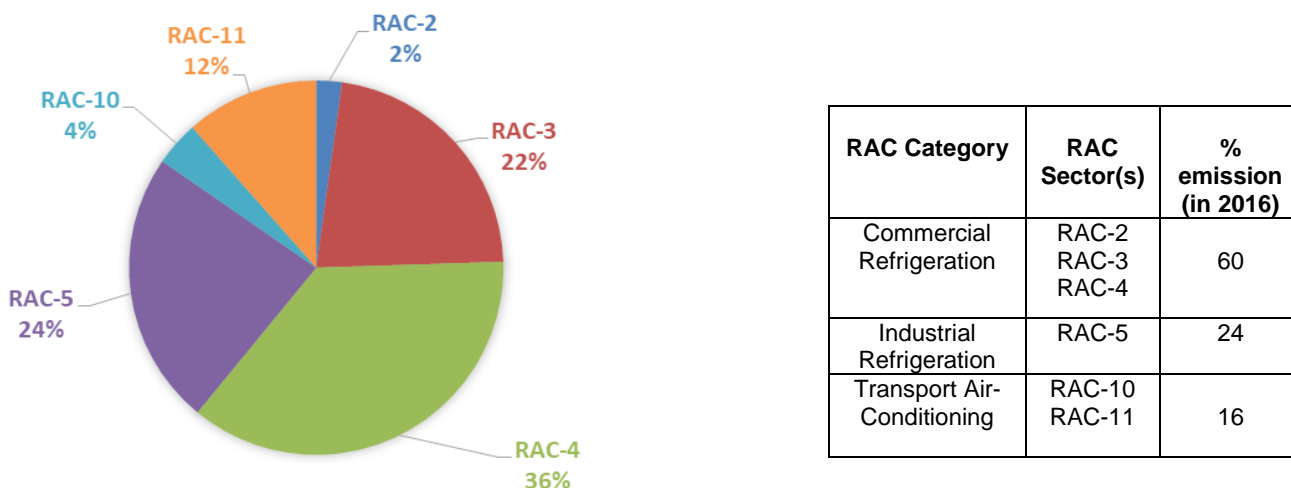


Figure 61: Total Emissions of HFC-143a in 2016.

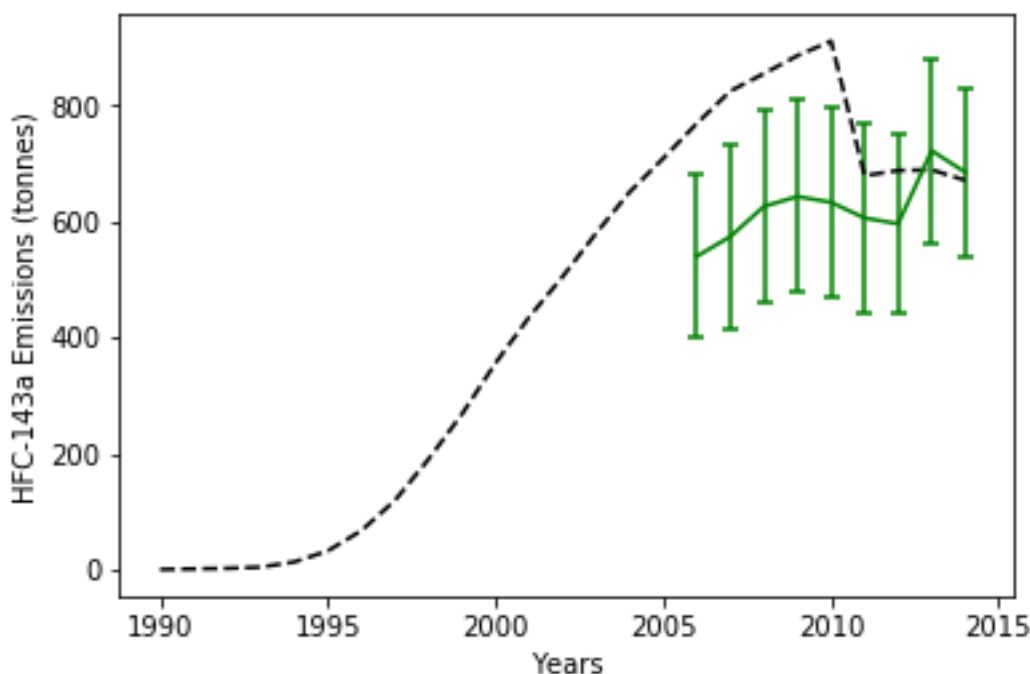


Figure 62: Comparison between UK's total inventory emissions reported to UNFCCC and Met Office's InTEM emissions (with uncertainties) of HFC-143a.

9.3.3 Bottom-up estimation of UK HFC-143a emissions

Five key input parameters in the RAC model were varied within the allowed range. The results are as follows:

Lifetime

Lifetime parameter was varied for each sector within the range given in parentheses (Figure 63). The default values of lifetime are 14, 18 and 25 for RAC-3, RAC-4 and RAC-5 respectively. Generally, lowering the unit's lifetime produce a lower total inventory emissions closer to InTEM values. This is expected due to the reduction of functioning RAC units, thus limiting gas emissions. Only minimal increase in inventory emissions is observed from increasing the lifetime, hence less effective in closing emission gaps in 2013 and 2014.

Lowering the lifetime in RAC-4 has a significant effect whereby the total inventory emissions fall agreeably within the range of InTEM uncertainties particularly in the later reporting years whereas only a slight decrease in inventory emissions due to the other two sectors. Indeed, lifetime of units

in each sector may possibly be lower than their respective default values assumed by the model depending on their usage, although longer lifetime should be expected as technology advance and units regularly maintained. Therefore, lifetime is expected to be a minor contributor in reducing the emission gap.

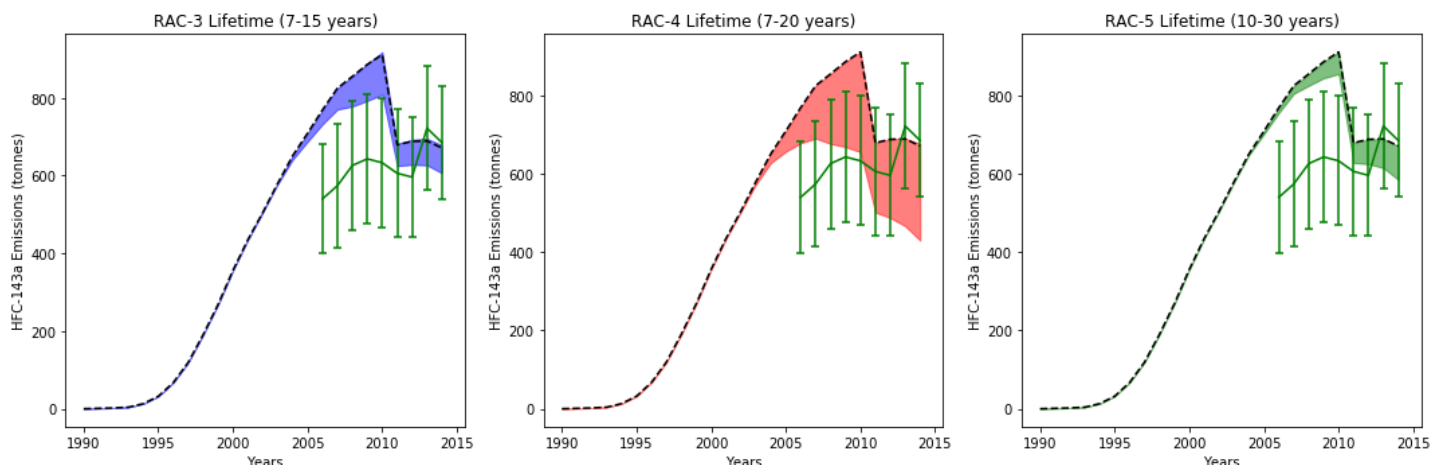


Figure 63: The effect of changing unit lifetime on UK’s total inventory emissions of HFC-143a.

Refill

The allowed input in refill parameter is either Yes or No. In all 3 sectors, the default input is Yes i.e. 100% refill. All units are assumed to be refilled annually thus, the amount of gas that leaks out is replaced by servicing each year. Changing to No i.e. 0% refill – no refill of units within unit lifetime, causes notable changes in the total inventory emissions by each sector (Figure 64). The switch leads to an agreement of total inventory emissions within InTEM emission uncertainties in all sectors. This is due to the decreasing amount of units as leaked gas is not replaced, hence suppressing subsequent emissions from refilling. However, changing refill parameter cannot justify the emission gaps in 2013 and 2014.

Although the assumption of no refill might not be plausible, varying the refill input within a scale between 0% and 100% would significantly reduce total emissions, allowing some improvements in the accuracy of RAC model. This might also be realistic as it is most likely that only a percentage of the total units, rather than either all or none of the units, in a sector is refilled. To illustrate this scenario, additional solid black lines (descending) in Figure 64 correspond to the expected inventory when 75%, 50% and 25% refill is assumed.

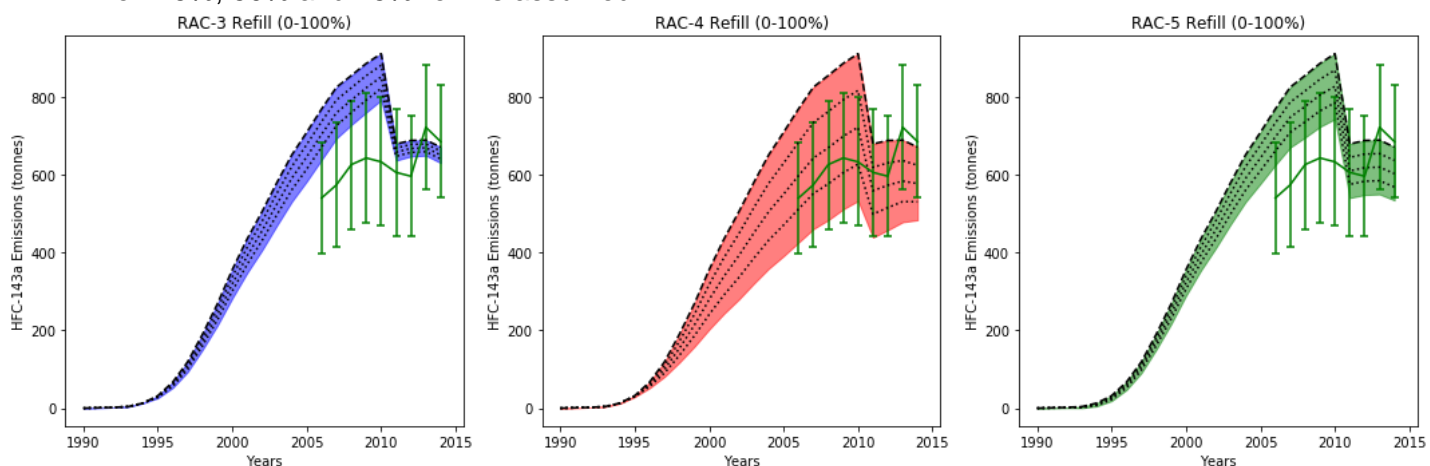


Figure 64: The effect of changing unit refill status on UK’s total inventory emissions of HFC-143a

Manufacturing Loss Rate

Manufacturing loss rates were varied within the range stated in parentheses (Figure 65). Although in RAC-3, the default manufacturing loss rates change over certain years, the rates were still varied between two extremes i.e. using a constant value of maximum and minimum for all the years. Altering the rates from each sector has an almost negligible effect on the total inventory emissions.

The reason is due to the smaller contribution of manufacturing emission factor (< 10%) towards the total HFC-143a emissions from model calculation (also manufacturing loss rates are usually very small < 10%). Therefore, it is not a suitable parameter to change to justify emission gap and improve the RAC model.

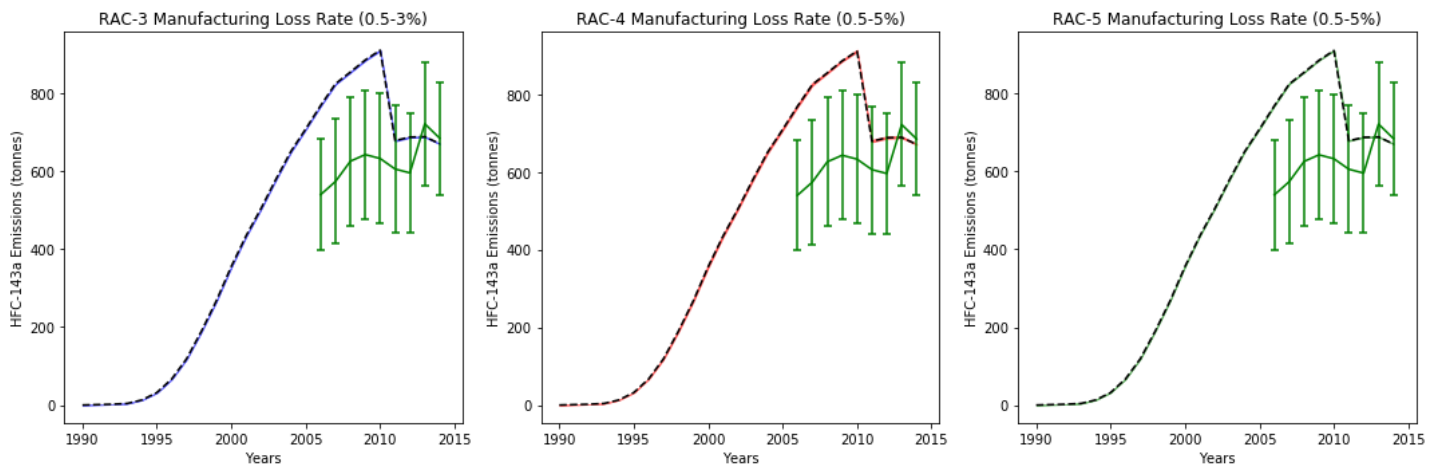


Figure 65: The effect of changing manufacturing loss rates on UK’s total inventory emissions of HFC-143a.

Operational Loss Rate

Operational loss rates were varied within the assumed range in the parentheses below (Figure 66). The default operational leak rates are: RAC-3 - 30% in 1990, 10% in 2010, linear decrease; RAC-4- 30% in 1990, 15% in 2010, linear decrease; RAC-5 - 20% in 1990, 20% in 2000, 10% in 2010, linear decrease from 2000 onwards. Despite the trend of linear decrease of default loss rates in all 3 sectors, rates were varied between a constant maximum and minimum throughout the entire reporting years. Generally, increase in the total inventory emissions are observed as the loss rates increase (and vice versa) due to the proportionality of emission factors with the loss rates.

Unlike the other two leak rates, the total inventory is sensitive to changes in operational loss rates. In all 3 sectors, increasing or decreasing loss rates from their default values resulted in significant changes whereby the inventory emissions fall within the InTEM uncertainties in all reporting years. This result is as expected as operational emission factor contributes massively towards the total HFC-143a emissions (> 90%). Hence, operational loss rate is the most important leak factor and a dominating parameter amongst others to be varied.

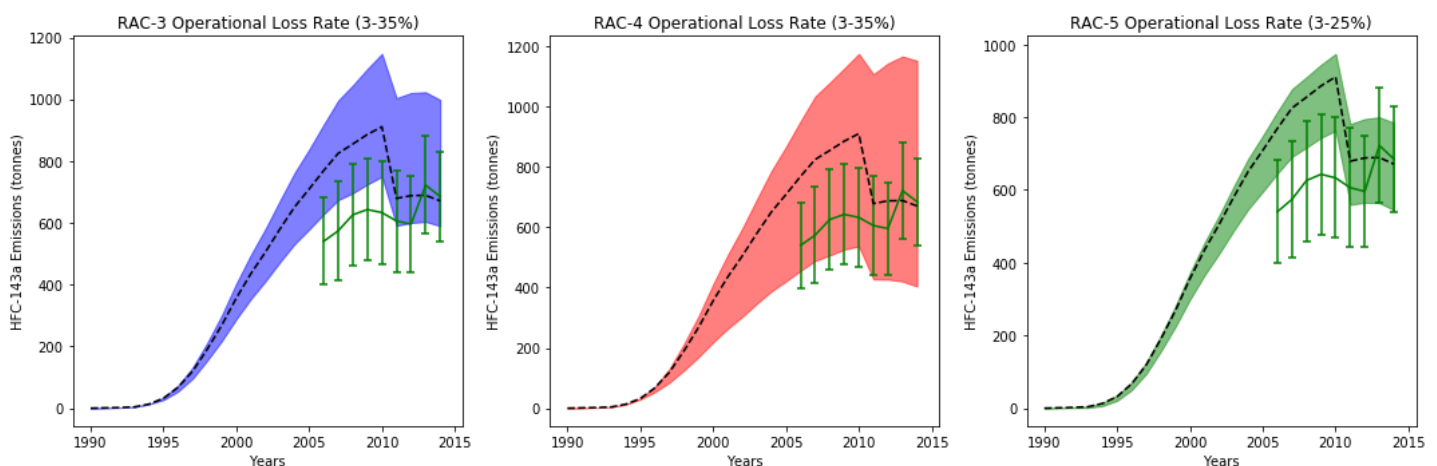


Figure 66: The effect of changing operational loss rates on UK’s total inventory emissions of HFC-143a.

Disposal Loss Rate

Disposal loss rates were varied within the specified range in the parentheses (Figure 67). The default values are: RAC-3 – 60% in 1990, 45% in 2000, 15% in 2010, linear decrease thereafter; RAC-4 – 50% in 1990, 25% in 2000, 6% in 2010, linear decrease thereafter; RAC-5 – 50% in 1990, 30% in 2000, 15% in 2010, linear decrease thereafter. Although the rates vary (decrease) as years

progress, the rates were varied between a maximum and a minimum throughout. However, in the earlier years (1990-1999), the default rates exceed the maximum value of the assumed range in each sector. Thus, only the rates from 2000 onwards were changed (to respective maximum) as to record the highest possible total inventory.

Generally, disposal loss rate has little significance towards the total inventory emissions from all 3 sectors although, leak rates are usually higher than the previous two. This might be due to the smaller amount of refrigerant remaining in the units being disposed, hence lower emission. However, the main reason is the fact that disposal emission factor has a smaller contribution towards the total gas emission (<10%) compared to the operational emission. However, increasing the loss rates in RAC-3, which leads to a slight increase in total inventory emissions in later years, is enough to compensate for the emission gaps found in 2013 and 2014. Regardless, disposal loss rate is generally an unsuitable parameter to alter to minimize emission gap.

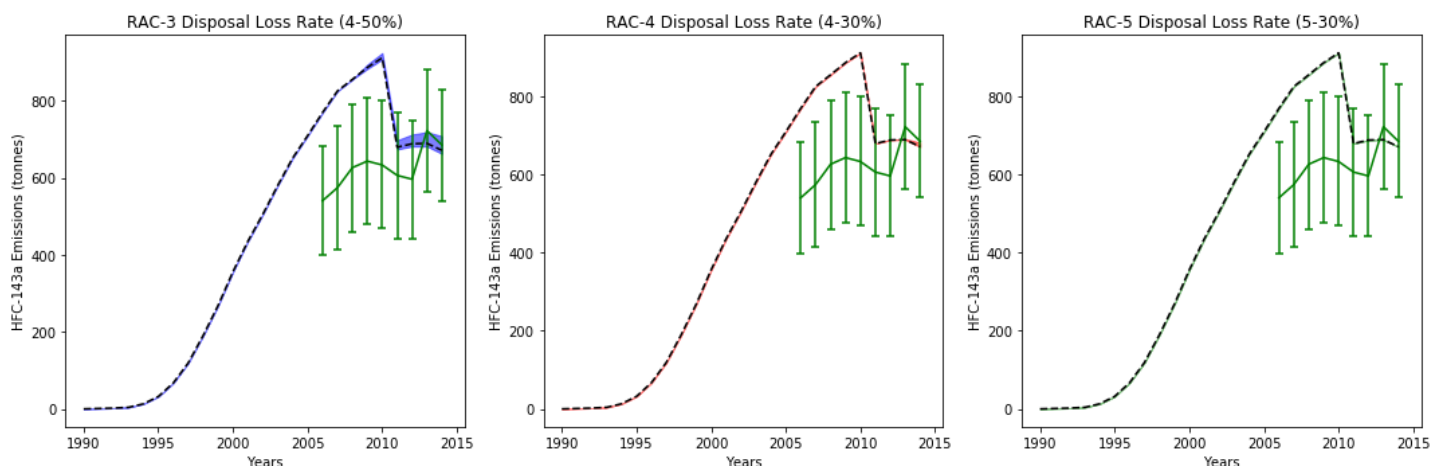


Figure 67: The effect of changing disposal loss rates on UK's total inventory emissions of HFC-143a.

Overall, the results above suggest that operational loss rate is the key parameter, among the others, appropriate for alteration to justify the gap between the predicted InTEM and total inventory emissions. Lifetime and refill parameters might also be acceptable for modification as proved to produce desired outcome for most years. Comparison between the effects on inventory emissions between sectors suggest that RAC-4 exerts a greater influence over the others, reflecting the larger proportion of RAC-4 in Figure 61. This could possibly be due to the large-scale use of refrigeration units having higher charge size found in big stores or supermarkets and high leakage rate due to pipe or joint failure and valves leakages.

9.4 Conclusions

Top-down approach in the estimation of HFC-143a emissions were conducted using the combination of atmospheric observations and air-history model (NAME) within InTEM inversion model. These data were compared with the bottom-up estimates calculated from RAC model which form the basis of UK's Inventory submitted to the UNFCCC. It was shown that there is a great discrepancy between the two sets of emission estimates especially in the earlier reporting years. These results highlight the importance in improving the methods used in quantifying gas emissions, i.e. the accuracy and reliability of RAC model.

Analysis of RAC model revealed the different effects of changing key input assumptions used in the model. From the results presented, operational loss rate is the most important and dominating parameter to alter to justify the emission gaps in all reporting years. Lifetime and refill parameters might also be suitable parameters to change to mitigate the discrepancy in emissions but not for 2013 and 2014.

In conclusion, further works in improving the techniques used in emissions estimates are necessary as to yield more accurate and reliable UK emissions data to be reported to the UNFCCC. Improvements should not only be specific to the RAC model but also the InTEM method as there are uncertainties associated with the data.

10 Use of optical methods for real-time atmospheric N₂O measurements

Summary based on Tom Richardson's MSc thesis (2017)

10.1 Introduction

A Los Gatos Research off-axis integrated cavity output spectrometer (OA-ICOS) was installed at Tacolneston tall tower (TAC), part of the UK Deriving Emissions linked to Climate Change (UK DECC) network, in September 2016 to measure N₂O and CO mole fractions in parallel with the gas chromatograph at site. This study compared the N₂O data obtained by the OA-ICOS and the gas chromatograph coupled with an electron detector (GC-ECD) at TAC from September 2016 to February 2017, specifically looking at instrument compatibility and comparability, examining differences in statistical sampling error and estimating errors induced by calibrating the OA-ICOS.

10.2 Instrumentation

An Agilent 6890 GC-ECD was installed at TAC in 2012 for N₂O analysis. A frontend system is used to select the air to be sampled, which is injected into the GC-ECD using 5/95% CH₄/Ar carrier gas. A multi-position Valco valve selects the gas to be analysed. Air is sampled from the 100m inlet and are filtered using a 40 and 7 µm filter. Calibration gas is made up of whole ambient air compressed into a 34 L stainless steel cylinder at MHD, where values are assigned. Sample air is dried using a Nafion dryer, with zero air used as the counterpurge gas, generated using a JunAir compressor and a zero air generator (Parker Balston 1250 TOC generator). The sample passes through an 8 mL loop under pressure for one minute, and then allowed to decay to ambient pressure before passing through the GC columns into the ECD. The GC-ECD is corrected for instrument nonlinearity over a concentration range from sub ambient to polluted air using a suite of cylinders, which were measured in April 2016 and a curve fitted to the results to assign the correction.

A LGR 30-EP model OA-ICOS with Scripps Institute of Oceanography modifications was installed at TAC in September 2016. Air from each inlet (54, 100 and 185 m.a.g.l.) at TAC is sampled from the primary intake lines with branched secondary lines through 40 and 7 µm filters before entering the frontend system. Each sample inlet was analysed sequentially for 20 minutes. A multi-position Valco valve selects gas to be analysed (sample air, target gas or calibration gas). Air is dried using a Nafion dryer in reflux mode, where a portion of the sample air after the Nafion dryer is cycled through as the counterpurge gas at a lower partial pressure. Calibration gas is made up of dried whole air spanning sub ambient to polluted air from MHD compressed into aluminium cylinders spanning the atmospheric mole fraction range and are calibrated at Empa, Switzerland. Calibration cylinders are analysed monthly and are used to define a nonlinearity correction.

10.3 Description of data analysis methods

All statistical analysis was conducted in R version 3.3 (R Core Team, 2014). To investigate the OA-ICOS and GC-ECD instrument compatibility, data from the OA-ICOS was averaged to one minute means. A one minute matrix was then created and data from both instruments were matched to the matrix. A number of basic statistics were then run on the matrix data.

The statistical sampling error between different sampling inlet heights was examined in two ways. Firstly, CO₂ and CH₄ data from a tall tower site within the UK DECC network (Tall Tower Angus; TTA) was explored to see if there was a difference between hourly means created using a whole hour and 20 or 30 minute subsets of data to create an hourly mean. Hourly means of 60, 30 and 20 minute data were created using the OpenAir package (Carslaw and Ropkins, 2012). A repeated measures ANOVA (R Core Team, 2014) was used to assess if there was a statistically significant difference between subset data and the true hourly average. Secondly, N₂O data from the OA-ICOS were used to assess stratification in mole fraction between the different sampling heights at TAC. Data were split by time of day using the lubricate and Plyr functions in R (Grolemund and Wickham, 2011; Wickham, 2011) and a new data frame was created using data from only between midday and 4pm, the time when the planetary boundary layer is at its most stable. Basic statistics were used to compare this data.

Error induced by instrument nonlinearity correction was studied by comparing data which had a correction based on data from all of the daily calibration sequences between 3rd and 24th October 2016 against individual corrections based on a single sequence between the same time period. Corrected data was analysed for statistical difference using a one-way ANOVA (R Core Team, 2014).

10.4 Results and discussion

Instrument compatibility (GC-ECD – OA-ICOS) showed good agreement for the comparison period (1st September 2016 to 28th February 2017), with a median difference in N₂O values of -0.32 ± 0.27 nmol mol⁻¹ and a strong significant correlation between the two instruments ($R = 0.929$, $p < 0.001$). The median bias remains outside of the World Meteorological compatibility guidelines of ± 0.1 nmol mol⁻¹ N₂O (WMO-GAW, 2016). The offset between instruments is thought to be caused due to values assigned to calibration gases came from two different laboratories (GC-ECD at Max Plank Institute, Germany, and OA-ICOS at Empa, Switzerland) and the nonlinearity correction assigned to each instrument.

Statistical sampling error on hourly averages were investigated for CO₂ and CH₄ at TTA for 2014. No statistically significant difference was observed in CO₂ or CH₄ hourly averages created with 60 minutes or 20 or 30 minute subsets of data. For 2014, hourly averages created using 60 minutes of data at TTA adequately encapsulated the hourly variability in CO₂ and CH₄. Similarly, little difference was seen in midday N₂O observations between different inlet heights at TAC on the OA-ICOS. A median bias of 0.074 ± 0.228 and -0.018 ± 0.415 nmol mol⁻¹ for 100m – 54 m and 185m, respectively. Time periods when there were the largest differences in N₂O between inlet heights correlated to low daily mean temperatures, when the planetary boundary layer was low.

A one-way independent ANOVA was used to determine if there was a statistical difference was found for changes in instrument nonlinearity over time, which was found to be not significant ($F_{1,16632} = 0.767$, $p = 0.381$, using a 95% confidence cut-off). This shows that the nonlinearity correction on the OA-ICOS does not drift significantly with time and an average of all calibration sequences adequately defines the nonlinearity curve on the instrument.

10.5 Conclusions

An in-situ comparison of two instruments; a GC-ECD that had been installed and running at TAC since 2012 and an OA-ICOS, which was installed in September 2016; showed that there was good instrument compatibility over the 6-month comparison period (1st September to 28th February). A median bias remains outside of the World Meteorological compatibility guidelines of ± 0.1 nmol mol⁻¹ N₂O (WMO-GAW, 2016). However, it is acknowledged that this target is ambitious and few laboratories have achieved it, especially when using older technologies, such as GC-ECDs.

The sampling error induced by analysing air from a number of inlets sequentially on a tall tower was investigated and found that 20-minute means for N₂O data at TAC from 1st September 2016 to 28th February 2017 would not likely affect results in lieu of hourly averages. Non-significant differences were found when both CO₂ and CH₄ data were compared from TTA.

Finally, instrument nonlinearity was shown not to vary significantly on the OA-ICOS whilst at TAC, meaning that a mean nonlinearity correction can be applied at site for a period, rather than having to calculate nonlinearity corrections every time a calibration sequence is conducted on the instrument.

11 Developments in methane isotopologue measurements

Using the tall tower network of total CH₄ mixing ratio measurements and regional scale inversion modelling, it is difficult to disaggregate emissions from specific CH₄ source categories with any significant certainty. Measurement of the CH₄ isotopologue ratios promise to provide additional information needed for more robust source attribution. The National Physical Laboratory is working to build an instrument capable of high precision isotopologue measurements for deployment to the Heathfield site in early 2019. This utilises spectroscopic measurement in the infrared by quantum cascade laser (QCL) absorption (a well-established technique to quantify the mixing ratios of trace species in atmospheric samples). If ambient air samples can be adequately concentrated before injection into the QCL then high-precision isotopologue measurements are possible.

12 References

- Arnold, T., Harth, C. M., Mühle, J., Manning, A. J., Salameh, P. K., Kim, J., Ivy, D. J., Steele, L. P., Petrenko, V. V., Severinghaus, J. P., Baggenstos, D. and Weiss, R. F.: Nitrogen trifluoride global emissions estimated from updated atmospheric measurements., *Proceedings of the National Academy of Sciences of the United States of America*, 110(6), 2029–34, doi:10.1073/pnas.1212346110, 2013.
- Buckle, G., “An independent verification of UK HFC-143a emissions based in atmospheric observations”, M.Sc project report, School of Chemistry (April 2016)
- Carslaw, D. C., and Ropkins, K.: openair --- an R package for air quality data analysis., *Environmental Modeling & Software*, 27-28, 52-61, 10.1016/j.envsoft.2011.09.008, 2012.
- Chevallier, F., P. Bergamaschi, D. Brunner, L. Feng, S. Houweling, T. Kaminski, W. Knorr, J. Marshall, P. I. Palmer, S. Pandey, M. Reuter, M. Scholze, and M. Voßbeck, *Climate Assessment Report for the GHG-CCI project of ESA's Climate Change Initiative*, pp. 96, version 4, 28 March 2017, 2017. [http://www.esa-ghg-cci.org/?q=webfm_send/385]
- Giusfredi et al, Theory of saturated-absorption cavity ring-down: radiocarbon dioxide detection, a case study, *Optical tech*: <https://doi.org/10.1364/JOSAB.32.002223>
- Grolemund, G., and Wickham, H.: *Dates and Times Made Easy with lubridate*, 2011, 40, 25, 10.18637/jss.v040.i03, 2011.
- Hausmann, P., Sussmann, R. and Smale, D.: Contribution of oil and natural gas production to renewed increase in atmospheric methane (2007–2014): top–down estimate from ethane and methane column observations, *Atmospheric Chemistry and Physics*, 16(5), 3227–3244, doi:10.5194/acp-16-3227-2016, 2016.
- Helmig, D., Rossabi, S., Hueber, J., Tans, P., Montzka, S. A., Masarie, K., Thoning, K., Plass-Duelmer, C., Claude, A., Carpenter, L. J., Lewis, A. C., Punjabi, S., Reimann, S., Vollmer, M. K., Steinbrecher, R., Hannigan, J. W., Emmons, L. K., Mahieu, E., Franco, B., Smale, D. and Pozzer, A.: Reversal of global atmospheric ethane and propane trends largely due to US oil and natural gas production, *Nature Geoscience*, 9(7), 490–495, doi:10.1038/ngeo2721, 2016.
- Keller, C. A., Matthias Hill, Martin K. Vollmer, Stephan Henne, Dominik Brunner, Stefan Reimann, Simon O’Doherty, Jgor Arduini, Michela Maione, Zita Ferenczi, Laszlo Haszpra, Alistair J. Manning, and Thomas Peter, “European Emissions of Halogenated Greenhouse Gases Inferred from Atmospheric Measurements” (2011)
- Kim, J., Fraser, P. J., Li, S., Mühle, J., Ganesan, A. L., Krummel, P. B., Steele, L. P., Park, S., Kim, S. K., Park, M. K., Arnold, T., Harth, C. M., Salameh, P. K., Prinn, R. G., Weiss, R. F. and Kim, K. R.: Quantifying aluminum and semiconductor industry perfluorocarbon emissions from atmospheric measurements, *Geophysical Research Letters*, 41, 4787–4794, doi:10.1002/2014GL059783, 2014.
- Ko, M. K. W., Newman, P. A., Reimann, S. and Strahan, S. E.: *Recommended Values for Steady-State Atmospheric Lifetimes and their Uncertainties, in SPARC Report on the Lifetimes of Stratospheric Ozone-Depleting Substances, Their Replacements, and Related Species*, edited by M. Ko, P. Newman, S. Reimann, and S. Strahan, *Stratospheric Processes And their Role in Climate*, Zurich, Switzerland., 2013.
- Lunt, M. F., Rigby, M., Ganesan, A. L., Manning, A. J., Prinn, R. G., O’Doherty, S., Mühle, J., Harth, C. M., Salameh, P. K., Arnold, T., Weiss, R. F., Saito, T., Yokouchi, Y., Krummel, P. B., Steele, L. P., Fraser, P. J., Li, S., Park, S., Reimann, S., Vollmer, M. K., Lunder, C., Hermansen, O., Schmidbauer, N., Maione, M., Arduini, J., Young, D. and Simmonds, P. G.: Reconciling reported and unreported HFC emissions with atmospheric observations, *Proceedings of the National Academy of Sciences*, 112(19), 5927–5931, doi:10.1073/pnas.1420247112, 2015.
- McCulloch, A. & Tim Vink, “Analysis of reported European emissions shows improvement in containment of hydrofluorocarbons” (2010)
- Mota-Babiloni, M., Pavel Makhnatch , Rahmatollah Khodabandeh, “Recent investigations in HFCs substitution with lower GWP synthetic alternatives: Focus on energetic performance and environmental impact” (2017)
- O’Doherty, S., M. Rigby, J. Mühle, D. J. Ivy, B. R. Miller, D. Young, P. G. Simmonds, S. Reimann, M. K. Vollmer, P. B. Krummel, P. J. Fraser, L. P. Steele, B. Dunse, P. K. Salameh, C. M. Harth, T. Arnold, R. F. Weiss, J. Kim, S. Park, S. Li, C. Lunder, O. Hermansen, N. Schmidbauer, L. X. Zhou, B. Yao, R. H. J. Wang, A. J. Manning, and R. G. Prinn, “Global emissions of HFC-143a (CH₃CF₃) and HFC-32 (CH₂F₂) from in situ and air archive atmospheric observations” (2014)
- Pickers PhD thesis: <https://ueaeprints.uea.ac.uk/id/eprint/61979>
- Prather, M. J., Hsu, J., DeLuca, N. M., Jackman, C. H., Oman, L. D., Douglass, A. R., Fleming, E. L., Strahan, S. E., Steenrod, S. D., Søvde, O. A., Isaksen, I. S. A., Froidevaux, L. and Funke, B.: Measuring and modeling the lifetime of nitrous oxide including its variability, *Journal of Geophysical Research: Atmospheres*, 120(11), 5693–5705, doi:10.1002/2015JD023267, 2015.
- Rigby, M., Prinn, R. G., O’Doherty, S., Montzka, S. a., McCulloch, A., Harth, C. M., Mühle, J., Salameh, P. K., Weiss, R. F., Young, D., Simmonds, P. G., Hall, B. D., Dutton, G. S., Nance, D., Mondeel, D. J., Elkins, J. W., Krummel, P. B., Steele, L. P. and Fraser, P. J.: Re-evaluation of the lifetimes of the major CFCs and CH₃CCl₃ using atmospheric trends, *Atmospheric Chemistry and Physics*, 13(5), 2691–2702, doi:10.5194/acp-13-2691-2013, 2013.

- Rigby, M., Prinn, R. G., O'Doherty, S., Miller, B. R., Ivy, D., Mühle, J., Harth, C. M., Salameh, P. K., Arnold, T., Weiss, R. F., Krummel, P. B., Steele, L. P., Fraser, P. J., Young, D. and Simmonds, P. G.: Recent and future trends in synthetic greenhouse gas radiative forcing, *Geophysical Research Letters*, 41(7), 2623–2630, doi:10.1002/2013GL059099, 2014.
- Rigby, M., Montzka, S. A., Prinn, R. G., White, J. W. C., Young, D., O'Doherty, S., Lunt, M. F., Ganesan, A. L., Manning, A. J., Simmonds, P. G., Salameh, P. K., Harth, C. M., Mühle, J., Weiss, R. F., Fraser, P. J., Steele, L. P., Krummel, P. B., McCulloch, A. and Park, S.: Role of atmospheric oxidation in recent methane growth, *Proceedings of the National Academy of Sciences*, 201616426, doi:10.1073/pnas.1616426114, 2017.
- Say, D., Alistair J. Manning, Simon O'Doherty, Matt Rigby, Dickon Young, and Aoife Grant, “Re-evaluation of the UK's HFC-134a Emissions Inventory Based on Atmospheric Observations”, Report for DECC (2016)
- Schaefer, H., Fletcher, S. E. M., Veidt, C., Lassey, K. R., Brailsford, G. W., Bromley, T. M., Dlugokencky, E. J., Michel, S. E., Miller, J. B., Levin, I., Lowe, D. C., Martin, R. J., Vaughn, B. H. and White, J. W. C.: A 21st-century shift from fossil-fuel to biogenic methane emissions indicated by $^{13}\text{CH}_4$, *Science*, 352(6281), 80–84, doi:10.1126/science.aad2705, 2016.
- Simmonds, P. G., Rigby, M., Manning, A. J., Lunt, M. F., O'Doherty, S., McCulloch, A., Fraser, P. J., Henne, S., Vollmer, M. K., Mühle, J., Weiss, R. F., Salameh, P. K., Young, D., Reimann, S., Wenger, A., Arnold, T., Harth, C. M., Krummel, P. B., Steele, L. P., Dunse, B. L., Miller, B. R., Lunder, C. R., Hermansen, O., Schmidbauer, N., Saito, T., Yokouchi, Y., Park, S., Li, S., Yao, B., Zhou, L. X., Arduini, J., Maione, M., Wang, R. H. J., Ivy, D. and Prinn, R. G.: Global and regional emissions estimates of 1,1-difluoroethane (HFC-152a, CH_3CHF_2) from in situ and air archive observations, *Atmospheric Chemistry and Physics*, 16(1), 365–382, doi:10.5194/acp-16-365-2016, 2016.
- Simmonds, P. G., Rigby, M., McCulloch, A., O'Doherty, S., Young, D., Mühle, J., Krummel, P. B., Steele, P., Fraser, P. J., Manning, A. J., Weiss, R. F., Salameh, P. K., Harth, C. M., Wang, R. H. J. and Prinn, R. G.: Changing trends and emissions of hydrochlorofluorocarbons (HCFCs) and their hydrofluorocarbon (HFCs) replacements, *Atmospheric Chemistry and Physics*, 17(7), 4641–4655, doi:10.5194/acp-17-4641-2017, 2017.
- Thompson, R. L., Ishijima, K., Saikawa, E., Corazza, M., Karstens, U., Patra, P. K., Bergamaschi, P., Chevallier, F., Dlugokencky, E., Prinn, R. G., Weiss, R. F., O'Doherty, S., Fraser, P. J., Steele, L. P., Krummel, P. B., Vermeulen, a., Tohjima, Y., Jordan, a., Haszpra, L., Steinbacher, M., Van der Laan, S., Aalto, T., Meinhardt, F., Popa, M. E., Moncrieff, J. and Bousquet, P.: TransCom N₂O model inter-comparison – Part 2: Atmospheric inversion estimates of N₂O emissions, *Atmospheric Chemistry and Physics*, 14(12), 6177–6194, doi:10.5194/acp-14-6177-2014, 2014.
- Trudinger, C. M., Fraser, P. J., Etheridge, D. M., Sturges, W. T., Vollmer, M. K., Rigby, M., Martinerie, P., Mühle, J., Worton, D. R., Krummel, P. B., Steele, L. P., Miller, B. R., Laube, J., Mani, F. S., Rayner, P. J., Harth, C. M., Witrant, E., Blunier, T., Schwander, J., O'Doherty, S. and Battle, M.: Atmospheric abundance and global emissions of perfluorocarbons CF_4 , C_2F_6 and C_3F_8 since 1800 inferred from ice core, firn, air archive and in situ measurements, *Atmospheric Chemistry and Physics*, 16(18), 11733–11754, doi:10.5194/acp-16-11733-2016, 2016.
- Turner, A. J., Frankenberg, C., Wennberg, P. O. and Jacob, D. J.: Ambiguity in the causes for decadal trends in atmospheric methane and hydroxyl, *Proceedings of the National Academy of Sciences*, 201616020, doi:10.1073/pnas.1616020114, 2017.
- Velders, G. J. M., Fahey, D. W., Daniel, J. S., McFarland, M. and Andersen, S. O.: The large contribution of projected HFC emissions to future climate forcing, *Proceedings of the National Academy of Sciences of the United States of America*, 106(27), 10949–10954, 2009.
- Wickham, H.: *The Split-Apply-Combine Strategy for Data Analysis*, 2011, 40, 29, 10.18637/jss.v040.i01, 2011.
- WMO-GAW: 18th WMO/IAEA Meeting on Carbon Dioxide, Other Greenhouse Gases and Related Tracers Measurement Techniques (GGMT-2015), La Jolla, CA, USA, 13 - 17 September 2015, WMO, Geneva, Switzerland, 2016.